Application of Nanomaterials in Precision Agriculture to Optimise Nitrogen Use Efficiency and Increase Global Food Security

By

JESSICA J. CHADWICK

A thesis submitted to the University of Birmingham for the degree of

DOCTOR OF PHILOSOPHY

School of Geography, Earth, and Environmental Sciences

College of Life and Environmental Sciences

University of Birmingham

November 2024

UNIVERSITY OF
BIRMINGHAM

University of Birmingham Research Archive

e-theses repository

This unpublished thesis/dissertation is copyright of the author and/or third parties. The intellectual property rights of the author or third parties in respect of this work are as defined by The Copyright Designs and Patents Act 1988 or as modified by any successor legislation.

Any use made of information contained in this thesis/dissertation must be in accordance with that legislation and must be properly acknowledged. Further distribution or reproduction in any format is prohibited without the permission of the copyright holder.

Abstract

Engineered nanomaterials (NM) are man-made nanoscale compounds, with at least one dimension between 1-100nm. Their utilisation presents a novel method to reduce the excessive use of synthetic fertiliser prevalent in industrial agriculture. The excess synthetic fertilisers are lost through the gaseous emission of N compounds, including N_2O, NH_3 and NO_Y, as well as through surface run-off and groundwater losses, increasing NO_3^- and NH_4^+ concentrations in waterways, impacting water quality. For NMs to be effective and sustainably used in agriculture there are several essential considerations that must be optimised: increased crop productivity and quality; positive effects on nutrient biogeochemical cycling, particularly N cycling to reduce emissions and run-off; and limiting impacts on soil biota including microbes and soil fauna, like earthworms.

The effects of NM exposure on seed germination were tested using seed priming experiments. NM effects were both species and NM dependent, although trends within "classes" of NMs were hard to predict, with constituent elements, concentration, agglomerate size, zeta potential and more sophisticated structure, like pore size, all impacting NM-plant interactions. NM application to soils in conjunction with reduced fertiliser application was used to determine NMs effects on plant growth and N cycling, using N_2O gas sampling and N compound losses in leachate. Zeolite NMs can have very different effects on terrestrial N cycling, with the sophisticated structure of the NM likely the root cause of these differences. Zeolites of the same type, like BEA-19 and BEA-150, were used in different soils and had very different impacts on N emissions and losses, reflecting the importance of NM characteristics, on NM environmental effects. BEA-150 triggered elevated N_2O emissions in the presence of microbes, while ZSM-5-15, another zeolite, decreased emissions in this soil type and increased them in another. This is indicative of the importance of soil abiotic factors, like soil moisture, clay and colloids, and soil microbial community composition on NM effect. Increased N_2O emissions may be generated through a process of ion exchange, with ZSM-5-15's extra-framework ion being exchanged for H^+ ions in its pores, leading to an increase in NH_4^+ accessible for nitrifying microbes to act upon and increasing nitrification derived N_2O. Wider effects of NMs on the soil environment were

studied using earthworm reproduction assays. ZSM-5-15 also triggered sub-lethal effects on reproduction of the earthworm *Eisenia fetida*, reducing the number of unhatched cocoons at 25 mg L^{-1}, a relatively low concentration. This may be through lower concentrations producing smaller NM agglomerates that are more able to pass through the worm epithelia and thus result in higher exposure at lower concentrations.

$Ce_{0.75}Zr_{0.25}O_2$ NMs didn't increase N_2O emissions in the loam soil studied but did in the sandy loam, also increasing NO_3^- leachate concentration. $Ce_{0.75}Zr_{0.25}O_2$ leaches Zr^{4+} ions into soil, transforming the NM into $Ce_{0.9}Zr_{0.1}O_2$ and CeO_2, as determined using X-ray near-edge absorption spectroscopy (XANES). $Ce_{0.75}Zr_{0.25}O_2$ is able to translocate from lettuce roots to shoots, with the NM found in aboveground lettuce tissue after soil-based NM application. Zr metal and $ZrCl_4$ were also found to be present in lettuce leaves, but whether these transformations occur in the soil before uptake and translocation or in lettuce shoots and leaves after uptake is uncertain. Other nano metal oxides used were TiO_2 PVP and $Co_{2.25}Fe_{0.75}O_4$ which were both applied in hydroponic medium. NM impact on N_2O emissions from hydroponics was minimal, however $K^{15}NO_3$ stable isotope application showed that the majority of the N_2O emissions were nitrification derived. This reflects the aeration of the rockwool substrate that the lettuce roots were grown in. TiO_2 PVP and $Co_{2.25}Fe_{0.75}O_4$ NMs may act on denitrifying microbes hence the minimal impact they have on total N_2O emissions.

NM co-application with synthetic fertiliser was found to increase the risk of N losses to the environment, while NMs with nutrients as part of their physical structure may be able to limit these losses. Urea-doped amorphous calcium phosphate (U-ACP), a hydroxyapatite NM with both N and P within its structure, was able to reduce NO_Y emissions from soil. The lack of N_2O and NH_3 gas data however means that there are several N cycling endpoints that are missed, so whether U-ACP application reduces net N losses or shifts the balance of the soil N cycle is unknown. U-ACP increased lettuce production as compared to urea, with this mostly being derived from urea application triggering soil acidification and limiting lettuce growth. U-ACP application also increased the community of nitric

oxide reductase (*qNorB* in particular) expressing soil bacteria, indicative of an increase in the soil microbial community active in denitrification.

Understanding NM impacts on N cycling is essential for a holistic view of fertilisation and for nano-enabled agriculture to truly increase sustainability while minimising the risk of regrettable substitutions. This thesis presents a first step towards achieving this holistic view.

Acknowledgements

This list of thanks is certainly not exhaustive, and my gratitude goes to all those I've met along the journey. PhDs, and thesis writing in particular, do not come easy and without the following this work would never have come to fruition.

First and foremost, thanks go to my co-supervisors Professor Iseult Lynch and Professor Sami Ullah. You have afforded me the most amazing opportunities, gently steered me in the right direction and pushed me to go further, dig deeper and achieve more. Thank you to my other supervisors, Peng Zhang and Arnoud Witteveen, your specialty advice and knowledge was invaluable. Ryan Mushinski, for launching me into the world of NO_Y, and Cynthia Kallenbach for her incredibly helpful advice and microbial ecology teaching.

Thank you to my collaborators, Aleksandar Radu, Ify Leonard Ugbomeh, Sam Parkinson, Swaroop Chakraborty and NanoSolveIT. I would like to thank Iuliia Mikulska at Diamond Light Source for her technical support and endless patience. Ross McCaffrey at Saturn Bioponics for all his help and good company. Fotis Sgouridis' GC and ^{15}N analysis and Chris Stark's ICP analyses. The behind the scenes teams in GEES, BBSRC, MIBTP and Mitacs-UKRI. Special thanks go to the lab staff at UoB; Nick Davidson, David Tubbs, Bethan Phillips, James Gore, I truly couldn't have done it without you.

Thanks are also richly deserved by the soil group, in particular Gianni, Manon and Yafei, for always being happy to help as fonts of gas flux sampling knowledge. Thanawan and Lisi for making WG be the place to be. The amazing Kallenbach group, particularly Sophie, Hannah and Jess, as well as Noura, Mohammed and Elias of the Whalen group for all your feedback, help in the lab and excellent company. Matt, Kieran, John and all the soil cultivators at Grand Union, working alongside you at the canal has been both a privilege and a pleasure.

My geography/mojito friends, for being the best people to have long lunches, post-work Bratby pints and experience my time in Birmingham with.

Kat, many tears have been shed on your shoulder, many glasses of wine drunk and an enormous number of laughs had. Grace, there since day one, a rock of wisdom, kindness and I truly couldn't have done it without our endless Zoom calls. Thank you for going through it all with me.

It is hard to summarise those who mean most to me and without whom this work could never have been done. We are changed by all those we love, and I am incredibly grateful to love such wonderful, interesting, funny people. Thank you to my family, for their love, support and also, my existence. Nana and Gran, two of the greats, if I have seen further, it is by standing on the shoulders of giants.

Thanks to the city of Birmingham, with all its jazz, old man pubs and secret delights, a good place to call home. This thesis has been written across many different cities, countries and even continents. Without the sea I fear I would have lost myself entirely.

There are three people who I would like to dedicate this thesis to. For Allan and Lourdes, thank you for your unwavering faith in me. And for Dinah, the voice in the back of my head.

Table of Contents

Abstract II
Acknowledgements VI
Table of Contents VII
List of Figures X
List of Tables XV
List of Abbreviations XVIII
Chapter 1. Aims and Hypotheses 20
Chapter 2. Introduction – Use of Nanotechnology to Increase Nutrient Use Efficiency, Enhance Crop Nutrition, and Reduce Agricultural Pollution 22
Acknowledgements 22
CReDIT statement 22
Chapter 3. Differential Impacts on Wheat and Lettuce Seedling Outcomes from Nano-Zeolite and Metal Oxide Seed Priming – A Comparative Study 48
Acknowledgements 49
CReDIT statement 49
3.1. Abstract 50
3.2. Introduction 51
3.3. Materials and Methods 54
3.3.1. Materials and characterisation 54
3.3.2. Seed priming 55
3.3.3. Bicinchoninic acid (BCA) Protein assay 56
3.3.4. Statistics 57
3.4. Results and Discussion 57
3.5. Conclusion 75
References 76
Chapter 4. Soil-based Zeolite and Metal Oxide Nanomaterial Application Alters Reactive Nitrogen Losses and Lettuce (*Lactuca sativa*) Growth 81
Acknowledgements 82
CReDIT statement 82
4.1. Abstract 83
4.2. Introduction 84
4.3. Materials and Methods 86
4.3.1. Materials 86
4.3.2. Greenhouse study, sampling and analysis 87
4.3.3. Soil characterisation and net nitrogen mineralisation 88
4.3.4. Greenhouse gas fluxes 88
4.3.5. Soil nutrient analysis 89
4.3.6. Macro- and micronutrients, NM constituent elements and plant stress marker analysis 90
4.3.7. X-ray Absorption Spectroscopy 90
4.3.8. Statistics 91
4.4. Results 92
4.5. Discussion 102
4.5.1. N_2O emissions and soil respiration are elevated under ZSM-5-15 treatment 102
4.5.2. Leaching loss dynamics over time and with NM treatment 104
4.5.3. NM zeta potential, ion exchange capacity, and transformations within the soil matrix, influence NM-soil component interactions 106
4.5.4. $Ce_{0.75}Zr_{0.25}O_2$ and ZSM-5-15 positively impact lettuce growth with maintained crop quality 108
4.5.5. Outlook 110

References ... 112
Chapter 5. Greenhouse Gas Emissions from Hydroponically Grown Lettuce Under Nano-Metal Oxide Treatment Monitored Using Stable ^{15}N Isotope Tracing ... 118
Acknowledgements ... 119
CReDIT statement ... 119
5.1. Abstract ... 120
5.2. Introduction ... 121
5.3. Methodology ... 124
5.3.1. Materials ... 124
5.3.2. Hydroponic experimental setup ... 125
5.3.3. Greenhouse gas fluxes and partitioning of N_2O emissions ... 125
5.3.4. Hydroponic medium nutrient analyses ... 126
5.3.5. Macro- and micronutrient and nanomaterial constituent elements analysis ... 127
5.3.6. X-ray Absorption Spectroscopy analysis of NMs bioaccumulation and transformation ... 127
5.3.7. Statistics ... 128
5.4. Results ... 129
5.5. Discussion ... 138
5.5.1. Impacts of TiO_2 PVP and $Co_{2.25}Fe_{0.75}O_4$ NMs on N-cycling are different but with similar outcomes ... 138
5.5.2. NM transformations and lettuce growth and quality ... 141
5.5.3. The rootzone has an important effect on nutrient accumulation and NM transformation ... 143
5.5.4. Conclusion ... 144
References ... 145
Chapter 6. Nanomaterial Interactions with Nitrogen Cycling Soil Microbial Communities and Ecotoxicological Implications for *Eisenia fetida* ... 149
Acknowledgements ... 150
CReDIT statement ... 150
6.1. Abstract ... 151
6.2. Introduction ... 152
6.3. Materials and Methods ... 155
6.3.1. Materials ... 155
6.3.2. Greenhouse study: experimental set up and sampling ... 155
6.3.3. Greenhouse gas flux sampling ... 157
6.3.4. Soil and leachate characterisation and nutrient analysis ... 157
6.3.5. Macro- and micronutrient and NM constituent element analysis ... 158
6.3.6. Extracellular microbial enzyme activity assays ... 158
6.3.7. Earthworm *Eisenia fetida* toxicology experiment ... 159
Eisenia fetida reproduction test and NM constituent element analysis ... 159
6.3.8. Statistics ... 160
6.4. Results and Discussion ... 161
6.4.1. Lettuce growth experiment comparing soil condition and NM amendments over time ... 162
6.4.2. *Eisenia fetida* dose response to zeolite application ... 172
6.5. Discussion ... 174
6.5.1. N_2O emissions are modulated by the interaction between NMs and soil microbes ... 174
6.5.2. NM and autoclaving impacts on extracellular activity and lettuce growth ... 176
6.5.3. ZSM-5-15 shows sublethal effects on *Eisenia fetida* at lower concentrations ... 178
6.5.4. Conclusion ... 179
References ... 180
Chapter 7. Urea-Doped Amorphous Calcium Phosphate Application During Lettuce Growth Decreases N Losses Compared to Conventional Fertilisation ... 183
Acknowledgements ... 184
CReDIT statement ... 184
7.1. Abstract ... 185

7.2. Introduction 186
7.3. Methods and Materials 189
7.3.1. U-ACP synthesis and characterisation 189
7.3.2. Soil characterisation 190
7.3.3. Lettuce pot experiment 190
7.3.4. Quantification of soil N gas fluxes 191
7.3.5. Leachate sampling and analysis 191
7.3.6. Soil sampling and pH testing 192
7.3.7. Soil microbial community analysis 192
7.3.8. Statistical analyses 193
7.4. Results 194
7.5. Discussion 200
7.5.1. Optimisation of the U-ACP 202
7.5.2. Conclusion 203
References 204
Chapter 8. General Discussion and Conclusion 207
References 212
Appendices 213

List of Figures

Figure 3.1. Wheat shoot (A) and root (B) length; germination rate at day 7 (C) and seedling vigour (D). Error bars reflect standard deviation. Stars are used to denote statistical significance ($p < 0.001$ ***). Note that the full set of 54 NMs effects can see seen in SI Table S3.1. 58

Figure 3.2. Lettuce shoot (A) and root (B) length; final germination rate (C) and seedling vigour (D). Error bars reflect standard deviation from the mean. Stars are used to denote statistical significance, p<0.05 *; p<0.01 **; p<0.001 ***. Note that the full set of 54 NMs effects can see seen in SI Table S3.1. 60

Figure 3.3. Wheat (A) biomass accumulation for NMs of interest. Lettuce (B) biomass estimation modelled from wheat-derived correlation for NMs of interest. Error bars depict standard error of the mean (SEM). 62

Figure 3.4. Seed exudate protein concentration of wheat (A) and lettuce (B) seeds after NM exposure. Error bars reflect SEM. 3.4B indicates that protein concentration results for $Ce_{0.75}Zr_{0.25}O_2$, CW and TiO_2 PVP were below the limit of detection. 69

Figure 3.5. PCA correlation biplots of wheat (A) and lettuce (B), looking at protein content of exudates, shoot and root length, total fresh biomass, final germination rate and seedling vigour (SV) in response to a subset of 8 NMs each. Lettuce biomass data used in (B) has been modelled using Equation 3.3 as derived from the relationship between total seedling length and biomass of wheat seedlings, detailed in the methods. PCA biplots of data from 54 NM seed priming experiments on wheat (C) and lettuce (D), where NMs have been grouped by NM type. 72

Figure 4.1. (A) Weekly time course of soil N_2O emissions across the five different treatments and control. Error bars indicate standard error from the mean (SEM) based on 4 replicates. (B) Weekly time course of soil CO_2 emissions across the five different treatments and control. Error bars indicate SEM of 4 replicates. (C) Soil NH_3 gas emissions in week 1 of the experiment. Error bars indicate SEM from 4 replicates. "***" is used to denote a statistically significant result as compared to the control of $p < 0.001$ 96

Figure 4.2. (A) NO_3^- concentration in leachate emissions recorded at weeks 1, 2, 4, and 8 across the six treatments. (B) PO_4^{3-} concentration in leachate across weeks 1, 2, 4 and 8. (C) NH_4^+ concentration in leachate recorded at weeks 1, 2, 4 and 8. Error bars reflect SEM based on 4 replicates. 98
Figure 4.3. (A) Lettuce aboveground biomass after destructive sampling at week 8. Error bars indicate standard deviation (n=4). Significantly different means compared to the control are denoted using '*' where $p<0.05$. (B) Malondialdehyde (MDA) concentration in lettuce shoot tissue including mean and SEM (n=4). Black dots signify outliers. (C) Relative concentration of macro- and micronutrient elements of interest in lettuce tissue compared across the six treatments (n=4), numerical element concentration data is available in SI Table S4.6. N content was determined via elemental analysis, all other nutrients were determined via ICP-OES. 100
Figure 4.4. (A) Ce L3-edge normalised XANES spectrum of $Ce_{0.75}Zr_{0.25}O_2$ treated soil samples and best linear combination fit of XANES profiles of Ce0.9Zr0.1O2 and CeO_2. (B) Zr K-edge normalised XANES spectrum of $Ce_{0.75}Zr_{0.25}O_2$ grown lettuce tissue and best linear combination fit of XANES profiles of pristine $Ce_{0.75}Zr_{0.25}O_2$ and $ZrCl_4$. 101
Figure 4.5. Summary image of proposed mechanisms of ZSM-5-15 and $Ce_{0.75}Zr_{0.25}O_2$ activity in agricultural soil and lettuce. 107
Figure 5.1. Summary of microbial pathways of N_2O production adapted from Rapson and Dacres (2013). 122
Figure 5.2. (A) Weekly time course of hydroponic N_2O emissions across the two NM treatments and control. Error bars indicate standard error from the mean (SEM) based on 3 replicates. (B) Proportion of denitrification derived N_2O emissions across the two NM treatments and control at weeks 1 and 3 of the experiment. (C) Weekly time course of hydroponic CO_2 emissions across the two NM treatments and control. Error bars indicate SEM of 3 replicates. (D) Weekly time course of hydroponic CH_4 emissions across the two NM treatments and control. Error bars indicate SEM of 3 replicates. 132
Figure 5.3. Lettuce fresh biomass for shoot (A) and root (B) tissues for each of the treatments (control or NM treated). Error bars indicate standard deviation from the mean. Statistical significance of $p < 0.05$ is denoted by '*' 134

Figure 5.4. Comparison of Co concentration for shoot (A) and root (B) tissues, and between the bulk hydroponic medium (C) and medium stored in the rockwool root zone (D). Error bars indicate standard deviation from the mean. 136

Figure 5.5. (A) Co K-edge XANES spectrum measured in hydroponic medium sample with 3000 mg L^{-1} added $Co_{2.25}Fe_{0.75}O_4$ NMs as compared to XANES spectra for $Co_{2.25}Fe_{0.75}O_4$, Co_3O_4 and $CoCO_3$. (B) Fe K-edge XANES spectrum measured on hydroponic media sample with 3000 mg L^{-1} added $Co_{2.25}Fe_{0.75}O_4$ NMs, compared to XANES profiles of pristine $Co_{2.25}Fe_{0.75}O_4$ NMs, Fe_2O_3 and Fe_3O_4. (C) Ti K-edge XANES spectrum measured on soil sample with added TiO_2 PVP NMs, compared to XANES profiles of pristine TiO_2 PVP and TiO_2 rutile..... 137

Figure 6.1. Concentration of ammonium (NH_4^+) in soil leachate from natural and autoclaved soil across the lettuce growth period of the experiment for different NM amendments (A and B); Concentration of nitrate (NO_3^-) in the leachate from natural and autoclaved soils across lettuce growth period of the experiment for different NM amendments (C and D). Error bars are standard error of the mean (SEM); n=3. 165

Figure 6.2. N_2O emissions from natural and autoclaved soils treated with different combinations of NM and NPK amendments over the lettuce growth period with gas sampling occurring at weeks 1, 2, 6 and 7 (A and B). CO_2 emissions from natural and autoclaved soils treated with different combinations of NMs and NPK amendment over the lettuce growth period with gas sampling occurring at weeks 1, 2, 6 and 7 (C and D). Error bars are standard error of the mean; n=3. 167

Figure 6.3. (A) Leucine aminopeptidase enzyme activity in autoclaved and natural soil under each of the amendments across the lettuce growth period. (B) Tyrosine aminopeptidase enzyme activity in autoclaved and natural soil under each of the amendments across the lettuce growth period. (C) NAG enzyme activity in autoclaved and natural soil under each of the amendments across the lettuce growth period. (D) Urease enzyme activity in autoclaved and natural soil under each of the amendments across the lettuce growth period. Error bars are standard error of the mean (SEM); n=3. 169

Figure 6.4. (A) Average fresh biomass of lettuce shoot tissue per amendment per soil condition at week 7 of the experiment. (B) Average lettuce height per amendment per soil condition at week 7 of the

experiment. Error bars are standard error of the mean (SEM). Statistically significant differences as compared to the negative control (Control) amendment are denoted with '*' ($p<0.05$)..... 171

Figure 6.5. (A) Average percentage change in *Eisenia fetida* worm body mass compared between day 0 and day 28. (B) Average proportion of survived versus dead worms after 28 days in each of the amendment soils. (C) Average number of juvenile worms produced per amendment as counted at day 56. (D) Average number of unhatched cocoons produced per amendment as counted at day 56. (E) Average Si concentration of each living worm at day 28. (F) Average Al concentration of each living worm at day 28..... 173

Figure 7.1. Outline of N compounds that occur throughout the nitrogen cycle, with NO_Y species highlighted in teal. NO_X refers to NO and NO_2. U-ACP may be acting to limit microbial access to N, reducing production of NO_Y. Sourced from Chadwick et al. (2023).. 187

Figure 7.2. TEM generated micrograph of pristine U-ACP nanocomposites. The pictured agglomerate was calculated to be 166 x 150 nm, with individual particles measuring ~2 nm. 194

Figure 7.3. (A) NO and (B) NO_Y-NO gas emissions from control, U-ACP and urea treated soils over a five-week period. Weeks 1 and 2 all had n = 5 per treatment, with weeks 3 to 5 having n = 4 for the control group, and n = 5 for the other two treatments. Error bars show the standard error of the mean (SEM).. 195

Figure 7.4. (A) Mean NH_4^+ concentration in soil leachate across the 6-week experiment from the three different soil treatments. (B) Mean NO_2^- concentration in soil leachate across the 6-week experiment from the three different soil treatments. (C) Mean NO_3^- concentration in soil leachate across the 6-week experiment from the three different soil treatments. Error bars show the standard error of the mean (SEM).. 197

Figure 7.5. (A) Abundance of betaproteobacteria AmoA relative to 16S rRNA bacterial gene abundance. (B) Abundance of periplasmic NxrB relative to 16S rRNA bacterial gene abundance. (C) Abundance of NirK clade I relative to 16S rRNA bacterial gene abundance. (D) Abundance of qNorB relative to 16S rRNA bacterial gene abundance. Outliers greater than 1.5 times the mean were excluded, as were 0 values. 198

Figure 7.6. (A) Mean lettuce height from weeks 2 to 5 for all three treatments. (B) Mean lettuce width from weeks 2 to 5 for all three treatments. (C) Mean lettuce leaf number from weeks 2 to 5 for all three treatments. Error bars indicate standard error. (D) Mean fresh biomass of lettuce week 5 for all three treatments. Black dots indicate outliers. 199

List of Tables

Table 3.1. Characterisation of the 38 NMs selected based on the seed priming results in terms of their hydrodynamic diameters and surface zeta potentials both pre- and post-exposure to either lettuce (*Lactuca sativa*) or wheat (*Triticum aestivum*) seeds. Orange shading indicates an increase/more negative value as compared to the pre-exposure characterisation and blue shading indicates a decrease/less negative. 64

Table 4.1. Nanomaterial characterisation using dynamic light scattering (DLS) before exposure to soil. Data are means ± standard deviation. 92

Table 4.2. Soil properties in the six different soil treatments after the eight-week growth period. Data are means ± standard error. Absent data is due to values being below the limit of detection of the specific method. 94

Table 5.1. NM characterisation summary for pre-exposure NMs and NMs in hydroponic medium at week 6. Data are for 25 mg L^{-1} NM dispersions in either deionised water (pre-exposure) or in hydroponic medium (week 6). Data presented are means ± standard deviation. 129

Table 5.2. Hydroponic medium characterisation from week 1 and week 6 for the three treatments. Rockwool hydroponic medium was only tested at week 6. Data presented are means ± standard deviation. 130

Table 6.1. Experimental amendments to study NM abiotic and biotic effects on lettuce growth, N cycling and extracellular enzyme activity. 156

Table 6.2. Summary of extracellular microbial enzymes of interest with their respective roles in N-cycling and substrates. 159

Table 6.3. NM characterisation by DLS before exposure to soil. Data are means ± standard deviation. 161

Table 6.4. Soil properties across the five different soil amendments in both the natural and autoclaved soil conditions before and after the seven-week growth period. Data are means ± standard error of the

mean (SEM). Absent data is due to values being below the limit of detection of the specific method. 163

Table 7.1. Soil pH of pre-conditioned (week 0) soil as compared to soil in week 5 of the experiment under each of the three treatments. 194

List of Abbreviations

BCA	Bicinchoninic acid
DLS	Dynamic light scattering
EA	Elemental Analysis
EC	Electrical conductivity
ECD	Electron capture detector
EEA	Extracellular enzyme activity
FID	Flame ionisation detector
GC	Gas Chromatography
GHG	Greenhouse gas
ICP-OES	Inductively coupled plasma-optical emission spectroscopy
LAP	Leucine aminopeptidase
LCF	Linear combination fitting
MDA	Malondialdehyde
MOF	Metal-organic framework
NAG	β-1,4-N-acetylglucosaminidase
NDVI	Normalised difference vegetation index
NM	Nanomaterial
NO_X	Nitrogen oxides ($NO + NO_2$)
NO_Y	Reactive nitrogen compounds (NO_X + HONO + HNO_3 + organic and particulate nitrates)
NPK	Nitrogen, Phosphorus, Potassium
Nr	Reactive nitrogen
OECD	Organisation for Economic Co-operation and Development
PVP	Polyvinylpyrrolidone
qPCR	Quantitative polymerase chain reaction
ROS	Reactive oxygen species
SEM	Scanning electron microscope
TAP	Tyrosine aminopeptidase
TEM	Transmission electron microscope
TI	Translocation factor
TN	Total nitrogen
TOC	Total organic carbon
U-ACP	Urea-doped amorphous calcium phosphate
WHC	Water holding capacity
XANES	X-ray near-edge absorption spectroscopy
XAS	X-ray absorption spectroscopy

Chapter 1. Aims and Hypotheses

The initial and overarching aim of this body of work was to optimise the choice of engineered nanomaterials (NMs) to be used as nanofertiliser as a remedy to over-fertilisation and losses of reactive nitrogen (Nr) pollution into the atmosphere and waterways. This aim for sustainable nanofertiliser development also required that certain crop qualities, like yield or nutritive quality, were maintained, or even enhanced. This aim led to the first experiment (Chapter 3), a large screening process whereby 54 NMs, including metal oxides, metal organic frameworks, biochar-based hydroxyapatites, nanopolymers and zeolites were tested in terms of their impacts on seeds. The screening process was thus a seed priming experiment on both lettuce (*Lactuca sativa*) and wheat (*Triticum aestivum*) which aimed to identify NMs for further study and help in identifying the NM characteristics responsible for positive and negative impacts on seed germination rate, seedling growth, biomass and vigour. From this initial screening experiment a subset of NMs were chosen for further study in growing lettuce in soil or hydroponically, presented in Chapters 4 and 5, respectively. In these experiments we aimed to improve crop yield and quality and interrogate the scale and form of Nr losses. We hypothesised that there would be differences between negative controls and NM grown crops in both growing systems for lettuce yield and nutritive quality, and Nr losses; with these resulting differences being a direct consequence of the specific characteristics, or combinations of characteristics, that the NMs may possess. Specifically, we hypothesised that NMs are able to reduce N volatilisation from soil and hydroponic medium, while improving crop yield and quality. In these experiments we also looked at understanding the microbial source of these N_2O emissions, which was done through the use of an adapted ^{15}N stable isotope experiment for the hydroponically grown lettuce. It was expected that Nr losses would be minimised through the action of NMs on soil microbes, with direct effects predicted on microbial community makeup or denitrifying enzyme activity.

Just as it was hypothesised that NMs will have an impact on soil microbes, the impact of the soil microbial community on the NMs was also explored. We therefore developed an experiment (Chapter 6) to determine how the presence/absence of soil microbes modulated soil Nr losses with NM

additions. We hypothesised that soil microbes may play an integral role in NM activity, acting with the NMs to alter the flux of Nr emissions. As soil is the main sink for NMs, especially in the case of purposeful NM additions, as with nanofertilisers, it is important to see how the NMs interact with other compartments of the agroecosystem. We therefore chose to explore how NM additions impact soil megafauna, in particular the worm *Eisenia fetida*, a commonly chosen model organism for terrestrial ecotoxicology studies. The NMs were expected to have a dose dependent impact on the worms, with biologically relevant concentrations chosen, as used throughout this body of work.

Predominantly, we used metal oxide and zeolite nanomaterials with co-application of a reduced dose of nitrogen, phosphorus and potassium (NPK) fertiliser. The final aim of the work was to explore how having a source of N as part of the nanofertiliser structure was able to alter NM efficacy. This was achieved looking at the hydroxyapatite urea-doped amorphous calcium phosphate (U-ACP) in Chapter 7. We anticipated that having urea as part of the nanofertiliser structure may aid in direct delivery and reduce Nr losses. This experiment also explored other facets of Nr emissions, looking at NO_Y and NO_X emissions, two compounds that contribute to poor respiratory health in humans. We expected that U-ACP addition to lettuce growing soils would alter NO_Y production, likely reducing it due to the structure of the compound limiting N losses.

Chapter 2. Introduction – Use of Nanotechnology to Increase Nutrient Use Efficiency, Enhance Crop Nutrition, and Reduce Agricultural Pollution

This chapter was published in "Nano-Enabled Sustainable and Precision Agriculture" by Academic Press (2023).

Acknowledgements

This work was supported by the Biotechnology and Biological Sciences Research Council (BBSRC) and University of Birmingham funded Midlands Integrative Biosciences Training Partnership (MIBTP) grant number BB/T00746X/1.

CReDIT statement

Jessica Chadwick: Writing – Original Draft, Visualisation. Peng Zhang: Supervision, Writing – Review and Editing, Funding acquisition. Sami Ullah: Supervision, Writing – Review and Editing, Funding acquisition. Iseult Lynch: Supervision, Writing – Review and Editing, Funding acquisition.

2

Use of nanotechnology to increase nutrient use efficiency, enhance crop nutrition, and reduce agrochemical pollution

J.J. Chadwick[1], *Peng Zhang*[2], *S. Ullah*[1] *and Iseult Lynch*[1]
[1]School of Geography, Earth and Environmental Sciences, University of Birmingham, Edgbaston, Birmingham, United Kingdom [2]Department of Environmental Science and Engineering, University of Science and Technology of China, Hefei, China

This chapter will introduce broadly how nanotechnology can improve the use of natural resources (nutrients, water, light) by plants and how this can enhance the overall nutritional value of crops.

2.1 Introduction

Crops, as with all plants, require a specific range of natural resources to grow. Light is essential for photosynthesis and is easily accessible for plants from the sun. Water is secured via roots from soils and transported into leaves where photosynthesis occurs: a process in which water and CO_2 from the air are eventually converted to glucose in the presence of chlorophyll (plant's green pigment molecule). Nutrients (e.g., nitrogen, phosphorus, and potassium) are obtained from the soil as part of the natural nutrient cycling process (through the decay of plant and animal matter) and are essential for plant growth and development. Limiting factors such as low availability of key nutrients put a damper on potential growth and reduce the nutritional value of the crop. The absence of key nutrients, which is increasingly occurring as a result of industrial agriculture and intensification of farming, leads to poor quality soils that are unable to supply the required nutrients, causing deficiencies in the plant, stunting their growth and, when sufficiently severe, triggering plant death. To resolve this, fertilizers are extensively used to supplement the soil's nutritive value and ensure consistent crop growth and quality. Crop quality includes a range of different aspects of a food crop, including nutritional value, which are

Nano-enabled Sustainable and Precision Agriculture. DOI: https://doi.org/10.1016/B978-0-323-91233-4.00010-7
© 2023 Elsevier Inc. All rights reserved.

important to consumers. This chapter will discuss nutrient management and the history of fertilizer, agricultural pollution due to excessive fertilizer use, and potential nanotechnology solutions to improve nutrient use efficiency (NUE) and thus enhance productivity while reducing the negative environmental impacts of agriculture.

2.2 Nutrient management and the development of fertilizer

Plants growing in the wild do not require nutrient inputs in the same way as crops do. Nutrient usage is a cycle; plant growth utilizes nutrients present in the soil, which are then stored in the plant, and upon plant death, these nutrients are returned to the soil for continuing usage by future plants. Agriculture disrupts this cycle, by growing plants and then removing them, thus also removing the nutrients that the crop has absorbed from the soil. The process of crop and associated nutrient removal is then repeated many times over successive seasons and years to continue food production for human and animal consumption. Continual growth and removal of crops result in a soil depleted of nutrients, which is less able to sustain further crop growth. Nutritionally depleted soils require new nutrient inputs to allow future crops to have productive growth, create the desired yields, and ensure that yield is of suitable quality. Yield quality can refer to size, mass, nutritive content, or esthetics of the edible part of a plant. In this chapter the focus will be on quantity (yield), with some aspects of nutritive content of yields produced also considered.

Nitrogen (N), phosphorus (P), and potassium (K) are the three essential mineral elements required for plant growth and development. Nitrogen is an essential element in amino acids, which are the building blocks of proteins. Rubisco is the most prevalent enzyme in plant leaves with an estimated 5 kg of rubisco for every person on Earth.[1] Rubisco is an essential enzyme that catalyzes the reduction of CO_2 into glucose, so N supply is directly linked to photosynthetic activity. Phosphorus is used in energy transfer as ADP and ATP (adenosine di- and triphosphate, respectively) and is an essential component of nucleotides, as well as being core to photosynthesis and aerobic respiration. Potassium is necessary for nutrient and water transport in plants as part of active transport processes via ion channels. Each of these nutrients cycle through organic and inorganic forms, with different oxidation states, as it becomes (bio)available or unavailable to plants through mineralization (oxidative breakdown in soil), immobilization by soil microbes, adsorption to soil particles, or loss to the environment. Nitrogen gas (N_2) is the primary component of the Earth's atmosphere, but this inorganic, inert gas is inaccessible to plants for use. Instead, it must be transformed into, like ammonia (NH_3), for plants to be able to absorb it. This process and the rest of the forms and processes that N undergoes

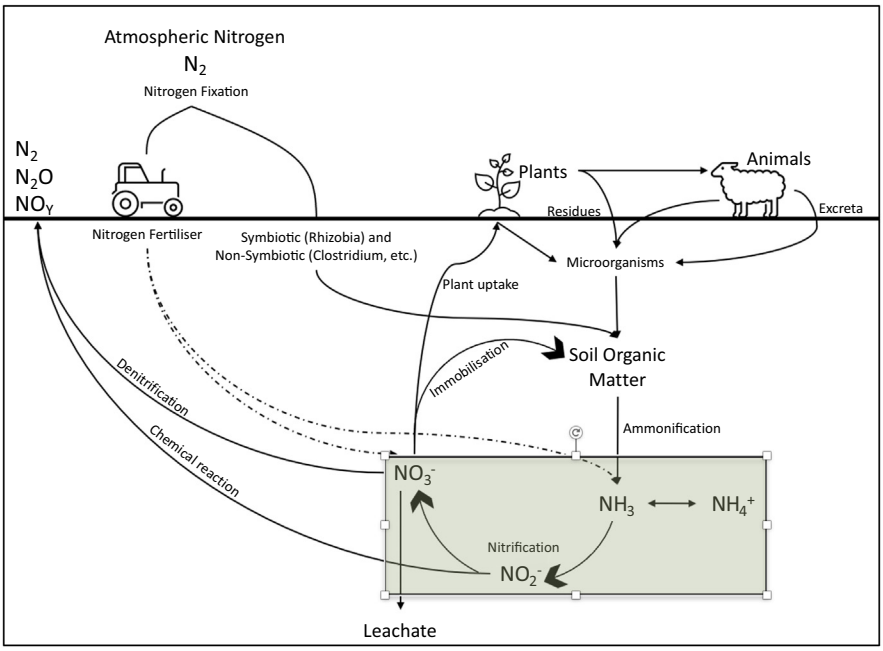


Figure 2.1 Diagram of the nitrogen cycle, including the major forms of N and the processes that convert N from one form to another. The four N species in the green box are bioavailable. *Source: Adapted from Myrold, D. D. Nitrogen Cycle. In* Environmental Geology*; Encyclopedia of Earth Science; Springer Netherlands: Dordrecht, 1999; pp 435–436. https://doi.org/10.1007/1-4020-4494-1_234.*

throughout the nitrogen cycle are illustrated in Fig. 2.1. Soil bacteria are instrumental in the N cycle and convert N into different species. Nitrification is the oxidation of reduced N forms into nitrite and then nitrate, making them accessible to plants. Denitrification is the reduction of nitrate and nitrite into gaseous forms of N, like N2. Incomplete denitrification can result in polluting N species formation.

Nutrient input can be achieved through a range of methods. Nitrogen can be gained using crop rotation, whereby leguminous plants, like peas or clover, are grown in alternative seasons to other, more nitrogen-demanding crops, for example, corn. Leguminous plants utilize their symbiotic association with Rhizobium bacteria to "fix" N from the air and convert it into an accessible form, typically NH_3, for plants to translocate and use. Alternatively, N can be added to the soil in the form of manure, crop residues, or as man-made fertilizer. Symbiotic partnerships between crop plants and mycorrhizal fungal partners can aid plants in gaining access to P and K. There is no soil microbial fixation process for P and K, which are naturally added through mineral weathering and must be manually added where soils are depleted of them. P and K are typically added as compound fertilizer, which contains differing ratios of N,

P, and K. The N component must be fixed into a plant available form, achieved through the Haber–Bosch process (or Haber process), an energy-intensive artificial N fixation process, created in the early 20th century. Nitrogen and hydrogen gases are combined under high temperatures and pressures with an iron-based catalyst to form ammonia, as per the equation given next.

$$N_2 + 3H_2 \rightarrow 2NH_3$$

This is an energetically expensive process and is currently dependent on fossil fuels for ammonia generation. The ammonia produced using the Haber–Bosch process can then be used in the Ostwald process, which reacts ammonia with nitric acid to form ammonium nitrate. The resulting ammonium nitrate was one of the most commonly used fertilizers globally due to its N supply in two different forms (ammonium and nitrate ions), but its popularity has waned over time due to its high water solubility (1.183 kg/L), which results in loss to the environment through runoff, toxic effects on animals, and its potential for use in explosives.[2] Insufficient supply of N to crops is of major concern to farmers and the problem of insufficient N for effective crop growth is exacerbated by how easily N is lost from soils into water or is converted into gaseous forms by soil microbes, in a process called denitrification (NO, N_2O, and N_2 gases). Also, ammonia gets volatilized from soil into air, thus polluting air whilst reducing the amount of bioavailable N to plants. As a result of this, N fertilizer inputs have to be greater than the amount directly required by plants to maximize the amount of N actually taken up by the plants. This is turn results in more N pollution to water and air (Table 2.1).

Phosphorus, unlike nitrogen, is not a renewable resource and has no substantial atmospheric component from which to draw. Instead, P must be mined from rock phosphate, with phosphate reserves expected to run out in the next 50–100 years.[3] An 85% of the demand for mined phosphate is for food production, with UK-grown cereals on average requiring 27 kg/ha in 2021.[4] There are large quantities of P present in soils and sediments; however, these are insoluble and not bioavailable, making them inaccessible to plants. The amount of P supplied atmospherically and from the soil is insufficient for nutritionally demanding crops, which is why P fertilizer is required. Once applied to soils, P is less subject

Table 2.1 N species, their roles in the N cycle, and their environmental effects.

Gas	Role	Environmental effects
NH_3	Used as fertilizer but can become airborne from soil surfaces	Impacts on plant and habitat biodiversity. Can form particulate matter with other gases, causing damage to heart and lung health in humans
N_2O	Produced by soil bacteria in nitrification and denitrification	Destroys ozone in the ozone layer leading to global warming
NO_x (NO and NO_2)	Produced by soil bacteria in nitrification and denitrification	Causes global warming and acid rain, impacting soils and waterways. Some forms can be damaging to human health and cause lung problems

to runoff and leaching through to groundwater than N, due to the high fixation capacity of mineral soils, that is, soils containing high quantities of minerals such as clay, sand, and silt and low in organic matter precipitate phosphorus, due to Ca, Al, or Fe content.[5] However, overapplication of P fertilizer can lead to leaching into groundwater over decades, and nitrate leaching can also promote P leaching in groundwater-fed wetlands.[6] Up to 40% of land is affected by P pollution,[7] making it essential to limit its use, and thus allow crops to use up legacy phosphorus and limit its long-term ability to leach through soils. As with N, P losses from soil mean that more P must be input to agricultural soils to counteract the losses and ensure that growing crops have a consistent supply of P as they are growing.

Potassium (K) is the last component of NPK fertilizer (the N, P and K indicate the three components of the fertilizer) and while there are large amounts of K present in soil, but it is largely inaccessible to plants. Due to this inaccessibility, water-soluble forms of potassium are added by farmers to support yield, maintain crop quality, and aid in plant stress resistance.[8] Soils that are particularly low in K are typically sandy, acidic, or waterlogged.[9] If K is not applied to soils, this can lead to a reduction in soil quality over time.

K can also become fixed in the soil, becoming adsorbed onto soil minerals quickly, and is released slowly due to strong binding between clay minerals and K.[10] K is able to transfer relatively easily between more readily and less readily available forms in the soil, forming part of the soil solution after its addition but becoming less accessible as $K+$ ions are bound between soil's silicate layers and immobilized. K is typically added to soils based on the N requirements of the crop, leading to excesses or shortages of K. Due to K's ability to adsorb onto clay minerals, there is minimal leaching and low mobility; however, this increases in lighter textured soils like sandy or loamy soils. K losses are primarily through surface runoff after application in nonoptimum conditions, for example, due to waterlogged soils or cracked soils. Maintaining soil reserves of K is essential but additions of K have no direct effect on crop yields, making soil's K contents a less focused upon aspect. To maintain reserves, K typically does not need isolated additions and is just added as part of NPK fertilizer as defined by the crop's need for N and P. The buffering capacity, defined as the ability of a soil to resist changes, for example, in pH, depends based on its soil type and makes maintaining K reserves more of a challenge in soils with less than 5% clay contents.

Where there is a lower exchange capacity, K must be added in smaller amounts more regularly or will be released from soils faster.[11] As seen in Fig. 2.2, N fertilizer is hugely overapplied in many nations globally, with no positive impact on yield and instead causing greater environmental pollution.

The risk of losses to water and air of the different components of N fertilizer has meant that overfertilization is common on commercial farms, with global increases in fertilizer usage over the last 60 years, as seen in Fig. 2.3. Overfertilization has significant effects, polluting the air and water and having a

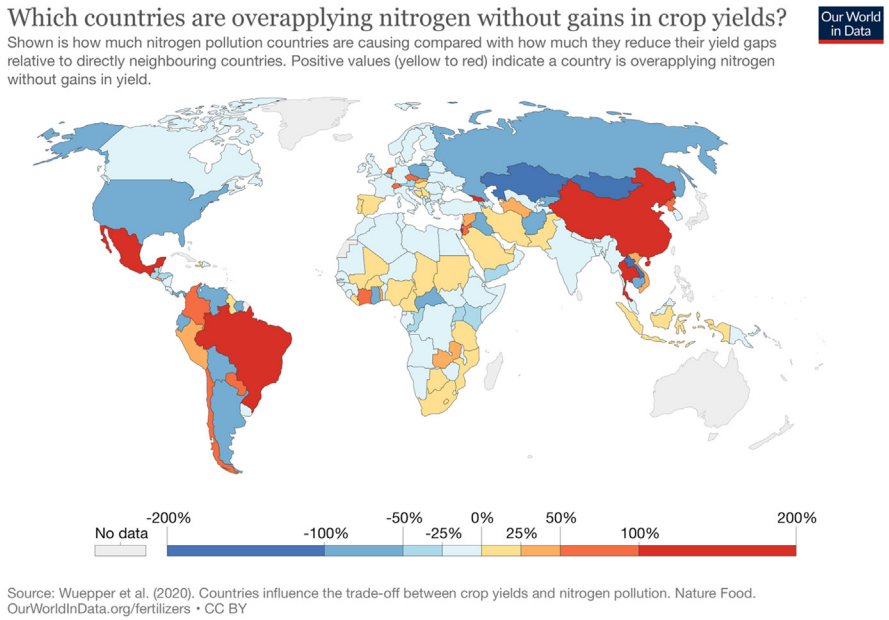
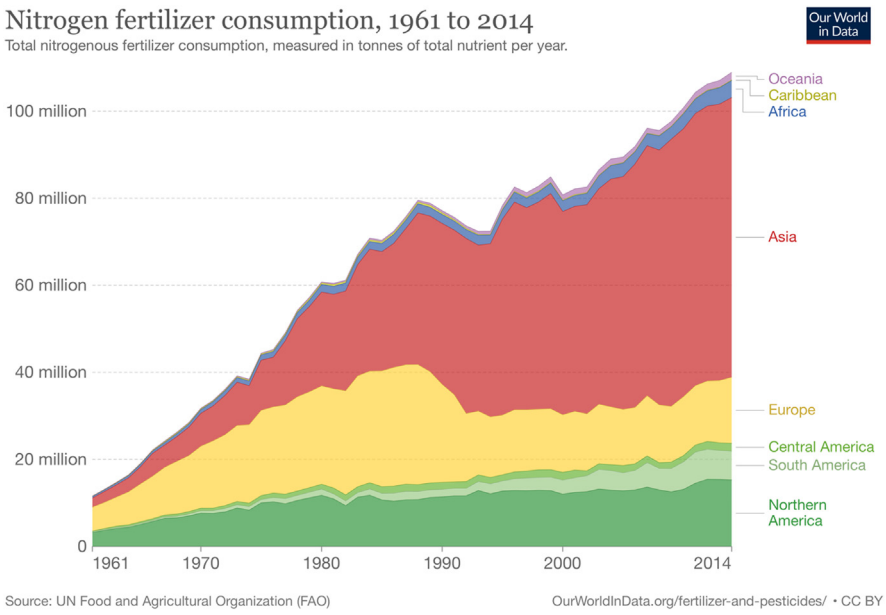


Figure 2.2 Proportion of N pollution a nation releases compared to the impact the increase in N fertilizer has on reducing yield gaps relative to their neighboring countries. Overapplication of fertilizer with no gain in yield is reflected in the positive values (yellow to red spectrum).[12] *Source: From Wuepper, D.; Borrelli, P.; Finger, R. Countries and the Global Rate of Soil Erosion.* Nat. Sustain. *2020,* 3 *(1), 51–55. https://doi.org/10.1038/s41893-019-0438-4.*

Figure 2.3 Nitrogen fertilizer use has increased globally, as shown in this graph of fertilizer usage from 1961 to 2014. Total nitrogen fertilizer consumption is measured in tons per year. *Source: From Hannah Ritchie, Max Roser and Pablo Rosado (2022) - "Fertilizers". Published online at OurWorldInData.org. Retrieved from: 'https://ourworldindata.org/fertilizers' [Online Resource]*



compounding effect on soil quality also. Over the last century, fertilizer use has increased massively, with the advent of synthetic N fixation estimated to support an additional 3 billion people globally, who without synthetic nitrogen fertilizer may never have been born.[13] With the affordability of fertilizer and the rise of industrial arable farming, fertilizer usage has spread and increased massively over the last century, particularly in the tropics and global south,[14] with fertilizer demand predicted to continue increasing over the coming century.[15] This allows yields to be maintained by farmers but does not tackle the crux of the issue—low NUE. Even with massive increases in the amount of fertilizer applied, only roughly 50% of the nutrients they contain are adsorbed by plants.[16] Effective nutrient management requires improvements in the efficiency of nutrient transfer to plants, with awareness of how different crops and soils leach nutrients, how timing and rate of fertilizer application affects likelihood of pollution, and how the type of fertilizer used also impacts on nutrient loss and utilization. In addition to these, improving the retention of N and P in soils is also important and can be achieved through better management or alternate sources of fertilization. For example, avoiding the use of urea as fertilizer, which is more susceptible to volatilization into NH_3, or timing fertilizer application to avoid heavy rains to prevent excessive leaching.

2.3 Nanotechnology: how it works and potential uses within agriculture

What is nanotechnology?

Nanotechnology refers to the manipulation and use of matter on an atomic, molecular, and supramolecular scale for industrial purposes, including in medicine and agriculture, using materials and particles whose dimensions occur on the nanoscale, typically 1−1000 nm. To put this in perspective, a nanometer is a million times smaller than an ant's leg! Popular examples include graphene, which won the 2010 Nobel Prize for Physics, and quantum dots, which have uses in computer screens and solar panels. Nanomaterials (NMs) have a range of different features which make them useful for this wide range of applications, as well as being of similar scales to biological machinery such as cellular receptors. They have been used in batteries, electronics, and industrial purposes, as well as in biological contexts, like in drug delivery or for controlled release of pesticides.[17,18] The main feature of NMs that enable them to be used in this many applications is their nano-size, making them differ from their bulk counterparts. Nanoscale materials are subject to quantum effects (depending on their composition) and have incredibly high surface-area-to-volume ratios. It is the very large surface area that confers high reactivity to NMs and increases their efficiency in different contexts, including as catalysts, sensors, for environmental remediation and to achieve high loading of cargoes such as fertilizers or pesticides.

Their large surface area, and porosity as in the case of some NMs like zeolites, permit high loading of N or urea and can allow key species to bind tightly to their surface, either in a specific or targeted manner (e.g., for pollution remediation) or through nonspecific interactions and so-called corona formation.[19,20] Utilization of the surface area and selectivity of binding could be applied to enhance NUE by using NMs to bind desirable N forms in the soil, allowing them to remain present for longer and preventing those nutrients from being subject to leaching or loss to air. The redox activity of NMs means that they are able to support electron transfer and convert N into different forms, up and down the redox ladder. The redox ladder refers to how energetically favorable a specific redox reaction is, with more energetically favorable reactions at the top of the ladder and progressively less energetically favorable reactions going down the rungs.

Volatilized and denitrified N species that are global warming gases or dangerous to human health are hypothesized to potentially be bound by NMs and, through electron transfer, convert the gases into different forms. Similarly, the catalytic activity of NMs could be utilized to prevent air pollution from the atmosphere, for example, nanoscale iron oxide particles are able to adsorb SO_2 from the atmosphere.[21] The nanomaterial could be developed to bind other trace soil elements that could aid the existing soil biodiversity to prevent nutrient pollution. An example of this could be using a copper-based nanomaterial to improve nitrous oxide reductase enzyme expression by soil bacteria which is a key enzyme in the reduction of N_2O to N_2 gas, rendering it nonharmful.[22]

Nanotechnology has been proposed as a solution to a range of different problems in agriculture, including pest control through enhanced targeted delivery, reduced disease, and improving the efficiency of nutrient usage. As mentioned previously, conventional fertilizers are typically very inefficient with up to 60% lost as leachate or through volatilization.[23] More efficient and environmental friendly fertilizers are required to increase food production in line with the globally increasing population, efforts to reduce food insecurity, and global sustainability goals. These combined potential positives of nanotechnology, of reducing air and water pollution, improving global crop yields, and decreasing the time and cost intensiveness of fertilizer treatment, make them a promising and sustainable alternative to commercial fertilizers. This work ties into two of the UN's global sustainable development goals (SDGs), zero hunger, and life on land. The SDGs are a worldwide blueprint to focus on sustainable development and reflect the intersectionality between many of the world's problems. The FAO (Food and Agriculture Organization of the United Nations) recognizes in its 2013 report the massive potential there is for using NMs in agriculture; however, a complete assessment of the long-term implications of their use on soil health and the impacts on wider food webs and in humans is required. Currently, most toxicity information on NMs is based off their bulk counterparts; however, nano versions of these materials can have very different

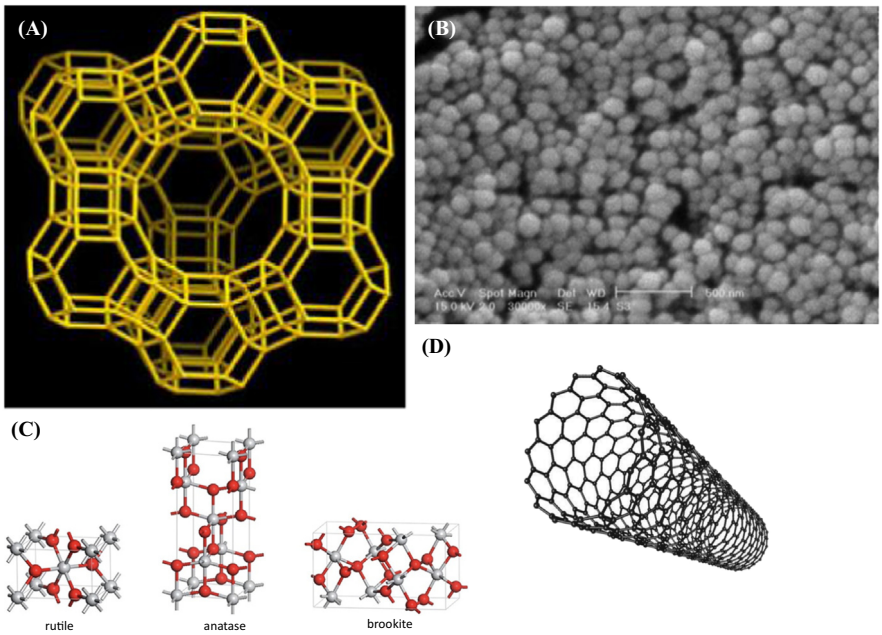


Figure 2.4 Nanomaterial structures can range widely but all are between 1 and 1000 nm (although many reports and regulatory definitions cap the size at 100 nm). (A) FAU-type zeolite, (B) chitosan nanoparticles, (C) three forms of TiO_2; rutile, anatase, and brookite, (D) carbon nanotube.[25,26] *FAU*, Faujasite. *Source: From Saremi, S. Tehran University of Medical Sciences via Open-i, US National Library of Medicine; Baranowska-Wójcik, E.; Szwajgier, D.; Oleszczuk, P.; Winiarska-Mieczan, A. Effects of Titanium Dioxide Nanoparticles Exposure on Human Health—A Review.* Biol Trace Elem. Res. *2020,* 193 *(1), 118–129. https://doi.org/10.1007/s12011-019-01706-6 and based on Samat, S. F. A.; Sarah, M. S. P.; Idros, M. F. M. In* High Optical Transmittance of Nanostructured TiO_2 Thin Film Using Dip Coating Method*, In 2016 7th IEEE Control and System Graduate Research Colloquium, pp 52–56; IEEE, 2016. https://doi.org/10.1109/ICSGRC.2016.7813300. AJC/flickr/CC BY-SA 2.0.*

effects, potentially becoming far less, or far more, potent. This is a by-product of the reactivity and accessibility of these nano-forms; NMs are more reactive due to their high surface areas and their size means they can access intracellular compartments that bulk materials cannot. The risks that NMs pose in these locations are greater, but if science is able to capitalize on the benefits, it could outweigh the risks.

NMs can be synthesized physically, chemically, and biologically, and these methods can either be bottom-up or top-down. Top-down synthesis involves processing bulk materials into their nanoscale counterparts, for example, physical or biological synthesis, while bottom-up synthesis is the formation of the NMs from the atomic level with self-assembly leading to the nanostructure, for example, chemical synthesis. NMs can be applied to plants through the leaves (foliar) or via the roots, and the form of application, for example, with or without nutrients, the shape of the nanomaterial, can differ widely. Examples of

different nanomaterial shapes and conformations can be seen in Fig. 2.4, the shape of a nanomaterial can have significant effects on its activity.[24] NMs used to carry fertilizers could be used to aid in controlled release of nutrients, reducing losses to the environment and enhancing NUE.

2.4 The problem of agricultural pollution and methods to minimize it

2.4.1 Soil pollution

Soil's productive capacity has been reduced over time due to soil erosion, cultivation, and atmospheric pollution, among other causes. Soil quality refers to the physical, chemical, and biological properties of soil and can be defined as "the ability of the soil to sustain the productivity, diversity, and environmental services of terrestrial ecosystems."[27] Soil pollution is defined as the degradation of soil quality, with negative effects on soil's ability to sequester carbon, overall structure, and ability to cycle nutrients, like phosphorus or nitrogen. Soil pollutants, like fertilizers, pesticides, and industrial waste, all impact on soil's physical, chemical, and biological properties. Additionally, soil pollution can have major impacts on soil structure and affect key ecosystem engineers, like earthworms, that create air gaps in the soil.

Soil structure impacts on crop growth and also has knock-on effects on water pollution through runoff and leachate, discussed in depth later in this chapter. Agricultural soil requires pores for root growth, water, and air movement throughout, with a 2:1:1 solid, air, and water ratio being optimal for plant growth. When soil is compacted through poor land management, crop productivity decreases as does biodiversity. This compaction also triggers a greater amount of surface runoff, leading to flooding and soil erosion; these processes also allow fertilizers to be washed into waterways faster leading to water pollution. There is also evidence that land management can affect the ability of soils to store organic carbon. Agricultural soils are one of the world's largest carbon sinks, and with decreases in soil quality that carbon has been depleted. Using agricultural soils for carbon sequestration is a potential method to help combat climate change.

There is potential for NMs to modulate soil biodiversity, altering both the diversity and abundance of different bacterial populations, in turn having knock-on effects on soil health and nutrient cycling.[28] NMs could even be used to aid in nitrogen fixation, as is the case with S-Fe_2O_3, which enhanced nodule development and delayed nodule senescence after foliar application to soybean.[29] Soil remediation using NMs is another method that NMs could be used to improve soil quality and prevent further degradation.[30] This could be achieved through using their surface area to bind and immobilize pollutants, aid pollutant uptake by plants, or to cause those bound pollutants to degrade, overall limiting their mobility through soil and therefore reducing their toxicological effects.[31–33]

There is limited viable agricultural land and while sustainable intensification of our existing agricultural land is important, rescuing land that is otherwise unusable is also an increasingly important option. Soil contaminants include heavy metals that can severely stress plants and massively inhibit growth, not to mention potential toxic effects from eating the edible parts of the crops grown here.

2.4.2 Water pollution

Due to the high release rate of conventional fertilizers, soils may become flooded with nutrients upon treatment. When the nutrients are unable to be absorbed by the crops due to exceeding the absorption rate of the plants, they are washed through the soil in a process called leaching. Leaching occurs as soil particles, phosphate, and nitrate are all negatively charged leading to repulsive forces and preventing adhesion of the nutrients onto the soil particles such that they remain in the water phase and remain mobile. High levels of fertilizer application cause significant amounts of fertilizer to be lost as leachate. Other factors impacting leaching include soil drainage, rainfall, and crop uptake. High levels of nutrient leaching lead to groundwater pollution, where the groundwater is made unfit for human consumption and can affect local wildlife that also relies on the water for drinking.

Eutrophication is the process where a body of water develops high levels of algal growth. This can occur naturally; however, human activity accelerates algal growth by runoff of nitrate and phosphate fertilizers from agriculture, sewage disposal, and industrial activity.[34] Total nitrogen loading from soil to water includes both organic and inorganic forms of N. This includes not just the N-based ions present in the soil but also the proteins and amino acids that can be oxidized into bioavailable forms and contribute to eutrophication. The effect of these algal blooms is that the water becomes hypoxic, where the oxygen content of the water is decreased to suboptimal levels, or even anoxic, when the water is completely lacking in oxygen. Reducing the water oxygen levels so severely impacts on the ability of organisms living in the water to survive, killing plants, fish, and other water-dwelling creatures. Once the water is anoxic, this forces the bacteria to switch to anaerobic respiration and utilize other chemicals down the redox ladder, for example, nitrate, iron, or methane, to maintain their energy source. This is less energetically productive for the bacteria and also has the effect of producing other chemical species, like sulfides and methane, which are themselves pollutants. Other negative effects as a result of eutrophication include blue-green algae growth; these blooms occur mostly in summer and are a form of cyanobacteria. They produce cyanotoxins that can affect the nervous system, liver function, and skin. Cyanotoxins can be detrimental to aquatic organisms they share the water with and can be lethal to other organisms in direct contact with the algal bloom, including birds, mammals, and other plants. This has particularly negative effects if the water is relied upon for human consumption,

causing methemoglobinemia, known commonly as Blue Baby syndrome. Additionally, there are links between one cyanotoxin produced by these blooms and Alzheimer's.[35] Current solutions to water pollution aim to minimize the effects of runoff by using NMs to trap bioavailable forms of N in the soil thus preventing runoff and subsequent eutrophication. Zhao et al.[22] have shown the effectiveness of using semiconducting NMs to catalyze the oxidation of organic pollutants, like nitrates, as a wastewater treatment method. The organic N undergoes mineralization, where organic molecules are converted into inorganic ones. Applying this technique to agriculture could prove an effective method to minimize runoff at source and could also potentially allow the reuse of the recovered N-fertilizers saving money for farmers.

These primary concerns with nutrient runoff into water bodies concern freshwater, eutrophication in lakes, and bodies of drinking water. However, nutrient runoff can also have major impacts on saltwater and create ocean dead zones due to algal blooms. This has major long-term impacts on delicate oceanic ecosystems and must also be rectified.

2.4.3 Air pollution

Phosphorus and potassium are not found in high proportions in the atmosphere, but there are a range of forms of nitrogen that are naturally present or that arise from human activities, including agriculture. After application of fertilizer to soil, soil microbes such as *Pseudomonas* act to either volatilize the ammonium ions or to denitrify the excess N present. This volatilization and denitrification, as seen in Fig. 2.1, release N-containing compounds into the atmosphere. Denitrification, when completed, releases nitrogen gas (N_2) into the atmosphere, which is an inert gas that comprises 78% of Earth's atmosphere. Incomplete denitrification can cause a number of different N-containing gases to be released, like NO, NO_2, or N_2O (Fig. 2.5).

Once produced, these gases are retained in the atmosphere and can go on to react with other atmospheric compounds. The largest proportion of these volatilized gases is nitrous oxide (N_2O), which is a major greenhouse gas, causing ozone depletion. In the late 20th century, chlorofluorocarbons, commonly known as

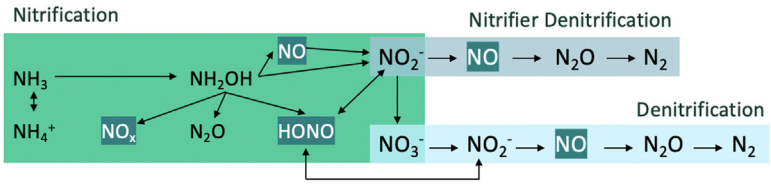


Figure 2.5 Outline of N compounds that occur throughout the nitrogen cycle, with NO_Y species (i.e., reactive nitrogen oxides in which the oxidation state of the N atom is +2 or greater) highlighted in teal. NO_X refers to NO and NO_2.

CFCs, were in common usage and could be found in fridges and deodorants. These CFCs were found to be ozone depleting and banned, with N_2O being the main ozone-depleting substance produced today. Solving the problem of N-based air pollution has been discussed using the hole-in-the-pipe model, first theorized by Firestone and Davidson.[36] One particularly damaging result from N air pollution is acid rain. Acid rain is formed when NO_X reacts with water and oxygen particles in the troposphere, the lowest layer of the atmosphere that surrounds Earth. Gentler acids, around pH 5, are typically neutralized by alkaline components in soil, bedrock, and bodies of water. Human activity has caused an increase in acid rain and an increase in the acidity of the rain formed. This means that the natural buffering systems in place, such as the carbonate buffering system, are incapable of neutralizing the acid rain. Acid rain causes damage to buildings made of limestone and other softer rocks but also has major effects on ecosystems and biodiversity. As acid rain falls, it acidifies the soil, lakes, and streams it enters. This disrupts the ecosystem and can have negative effects on soil and water biodiversity. Soil acidification has other impacts also, as the pH of soils is lowered, the carbon losses from those soils increase, this could have long-term impacts on global efforts to carbon sequester using soil.[37] Reduced and oxidized forms of N, like NO_Y, have health implications in lower parts of the atmosphere.

N_2O has 300 times the radiative forcing effect of CO_2 due to its ability to degrade ozone. N_2O is released from incomplete denitrification (Fig. 2.5) and the amount that is produced depends on the nitrogen inputs into the soil, the soil moisture, and the temperature. N_2O emissions occur mainly from agriculture (Fig. 2.6). NO_Y is also produced from incomplete denitrification and has severe effects on human health, being incredibly dangerous for people with lung conditions, including asthma.

The effect of N_2O and NO_Y on humans and the environment is significant and for agriculture to become more sustainable methods to reduce these dangerous N species from being produced is necessary. Using NMs to provide a more efficient source of N to plants is one option, reducing the excess organic N that soil microbes can act on. Other potential methods using NMs would instead seek to change the N_2O and NO_Y into less damaging compounds. Nanocatalysts are NMs with catalytic properties. One use of nanocatalysis is to create the ammonia required for fertilizers using a more sustainable and environmental friendly method by reducing atmospheric nitrogen, with water and electricity using hollow gold nanocages.[39] This principle of using NMs in catalysis could provide an opportunity to apply a similar nanomaterial to minimize dangerous N emissions from soils. If a nanomaterial was found that was able to act without the presence of electricity (e.g., through solar power or via a redox reaction) and was able to catalyze the conversion of N_2O and other harmful forms of N to neutral ones, this would be of massive benefit to agriculture and reduce agricultural N emissions massively.

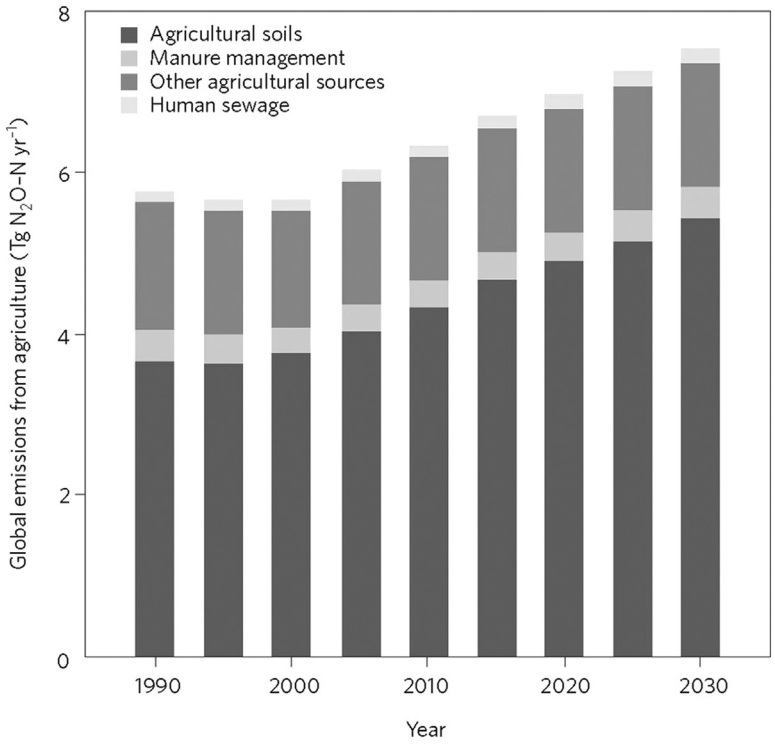


Figure 2.6
Global nitrous oxide (N_2O) emissions from 1990 to 2030.[38] *Source: From Reay, D. S.; Davidson, E. A.; Smith, K. A.; Smith, P.; Melillo, J. M.; Dentener, F.; Crutzen, P. J. Global Agriculture and Nitrous Oxide Emissions.* Nat. Clim. Change. *2012, 2 (6), 410–416. https://doi.org/10.1038/nclimate1458.*

2.5 Nanotechnology as a solution for the inefficiencies of conventional fertilizers

2.5.1 Improvements to nutrient use efficiency

Nanotechnology has been shown to be a promising solution to overfertilization and its resulting impacts on the environment. To improve NUE of crop plants, there are four keyways in which fertilizer application must be optimized: (1) the form that the nutrient takes should be most appropriate for its use, as should; (2) the rate; (3) the timing; and (4) the location of application. Low NUE results from the release rate of a fertilizer being greater than the absorption rate of the crop plant. Absorption rate is influenced by environmental factors like humidity, temperature, and soil compaction; biological factors like species, developmental stage, and nutrient status; and nutrient factors like concentration or pH. This can be further affected by any transformations the fertilizers undergo (like mineralization) which could affect the nutrient's bioavailability.[40]

To align the release and absorption rates, and therefore increase nutrient efficiency, a range of different solutions have been suggested. These include precision fertilizer application, where satellite or drone imagery is used to inform farmers about exactly when and where to apply fertilizer, or fertigation where low levels of fertilizer are added to the irrigation system in a drip-feed style. A less technology-intensive version of this approach is applying fertilizers in a localized or split way. Localized fertilizer is buried in the soil, typically before or during sowing, this allows the nutrients to be available to the plants without rain or irrigation and can decrease the amount of fertilizer required overall. Split fertilizer application applies fertilizer at two or more distinct times in the crop's growing season, rather than all at once at the start. This helps the nutrients to be applied at the correct rate for the plant's roots to be able to adsorb the nutrients appropriately, minimizing the period of time over which nutrient loss can occur. Using cover crops after the main crop's growing season is finished can help to minimize nutrient losses to the environment; however, this is a solution to the symptom not the cause of the problem. The use of microencapsulation has been previously used in agriculture to allow slow release of fertilizers or pesticides in soils. The casing of the fertilizers is made of plastic, which is unable to biodegrade and instead forms microplastics in the soil. The plastic casing is used to slow the release of the nutrients, and also to prevent potentially severe health effects on farmers and those applying the nutrients or pesticides. The long-term effects of microplastics on soil systems is unknown, with fears that they will have effects on soil microorganisms and in turn effect biodiversity and food chains.[41,42] Using nanoencapsulation is a similar alternative that reduces the amount of plastic introduced into the soil. In nanoencapsulation, nanoparticles are used as a nanoscale packaging layer over the target compound. This produces a film over the surface of the molecules being packaged and gives it a nanoscale defense; this could increase the bioavailability of the packaged molecules and allow a targeted release mechanism to be enacted. An example from agriculture is using a chitosan nano-matrix to encapsulate silicon; this nanofertilizer allows slow and controlled release and has been shown to enhance maize yield by more than 40% per plot.[43]

Nitrogen has low retention in soil typically; however, NMs can be doped with sources of N with the aim of aiding N retention in the soil for longer periods of time and improved access to the roots. NMs are able to bind different molecules with different levels of affinity/specificity/strength and identify particles that are able to bind specific N, P, and/or K species at the correct level, where they are still available to plant roots could solve issues around nutrient leaching. NMs that are able to bind N_2 gas have already been identified, as is the case with carbon nanotubes used in catalysis[44] Another issue is the difficulty of getting nutrients from the soil into the plant. Low uptake of nutrients is a problem, with nutrients transported into plant roots using active transport and requiring a sufficiently extensive root network to be functional. NM–nutrient composites

or NMs that can bind or contain nutrients themselves may be able to help transport of nutrients into plants and then release them in situ. Some NMs, dependent on size and shape, are able to enter plants and travel through the xylem or phloem before crossing the cell wall barrier and are transported through the apoplast pathway.[45] Crossing through the cell membrane occurs through several different mechanisms, as shown in Fig. 2.7, including through endocytosis where the cell membrane invaginates to allow nanoparticles to be stored in endosomes (membrane-bound organelles that sort transportation inside cells) within the plant cytosol, or through gaps in the cell membrane called plasmodesmata.[46] Foliar sprays can allow NMs to enter plant leaves through their stomata. NMs can also be used on plants that are not yet mature, for example, seed treatments with NMs, where NMs are able to penetrate the seed coating, as demonstrated by carbon nanotubes entering tomato seeds.[47]

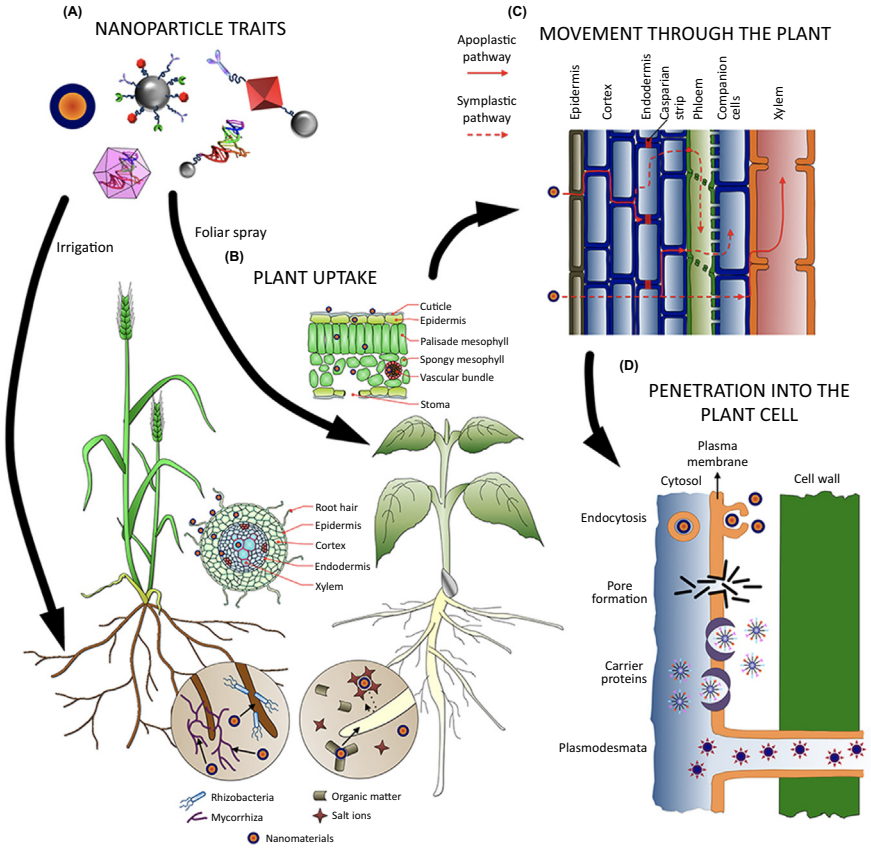


Figure 2.7 Nanoparticle absorption, uptake, and transport in plants. *Source*: From A., Pérez-de-Luque; Interaction of Nanomaterials with Plants: What Do We Need for Real Applications in Agriculture. *Front. Environ. Sci.* **2017**, 5. https://doi.org/10.3389/fenvs.2017.000121.

Table 2.2 Key features of nutrient use efficiency and how each aspect can be tackled by nanotechnology.

Feature	Problem	Nanotechnology solution
Nutrient uptake	Nutrients enter roots through active transport	NMs have been shown to enter plants through roots, with particularly small NMs passing through cell wall openings, and stomatal pores or cuticle pores in leaves also. Some NMs are unable to be taken up and instead coat the root epidermis
Transport	Nutrients are transported through the phloem along with sucrose	NMs are smaller and able to be transported either through the phloem or xylem (depending on composition) and can travel by different routes within the plant, e.g., apoplast (extracellular) and symplast (intracellular) pathways
Storage	Nutrients are stored in sinks, like leaves, fruits, roots, and stems	NMs are hypothesized to be stored in the vacuole of plant cells[48]
Mobility	N and P both quite mobile through soil, K far less mobile	NMs adsorb to soil particles upon application and are far less mobile than traditional forms of fertilizer like urea and ammonia but do still migrate through soil

Using nanobionics to improve plant photosynthesis was achieved using carbon nanotubes to improve chloroplast functioning and increase the photosynthetic activity of the plant.[49] Improving a plant's photosynthetic efficiency should allow a greater amount of sugars to be available to the plant, imparting it with more energy to put into increasing yield or other aspects of growth, affecting NUE. Plant nanobionics is discussed further in Chapter 7.

Often, the effect on NUE of an NM can be seen experimentally, but the mechanism by which this takes place is unknown, with some proposed solutions seen in Table 2.2. Urea-doped amorphous calcium phosphate (U-ACP) has been shown to maintain crop quality even when the N applied is in far smaller quantities than would have been added with conventional fertilizers, like urea. This has been shown in wine grapes (Fig. 2.8), with applications of 0.4 kg/ha of U-ACP maintaining grape quality when compared to conventional fertilizer application with 6 kg/ha of N added.[50] Similar effects have been seen in cucumber (20% increase in NUE as compared to conventional fertilizer) and wheat (N reduction of 40% with no impact on yield), indicating the potential improvements in NUE that can be enabled using nanofertilisers.[51,52] This growing body of work also indicates that nanotechnological improvements to yield and crop quality can be derived for both monocots and dicots, with different NMs proving effective for different species.

2.5.2 Improvements to crop growth, quality, and resilience

Crop quality includes a range of different features other than yield. The size and mass of the crop are of significant interest as are the nutritional content, shape, and esthetic value of the crop. For example, the number of tomatoes produced is not the only factor that farmers will be concerned with. Variety,



Figure 2.8 Wine grapes are a major crop worldwide, with the global wine market estimated to be worth $326.6 billion in 2020. Growing wine grapes is a water and nutrient-intensive activity where quality and yield cannot be compromised on. Application of U-ACP on wine grapes generated a massive increase in nutrient use efficiency, with the amount of N applied 15 times lower than with conventional fertiliser.[50] *U-ACP*, Urea-doped amorphous calcium phosphate.

shape, size, flavor quality, and nutritional composition are all significant factors that will affect consumer satisfaction. Additionally, food esthetics have come under scrutiny in recent years, with many supermarkets opting to sell "wonky" fruit and vegetables at a reduced rate rather than disposing of them due to concerns about lack of consumer acceptance. NMs are able to affect multiple different facets of plant growth and development. From increasing stem length and diameter in watermelon[53] to altering the nutritive content of a plant, NMs are poised to make major impacts on crops in a range of ways. In rice treated with cerium oxide nanoparticles, there was less starch, storage proteins (prolamins), fatty acids (lauric and valeric acids), and antioxidants.[54] However, tomatoes treated with nutrient loaded 100 nm liposomes were able to overcome their acute nutrient deficiencies in Mg and Fe, which conventional treatments were unable to do.[55] This highlights further how different NMs, and different crops will interact differently and conclusions from one case cannot be extrapolated to others.

Beyond crop quality, to have effective plant growth, stress must be minimized for plants. If a plant is forced to grow with insufficient water, in contaminated soils, is too hot or cold or is subject to biological pests and pathogens, it will never grow to its full potential and the quality of the resulting crop will be similarly stunted. Using NMs to aid in crop resilience and stress tolerance, or as nanopesticides to help defend against pests, can also impact crop growth and quality. Improvements to plant salt stress tolerance have been achieved in the oil crop rapeseed (*Brassica napus*) and model plant *Arabidopsis thaliana* through

application of CeO_2 NMs, which is achieved through the antioxidant nature of the CeO_2 NMs whereby hydroxyl (OH) radicals are scavenged leading to long-term retention of K^+ ions, allowing photosynthesis to persist under salinity stress.[56,57] Soil water retention using zeolites, a cage-structured nanomaterial, could help prevent osmotic and drought stress for crops by retaining water in the pores and enabling slow release. Soil water retention is largely dependent on soil particle size and therefore soil type, for example, clay and silt. Adding zeolites to soil has been shown to improve infiltration of water into the soil, to help in minimizing runoff and to increase soil moisture.[58] This could aid in minimizing the amount of freshwater and irrigation required in commercial arable farming, with agriculture being the number one use of freshwater globally, using ~70% of freshwater supplies.[59] Drought stress, which is predicted to increase further as a result of climate change, has major impacts on crop productivity and minimizing water inputs where possible is of major interest in many regions globally. Other stresses, like salt stress, are similar to drought stress in that they both cause osmotic stress to the plant where there is insufficient water accessible to the cells. This generates the production of reactive oxygen species (ROS) which cause harm to plant cells and uses up energy the plant would ideally be putting into growth to fight the oxidative stress arising from excessive ROS. Carbon-based NMs have been shown to improve salt stress tolerance and increase both germination and total biomass in a range of crops. The carbon nanotubes used were able to significantly reduce the concentration of Na^+ ions and the carbon-based NMs upregulated expression of water channel genes called aquaporins.[60]

Other modes of action for NMs to improve total growth include using NMs to defend against pathogens. Silver nanoparticles when applied to the leaves of tomatoes have been shown to improve resistance to foliar pathogens, with 79%–98% improved resistance as compared to the control.[61] Similarly, using nanoscale copper can aid in reducing Fusarium (a soil fungus that can have devastating impacts on crops, resulting in root rot, wilting or stem cankers to develop) with a concentration of 450 ppm inhibiting 93.98% of Fusarium fungus growth, with conventional fungicide products typically inhibiting growth by 62%–68%.[62,63] Please see Chapter 3 on nanofertilizers for more information on how NMs can improve crop nutrition and Chapters 4 and 5 for information on nanopesticides and NMs for plant pathogen control.

2.6 Summary

2.6.1 Nutrient use in farming and how nanotechnology can improve yields and reduce pollution

NMs can be applied in a range of techniques to improve NUE, these range from being used as fertilizers, to improving soil water retention, minimizing pests and disease, or catalyzing conversion of nutrients to less harmful forms to

minimize wastage and pollution. There is a significant body of research already existing looking at natural and engineered NMs effects on different aspects of a range of crop plants growth, including yield, nutritive content, and resilience to stress. By reducing total nutrient inputs into soil, it is hoped that this will in turn minimize excess nutrients being converted into volatile species that impact on climate change and air quality, prevent leaching into waterways and the associated effects on biodiversity, and also prevent soil degradation.

2.6.2 Areas of concern regarding nanotechnology?

NMs' long-term effects have not yet been fully determined and how they respond and transform in different environments is still being researched. If NMs persist in soil, they may even be considered a soil pollutant themselves, along the lines of the microplastic capsules currently utilized in controlled pesticide release. Utilization of naturally derived nanoscale materials such as nanocellulose and zeolites may offer advantages from a regulatory perspective. For deep understanding of whether NMs provide a holistic solution to current fertilizer inadequacy, their impact on nutrient cycling, toxicity to soil microbes and fauna, and their cumulative effects in food chains need to be explored over multiple growth cycles and under field conditions.

Public knowledge of nanotechnology is low, with knowledge on applications in agriculture not commonly considered or well publicized, although it is likely there would be less resistance to nano-enabled agriculture than there has been to use of genetically modified crops in Europe. However, the toxicity of NMs and their effect if ingested is dependent on the composition of the NMs and the amount. Some NMs have been approved for use in food, for example, silica and titanium dioxide, and others have previously been used in food with permissions revoked due to new findings.

2.7 Study questions

1. Make a list of the pros and cons of using NMs in agriculture, what problems do they solve and what potential issues could their use raise?
2. Seed germination experiments are popular for understanding nanomaterial phytotoxicity; describe how you would set up a seed germination experiment. What factors might you need to consider/control?
3. Which points in the nitrogen cycle are most amendable to intervention through use of nanotechnology, and why?

References

1. Phillips, R.; Milo, R. A Feeling for the Numbers in Biology. *Proc. Natl. Acad. Sci. U.S.A* **2009,** *106* (51), 21465–21471. Available from: https://doi.org/10.1073/pnas.0907732106.

2. Hecnar, S. Acute and Chronic Toxicity of Ammonium Nitrate Fertilizer to Amphibians from Southern Ontario. *Environ. Toxicol. Chem.* **1995,** *14* (12), 2131−2137.
3. Steen, I. Phosphorus Availability in the 21st Century: Management of a Non-Renewable Resource. *Phosphor. Potassium* **1998,** *217*, 25−31.
4. Cordell, D.; Drangert, J.-O.; White, S. The Story of Phosphorus: Global Food Security and Food for Thought. *Glob. Environ. Change* **2009,** *19* (2), 292−305. Available from: https://doi.org/10.1016/j.gloenvcha.2008.10.009.
5. Taylor, A. W.; Gurney, E. L. Precipitation of Phosphate by Iron Oxide and Aluminum Hydroxide From Solutions Containing Calcium and Potassium. *Soil Science Society of America Journal* **1965,** *29* (1), 18−22. Available from: https://doi.org/10.2136/sssaj1965.03615995002900010008x.
6. Smolders, A. J. P.; Lucassen, E. C. H. E. T.; Bobbink, R.; Roelofs, J. G. M.; Lamers, L. P. M. How Nitrate Leaching from Agricultural Lands Provokes Phosphate Eutrophication in Groundwater Fed Wetlands: The Sulphur Bridge. *Biogeochemistry* **2010,** *98* (1−3), 1−7. Available from: https://doi.org/10.1007/s10533-009-9387-8.
7. Mekonnen, M. M.; Hoekstra, A. Y. Global Anthropogenic Phosphorus Loads to Freshwater and Associated Grey Water Footprints and Water Pollution Levels: A High-Resolution Global Study. *Water Resour. Res.* **2018,** *54* (1), 345−358. Available from: https://doi.org/10.1002/2017WR020448.
8. Wang, M.; Zheng, Q.; Shen, Q.; Guo, S. The Critical Role of Potassium in Plant Stress Response. *IJMS* **2013,** *14* (4), 7370−7390. Available from: https://doi.org/10.3390/ijms14047370.
9. Zörb, C.; Senbayram, M.; Peiter, E. Potassium in Agriculture − Status and Perspectives. *J. Plant Physiol.* **2014,** *171* (9), 656−669. Available from: https://doi.org/10.1016/j.jplph.2013.08.008.
10. Öborn, I.; Andrist-Rangel, Y.; Askekaard, M.; Grant, C. A.; Watson, C. A.; Edwards, A. C. Critical Aspects of Potassium Management in Agricultural Systems. *Soil Use Manag.* **2008,** *21* (1), 102−112. Available from: https://doi.org/10.1111/j.1475-2743.2005.tb00114.x.
11. Munson, R. D.; Nelson, W. L. Movement of Applied Potassium in Soils. *J. Agric. Food Chem* **1963,** *11* (3), 193−201. Available from: https://doi.org/10.1021/jf60127a015.
12. Wuepper, D.; Borrelli, P.; Finger, R. Countries and the Global Rate of Soil Erosion. *Nat. Sustain.* **2020,** *3* (1), 51−55. Available from: https://doi.org/10.1038/s41893-019-0438-4.
13. Erisman, J. W.; Sutton, M. A.; Galloway, J.; Klimont, Z.; Winiwarter, W. How a Century of Ammonia Synthesis Changed the World. *Nat. Geosci.* **2008,** *1*, 636−639.
14. FAO. *World Food and Agriculture − Statistical Yearbook 2021;* FAO: Rome, **2021**. Available from: https://doi.org/10.4060/cb4477en.
15. Food and Agriculture Organization of the United Nations. *World Fertilizer Trends and Outlook to 2022*; Rome, **2019**.
16. Lassaletta, L.; Billen, G.; Grizzetti, B.; Anglade, J.; Garnier, J. 50 Year Trends in Nitrogen Use Efficiency of World Cropping Systems: The Relationship between Yield and Nitrogen Input to Cropland. *Environ. Res. Lett.* **2014,** *9* (10), 105011. Available from: https://doi.org/10.1088/1748-9326/9/10/105011.
17. Gogotsi, Y.; Penner, R. M. Energy Storage in Nanomaterials − Capacitive, Pseudocapacitive, or Battery-Like? *ACS Nano* **2018,** *12* (3), 2081−2083. Available from: https://doi.org/10.1021/acsnano.8b01914.
18. Hubbell, J. A.; Chilkoti, A. Nanomaterials for Drug Delivery. *Science* **2012,** *337* (6092), 303−305. Available from: https://doi.org/10.1126/science.1219657.
19. Wheeler, K. E.; Chetwynd, A. J.; Fahy, K. M.; Hong, B. S.; Tochihuitl, J. A.; Foster, L. A.; Lynch, I. Environmental Dimensions of the Protein Corona. *Nat. Nanotechnol.* **2021,** *16* (6), 617−629. Available from: https://doi.org/10.1038/s41565-021-00924-1.
20. Zhu, Y.; Xu, F.; Liu, Q.; Chen, M.; Liu, X.; Wang, Y.; Sun, Y.; Zhang, L. Nanomaterials and Plants: Positive Effects, Toxicity and the Remediation of Metal and Metalloid

Pollution in Soil. *Sci. Total Environ.* **2019,** *662*, 414−421. Available from: https://doi.org/10.1016/j.scitotenv.2019.01.234.

21. Ding, J.; Zhong, Q.; Zhang, S.; Cai, W. Size- and Shape-Controlled Synthesis and Catalytic Performance of Iron−Aluminum Mixed Oxide Nanoparticles for NO_X and SO_2 Removal with Hydrogen Peroxide. *J. Hazard. Mater.* **2015,** *283*, 633−642.
22. Zhao, S.; Su, X.; Wang, Y.; Yang, X.; Bi, M.; He, Q.; Chen, Y. Copper Oxide Nanoparticles Inhibited Denitrifying Enzymes and Electron Transport System Activities to Influence Soil Denitrification and N_2O Emission. *Chemosphere* **2020,** *245*, 125394. Available from: https://doi.org/10.1016/j.chemosphere.2019.125394.
23. Galloway, J. N.; Cowling, E. B. Reactive Nitrogen and the World: 200 Years of Change. *AMBIO: A J. Hum. Environ.* **2002,** *31* (2), 64−71. Available from: https://doi.org/10.1579/0044-7447-31.2.64.
24. Guisbiers, G.; Mejía-Rosales, S.; Leonard Deepak, F. Nanomaterial Properties: Size and Shape Dependencies. *J. Nanomater.* **2012,** *2012*, 1−2. Available from: https://doi.org/10.1155/2012/180976.
25. Baranowska-Wójcik, E.; Szwajgier, D.; Oleszczuk, P.; Winiarska-Mieczan, A. Effects of Titanium Dioxide Nanoparticles Exposure on Human Health—A Review. *Biol Trace Elem. Res.* **2020,** *193* (1), 118−129. Available from: https://doi.org/10.1007/s12011-019-01706-6.
26. Samat, S. F. A.; Sarah, M. S. P.; Idros, M. F. M. In *High Optical Transmittance of Nanostructured TiO_2 Thin Film Using Dip Coating Method*, In 2016 7th IEEE Control and System Graduate Research Colloquium, pp 52−56; IEEE, **2016**. https://doi.org/10.1109/ICSGRC.2016.7813300.
27. ITPS Soil Letters. Towards a Definition of Soil Health; FAO: Rome, Italy, 2020, p. 3.
28. Nogueira, V.; Lopes, I.; Rocha-Santos, T.; Santos, A. L.; Rasteiro, G. M.; Antunes, F.; Gonçalves, F.; Soares, A. M. V. M.; Cunha, A.; Almeida, A., et al. Impact of Organic and Inorganic Nanomaterials in the Soil Microbial Community Structure. *Sci. Total Environ.* **2012,** *424*, 344−350. Available from: https://doi.org/10.1016/j.scitotenv.2012.02.041.
29. Cao, X.; Yue, L.; Wang, C.; Luo, X.; Zhang, C.; Zhao, X.; Wu, F.; White, J. C.; Wang, Z.; Xing, B. Foliar Application with Iron Oxide Nanomaterials Stimulate Nitrogen Fixation, Yield, and Nutritional Quality of Soybean. *ACS Nano* **2022,** *16* (1), 1170−1181. Available from: https://doi.org/10.1021/acsnano.1c08977.
30. Gong, X.; Huang, D.; Liu, Y.; Peng, Z.; Zeng, G.; Xu, P.; Cheng, M.; Wang, R.; Wan, J. Remediation of Contaminated Soils by Biotechnology with Nanomaterials: Bio-Behavior, Applications, and Perspectives. *Crit. Rev. Biotechnol.* **2018,** *38* (3), 455−468. Available from: https://doi.org/10.1080/07388551.2017.1368446.
31. El-Temser, Y.; Joner, E. Effects of Nano-Sized Zero-Valent Iron (NZVI) on DDT Degradation in Soil and Its Toxicity to Collembola and Ostracods. *Chemosphere* **2013,** *92*, 131−137. Available from: https://doi.org/10.1016/j.chemosphere.2013.02.039.
32. Li, S.; Turaga, U.; Shrestha, B.; Anderson, T.; Ramkumar, S.; Green, M.; Das, S.; Cañas-Carrell, J. Mobility of Polyaromatic Hydrocarbons (PAHs) in Soil in the Presence of Carbon Nanotubes. *Ecotoxicol. Environ. Saf.* **2013,** *96*, 168−174. Available from: https://doi.org/10.1016/j.ecoenv.2013.07.005.
33. Singh, J.; Lee, B.-K. Influence of Nano-TiO_2 Particles on the Bioaccumulation of Cd in Soybean Plants (*Glycine max*): A Possible Mechanism for the Removal of Cd from the Contaminated Soil. *J. Environ. Manage.* **2016,** *170*, 88−96. Available from: https://doi.org/10.1016/j.jenvman.2016.01.015.
34. Schindler, D. W. Eutrophication and Recovery in Experimental Lakes: Implications for Lake Management. *Science* **1974,** *184* (4139), 897−899. Available from: https://doi.org/10.1126/science.184.4139.897.
35. Funari, E.; Testai, E. Human Health Risk Assessment Related to Cyanotoxins Exposure. *Crit. Rev. Toxicol.* **2008,** *38* (2), 97−125. Available from: https://doi.org/10.1080/10408440701749454.

36. Firestone, M.; Davidson, E. Microbiological Basis of NO and N_2O Production and Consumption in Soil. In *Exchange of Trace Gases Between Terrestrial Ecosystems and the Atmosphere*; Andreae M.O., Schimel D.S., Eds; John Wiley and Sons: Chichester, **1989**; 47, pp 7–21.
37. Raza, S.; Zamanian, K.; Ullah, S.; Kuzyakov, Y.; Virto, I.; Zhou, J. Inorganic Carbon Losses by Soil Acidification Jeopardize Global Efforts on Carbon Sequestration and Climate Change Mitigation. *J. Clean. Prod.* **2021,** *315*, 128036. Available from: https://doi.org/10.1016/j.jclepro.2021.128036.
38. Reay, D. S.; Davidson, E. A.; Smith, K. A.; Smith, P.; Melillo, J. M.; Dentener, F.; Crutzen, P. J. Global Agriculture and Nitrous Oxide Emissions. *Nat. Clim. Change* **2012,** *2* (6), 410–416. Available from: https://doi.org/10.1038/nclimate1458.
39. Nazemi, M.; Panikkanvalappil, S. R.; El-Sayed, M. A. Enhancing the Rate of Electrochemical Nitrogen Reduction Reaction for Ammonia Synthesis under Ambient Conditions Using Hollow Gold Nanocages. *Nano Energy* **2018,** *49*, 316–323. Available from: https://doi.org/10.1016/j.nanoen.2018.04.039.
40. Chhipa, H. Nanofertilizers and Nanopesticides for Agriculture. *Environ. Chem. Lett.* **2017,** *15* (1), 15–22. Available from: https://doi.org/10.1007/s10311-016-0600-4.
41. Zhang, P.; Guo, Z.; Ullah, S.; Melagraki, G.; Afantitis, A.; Lynch, I. Nanotechnology and Artificial Intelligence to Enable Sustainable and Precision Agriculture. *Nat. Plants* **2021,** *7* (7), 864–876. Available from: https://doi.org/10.1038/s41477-021-00946-6.
42. Zhang, X.; Li, Y.; Ouyang, D.; Lei, J.; Tan, Q.; Xie, L.; Li, Z.; Liu, T.; Xiao, Y.; Farooq, T. H., et al. Systematical Review of Interactions between Microplastics and Microorganisms in the Soil Environment. *J. Hazard. Mater.* **2021,** *418*, 126288. Available from: https://doi.org/10.1016/j.jhazmat.2021.126288.
43. Kumaraswamy, R. V.; Saharan, V.; Kumari, S.; Chandra Choudhary, R.; Pal, A.; Sharma, S. S.; Rakshit, S.; Raliya, R.; Biswas, P. Chitosan-Silicon Nanofertilizer to Enhance Plant Growth and Yield in Maize (*Zea mays* L.). *Plant Physiol. Biochem.* **2021,** *159*, 53–66. Available from: https://doi.org/10.1016/j.plaphy.2020.11.054.
44. Mabena, L. F.; Sinha Ray, S.; Mhlanga, S. D.; Coville, N. J. Nitrogen-Doped Carbon Nanotubes as a Metal Catalyst Support. *Appl. Nanosci.* **2011,** *1* (2), 67–77. Available from: https://doi.org/10.1007/s13204-011-0013-4.
45. Kurczyńska, E.; Godel-Jędrychowska, K.; Sala, K.; Milewska-Hendel, A. Nanoparticles—Plant Interaction: What We Know, Where We Are? *Appl. Sci.* **2021,** *11* (12), 5473. Available from: https://doi.org/10.3390/app11125473.
46. Pérez-de-Luque, A. Interaction of Nanomaterials with Plants: What Do We Need for Real Applications in Agriculture. *? Front. Environ. Sci.* **2017,** 5. Available from: https://doi.org/10.3389/fenvs.2017.00012.
47. Khodakovskaya, M.; Dervishi, E.; Mahmood, M.; Xu, Y.; Li, Z.; Watanabe, F.; Biris, A. S. Carbon Nanotubes Are Able To Penetrate Plant Seed Coat and Dramatically Affect Seed Germination and Plant Growth. *ACS Nano* **2009,** *3* (10), 3221–3227. Available from: https://doi.org/10.1021/nn900887m.
48. da Cruz, T. N. M.; Savassa, S. M.; Montanha, G. S.; Ishida, J. K.; de Almeida, E.; Tsai, S. M.; Lavres Junior, J.; Pereira de Carvalho, H. W. A New Glance on Root-to-Shoot in Vivo Zinc Transport and Time-Dependent Physiological Effects of $ZnSO_4$ and ZnO Nanoparticles on Plants. *Sci. Rep.* **2019,** *9* (1), 10416. Available from: https://doi.org/10.1038/s41598-019-46796-3.
49. Giraldo, J. P.; Landry, M. P.; Faltermeier, S. M.; McNicholas, T. P.; Iverson, N. M.; Boghossian, A. A.; Reuel, N. F.; Hilmer, A. J.; Sen, F.; Brew, J. A., et al. Plant Nanobionics Approach to Augment Photosynthesis and Biochemical Sensing. *Nat. Mat.* **2014,** *13* (4), 400–408. Available from: https://doi.org/10.1038/nmat3890.
50. Pérez-Álvarez, E. P.; Ramírez-Rodríguez, G. B.; Carmona, F. J.; Martínez-Vidaurre, J. M.; Masciocchi, N.; Guagliardi, A.; Garde-Cerdán, T.; Delgado-López, J. M. Towards a More

Sustainable Viticulture: Foliar Application of N-Doped Calcium Phosphate Nanoparticles on Tempranillo Grapes. *J. Sci. Food Agric.* **2021,** *101* (4), 1307−1313. Available from: https://doi.org/10.1002/jsfa.10738.

51. Carmona, F. J.; Dal Sasso, G.; Ramírez-Rodríguez, G. B.; Pii, Y.; Delgado-López, J. M.; Guagliardi, A.; Masciocchi, N. Urea-Functionalized Amorphous Calcium Phosphate Nanofertilizers: Optimizing the Synthetic Strategy towards Environmental Sustainability and Manufacturing Costs. *Sci. Rep.* **2021,** *11* (1), 3419. Available from: https://doi.org/10.1038/s41598-021-83048-9.
52. Ramírez-Rodríguez, G. B.; Miguel-Rojas, C.; Montanha, G. S.; Carmona, F. J.; Dal Sasso, G.; Sillero, J. C.; Skov Pedersen, J.; Masciocchi, N.; Guagliardi, A.; Pérez-de-Luque, A., et al. Reducing Nitrogen Dosage in Triticum Durum Plants with Urea-Doped Nanofertilizers. *Nanomaterials* **2020,** *10* (6), 1043. Available from: https://doi.org/10.3390/nano10061043.
53. Acharya, P.; Jayaprakasha, G. K.; Crosby, K. M., et al. Nanoparticle-Mediated Seed Priming Improves Germination, Growth, Yield, and Quality of Watermelons (Citrullus Lanatus) at Multi-Locations in Texas. *Sci. Rep.* **2020,** *10* (1), 5037. Available from: https://doi.org/10.1038/s41598-020-61696-7.
54. Rico, C. M.; Morales, M. I.; Barrios, A. C.; McCreary, R.; Hong, J.; Lee, W.-Y.; Nunez, J.; Peralta-Videa, J. R.; Gardea-Torresdey, J. L. Effect of Cerium Oxide Nanoparticles on the Quality of Rice (*Oryza sativa* L.) Grains. *J. Agric. Food Chem.* **2013,** *61* (47), 11278−11285. Available from: https://doi.org/10.1021/jf404046v.
55. Karny, A.; Zinger, A.; Kajal, A.; Shainsky-Roitman, J.; Schroeder, A. Therapeutic Nanoparticles Penetrate Leaves and Deliver Nutrients to Agricultural Crops. *Sci. Rep.* **2018,** *8* (1), 7589. Available from: https://doi.org/10.1038/s41598-018-25197-y.
56. Rossi, L.; Zhang, W.; Lombardini, L.; Ma, X. The Impact of Cerium Oxide Nanoparticles on the Salt Stress Responses of *Brassica napus* L. *Environ. Pollut.* **2016,** *219*, 28−36. Available from: https://doi.org/10.1016/j.envpol.2016.09.060.
57. Wu, H.; Shabala, L.; Shabala, S.; Giraldo, J. P. Hydroxyl Radical Scavenging by Cerium Oxide Nanoparticles Improves Arabidopsis Salinity Tolerance by Enhancing Leaf Mesophyll Potassium Retention. *Environ. Sci.: Nano* **2018,** *5* (7), 1567−1583. Available from: https://doi.org/10.1039/C8EN00323H.
58. Xiubin, H.; Zhanbin, H. Zeolite Application for Enhancing Water Infiltration and Retention in Loess Soil. *Resour. Conserv. Recycl.* **2001,** *34* (1), 45−52. Available from: https://doi.org/10.1016/S0921-3449(01)00094-5.
59. FAO. *The State of the World's Land and Water Resources for Food and Agriculture (SOLAW) − Managing Systems at Risk*. Food and Agriculture Organization of the United Nations: Rome and Earthscan, London, 2011.
60. Pandey, K.; Lahiani, M. H.; Hicks, V. K.; Hudson, M. K.; Green, M. J.; Khodakovskaya, M. Effects of Carbon-Based Nanomaterials on Seed Germination, Biomass Accumulation and Salt Stress Response of Bioenergy Crops. *PLoS One* **2018,** *13* (8), e0202274. Available from: https://doi.org/10.1371/journal.pone.0202274.
61. Ashraf, H.; Anjum, T.; Riaz, S.; Naseem, S. Microwave-Assisted Green Synthesis and Characterization of Silver Nanoparticles Using Melia Azedarach for the Management of Fusarium Wilt in Tomato. *Front. Microbiol.* **2020,** *11*, 238. Available from: https://doi.org/10.3389/fmicb.2020.00238.
62. Larkin, R. P.; Fravel, D. R. Efficacy of Various Fungal and Bacterial Biocontrol Organisms for Control of Fusarium Wilt of Tomato. *Plant Dis.* **1998,** *82* (9), 1022−1028. Available from: https://doi.org/10.1094/PDIS.1998.82.9.1022.
63. Viet, P. V.; Nguyen, H. T.; Cao, T. M.; Hieu, L. V. Fusarium Antifungal Activities of Copper Nanoparticles Synthesized by a Chemical Reduction Method. *J. Nanomater.* **2016,** *2016*, 1−7. Available from: https://doi.org/10.1155/2016/1957612.

Further reading

Doran, J. W.; Parkin, T. B. *Quantitative Indicators of Soil Quality: A Minimum Data Set*. In *SSSA Special Publications;* Doran, J. W., Jones, A. J., Eds.; Soil Science Society of America: Madison, WI, USA, **1997**; pp 25−37. Available from: https://doi.org/10.2136/sssaspecpub49.c2.

Doran, J. W.; Zeiss, M. R. Soil Health and Sustainability: Managing the Biotic Component of Soil Quality. *Appl. Soil Ecol.* **2000,** *15* (1), 3−11. Available from: https://doi.org/10.1016/S0929-1393(00)00067-6.

Megonigal, J.; Hines, M.; Visscher, P. Anaerobic Metabolism: Linkages to Trace Gases and Aerobic Processes. *Biogeochemistry* **2004**.

de la Rosa, G.; Vázquez-Núñez, E.; Molina-Guerrero, C.; Serafín-Muñoz, A. H.; Vera-Reyes, I. Interactions of Nanomaterials and Plants at the Cellular Level: Current Knowledge and Relevant Gaps. *Nanotechnol. Environ. Eng* **2021,** *6* (1), 7. Available from: https://doi.org/10.1007/s41204-020-00100-1.

World Health Organization & Food and Agriculture Organization of the United Nations. State of the Art on the Initiatives and Activities Relevant to Risk Assessment and Risk Management of Nanotechnologies in the Food and Agriculture Sectors: FAO/WHO technical paper; Food and Agriculture Organization of the United Nations and World Health Organization: Rome, **2013**.

Zhang, X; Li, Y.; Ouyang, D.; Lei, J.; Tan, Q.; Xie, L.; Li, Z.; Liu, T.; Xiao, Y.; Farooq, T. H. Systematical Review of Interactions Between Microplastics And Microorganisms in the Soil Environment. J. Hazard. Mater. **2021**, *418*, 126288. DOI: https://doi.org/10.1016/j.jhazmat.2021.126288. https://reader.elsevier.com/reader/sd/pii/S0304389421012528?token = 8D75C099ACCAD678A30089D8678EC860D9D191B1BDCE2FC152F204B831-F99ED765EC788A0329935523F05D33315C7A3A&originRegion = eu-west-1&originCreation = 20220630152127 (accessed June 30, 2022).

United Kingdom Food Security Report 2021: Theme 2: UK Food Supply Sources; Department for Environment, Food & Rural Affairs, **2021**. https://www.gov.uk/government/statistics/united-kingdom-food-security-report-2021/united-kingdom-food-security-report-2021-theme-2-uk-food-supply-sources (accessed March 8, 2022).

Chapter 3. Differential Impacts on Wheat and Lettuce Seedling Outcomes from Nano-Zeolite and Metal Oxide Seed Priming – A Comparative Study

Jessica J Chadwick[1], Aleksandar Radu[2], Sam Parkinson[3], Ify Leonard Ugbomeh[1], Peng Zhang[1], Sami Ullah[1], Iseult Lynch[1]

[1] School of Geography, Earth and Environmental Sciences, University of Birmingham, Edgbaston, B15 2TT Birmingham, United Kingdom

[2] School of Chemistry, University of Lincoln, Lincoln LN6 7TS, UK

[3] School of Chemistry, University of Birmingham, Edgbaston, B15 2TT Birmingham, United Kingdom

[*] Corresponding authors: Jessica J. Chadwick, jxc1326@student.bham.ac.uk; Iseult Lynch, i.lynch@bham.ac.uk

Acknowledgements

This work was supported by the Biotechnology and Biological Sciences Research Council (BBSRC) and University of Birmingham funded Midlands Integrative Biosciences Training Partnership (MIBTP) grant number BB/T00746X/1. Materials were supplied by the NanoSolveIT project (Grant Agreement No, 814572) and Promethean Particles Ltd.

CReDIT statement

Jessica Chadwick: Writing – Original Draft, Investigation, Formal analysis, Visualisation, Conceptualisation. Aleksandar Radu: Materials. Sam Parkinson: Materials. Ify Leonard Ugbomeh: Materials. Peng Zhang: Supervision, Funding acquisition. Sami Ullah: Supervision, Funding acquisition. Iseult Lynch: Supervision, Writing – Review and Editing, Funding acquisition.

3.1. Abstract

Seed priming, through managing the temperature and moisture of seeds, aids in promoting seed germination and giving seeds an early growth advantage. Nanomaterials have been used in seed priming to aid in water uptake, and trigger improved stress resilience, priming them for adverse conditions later in development. This experiment directly compared 54 nanomaterials at 500 mg L^{-1} to develop a method for identifying nanomaterials with positive effects on seeds, enhancing germination rate as well as early shoot and root growth. Equally, investigation of the changes in NM characteristics after exposure to different crop seeds was studied. The crop species used were wheat and lettuce, representing monocot and dicot crops respectively, with nanomaterial effect expected to at least partly depend on the plant development strategy. Metal oxides and zeolites were found to have the best impacts on seed germination for both species. Other tested nanomaterials, like metal organic frameworks, produced a toxic effect and inhibited growth at the same concentration. Exposure to seeds has a significant impact on nanomaterial characteristics, triggering aggregation of metal oxides and an increase in zeta potential of zeolites. These effects are predicted to be through the action of seed exudates, with nanomaterial application having differing effects on the protein concentration of wheat and lettuce seed exudates. Other components of seed exudates, like organic acids, should be studied in further depth. Correlative analysis was performed on the outputs of this dataset indicates that some initial nanomaterial characteristics, like agglomerate size and zeta potential can be indicative of effects on wheat seed growth and germination. Further dose-response testing for both lettuce and wheat would extend current knowledge and enable modelling and optimisation of nanomaterials properties for effective seed priming.

3.2. Introduction

Study of seed physiology began with the ancient Greeks, with records dating back to 300 B.C.E. (Evenari, 1984). Seed priming, or regulating the germination process of seeds by managing the temperature and seed moisture content, is commonly used pre-sowing to aid in germination and seedling vigour, in turn impacting on crop productivity and quality later in development (Paparella et al., 2015). Seed priming can trigger positive effects on plant growth, either through initiating the first stage of germination, or aiding the plant in early establishment due to an enhanced resilience to environmental stressors (Chen and Arora, 2013). These effects can be achieved with water, known as hydropriming, or other chemicals such as hydrogen peroxide (H_2O_2). Other priming methods include using phytohormones to trigger germination, prime plants for stresses later in development or improving crop yield under adverse conditions through modulating ion uptake (Rhaman et al., 2021; Bertini et al., 2018; Iqbal and Ashraf, 2013).

Seed desiccation permits seeds to survive for long periods of time until ideal conditions are met for germination There are three core phases of seed germination, beginning with water imbibition. In the first stage a proportionally large volume of water is taken up by the seed, permitting preparation for stage two. At stage two the uptake of water slows, but a massive increase in metabolic activity is seen. The uptake of water is a core part of the transition to activity; this permits the breakdown of starch stores in the seed's endosperm, releasing energy and enzymes for further stages of development. These contribute to the final phase of seed germination, where the radicle begins to emerge from the seed and water uptake is again increased to enable new growth (Bewley, 1997). Seed priming acts on stages one and two of germination, resulting in faster emergence of the radicle (Paparella et al., 2015). The timeline of generalised physiological seed germination and post-germination responses are displayed in SI Figure S3.1.

Engineered nanomaterials (NMs) have been used in the context of seed priming for a range of major crops including rice, tomato, and wheat (Bertini et al., 2018; López-Vargas et al., 2020; Bayat et al., 2022). NM effects depend heavily on their physico-chemical properties, in particular size, surface charge, shape and concentration (Avellan et al., 2019, Kladko et al., 2021, Hao et al., 2016). Depending

on these properties, NM effects on plants differ significantly. Whilst some show phytotoxic effects, inhibiting plant germination and growth, others can positively enhance seed germination, causing signalling cascades that trigger growth or aid in priming plants for resilience to biotic and abiotic stresses (do Espirito Santa Pereira et al., 2021). Some of these positive responses may be due to NM application to seeds inducing hormetic effects, aiding in water uptake, or triggering internal plant molecular signalling when exposed at low concentrations (Wang et al., 2022; Rai et al., 2023). NMs have also been shown to increase accumulation and production of reactive oxygen species (ROS), triggering oxidative stress and activating multiple signalling pathways at higher exposure doses (Khan et al., 2017). ROS production in plants may aid in water uptake, as well as triggering signalling cascades and phytohormone production (Mittler et al., 2022). Enabling faster germination rates for crops and increasing seedling vigour allows crops to establish a strong root network early in their development, meaning they gain vital nutrients and water access (Motte et al., 2019). Slower germination leaves young plants vulnerable to stress and disease, further limiting growth and crop productivity resulting in losses (Kanojia and Dijkwel, 2018).

The stages of germination are consistent across seeds, however the specific morphology and molecular and physiological mechanisms that a seed undergoes are dependent on its evolutionary history (Sreenivasulu and Wobus, 2013). There are two main plant families of flowering plants, dicotyledonous (dicots) and monocotyledonous (monocots), referring to their number of cotyledons (embryonic leaves in seed-bearing plants, which are the first to appear) upon germination. Monocots early growth focuses on the emergence of a single leaf, while dicots begin life with a leaf pair. Monocots include all cereals, like wheat, a commonly used cereal that was worth £4.1bn to the UK economy in 2022, with similarities to other major crops of global financial significance, like rice and maize, which are both also monocots (DEFRA, 2024). Lettuce is one of the top three vegetables grown under cover that are imported into the UK (DEFRA, 2021). While variation within taxa are significant, generalised monocots and dicot growth and development differ, with different seed storage proteins, starch contents and morphophysiological events in seed development (Yang et al., 2023). Lettuce is a common dicot leaf vegetable that has also been shown to be more sensitive to NMs than other crops (like cucumber and radish) (Rizwan et al., 2017). Understanding the differences in response to NM between monocots and dicots will increase

knowledge and ability to tailor future NM development and application protocols for specific crop growth.

Tailoring NMs for use in agriculture also requires a deep understanding of how their specific physio-chemical properties impact on their interactions with different types of crop seeds. Present literature has focussed on a small selection of metal and metal oxide NMs, with substantial research done on TiO_2, ZnO, CeO_2, iron oxides, silica, Ag and Au nanoparticles (Rojas et al., 2022; do Espirito Santa Pereira et al., 2021; An et al., 2020). Several meta-analyses and reviews compare between NMs for seed priming effects, however differing concentrations and test species make direct comparison more challenging (Guo et al., 2024; Khan et al., 2023). Thus, the experiments presented here aimed to compare a wide range of NMs with varying chemical constituents and elemental ratios, and physical characteristics to identify and distinguish which compositions and properties aided monocot and dicot crop seed germination. This study utilised engineered NMs to prime either wheat or lettuce seeds, with a total 54 NMs compared. These included zeolites, metal oxides, nanopolymers, metal organic frameworks (MOFs), and biochar-hydroxyapatites effects on lettuce and wheat seeds. The concentration chosen was 500 mg L^{-1}, a relatively high NM concentration, to test the likelihood of inhibitory or phytotoxic effects compared to growth-enhancing ones. As well as understanding the impacts of the NMs on seed germination and seedling vigour, the study also aimed to examine the impact of contact with the seeds on the NMs physical characteristics through pre- and post-priming characterisation of NMs. Analysis of seed exudates post-exposure to a subset of the initially screened NMs will help inform how NMs may influence seed signalling pathways as well as providing information on how the exudates may be interacting with the NMs to cause different transformations., e.g. homoaggregation or corona formation evidenced as changes in zeta potential. Hydrodynamic size and zeta potential based characterisation occurred for 38 of the initial 54 nanomaterials tested. A subset of 14 of these NMs underwent further testing to investigate their impact on seed biomass and NM impacts on seed exudation contents. Experiment progression and NMs chosen for later experiments is visualised in Supplementary Information (SI) Scheme S3.1. Identifying which NM characteristics are most significant for predicting crop seed responses will aid in furthering understanding of which existing NMs are best suited to further

research. This would aid in permitting future commercialisation and will aid in re-design of NMs with enhanced properties.

3.3. Materials and Methods

3.3.1. Materials and characterisation

Metal oxides: TiO_2, TiO_2 coated with polyvinylpyrrolidine (PVP), TiO_2 coated with the polymer Solpus D540, a series of Zr-doped cerium oxide NMs starting from CeO_2, $Ce_{0.1}Zr_{0.9}O_2$, $Ce_{0.25}Zr_{0.75}O_2$, $Ce_{0.5}Zr_{0.5}O_2$, $Ce_{0.75}Zr_{0.25}O_2$, $Ce_{0.9}Zr_{0.1}O_2$ and a pure ZrO_2 for comparison, AlOOH, Fe_3O_4, CeO_2/Co_3O_4, $Co_{1.5}Fe_{1.5}O_4$, $Co_{2.25}Fe_{0.75}O_4$, $Co_{0.75}Fe_{2.25}O_4$, Fe_2O_3, Co_3O_4, ;

Zeolites: There were three beta structured zeolites (BEA) of different Si:Al ratios, BEA-12, BEA-19, BEA-150, three Socony Mobil-5 (ZSM-5) zeolites ZSM-5-40, ZSM-5-25, ZSM-5-15, mordenite zolite (MOR-10), ferrierite (FER), three crystalline sodium zeolites NaX, NaY, NaA, three crystalline potassium zeolites KX, KY, KA, maximum aluminiuum zeolite (MAP), Linde type L zeolite (LTL), and three natural clinoptilolite zeolites CW, CVZA, CVZB;

Metal organic frameworks: aluminium fumarate (AlFu), nickel-2,5-dioxido-1,4-benzenedicarboxylate (CPO-27(Ni)), iron-1,3,5-benzenetricarboxylate (Fe BTC), copper benzene-1,3,5-tricarboxylate (HKUST-1), $M_3O(H_2O)_2OH$(1,3,5-benzenetricarboxylate)$_2$ (MIL-100), $[K(H_2O)_2Co_3(cit)(Hcit)]$ (UTSA-16 (Co));

Nanopolymers: Three Poly([2-(Methacryloyloxy)ethyl]trimethylammonium chloride)-block-Poly(methyl methacrylate) (PQDMAEMA-PMMA) variants including $PQDMAEMA_{70}$-$P(MMA_{297}$-$MBA_3)$, $PQDMAEMA_{70}$-$P(MMA_{198}$-$MBA_2)$, $PQDMAEMA_{70}$-$P(MMA_{99}$-$MBA_1)$; two Poly(Dimethylacrylamide)-block-Poly(diacetone acrylamide) (PDMAm - PDAAm) variants, $PDMAm_{70}$-$P(DAAm_{45}$-$MBA_5)$ and $PDMAm_{70}$-$P(DAAm_{90}$-$MBA_{10})$;

Biochar derivatives: Beech biochar, hydroxyapatite-modified beech biochar, magnetite and hydroxyapatite dual functionalised beech biochar, magnetite-modified beech biochar, magnetite-modified hydroxyapatite particles.

A sub-set of 38 NMs based on the seed priming results were characterised pre- and post-exposure to wheat and lettuce seeds. Characterisation was achieved using the dynamic light scattering (DLS) instrument (Zetasizer, Malvern Instruments, UK) for hydrodynamic diameter of NMs to be captured, and zeta-potential of the NMs. NMs were dispersed in deionised (DI) water to 500 mg L^{-1}. NM samples underwent 15 minutes of continuous sonication in a sonic Elmasonic S 10 H sonic bath at <30˚C at 37kHz (Elma Schmidbauer GmbH, Singen, Germany) prior to measurements. Metal oxide nanomaterials were provided via the NanoSolveIT project (Grant Agreement No. 814572) and originally from Promethean Particles (UK), metal organic frameworks (MOFs) by Promethean Particles (UK), zeolites from Keele University (Stoke-on-Trent, UK), nanopolymers were synthesised and provided by Sam Parkinson (University of Birmingham, UK) following the synthesis procedure detailed in Parkinson et al. (2022). Further details on nanopolymer characterisation are in SI Figure S3.3. Beech biochar and its derivatives were synthesised and provided by Ify Leonard Ugbomeh (University of Birmingham, Birmingham, UK).

3.3.2. Seed priming

Wheat (*Triticum aestivum*) and lettuce (*Lactuca sativa*) seeds were used in seed priming experiments, representing dicot and monocot crops respectively. Seed sterilisation was performed using 1.5% NaClO solution (Sigma-Aldrich) for 15 minutes before thorough washing with DI water. 500 mg L^{-1} nanomaterial suspensions in DI water were sonicated for 15 minutes prior to exposure. Seeds were then incubated for 24 hours in these NM suspensions. DI water was used as a negative control. Seeds were separated from the NM suspensions and the leftover NM suspensions were stored at 4˚C before undergoing characterisation. The post-exposure seeds were plated on UV sterilised petri dishes with filter paper and 5 mL DI water before sealing with parafilm. Treatments were done in triplicate with 14 seeds per petri dish. The conditions for their incubation can be seen in SI Table S3.1. Seed germination counts were done at 0 hours, 24 hours, 48 hours and five days for lettuce seeds, and at 24 hours, 48 hours and seven days for wheat seeds. At the final day for each, all germinated seeds had their shoot and root lengths recorded. The remaining water in the petri dishes at the end of the incubation were stored for bicinchoninic acid (BCA) analysis to quantify proteins in the exudate. A seed was considered to have

germinated when the emergent radicle was determined to be half of the seed length or more. Shoot and root length were measured at the end of the incubation period for each crop species. Germination rate (Equation 3.1) and seedling vigour (Equation 3.2) were calculated.

$$\text{Germination rate (\%)} = \text{NG/NT x 100[Equation 3.1]}$$

[Equation 3.1]

where N_G is the number of germinated seedlings and N_T is the total number of seeds per plate.

$$Seedling\ vigour\ (cm\ \%) = (Root\ length + Shoot\ length)\ \times\ Germination\ rate$$

[Equation 3.2]

Root and shoot lengths were recorded for wheat and lettuce at day 7 and day 5, respectively.

Lettuce biomass was modelled using the collected fresh wheat seedling biomass. Wheat seedling biomass was recorded at the end of the 7 day growing period, with dry weight recorded after 48 hours in a 70˚C oven. To estimate lettuce fresh biomass, the combined root and shoot length of the wheat was plotted against wheat fresh biomass (Equation 3.3). The resulting equation of the line of best fit was calculated for wheat:

$$Biomass = 0.0809\ \times\ (Root\ length + Shoot\ length) + 0.7279$$

[Equation 3.3]

This equation (R^2 = 0.8455) was then applied to the subset of NMs used for lettuce protein exudate analysis to estimate fresh lettuce seedling biomass at the end of the studied germination period.

3.3.3. Bicinchoninic acid (BCA) Protein assay

Seed exudate protein content was analysed using the BCA assay (ThermoFisher, UK). After the 5 or 7 day incubation period, the remaining water in each petri dish was removed (~5 mL) and stored at 4˚C before analysis. The BCA assay was performed using bovine serum albumin (BSA) standards according

to the detailed ThermoFisher protocol. Readings were taken from the Tecan Spark microplate (Tecan, UK) at 562 nm absorbance. Blank readings containing DI water in place of the sample were subtracted for base-corrected protein concentrations.

3.3.4. Statistics

All statistical analyses were conducted using R Studio (v4.3.1; R Core Team, 2024). The significance level was set at $p = 0.05$. Data was assessed for normality and homogeneity of variance using Shapiro-Wilk and Levene's tests. Statistical analyses were performed on the root length, shoot length, germination rate, seedling vigour, biomass and seed exudate protein concentration data to determine the significance of results. When the assumptions of normality and homogeneity of variance were met, parametric analysis was used. A one-way analysis of variance (ANOVA) followed by a Tukey post-hoc test was used. If data were not normally distributed then a non-parametric equivalent was used, the Kruskal-Wallis with a Dunn post-hoc. A principal component analysis (PCA) was performed on root and shoot length, germination rate, seedling vigour, fresh biomass and seed exudate protein content data for lettuce and wheat. Another PCA was performed using the 54 NM set of results for root and shoot length, germination rate and seedling vigour also. A spearman rank correlation test was performed on pre- and post-exposure characterisation data for the 38 NMs in comparison with their results for root length, shoot length and final germination rate for wheat and lettuce.

3.4. Results and Discussion

Wheat and lettuce display differential responses between and within themselves to different NM treatments across all studied seed growth parameters. There are also clear distinctions between NM groups. Metal oxides and zeolites showed a range of different effects on wheat and lettuce seeds, with the same NM being affected very differently by wheat or lettuce seed exposure. MOFs had toxic inhibitory effects at this concentration. A subset of the results is displayed in Figures 3.1 and 3.2 for clarity. For the full set of results see SI Table S3.2.

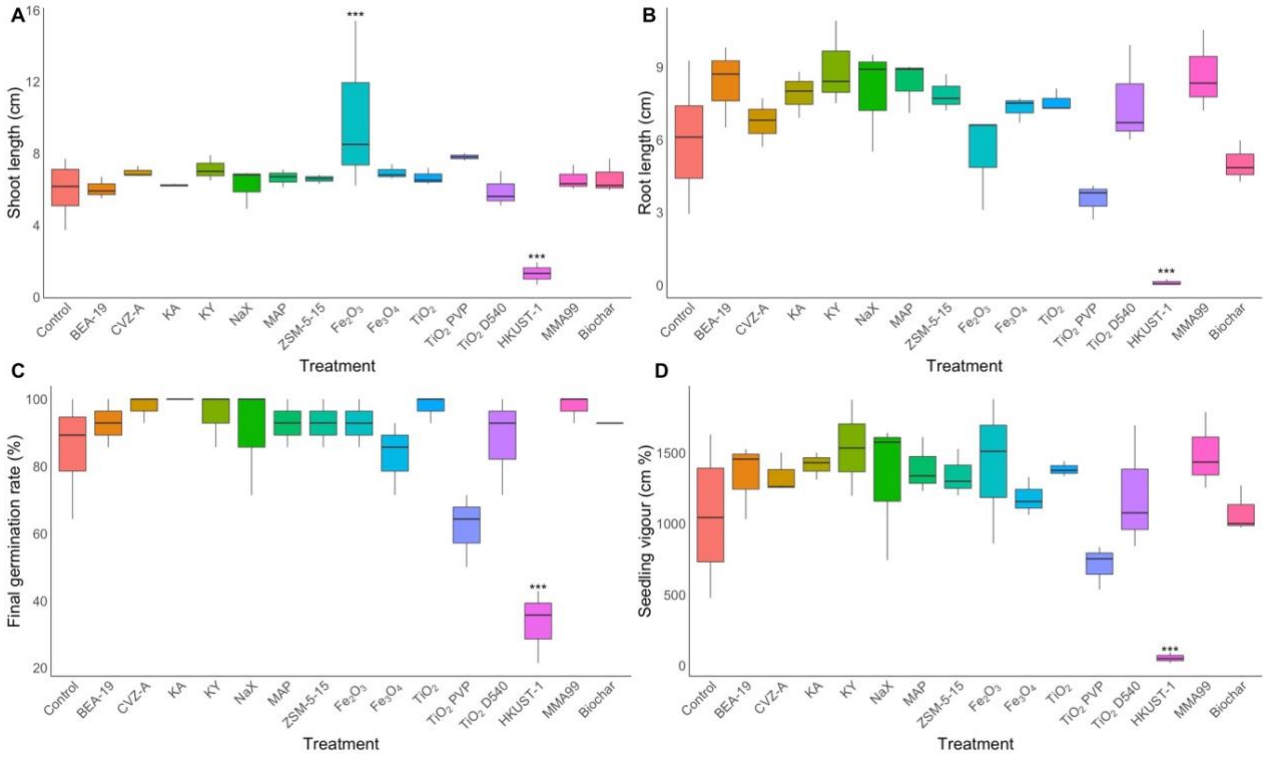


Figure 3.1. Wheat shoot (A) and root (B) length; germination rate at day 7 (C) and seedling vigour (D). Error bars reflect standard deviation. Data were analysed using ANOVA tests followed by Tukey tests for post-hoc analysis. Stars are used to denote statistically significantly different results relative to the Control ($p < 0.001$ ***). Note that the full set of 54 NMs effects can see seen in SI Table S3.2.

After germination, seeds typically invest greater energy into shoot rather than root growth, as seen in Fig. 3.1A and 3.1B. Wheat seeds showed improved shoot length under treatment with Fe_2O_3, ($p=1.15x10^{-4}$). Fe_2O_3 is a metal oxide, however observed responses by other metal oxides varied. Fe-based metal oxide performance differed depending on the oxidation state of Fe, with Fe_3O_4 having average or below average germination. Another metal oxide studied, TiO_2 produced different effects on wheat seeds depending on its coating. TiO_2 with the polymer poly-vinyl pyrrolidone (PVP) reduced wheat germination and root growth compared to TiO_2 without a polymer coating. PVP has been used to increase NM stability but may also limit its effects (Rafiei et al., 2021). TiO_2 D540 is a TiO_2 NM with a Solplus D540 polymer coating; the D540 coated TiO_2 decreased wheat seedling vigour, indicating that polymeric coatings of TiO_2 can have significant impacts on NM reactivity.

Another group of NMs, MOFs, showed different effects on wheat seeds The MOF HKUST-1 had a statistically significant negative effect, reducing germination rate, root and shoot growth and seedling vigour in wheat seeds. For HKUST-1 this inhibitory trend was consistently significantly different to the control ($p=1.19x10^{-6}$) and most of the other NM treatments (Fig. 3.1A-D). HKUST-1 is a copper-based benzene MOF, and agricultural soils typically have copper concentrations in the range of 2-100 mg kg^{-1} (Kumar et al., 2021). Dissolution of the copper from the rest of the metal organic framework is likely causing this toxic effect to the seeds, with 500 mg L^{-1} HKUST-1 shown to release ~4.5 mg L^{-1} Cu (Loera-Serna et al., 2024). Aggregation and dissolution of metal ions from their NM structures occurs in response to biotic and abiotic changes in their environment, including shifts in pH, dissolved oxygen, and biologically induced transformations, e.g. sulfidation, phosphorylation, and adsorption of proteins (Louie et al., 2014). The dissolution predicted here may be influenced by seed exudates, with previous research showing that Ag NPs dissociate to release Ag^{+} in response to dissolved organic matter (DOM) exuded by aquatic plants (Unrine, et al., 2012). Lower NM concentrations may be preferable in seed priming applications of MOFs. Also, using MOFs that consist of elements that are more tolerable to, or actively used by, microbial metabolism may prove to be a more sustainable option, as indicated by Anstoetz et al. (2016) work on oxalate-phosphate-amine (OPA) MOFs. Anstoetz et al. (2016) concluded that a concentration of 1-50 mg L^{-1} was optimal for OPA-MOF applications in agriculture. A dose-response study of HKUST-1, and the other MOFs utilised in this study, may show positive effects on wheat germination parameters at lower concentrations than used here, potentially showing hormetic effect at sufficiently low concentrations.

Wheat root growth (Fig. 3.1B) shows a positive effect in response to multiple NMs, including several zeolites, like BEA-19, KA, KY, MAP and ZSM-5-15. Engineered zeolites have regular structures, with varying Si:Al ratios, pore sizes and extra-framework cations. These zeolites had either NH_4^{+} ions (ZSM-5-15 and BEA-19) or Na^{+} and K^{+} ions (KY), with widely varying Si:Al ratios and pore sizes (see SI Table S3.4). BEA-19 and KY resulted in the most improved wheat seedling growth of the applied zeolites. The ions that they carry in their pores as part of the 3D structure may be acting to enhance growth through increased osmosis, due to the action of Na^{+} and K^{+} ions, which may act to

maintain a high water potential gradient allowing continued entrance of water into the seed (Zhou and Xiao, 2009).

The nanopolymer MMA99 displayed non-significant, elevated wheat root growth. These are the smallest of the Poly[2 (Dimethylamino)ethyl Methacrylate]-poly(methyl methacrylate (PQDMAEMA-PMMA) particles with recorded size of 71nm and positive surface charge. These soft plastic nanopolymers are self-assembled from differently charged homopolymers to create nanopolymers of varying polymer chain lengths and charges and can be utilised in agrochemical delivery (Parkinson et al., 2022; Sikder et al., 2021). The positive charge may allow them to bind to the seed tissues better than other, negatively charged nanopolymers which may be subject to uptake. Positive charge has been shown to limit passage into cells due to electrostatic interactions with plant cell walls, which may be occurring here also (Parkinson et al., 2022; He et al., 2010).

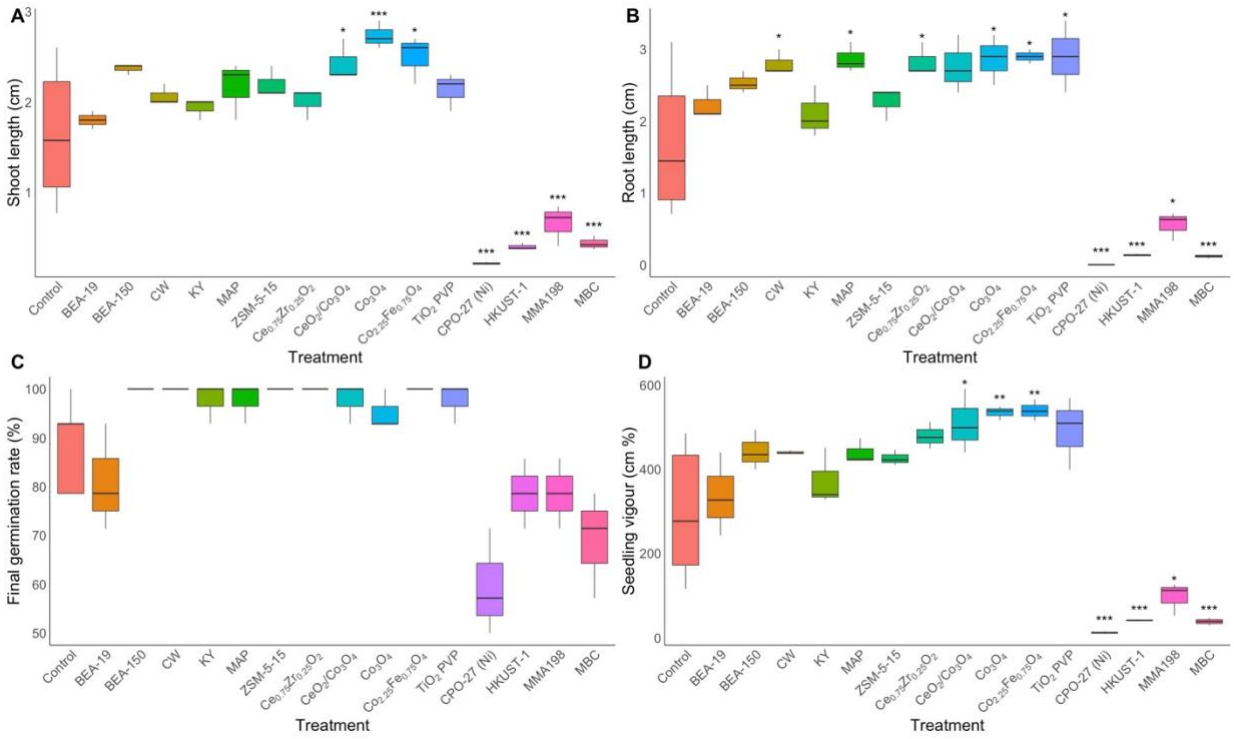


Figure 3.2. Lettuce shoot (A) and root (B) length; final germination rate (C) and seedling vigour (D). Error bars reflect standard deviation from the mean. Data for shoot length, root length and seedling vigour were analysed using ANOVA tests followed by Tukey tests for post-hoc analysis. Final germination rate data was tested for statistical significance using a Kruskal-Wallis test followed by a Bonferroni corrected Dunn's test. Stars are used to denote statistically significantly different results compared to the Control ($p < 0.05$ *; $p < 0.01$ **; $p < 0.001$ ***). Note that the full set of 54 NMs effects can see seen in SI Table S3.2.

Several cobalt-based metal oxides performed positively across lettuce seed metrics (Fig. 3.2), including Co_3O_4, $Co_{1.5}Fe_{1.5}O_4$, $Co_{2.25}Fe_{0.75}O_4$ and CeO_2/Co_3O_4. Co isn't an essential element for plant growth however it does have important roles as cofactors in several important plant enzymes, with high concentrations of Co leading to tissue necrosis and abnormal root development (Hu et al., 2021; Minz et al., 2018). The Co containing UTSA-16 MOF's seedling vigour was statistically significantly lower than the control ($p= 0.0133$), with average seedling vigour reduced to 87 cm %, as compared to the control treatment's average seedling vigour of 299 cm %. Several of the NMs had full germination success for lettuce (100% germination rate across all 14 seeds for all three biological replicates) as shown in Fig. 3.2C, with BEA-150, $Ce_{0.75}Zr_{0.25}O_2$, $Co_{2.25}Fe_{0.75}O_4$, CW and ZSM-5-15 proving to significantly improve germination compared to the control ($p=0.021$). While the nanopolymer MMA99 provided a positive effect for wheat seed root growth, the nanopolymer MMA297 reduced lettuce seed germination significantly (Fig. 3.2C). Both are PQDMAEMA coated -PMMA particles with positive surface charges of ~3-mV and have been shown to accumulate on root surfaces rather than being taken up as with neutral or negatively charged polymeric NMs (Parkinson et al., 2022). These NMs are block-poly(methyl methacrylate) copolymers that self-assemble into different morphologies, like micelles or rods, and have been shown to be applicable in catalysis and biomedical applications (Antoun et al., 2001; Wan et al., 2022). NM shape has been shown to be important in biomedical contexts, altering NM entry into cells and their biodistribution (Khor et al., 2019). The effect of differing morphology and concentration of nanopolymers on lettuce and wheat was not studied in this body of work but could be a promising avenue for future research.

The MOF HKUST-1 had a negative effect on lettuce seed germination ($p=2.64x10^{-4}$) and other measured growth parameters as it had in wheat also, but another MOF, CPO-27 had an even greater negative impact on lettuce ($p=1.61x10^{-5}$), as seen in Fig. 3.2 A-D. CPO-27 is a nickel-based MOF that is well studied in industrial contexts and is utilised for its gas storage and separation abilities (Garzón-Tovar et al., 2015). Nickel is an essential plant micronutrient that is required at only 0.5 mg kg^{-1} and has been shown to be toxic to sensitive crop species at 10 mg kg^{-1} or greater (Liu et al., 2011). As with HKUST-1, the concentration utilised in this experiment is too great for the seeds and phytotoxicity is

the result. The strong negative impact of MOFs on seed germination may be through NM dissolution, with previous research indicating that metal oxide NMs can have greater impact on seeds than free metal ions (Tang et al., 2012).

The initial hypothesis expected that monocots and dicots would respond differently to the tested NMs, due to their differing seed morphologies, in particular the different seed coat thicknesses. This data reflects that lettuce seed responses to the same NMs as exposed to wheat varied significantly, with some responses similar across species, for example, MOF treatment stunted growth of both lettuce and wheat. Other NMs, like several metal oxides studied, produced species-specific effects. Positive effects on seed growth parameters were found in both wheat and lettuce exposed to KY, ZSM-5-15 and BEA-19, and all zeolites. Similarly, MOFs, like HKUST-1, consistently limited growth and germination across species. Metal oxides displayed highly species specific efficacy in seed germination enhancement and impact in general, with nanopolymers and biochar derivatives having limited or negative effects on both of the study species.

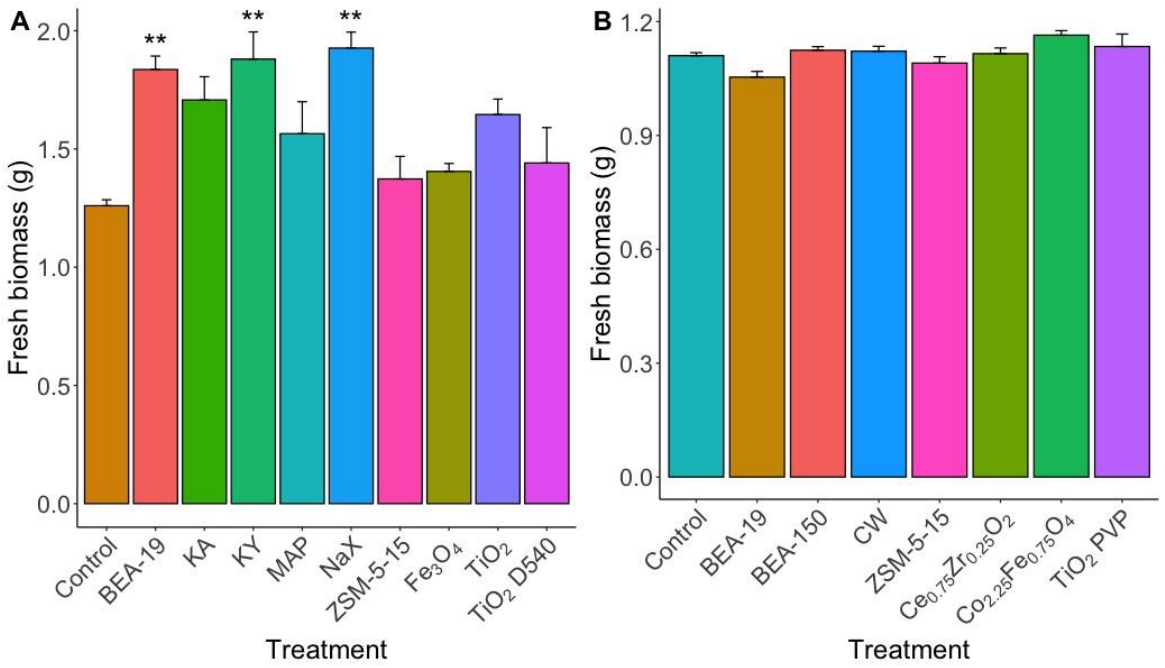


Figure 3.3. Wheat (A) biomass accumulation for NMs of interest. Lettuce (B) biomass estimation modelled from wheat-derived correlation for NMs of interest. Error bars depict standard error of the mean (SEM).

An initial 54 NMs were studied for their effects on wheat and lettuce seed priming, with a subset of 38 NMs taken forward for full characterisation based on the significance of results relative to the untreated control plants. Of these, a further 14 NMs had their biomass and seed exudates analysed, with full results for these available in SI Table S3.3.

Based on the data in Figures 3.1 and 3.2, a subset of the NMs used for the germination study were taken forward for further analysis comparing seedling fresh biomass and seed exudate protein contents between NM treatments. Of the tested NMs, 38 were selected and their detailed characterisation in deionised water was determined, as shown in Table 3.1. Based off the data in Figure 3.2A and 3.2B, lettuce biomass accumulation was modelled using an equation derived from the data in Figure 3.3A that linked root and shoot length of wheat seeds with their biomass ($R^2 = 0.8455$). NMs were chosen for their significance in at least one parameter of seed growth. Wheat seeds are larger than lettuce seeds and were able to accumulate more biomass, as expected, due to their morphological differences, e.g. differing sizes of their nutritive stores, different seed coat thickness. Wheat fresh biomass showed some statistically significant results, including between the negative control and BEA-19 (*p=0.0085*), KY (*p=0.0041*) and NaX (*p=0.00188*), as shown in Figure 3.3A. All three of the NMs that produced significant different in biomass are zeolites, with both KY and NaX producing positive impacts on wheat growth. Ky and NaX both have low Si:Al ratios of 2.6 and 1.3, respectively. Their extra-framework cations include Na^+, with KY also having K^+ ions present, and both zeolites have pore sizes of 7.4Å (as shown in SI Table S3.3). These cations and the zeolite's structures may be aiding in water absorption and osmotic entry of water into the seeds, promoting biomass accumulation. BEA-19 however, has a smaller pore size (6.8Å), NH_4^+ as its extra-framework cation and a high Si:Al ratio of 19. These results were not replicated in lettuce seedling biomass accumulation. In Fig. 3.3B, none of the treatments generated a meaningful difference in lettuce biomass relative to the control, with $Co_{2.25}Fe_{0.75}O_4$ and BEA-19 being significantly different to one another only (*p=0.0051*). Lettuce and wheat seeds' responses to zeolites were different for the fresh biomass values, even though lettuce seed biomass was modelled off of that for the wheat. This is potentially due to different modes of growth and morphological differences between monocot and dicot seed structures. Wheat seeds have a pericarp, an extra layer outside of the seed coat, this makes water imbibition more essential as wheat seeds are more

able to desiccate than dicot seeds and require greater water to regain metabolic activity (Sreenivasulu and Wobus, 2013). This, therefore, could explain the difference in zeolite efficacy at increasing seedling biomass in wheat but not lettuce. As zeolites have extra-framework ions, the ions may act on the wheat seed pericarp to promote osmosis and continued uptake of water, or there may be a direct interaction between the zeolites and the seed surface. Future studies should look at lettuce fresh biomass accumulation directly to provide a comparison to both modelled data and wheat data. Therefore, if the directly collected fresh biomass data is sufficiently comparable to the modelled data, this would provide evidence to support a future method for shorter seed priming comparison studies. However, due to differing modes of growth, with longer root and shoot lengths seen for wheat seedlings, there may be limited modelling from wheat to lettuce data, with more extreme differences in wheat seedlings seen as compared to in lettuce seedlings.

Table 3.1. Characterisation of the 38 NMs selected based on the seed priming results in terms of their hydrodynamic diameters and surface zeta potentials both pre- and post-exposure to either lettuce (*Lactuca sativa*) or wheat (*Triticum aestivum*) seeds. Orange shading indicates an increase/more negative value as compared to the pre-exposure characterisation and blue shading indicates a decrease/less negative.

Nanomaterial	**Hydrodynamic diameter (nm) (n=3)**			**Zeta potential (mV) (n=3)**		
	Pre-exposure	Post-exposure Lettuce	Post-exposure Wheat	Pre-exposure	Post-exposure Lettuce	Post-exposure Wheat
Metal oxides						
TiO_2	426.3 (±43.2)	634.1 (±160)	363.5 (±20.8)	-17.5 (±1.46)	-19.7 (±19.8)	-34.6 (±0.51)
TiO_2 D540	1227 (±103.6)	675 (±15.1)	151.3 (±3.03)	-45.8 (±0.25)	-39.1 (±1.27)	-33.2 (±1.06)
$Ce_{0.5}Zr_{0.5}O_2$	114.5 (±2.41)	203.3 (±7)	159.1 (±3.21)	52.1 (±6.7)	-34.5 (±0.29)	-18.9 (±1.77)
ZrO_2	99.11 (±108.3)	210.6 (±1.19)	115.9 (±2.32)	42.5 (±0.35)	29.8 (±0.56)	-24.8 (±0.67)
$Ce_{0.1}Zr_{0.9}O_2$	233.8 (±101.5)	221.4 (±2.63)	150.4 (±2)	45.4 (±1.62)	24.4 (±0.7)	-2.68 (± (±0.38)

Nanomaterial	Hydrodynamic diameter (nm) (n=3)			Zeta potential (mV) (n=3)		
	Pre-exposure	Post-exposure Lettuce	Post-exposure Wheat	Pre-exposure	Post-exposure Lettuce	Post-exposure Wheat
$Ce_{0.75}Zr_{0.25}O_2$	104.5 (±4.37)	1319 (±385.9)	9017.3 (±11798.5)	45.2 (±0.75)	-15.4 (±0.5)	-26.7 (±0.7)
$Ce_{0.25}Zr_{0.75}O_2$	69.91 (±14.6)	104.5 (±2.1)	161.9 (±3.99)	56.4 (±2.3)	34.9 (±1.18)	-20.9 (±0.59)
AlOOH	142.8 (±1.21)	3376 (±323.1)	26626.7 (±9805.8)	47.8 (±1.3)	4.18 (±0.09)	2.12 (±0.86)
$Ce_{0.9}Zr_{0.1}O_2$	271.5 (±33.9)	431.1 (±13.5)	286.0 (±14.2)	56.1 (±1.07)	0.413 (±3.32)	-27.1 (±0.36)
Fe_3O_4	108.9 (±1.44)	125.6 (±2.91)	97.0 (±2.77)	-48.3 (±1.56)	-34.5 (±0.68)	-37.9 (±1.2)
CeO_2/Co_3O_4	133.4 (±0.63)	718 (±96.6)	159.7 (±3.04)	51.1 (±1.03)	-18.9 (±0.17)	-25.1 (±0.85)
TiO_2 PVP	742.8 (±14.2)	2780 (±1480)	186.3 (±2.23)	-14.2 (±1.5)	-36 (±3.41)	-17.6 (±1.02)
$Co_{1.5}Fe_{1.5}O_4$	410.3 (±2.83)	170.7 (±0.6)	610.6 (±75.7)	17.8 (±0.25)	-28.3 (±0.9)	-28.8 (±0.1)
$Co_{2.25}Fe_{0.75}O_4$	511.6 (±7.31)	577.6 (±139.6)	141.7 (±6.39)	34.2 (±0.2)	-30.7 (±0.27)	-25.7 (±0.91)
$Co_{0.75}Fe_{2.25}O_4$	920.8 (±234.5)	344.3 (±2.4)	155.5 (±6.49)	-3.79 (±1.72)	-31.6 (±0.47)	-24.1 (±4.35)
Fe_2O_3	169.3 (±10.7)	655 (±85.6)	205.7 (±6.58)	47.5 (±1.36)	-31.3 (±0.15)	-28.7 (±0.2)
Co_3O_4	127.4 (±2.6)	177.1 (±3.67)	101.8 (±1.55)	45.5 (±0.95)	-30.3 (±0.66)	-26 (±0.4)
CeO_2	158.2 (±1.69)	286.3 (±9.91)	169.5 (±7.37)	54.7 (±0.72)	19 (±0.72)	-28.4 (±0.76)
Average change (%)		118	550		-151	-191
Zeolites						
BEA-12	925.2 (±313.8)	273.1 (±70.9)	228.4 (±33.7)	-34.7 (±0.67)	-33 (±2.93)	-28.2 (±0.83)

Nanomaterial	Hydrodynamic diameter (nm) (n=3)			Zeta potential (mV) (n=3)		
	Pre-exposure	Post-exposure Lettuce	Post-exposure Wheat	Pre-exposure	Post-exposure Lettuce	Post-exposure Wheat
BEA-19	997.8 (±196.8)	1182 (±55.8)	390.5 (±56.8)	-39.5 (±0.95)	-39.5 (±0.69)	-22.1 (±0.55)
MOR-10	564.5 (±27.9)	464.9 (±12.1)	285.4 (±11.8)	-45.7 (±0.27)	-41.9 (±0.78)	-40.8 (±0.79)
FER	753.8 (±29)	489.2 (±0.1)	310.2 (±22.7)	-25.4 (±0.36)	-34.9 (±3.01)	-33 (±0.27)
NaX	2291 (±152.2)	1773 (±839.5)	267.2 (±18.6)	-31.3 (±0.62)	-29.1 (±3.12)	-25 (±3.35)
NaY	870 (±45.2)	1389 (±197.2)	404.6 (±58.8)	-36.9 (±0.47)	-38.5 (±1.27)	-29.2 (±0.47)
NaA	704.7 (±37.4)	1092 (±216.9)	508 (±190)	-38.1 (±0.32)	-35.3 (±0.91)	-33.1 (±1.15)
KX	2004 (±378.9)	1064 (±78.6)	410.3 (±11.9)	-33.5 (±1.44)	-40.8 (±2.6)	-29 (±1.72)
KY	605.7 (±1.48)	346.5 (±55.6)	440.6 (±19.9)	-39.6 (±0.44)	-36.5 (±1.21)	-27.2 (±0.83)
KA	372.4 (±22.9)	20050 (±16110)	436.6 (±51.2)	-47.3 (±0.87)	-39.6 (±1.47)	-34.1 (±1.74)
MAP	452.4 (±7.11)	921.9 (±60.7)	142 (±18.7)	-44.9 (±0.71)	-41.3 (±0.79)	-30.9 (±1.11)
CW	502.7 (±37.8)	460 (±15.8)	361 (±26.5)	-27.1 (±0.95)	-34.1 (±0.51)	-26.4 (±1.22)
CVZA	991.4 (±156.3)	19940 (±32430)	256.4 (±7.27)	-42.7 (±2.08)	-29 (±2.7)	-28.8 (±0.96)
CVZB	572.2 (±52)	315.1 (±5.8)	176.1 (±4.82)	-32.8 (±0.66)	-24.1 (±4.15)	-28.1 (±1.11)
LTL	539.1 (±13.1)	447.3 (±9.73)	293.3 (±9.91)	-46.2 (±1.26)	-41.1 (±1.7)	-38.2 (±1.35)
BEA-150	704.4 (±2.71)	511 (±7.48)	270.9 (±9.5)	-42.5 (±0.64)	-39.1 (±0.84)	-30.4 (±1.42)
ZSM-5-40	1085 (±72.9)	773.2 (±95.8)	328.2 (±12.3)	-45.2 (±0.29)	-40.2 (±1.67)	-23.6 (±0.78)

Nanomaterial	Hydrodynamic diameter (nm) (n=3)			Zeta potential (mV) (n=3)		
	Pre-exposure	Post-exposure Lettuce	Post-exposure Wheat	Pre-exposure	Post-exposure Lettuce	Post-exposure Wheat
ZSM-5-25	425 (±37)	321.3 (±4.41)	210.5 (±4.19)	-38.6 (±0.86)	-37 (±0.92)	-31.6 (±2.01)
ZSM-5-15	631.3 (±12.7)	356.6 (±43.5)	250.9 (±4.71)	-28 (±0.66)	-41.4 (±0.59)	-27 (±0.74)
Average change (%)		226	-63		-3.28	-21.3

From the characterisation data presented in Table 3.1, it is clear that both hydrodynamic size and zeta potential vary widely across the NM groups. While there is a lot of variation in the dataset there are some visible trends, with initial hydrodynamic sizes of zeolites being larger than those of metal oxides by ~500 nm. This may be due to zeolites forming larger agglomerates than metal oxides rather than primary particle sizes being greater, something which requires verification through TEM. After exposure to seeds, whether lettuce or wheat, the average size of metal oxides increased, with a greater proportion increasing after exposure to lettuce than wheat seeds. This may be due to the higher surface area to volume ratio of the lettuce seeds resulting in a greater surface area for the NMs to interact with, or the greater surface area could be linked with a greater volume of seed exudates produced or seed exudates of a different composition to those of wheat. Nanomaterials in root exudates respond differently based on composition, with root exudates triggering NM agglomeration, creating larger aggregates over the course of five days (Cervantes-Avilés et al., 2021). Seed exudates typically contain sugars, in particular fructose and glucose, as well as proteins, amino acids, organic acids, ions and minerals. The most common organic acids to find in seed exudates are citric, succinic and malic acids, all of which have the potential to interact with the NMs, with organic acid production also being altered by NM treatment (Kamilova et al., 2006; Ghoto et al., 2020). Amino acids have varying charges as do proteins, which could be causing binding interactions and modulating zeta potential in this way. With the high proportion of zeolite's that became less negative after seed exposure, there is potential that the electrostatic

interactions that are possible between the NMs and the protein are causing the overall zeta potential of the compound to change (Patil et al., 2007; Xu et al., 2020).

The zeolite size and charge data differs here, with zeolite's recorded hydrodynamic sizes decreasing after exposure to lettuce and wheat seeds. This may be due to even greater aggregation of zeolites in response to seed exudates, which would lead to sedimentation and thus only smaller aggregates being detectable. It may also reflect that more negatively charged zeolites are more able to be taken up by seeds or bind to seed exudate compounds, as is seen in the high proportion of Fe_3O_4 NMs that were translocated in a study by Lau et al. (2020). TEM would be a useful method to distinguish to what extent the zeolites are aggregating and whether they are forming homoaggregates or binding to seed surface components or exudates.

Zeta potential also changes after exposure, with different patterns emerging for metal oxides compared to zeolites, and for those exposed to lettuce rather than wheat. Lettuce exposure causes the NMs to change their zeta potential less than after wheat seed exposure, -77 mV as opposed to -106 mV. After metal oxide exposure to wheat the zeta potential reduces by 191 mV, making the initially, largely positively charged particles negatively charged. Lettuce seeds have a similar effect on metal oxides but to a slightly lesser extent, as seen in Table 3.1. Zeolites, however, have negative zeta potential pre-exposure to seeds and become more positive after wheat seed exposure, on average by +8mV. After exposure to lettuce, zeta potential only increased by +1mV. Zeta potential is dependent on both the NM and the environment it is in, with adsorbed macromolecules likes proteins and polymers altering zeta potential (Lowry et al., 2016). Metal oxides zeta potential has been shown to be responsive to organic matter present in soybean root exudates and soil leachate, becoming more negative after contact, a trend that is also seen here with lettuce and wheat seed exudates (Cervantes-Aviles et al., 2021). Similarly, in the case of positively charged nanoceria (CeO_2) more positively charged NMs interacted with proteins more, altering their biocorona and onward reactivity or uptake (Patil et al., 2007). Seed, seedling and root exudates all differ in constituents and proportions; however, this research is unable to conclude whether it is the action of organic acids or proteins that have the greatest impact on NM transformations, and how they therefore alter NM fate, toxicity and bioavailability.

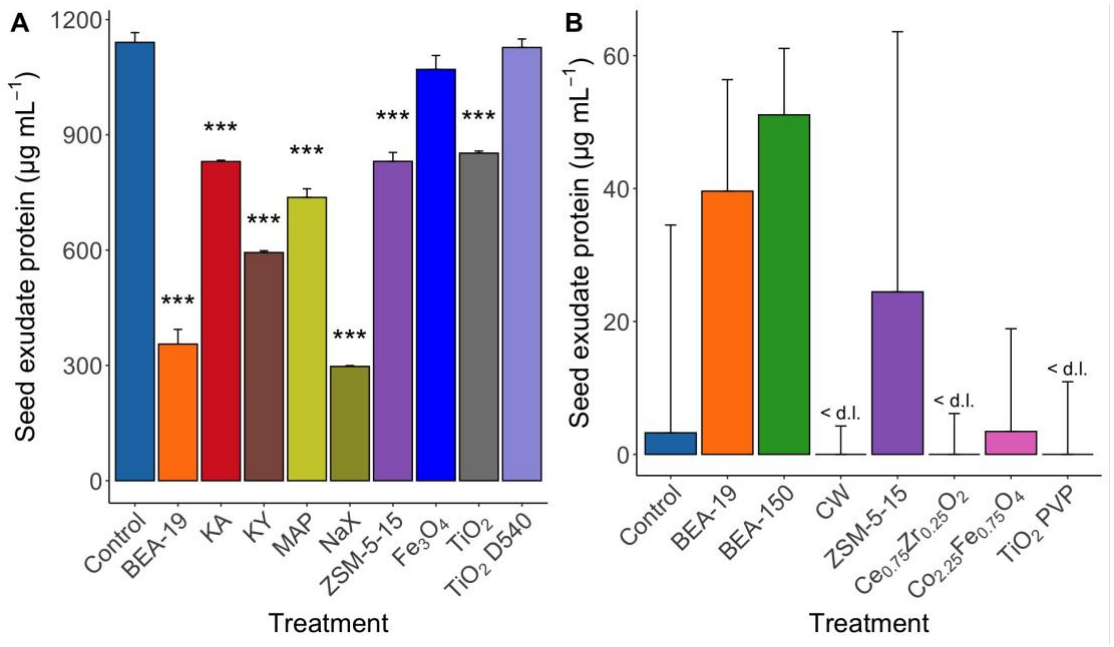


Figure 3.4. Seed exudate protein concentrations of wheat (A) and lettuce (B) seeds after NM exposure. Error bars reflect SEM. 3.4B indicates that protein concentration results for $Ce_{0.75}Zr_{0.25}O_2$, CW and TiO_2 PVP were below the limit of detection.

In order to further understand these impacts on the NMs, a final subset of the characterised NMs were used for a further seed priming experiment where seed exudates were collected after final germination rate was achieved and they were analysed for protein content. Seed exudates have previously been used in the biosynthesis of NMs, for example with Ag and Au nanoparticles (Lukman et al., 2011; Khatami et al., 2015). Seed exudates have been shown in these studies to change the oxidation state of a NM during synthesis, reflecting that redox reactions with NMs are an important avenue for NM transformation in biological systems. A positive correlation was found between seed size and amount of exudate released, due to increased storage material present inside larger seeds (Vančura and Hanzlíková, 1972). A BCA assay on the seed exudates, seen in Figure 3.4, shows highly differential protein exudation from wheat and lettuces seeds, with different accompanying trends. The greatest concentration of protein was present in the control wheat seeds, producing on average 1140 µg/mL of protein. Statistically significant differences to the control include BEA-19 ($p=2.88x10^{-14}$), KA ($p=1.73x10^{-7}$), KY ($p=7x10^{-12}$), MAP ($p=1.83x10^{-9}$), NaX ($p=2.18x10^{-14}$), TiO2 ($p=5.7x10^{-7}$) and ZSM-5-15 ($p=1.77x10^{-7}$). These significant results all reduced protein concentration in seed exudates as compared to the control, with varying effects on wheat seedling growth parameters. This may reflect an

imperfect link between NM effectiveness on seedling growth and impact on protein exudation. Seed and root exudates are used by plants to recruit mycorrhizal interactions that aid in delivery of water and nutrients to the crop (Nelson, 1990). In this context it may be that when nutrients are plentiful or osmotic pressure is permitting sufficient access to water then fewer exudates are produced. There are also major differences between these zeolites, in terms of Si:Al ratio, pore size, and extra-framework cations. There are high Si:Al ratios for BEA-19 (19) and ZSM-5-15 (15), similar particle sizes as determined by SEM (0.1 and 0.2µm, respectively) and the same extra-framework cation of NH_4^+. However, these very similar zeolites have significantly different results to one another also ($p=9.66x10^{-11}$).

The changes in protein exudation induced in wheat by the NMs are different to the effects of the same NMs on lettuce seed exudates. Lettuce seeds appear to exude far less protein in general than wheat, at 3 µg/mL for lettuce compared to wheat's 1140 µg/mL. But while wheat's significant changes showed a reduction in protein exudation, many of lettuce's protein exudate concentrations increased, particularly in response to zeolites. BEA-19 reduced wheat protein exudation and increased lettuce protein concentration as seen in Fig. 3.4B. BEA-150, BEA-19 and ZSM-5-15 increased protein concentration while CW, $Ce_{0.75}Zr_{0.25}O_2$ and TiO_2 reduced protein concentration to below the limit of detection. CW is a naturally occurring clinoptilolite zeolite with the extra-framework cations of K^+, Na^+, Ca^{2+} and Fe^{3+}. It may be that these ions increased water uptake or were themselves used in seed metabolism, reducing the plant's need to produce seed exudates to encourage microbial interactions with the plant (Martins et al., 2018). BEA-150 has a much larger Si:Al ratio than any of the other zeolites studied and, while not statistically significant, it increased the protein concentration in lettuce exudate. The most effective NMs in increasing lettuce protein exudation were the three zeolites listed above, all of which had relatively high Si:Al ratios. It may be due to this ratio that the positive effect on protein exudation has occurred, but why in lettuce and not in wheat remains unclear.

The core limitation to studying protein content of seed exudates only is while the BCA assay is able to detect several amino acids it cannot detect all of them. Seed exudates contain more amino acids than chained proteins, with NM exposure previously shown to reduce protein content of vegetable seed exudates (Kamilova et al., 2006). Future research should study a wider breadth of exudate constituents, for example, using total organic carbon (TOC) and total nitrogen (TN) analyses of seed exudates to

better determine overall chemical makeup of exudates and changing C:N ratios in response to NMs. As mentioned earlier, organic acids may be crucial to understanding NM transformations in response to plant exudates; confirmation of this would require a dedicated exudate response study and analysis by liquid chromatography with triple quadrupole mass spectrometry (LC-MS/MS).

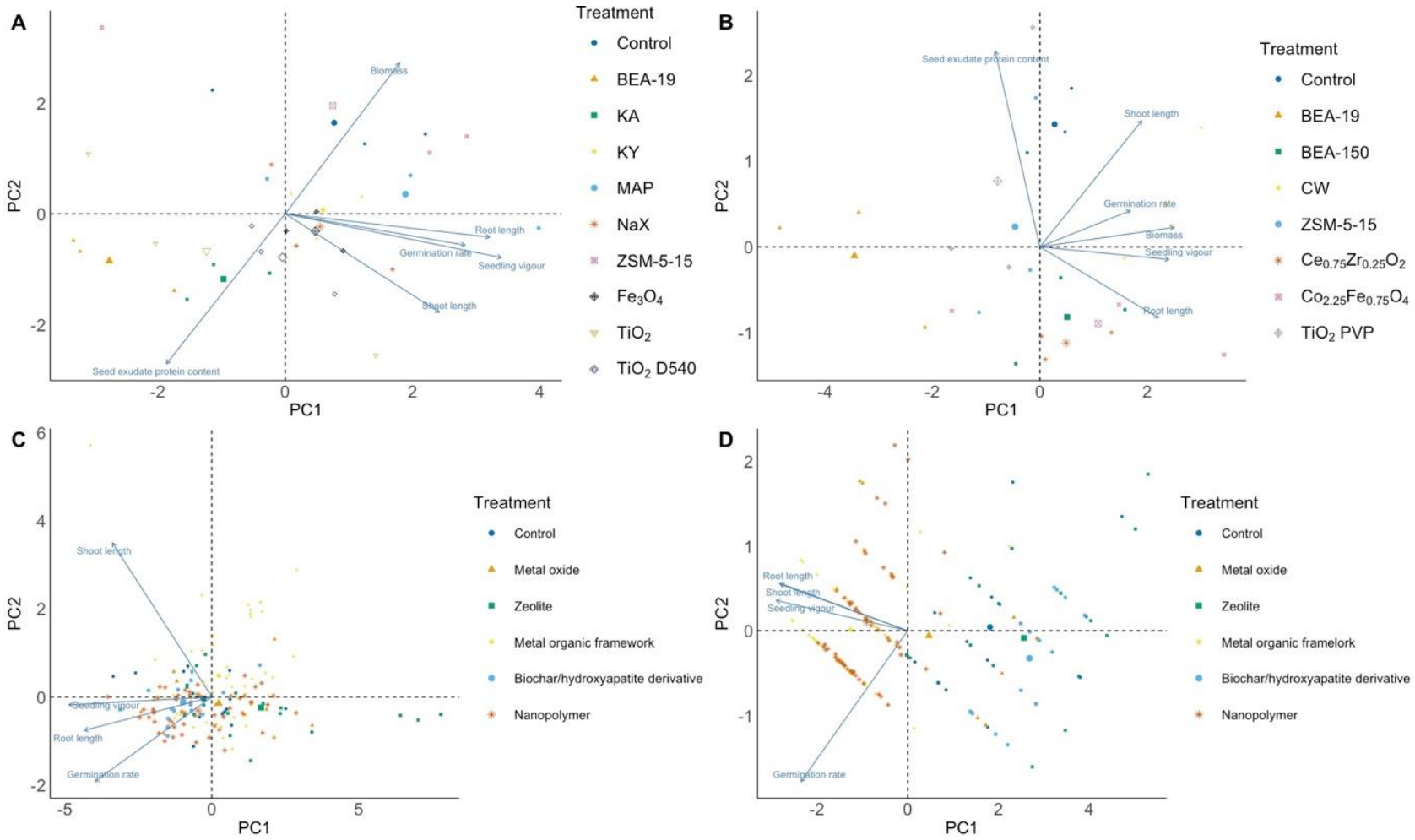


Figure 3.5. PCA correlation biplots of wheat (A) and lettuce (B), looking at protein content of exudates, shoot and root length, total fresh biomass, final germination rate and seedling vigour (SV) in response to a subset of 8 NMs each. Lettuce biomass data used in (B) has been modelled using Equation 3.3 as derived from the relationship between total seedling length and biomass of wheat seedlings, detailed in the methods. PCA biplots of data from 54 NM seed priming experiments on wheat (C) and lettuce (D), where NMs have been grouped by NM type.

In Fig 3.5A, the protein content of the wheat exudate and the wheat seedlings fresh biomass show a negative correlation. This reflects a link between growth and exudate, with greater biomass accumulation resulting in wheat seedling's focussing their efforts on energetically productive internal metabolism, reducing the amount of nutrient and amino acids lost as exudates. If a plant is successful by itself then it doesn't need to attract mycorrhizal fungi to aid it in its acquisition of nutrients and water (Huey et al., 2020). As seeds germinate, they undergo a fundamental shift in gene expression and development, triggering a release of metabolites, like carbohydrates, vitamins and amino acids. The function of these seed exudates is varied, generating ecochemical zones to aid nodulation by *Rhizobium* bacteria or inhibit growth of pathogenic fungi and bacteria (Hartwig et al., 1991). NMs have been shown to interfere with symbiotic nitrogen fixation, with a change in gene expression resulting in suppression of nodulation and downstream responses to root exudates (Mortimer et al., 2020). The changes seen in response to NM presence in seed exudate protein concentration could indicate a shift in strategy by the seeds. Under high nutrient availability growth and biomass accumulation may be prioritised, and the requirement to form mycorrhizal relationships will be reduced. This would aid in explaining why there is such a negative correlation between protein concentration in exudates and seedling biomass. While the Mortimer et al. (2020) study links NMs, seed exudates and symbiotic nitrogen fixation, the molecular basis of mycorrhizal interactions is similar to that of N-fixing bacteria-plant root interactions, with plant derived signalling compounds secreted to allow mycorrhizae to initiate the interaction in soil. Alternatively, previous studies have found that NM application deteriorates the symbiotic relationship between plants and mycorrhizal fungi (Feng et al., 2013). This has been stated to be via a range of mechanisms including reducing root mycorrhizal colonisation (Cao et al., 2017). A potential mechanism to reduce mycorrhizal colonisation could be through disruption of the initial signalling mechanism between roots and mycorrhiza, which is mediated through root exudates.

Positively correlated wheat growth parameters are germination, root length and seedling vigour. Seedling vigour is calculated from root and shoot length, and germination rate, explaining the close relationship between these parameters. Most of the wheat data's range (Fig. 3.5A) is derived from its

protein and biomass parameters, while in lettuce the spread of data is defined largely by protein concentration and root length, two negatively correlated parameters (Fig. 3.5B). In lettuce the main positive correlation is between seedling vigour and biomass, both of which are heavily impacted by shoot and root lengths, however these show no correlation in wheat. This is due to the modelling methods used where lettuce biomass was estimated from root and shoot lengths, which is why it sits between the two and is therefore not an independent parameter. With the lack of correlation shown between wheat biomass and shoot and root lengths in Fig. 3.5A, this indicates that using these parameters to model biomass may have large inaccuracies and other factors may play a more integral role in determining fresh biomass.

Figure 3.5C and 3.5D uses data from the full 54 NM seed priming screening. Fig. 3.5C shows that the wheat data's diversity is generated through the germination rate and shoot length, while root length and seedling vigour remain highly positively correlated. Lettuce data in Fig. 3.5D presents data that is overall less correlated. Germination rate continues to be a core driver of data diversity, but no correlative relationships between parameters appears to be very strong.

Correlation tests of how NM hydrodynamic size and zeta-potential can be used to indicate clearly how NMs' physical characteristics may be impacting on monocot and dicot seedling growth and germination. From these correlative tests it may be more possible to identify qualities to screen for in nanopriming, and which to avoid. There is limited presence of a pattern based on the NM chemical characteristics reported here. While Co-based metal oxides improved lettuce germination parameters, MOFs, including the ones containing Co, stunted seedling vigour at the studied concentration of 500 mg L^{-1}. Zeolites can affect wheat and lettuce exudates differently and even zeolites with similar Si:Al ratios, extra-framework cations, pore sizes and primary particle sizes can produce different results within the same species. A negative correlation was found between the pre-exposure zeta potentials of NMs and seedling vigour in wheat ($\rho = -0.433, p = 0.00788$), slightly weaker negative correlation seen between zeta potential of NMs after exposure to wheat seeds, approaching statistical significance ($\rho = -0.286, p = 0.086$). The zeta potential of NMs pre- and post-exposure to wheat seeds is linked but the effect of exposure to the wheat seeds on zeta potential is not consistent across the NMs, as seen in Table

3.1. There was also a positive correlation between wheat root length and pre-exposure size of NMs ($\rho = 0.359, p = 0.029$) and shoot length and post-exposure zeta of NMs ($\rho = 0.337, p = 0.0417$). Negative correlations were found between wheat shoot length and post-exposure hydrodynamic size ($\rho = -0.367, p = 0.0265$); root length and pre-exposure zeta potential ($\rho = -0.589, p = 0.000125$) and final germination rate and pre-exposure zeta potential ($\rho = -0.355, p = 0.0309$). Lettuce seed growth also had no statistically significant correlative relationships with any of the NM parameters recorded. These correlations could be indicative that pre-exposure characteristics are more influential on root growth, with larger NM agglomerates that are more negatively charged increasing root length. Post-exposure characteristics are more significant for shoot length, with more positive and smaller NMs correlated with longer shoots. Due to the lack of correlation found for the lettuce seeds, it may be that other NM characteristics are of greater significance, for example, NM composition or extent of dissolution (Liu et al., 2016; Liu et al., 2021).

3.5. Conclusion

Hydrodynamic size and zeta potential of zeolites and metal oxides can be used to predict the general trend of lettuce and wheat responses; however, correlations are NM-crop species specific and further modelling is required to disentangle which NM properties have the most significant effect on improving crop growth efficacy. Metal oxides show species-specific responses, with nanopolymers and biochar derivatives having limited impact. MOFs, like HKUST-1 and CPO-27, showed highly inhibitory effects on both wheat and lettuce growth, potentially through ion dissolution. 500 mg L^{-1} was seen to be an appropriate concentration for some of the NMs but sufficiently high for others to trigger toxicity in the seeds, for example, the MOFs HKUST-1 and CPO-27. Interrogating dose-responses of the two crop species' seeds would permit insights into functional concentrations for future commercialisation and reflect any potential dose-based phytotoxic or hormetic effects. While the conclusions from this study are specifically relating to lettuce and wheat, they may inform directions for NM seed priming research in other dicot and monocot crops.

Responses of wheat and lettuce seeds differ for the same NMs, and different trends are seen in NM agglomeration and surface charge in response to seed exposure and resulting seed exudates. NM aggregation may be induced by seed exposure or binding of NMs to seed surfaces, leading to post-exposure hydrodynamic sizes being reduced. TEM imaging of particles before and after exposure would aid in elucidating to what extent the NMs' hydrodynamic size changes are through seed coat interactions, homo- or heteroaggregation. There is potential that some of the responses induced in seeds by NMs exposure is through the action of seed exudates. Protein in wheat seed exudates is decreased by NM exposure but increases upon lettuce seed exposure to some zeolites; this is predicted to be due to nutrient and water uptake where optimal growth conditions reduce seed exudation. Analysis of seed exudates for organic acids, proteins and amino acids that are undetectable by BCA assay could also prove to be of interest.

References

An, J., Hu, P., Li, F., Wu, H., Shen, Y., White, J.C., Tian, X., Li, Z., Giraldo, J.P., 2020. Emerging investigator series: molecular mechanisms of plant salinity stress tolerance improvement by seed priming with cerium oxide nanoparticles. Environ. Sci.: Nano 7, 2214–2228. https://doi.org/10.1039/D0EN00387E

Anstoetz, M., Sharma, N., Clark, M., Yee, L.H., 2016. Characterization of an oxalate-phosphate-amine metal–organic framework (OPA-MOF) exhibiting properties suited for innovative applications in agriculture. J Mater Sci 51, 9239–9252. https://doi.org/10.1007/s10853-016-0171-6

Antoun, S., Gohy, J.-F., Jérôme, R., 2001. Micellization of quaternized poly(2-(dimethylamino)ethyl methacrylate)-*block*-poly(methyl methacrylate) copolymers in water. Polymer 42, 3641–3648. https://doi.org/10.1016/S0032-3861(00)00746-1

Avellan, A., Yun, J., Zhang, Y., Spielman-Sun, E., Unrine, J.M., Thieme, J., Li, J., Lombi, E., Bland, G., Lowry, G.V., 2019. Nanoparticle Size and Coating Chemistry Control Foliar Uptake Pathways, Translocation, and Leaf-to-Rhizosphere Transport in Wheat. ACS Nano 13, 5291–5305. https://doi.org/10.1021/acsnano.8b09781

Bayat, M., Zargar, M., Murtazova, K.M.-S., Nakhaev, M.R., Shkurkin, S.I., 2022. Ameliorating Seed Germination and Seedling Growth of Nano-Primed Wheat and Flax Seeds Using Seven Biogenic Metal-Based Nanoparticles. Agronomy 12, 811. https://doi.org/10.3390/agronomy12040811

Bertini, L., Proietti, S., Focaracci, F., Sabatini, B., Caruso, C., 2018. Epigenetic control of defense genes following MeJA-induced priming in rice (Oryza sativa). Journal of Plant Physiology 228, 166–177. https://doi.org/10.1016/j.jplph.2018.06.007

Bewley, J., 1997. Seed Germination and Dormancy. Plant Cell 9, 1055–1066.

Cao, J., Feng, Y., Lin, X., Wang, J., Xie, X., 2017. Iron oxide magnetic nanoparticles deteriorate the mutual interaction between arbuscular mycorrhizal fungi and plant. J Soils Sediments 17, 841–851. https://doi.org/10.1007/s11368-016-1561-8

Cervantes-Avilés, P., Huang, X., Keller, A.A., 2021. Dissolution and Aggregation of Metal Oxide Nanoparticles in Root Exudates and Soil Leachate: Implications for Nanoagrochemical Application. Environ. Sci. Technol. 55, 13443–13451. https://doi.org/10.1021/acs.est.1c00767

Chen, K., Arora, R., 2013. Priming memory invokes seed stress-tolerance. Environmental and Experimental Botany, Cross-stress tolerance and stress "memory" in plants 94, 33–45. https://doi.org/10.1016/j.envexpbot.2012.03.005

DEFRA, 2024. Agriculture in the UK 2023: Chapter 7 - Crops [WWW Document]. GOV.UK. URL https://www.gov.uk/government/statistics/agriculture-in-the-united-kingdom-2022/chapter-7-crops (accessed 9.19.24).

DEFRA, 2021. Horticulture Statistics 2020.

do Espirito Santo Pereira, A., Caixeta Oliveira, H., Fernandes Fraceto, L., Santaella, C., 2021. Nanotechnology Potential in Seed Priming for Sustainable Agriculture. Nanomaterials 11, 267. https://doi.org/10.3390/nano11020267

Evenari, M., 1984. Seed Physiology: Its History from antiquity to the beginning of the 20th century. Bot. Rev 50, 119–142. https://doi.org/10.1007/BF02861090

Feng, Y., Cui, X., He, S., Dong, G., Chen, M., Wang, J., Lin, X., 2013. The Role of Metal Nanoparticles in Influencing Arbuscular Mycorrhizal Fungi Effects on Plant Growth. Environ. Sci. Technol. 47, 9496–9504. https://doi.org/10.1021/es402109n

Garzón-Tovar, L., Carné-Sánchez, A., Carbonell, C., Imaz, I., Maspoch, D., 2015. Optimised room temperature, water-based synthesis of CPO-27-M metal-organic frameworks with high space-time yields. J Mater Chem A Mater Energy Sustain 3, 20819–20826. https://doi.org/10.1039/C5TA04923G

Ghoto, K., Simon, M., Shen, Z.-J., Gao, G.-F., Li, P.-F., Li, H., Zheng, H.-L., 2020. Physiological and Root Exudation Response of Maize Seedlings to TiO2 and SiO2 Nanoparticles Exposure. BioNanoSci. 10, 473–485. https://doi.org/10.1007/s12668-020-00724-2

Guo, Z., Zhang, P., Chakraborty, S., Chetwynd, A.J., Abdolahpur Monikh, F., Stark, C., Ali-Boucetta, H., Wilson, S., Lynch, I., Valsami-Jones, E., 2021. Biotransformation modulates the penetration of metallic nanomaterials across an artificial blood–brain barrier model. Proceedings of the National Academy of Sciences 118, e2105245118. https://doi.org/10.1073/pnas.2105245118

Hao, Y., Zhang, Z.-T., Rui, Y.-K., Ren, J.-Y., Hou, T.-Q., Wu, S.-J., Rui, M.-M., Jiang, F.-P., Liu, L.-M., 2016. Effect of Different Nanoparticles on Seed Germination and Seedling Growth in Rice. Presented at the 2nd Annual International Conference on Advanced Material Engineering (AME 2016), Atlantis Press, pp. 166–173. https://doi.org/10.2991/ame-16.2016.28

Hartwig, U.A., Joseph, C.M., Phillips, D.A., 1991. Flavonoids Released Naturally from Alfalfa Seeds Enhance Growth Rate of *Rhizobium meliloti*. Plant Physiol. 95, 797–803. https://doi.org/10.1104/pp.95.3.797

He, C., Hu, Y., Yin, L., Tang, C., Yin, C., 2010. Effects of particle size and surface charge on cellular uptake and biodistribution of polymeric nanoparticles. Biomaterials 31, 3657–3666. https://doi.org/10.1016/j.biomaterials.2010.01.065

Hu, X., Wei, X., Ling, J., Chen, J., 2021. Cobalt: An Essential Micronutrient for Plant Growth? Front. Plant Sci. 12. https://doi.org/10.3389/fpls.2021.768523

Huey, C.J., Gopinath, S.C.B., Uda, M.N.A., Zulhaimi, H.I., Jaafar, M.N., Kasim, F.H., Yaakub, A.R.W., 2020. Mycorrhiza: a natural resource assists plant growth under varied soil conditions. 3 Biotech 10, 204. https://doi.org/10.1007/s13205-020-02188-3

Iqbal, M., Ashraf, M., 2013. Gibberellic acid mediated induction of salt tolerance in wheat plants: Growth, ionic partitioning, photosynthesis, yield and hormonal homeostasis. Environmental and Experimental Botany, Special Issue: Phytohormones and Stress 86, 76–85. https://doi.org/10.1016/j.envexpbot.2010.06.002

Kamilova, F., Kravchenko, L., Shaposhnikov, A., Azarova, T., Makarova, N., Lugtenberg, B., 2006. Organic Acids, Sugars, and l -Tryptophane in Exudates of Vegetables Growing on Stonewool and Their Effects on Activities of Rhizosphere Bacteria. Molecular plant-microbe interactions : MPMI 19, 250–6. https://doi.org/10.1094/MPMI-19-0250

Kanojia, A., Dijkwel, P.P., 2018. Abiotic Stress Responses are Governed by Reactive Oxygen Species and Age, in: Roberts, J.A. (Ed.), Annual Plant Reviews Online. Wiley, pp. 295–326. https://doi.org/10.1002/9781119312994.apr0611

Khan, M.N., Fu, C., Li, J., Tao, Y., Li, Y., Hu, J., Chen, L., Khan, Z., Wu, H., Li, Z., 2023. Seed nanopriming: How do nanomaterials improve seed tolerance to salinity and drought? Chemosphere 310, 136911. https://doi.org/10.1016/j.chemosphere.2022.136911

Khan, M.N., Mobin, M., Abbas, Z.K., AlMutairi, K.A., Siddiqui, Z.H., 2017. Role of nanomaterials in plants under challenging environments. Plant Physiology and Biochemistry, Effects of Nanomaterials in Plants 110, 194–209. https://doi.org/10.1016/j.plaphy.2016.05.038

Khatami, Mehrdad, Pourseyedi, S., Khatami, Mansour, Hamidi, H., Zaeifi, M., Soltani, L., 2015. Synthesis of silver nanoparticles using seed exudates of Sinapis arvensis as a novel bioresource, and evaluation of their antifungal activity. Bioresour. Bioprocess. 2, 19. https://doi.org/10.1186/s40643-015-0043-y

Khor, S.Y., Quinn, J.F., Whittaker, M.R., Truong, N.P., Davis, T.P., 2019. Controlling Nanomaterial Size and Shape for Biomedical Applications via Polymerization-Induced Self-Assembly. Macromolecular Rapid Communications 40, 1800438. https://doi.org/10.1002/marc.201800438

Kladko, D.V., Falchevskaya, A.S., Serov, N.S., Prilepskii, A.Y., 2021. Nanomaterial Shape Influence on Cell Behavior. International Journal of Molecular Sciences 22, 5266. https://doi.org/10.3390/ijms22105266

Kumar, V., Pandita, S., Singh Sidhu, G.P., Sharma, A., Khanna, K., Kaur, P., Bali, A.S., Setia, R., 2021. Copper bioavailability, uptake, toxicity and tolerance in plants: A comprehensive review. Chemosphere 262, 127810. https://doi.org/10.1016/j.chemosphere.2020.127810

Lau, E.C.H.T., Carvalho, L.B., Pereira, A.E.S., Montanha, G.S., Corrêa, C.G., Carvalho, H.W.P., Ganin, A.Y., Fraceto, L.F., Yiu, H.H.P., 2020. Localization of Coated Iron Oxide (Fe3O4) Nanoparticles on Tomato Seeds and Their Effects on Growth. ACS Appl. Bio Mater. 3, 4109–4117. https://doi.org/10.1021/acsabm.0c00216

Liu, G., Simonne, E.H., Li, Y., 2011. Nickel Nutrition in Plants.

Liu, R., Zhang, H., Lal, R., 2016. Effects of Stabilized Nanoparticles of Copper, Zinc, Manganese, and Iron Oxides in Low Concentrations on Lettuce (Lactuca sativa) Seed Germination: Nanotoxicants or Nanonutrients? Water Air Soil Pollut 227, 42. https://doi.org/10.1007/s11270-015-2738-2

Liu, Y., Ma, Y., Jiao, C., Liu, M., Luo, W., Dong, C., Fan, S., He, X., Yang, F., Zhang, Z., 2021. Comparative toxicity of rod-shaped nano-CeO2 and nano-CePO4 to lettuce. Metallomics 13, mfab033. https://doi.org/10.1093/mtomcs/mfab033

Loera-Serna, S., Beltrán, H.I., Mendoza-Sánchez, M., Álvarez-Zeferino, J.C., Almanza, F., Fernández-Luqueño, F., 2024. Effect of HKUST-1 metal–organic framework in root and shoot systems, as well as

seed germination. Environ Sci Pollut Res Int 31, 13270–13283. https://doi.org/10.1007/s11356-023-31728-6

López-Vargas, E.R., González-García, Y., Pérez-Álvarez, M., Cadenas-Pliego, G., González-Morales, S., Benavides-Mendoza, A., Cabrera, R.I., Juárez-Maldonado, A., 2020. Seed Priming with Carbon Nanomaterials to Modify the Germination, Growth, and Antioxidant Status of Tomato Seedlings. Agronomy 10, 639. https://doi.org/10.3390/agronomy10050639

Louie, S.M., Ma, R., Lowry, G.V., 2014. Chapter 2 - Transformations of Nanomaterials in the Environment, in: Lead, J.R., Valsami-Jones, E. (Eds.), Frontiers of Nanoscience, Nanoscience and the Environment. Elsevier, pp. 55–87. https://doi.org/10.1016/B978-0-08-099408-6.00002-5

Lowry, G.V., Hill, R.J., Harper, S., Rawle, A.F., Hendren, C.O., Klaessig, F., Nobbmann, U., Sayre, P., Rumble, J., 2016. Guidance to improve the scientific value of zeta-potential measurements in nanoEHS. Environ. Sci.: Nano 3, 953–965. https://doi.org/10.1039/C6EN00136J

Lukman, A.I., Gong, B., Marjo, C.E., Roessner, U., Harris, A.T., 2011. Facile synthesis, stabilization, and anti-bacterial performance of discrete Ag nanoparticles using Medicago sativa seed exudates. Journal of Colloid and Interface Science 353, 433–444. https://doi.org/10.1016/j.jcis.2010.09.088

Martins, S.J., Medeiros, F.H.V., Lakshmanan, V., Bais, H.P., 2018. Impact of Seed Exudates on Growth and Biofilm Formation of Bacillus amyloliquefaciens ALB629 in Common Bean. Front Microbiol 8, 2631. https://doi.org/10.3389/fmicb.2017.02631

Minz, A., Kumari Sinha, A., Kumar, R., 2018. A Review on Importance of Cobalt in Crop Growth and Production. Int.J.Curr.Microbiol.App.Sci 2978–2984.

Mittler, R., Zandalinas, S.I., Fichman, Y., Van Breusegem, F., 2022. Reactive oxygen species signalling in plant stress responses. Nat Rev Mol Cell Biol 23, 663–679. https://doi.org/10.1038/s41580-022-00499-2

Mortimer, M., Li, D., Wang, Y., Holden, P.A., 2020. Physical Properties of Carbon Nanomaterials and Nanoceria Affect Pathways Important to the Nodulation Competitiveness of the Symbiotic N2-Fixing Bacterium Bradyrhizobium diazoefficiens. Small 16, 1906055. https://doi.org/10.1002/smll.201906055

Motte, H., Vanneste, S., Beeckman, T., 2019. Molecular and Environmental Regulation of Root Development. Annual Review of Plant Biology 70, 465–488. https://doi.org/10.1146/annurev-arplant-050718-100423

Nelson, E.B., 1990. Exudate molecules initiating fungal responses to seeds and roots. Plant Soil 129, 61–73. https://doi.org/10.1007/BF00011692

Paparella, S., Araújo, S.S., Rossi, G., Wijayasinghe, M., Carbonera, D., Balestrazzi, A., 2015. Seed priming: state of the art and new perspectives. Plant Cell Rep 34, 1281–1293. https://doi.org/10.1007/s00299-015-1784-y

Parkinson, S.J., Tungsirisurp, S., Joshi, C., Richmond, B.L., Gifford, M.L., Sikder, A., Lynch, I., O'Reilly, R.K., Napier, R.M., 2022. Polymer nanoparticles pass the plant interface. Nat Commun 13, 7385. https://doi.org/10.1038/s41467-022-35066-y

Patil, S., Sandberg, A., Heckert, E., Self, W., Seal, S., 2007. Protein adsorption and cellular uptake of cerium oxide nanoparticles as a function of zeta potential. Biomaterials 28, 4600–4607. https://doi.org/10.1016/j.biomaterials.2007.07.029

Rafiei, H., Abbasian, M., Yegani, R., 2021. Polyvinylidene fluoride as a neat and the synthesized novel membranes based on PVDF/polyvinyl pyrrolidone polymer grafted with TiO2 nanoparticles through RAFT method for water purification. Iran Polym J 30, 769–780. https://doi.org/10.1007/s13726-021-00928-7

Rai, P.K., Song, H., Kim, K.-H., 2023. Nanoparticles modulate heavy-metal and arsenic stress in food crops: Hormesis for food security/safety and public health. Science of The Total Environment 902, 166064. https://doi.org/10.1016/j.scitotenv.2023.166064

R Core Team (2023). R: A language and environment for statistical computing. R Foundation for Statistical Computing, Vienna, Austria. URL https://www.R-project.org/.

Rhaman, M.S., Imran, S., Rauf, F., Khatun, M., Baskin, C.C., Murata, Y., Hasanuzzaman, M., 2021. Seed Priming with Phytohormones: An Effective Approach for the Mitigation of Abiotic Stress. Plants 10, 37. https://doi.org/10.3390/plants10010037

Rizwan, M., Ali, S., Qayyum, M.F., Ok, Y.S., Adrees, M., Ibrahim, M., Zia-ur-Rehman, M., Farid, M., Abbas, F., 2017. Effect of metal and metal oxide nanoparticles on growth and physiology of globally important food crops: A critical review. Journal of Hazardous Materials, SI:Environmental Nanotechnol 322, 2–16. https://doi.org/10.1016/j.jhazmat.2016.05.061

Rojas, S., Rodríguez-Diéguez, A., Horcajada, P., 2022. Metal–Organic Frameworks in Agriculture. ACS Appl. Mater. Interfaces 14, 16983–17007. https://doi.org/10.1021/acsami.2c00615

Sikder, A., Pearce, A.K., Parkinson, S.J., Napier, R., O'Reilly, R.K., 2021. Recent Trends in Advanced Polymer Materials in Agriculture Related Applications. ACS Appl. Polym. Mater. 3, 1203–1217. https://doi.org/10.1021/acsapm.0c00982

Sreenivasulu, N., Wobus, U., 2013. Seed-Development Programs: A Systems Biology–Based Comparison Between Dicots and Monocots. Annual Review of Plant Biology 64, 189–217. https://doi.org/10.1146/annurev-arplant-050312-120215

Tang, Y.J., Wu, S.G., Huang, L., Head, J., Chen, D., Kong, I.C., 2012. Phytotoxicity of Metal Oxide Nanoparticles is Related to Both Dissolved Metals Ions and Adsorption of Particles on Seed Surfaces. J Pet Environ Biotechnol 03. https://doi.org/10.4172/2157-7463.1000126

Unrine, J.M., Colman, B.P., Bone, A.J., Gondikas, A.P., Matson, C.W., 2012. Biotic and Abiotic Interactions in Aquatic Microcosms Determine Fate and Toxicity of Ag Nanoparticles. Part 1. Aggregation and Dissolution. Environ. Sci. Technol. 46, 6915–6924. https://doi.org/10.1021/es204682q

Vančura, V., Hanzlíková, A., 1972. Root exudates of plants. Plant Soil 36, 271–282. https://doi.org/10.1007/BF01373482

Wan, J., Fan, B., H. Thang, S., 2022. RAFT-mediated polymerization-induced self-assembly (RAFT-PISA): current status and future directions. Chemical Science 13, 4192–4224. https://doi.org/10.1039/D2SC00762B

Wang, Z., Tang, J., Zhu, L., Feng, Y., Yue, L., Wang, C., Xiao, Z., Chen, F., 2022. Nanomaterial-induced modulation of hormonal pathways enhances plant cell growth. Environ. Sci.: Nano 9, 1578–1590. https://doi.org/10.1039/D2EN00251E

Xu, L., Xu, M., Wang, R., Yin, Y., Lynch, I., Liu, S., 2020. The Crucial Role of Environmental Coronas in Determining the Biological Effects of Engineered Nanomaterials. Small 16, 2003691. https://doi.org/10.1002/smll.202003691

Yang, T., Wu, X., Wang, W., Wu, Y., 2023. Regulation of seed storage protein synthesis in monocot and dicot plants: A comparative review. Molecular Plant 16, 145–167. https://doi.org/10.1016/j.molp.2022.12.004

Zhou, D., Xiao, M., 2010. Specific Ion Effects on the Seed Germination of Sunflower. Journal of Plant Nutrition 33, 255–266. https://doi.org/10.1080/01904160903434295

Chapter 4. Soil-based Zeolite and Metal Oxide Nanomaterial Application Alters Reactive Nitrogen Losses and Lettuce (*Lactuca sativa*) Growth

Jessica J. Chadwick,[1]* Aleksandar Radu,[2] Iuliia Mikulska,[3] Swaroop Chakraborty,[1] Peng Zhang,[1] Sami Ullah,[1] Iseult Lynch[1]*

[1] School of Geography, Earth and Environmental Sciences, University of Birmingham, Edgbaston, Birmingham B15 2TT, UK

[2] School of Chemistry, University of Lincoln, Lincoln LN6 7TS, UK

[3] Diamond Light Source Ltd, Harwell Science & Innovation Campus, Didcot, Oxfordshire OX11 0DE, UK

* Corresponding authors: Jessica J. Chadwick, jessicajchadwick@gmail.com; Iseult Lynch, i.lynch@bham.ac.uk

Acknowledgements

This work was supported by the Biotechnology and Biological Sciences Research Council (BBSRC) and University of Birmingham funded Midlands Integrative Biosciences Training Partnership (MIBTP) grant number BB/T00746X/1. Assistance with figures was provided by Chantal Jackson (University of Birmingham, UK). Gas chromatography and lettuce elemental analysis was undertaken by Fotis Sgouridis (University of Bristol, UK). Soil elemental analysis was performed at the Analytical Facility, Department of Chemistry (University of Birmingham, UK). ICP-OES assistance was provided by Chris Stark (University of Birmingham, UK). Cerium-zirconium oxide nanomaterials were obtained from Promethean Particles via the EU-funded NanoSolveIT project (Grant Agreement Nº 814572). Funding for XAS experiments (experiment numbers SP34510-1 and SP39677-1) was won by Swaroop Chakraborty, Iseult Lynch, Iuliia Mikulska, and Jessica Chadwick and provided via the University of Birmingham and Diamond Light Source collaboration. Swaroop Chakraborty acknowledges NERC Independent Research Fellowship (UKRI187) to support Jessica Chadwick with B18 XAS work at Diamond Light Source for this project.

CReDIT statement

Jessica Chadwick: Writing – Original Draft, Investigation, Formal analysis, Visualisation, Conceptualization, Funding acquisition. Aleksandar Radu: Resources, Writing – Review and Editing. Iuliia Mikulska: Formal analysis, Visualisation, Funding acquisition, Writing – Review and Editing. Swaroop Chakraborty: Investigation, Funding acquisition, Writing – Review and Editing. Peng Zhang: Supervision, Funding acquisition. Sami Ullah: Conceptualization, Supervision, Writing – Review and Editing, Funding acquisition. Iseult Lynch: Conceptualization, Supervision, Writing – Review and Editing, Funding acquisition.

4.1. Abstract

Excessive nitrogen fertiliser use has resulted in reactive nitrogen losses to the environment through gaseous N emissions, like N_2O, resulting in agriculture being a major anthropogenic source of N_2O gas emissions globally. Using engineered nanomaterials to deliver reactive nitrogen can aid in more efficient nutrient delivery to crops, maximising yield and crop quality, while minimising reactive losses to the environment. The impact of three engineered nanomaterials on soil N emissions and losses was interrogated by co-application with a reduced dose of conventional fertiliser to soils to grow lettuce. Nanomaterial addition to soils was hypothesised to reduce N losses to the environment while maintaining lettuce yield and quality. ZSM-5-15, a nano-zeolite, increased cumulative N_2O emissions by 42% when applied in combination with a 50% dose of conventional nitrogen fertiliser. This is theorised to be through ion exchange of ZSM-5-15's extra-framework NH_4^+ ion load being released, allowing nitrifying microbes to act on the newly released NH_4^+ and increase N_2O emissions. BEA-19, a similar zeolite to ZSM-5-15 but with a slightly altered Si:Al ratio, size and charge, causes no increase in N_2O emissions. While ZSM-5-15 increases reactive N emissions it also drives improved lettuce growth. $Ce_{0.75}Zr_{0.25}O_2$, a nano-metal oxide, improves growth and maintains nutritive quality of lettuce without increasing N_2O emissions. Nano-$Ce_{0.75}Zr_{0.25}O_2$ transforms in soil to form CeO_2 and $Ce_{0.9}Zr_{0.1}O_2$, leaching Zr^{4+} ions which partly form $ZrCl_4$. These compounds may then act on lettuce roots and soil microbes independently. These results indicate how nanomaterials may impact reactive nitrogen emissions through effects on soil microbial communities.

4.2. Introduction

Since the discovery of the Haber-Bosch process in 1913 the total input of reactive nitrogen (Nr) into agricultural ecosystems has more than doubled due to excessive use of synthetic fertiliser (Galloway and Cowling, 2002). Increased fertiliser use has supported global food security and human population growth, with over half of the world's current population eating food produced from nitrogen fertiliser (Smil, 2001). While synthetic fertiliser additions have permitted an increase in crop productivity, their low uptake efficiencies from soils (by crops) have enriched agricultural soils with reactive nitrogen (Nr) thus resulting in its loss to the environment through aqueous run-off and gaseous emissions. These losses include gaseous N compounds that contribute to climate change, primarily through the production of N_2O, which has a global warming potential (GWP) of ~300 as compared to CO_2 and whose atmospheric concentration has increased to 332 ppb in 2021, compared to pre-industrial levels of 275 ppb (IPCC, 2023). Other volatile N compounds include NH_3 and NO_x, that are formed through different stages of N transformations and contribute to climate change as well as impacting air quality. There are also Nr losses through run-off and groundwater leaching in the form of NO_3^- and NH_4^+, contributing to eutrophication and reducing water quality. It is essential to reduce the impact of synthetic fertiliser on the environment without compromising crop productivity, the ability of global agriculture to support the population, and the livelihoods of farmers.

Nanomaterials (NM) have been posited as a solution for precision agriculture, aiding in efficient nutrient delivery (and thus reducing the amounts needed) and promoting crop growth and stress tolerance. NMs have at least one dimension between 1 and 1000 nm, with a huge surface area to volume ratio permitting environment-dependent transformations (amongst other qualities). NM function is highly dependent on their characteristics, including size, shape, surface charge and chemistry, which in turn alter their reactivity, adsorption/binding kinetics and mobility (Wang et al., 2017; Spielman-Sun et al., 2017; Rizwan et al., 2017). The dynamic nature of NMs (as indicated by their propensity to transform) presents a challenge, as generalisations about the behaviour and impacts of different classes of NMs are difficult to make, with changes in shape, size and constituent element ratio altering their fate and effects significantly (Svendsen et al., 2020). This is particularly true of adding NMs into

biological systems. Soil is a highly heterogeneous environment, and NM interactions with minerals, organic matter and microorganisms can trigger ion dissociation and biotransformation of the NMs (Avellan et al., 2018; Svendsen et al., 2020). Similarly, plants with their varied solute concentrations and highly specialised internal environments, can further alter NM transformations, resulting in highly specific interactions between different NMs, soil types and plant species (Pagano et al., 2023; Zhu et al., 2024). NM introduction to the soil environment causes changes to the physicochemical properties of NMs, altering NM behaviour, fate, and biological activity, with NMs impacted by soil pH, organic matter and water content (Xu et al., 2015; Li et al., 2024). These in turn can cause NM agglomeration, transformation, adsorption to the soil matrix or other compounds present and influence NM dissolution, having further impacts on NM behaviour as well as on nutrient supply, including N. Characterising NMs in soil and plants is a further challenge due to the difficulties in tracing the NMs through the whole agricultural system and the requirement that NMs are dispersed for most characterisation methods and in many cases separated from the complex environmental matrix (Mudalige et al., 2019).

Previous research indicates that NM application is able to reduce the nitrogen, phosphorus and potassium (NPK) input needs of crop plants, with metallic NMs shown to impact the cycling of N, P and C (Ditta and Arshad, 2016; Simonin et al., 2018). Here, research is focussed on three metallic NMs, two nano-zeolites, BEA-19 and ZSM-5-15, and a mixed metal oxide, $Ce_{0.75}Zr_{0.25}O_2$. Zeolites are highly porous aluminosilicates, which are often used as industrial catalysts due to their porosity which lends itself to specific ion exchange capabilities. In particular, metal-exchanged ZSM-5 NMs have been used in N_2O decomposition (Abu-Zied et al., 2008). Previous research has shown that CeO_2 and ZrO_2 both have antioxidative properties (Narasaiah et al., 2022), with significant research already exploring the application of nanoceria (CeO_2) to different crops (Gui et al., 2015; Zhang et al., 2011; Rodrigues et al., 2021). The mixed metal oxide utilised here is $Ce_{0.75}Zr_{0.25}O_2$, which follows the nanostructure $Ce_{1-x}Zr_xO_2$. Previous research has utilised $Ce_{0.75}Zr_{0.25}O_2$ NMs as catalysts due to their high dynamic oxygen exchange capacity (Stark et al., 2003; Zheng et al., 2011). This catalytic activity may enable them to function as nanozymes, directly mimicking the action of biological enzymes in the soil to minimise gaseous N emissions (Jiang et al., 2019).

Sustainable intensification of agriculture is described as maintaining or improving yield without compromising on healthy ecosystem functioning. The experiments presented herein aimed to investigate how soil-based NM application with reduced NPK fertiliser input affected crop growth and yield and soil N gaseous fluxes. The hypothesised mechanism is that binding of the NPK nutrients to the surface of the NMs results in a binding dynamic that allows slow nutrient release and, due to the NMs ability to cross biological barriers and be taken up into plants, would allow a more direct nutrient release, thereby minimising the potential for nutrient losses to the environment. Parameters studied include biomass as a measure of plant growth, antioxidative response to assess NM toxicity or stress initiation to aid in deciphering NM mechanism of action, and elemental analysis in order to determine how NM application altered macro- and micronutrient accumulation in lettuce tissue and if there was above-ground accumulation of the NMs based on analysis of their constituent elements. To understand the nutrient cycling that occurred, CO_2, N_2O and NH_3 gas fluxes were captured via gas sampling and analysis. Nitrate, phosphate and ammonium content of the soil and leachate were also analysed to determine how the nutrient supply was influenced by NMs and fertilization. X-ray absorption spectroscopy (XAS) was utilised to determine $Ce_{0.75}Zr_{0.25}O_2$ NM transformations in the soil environment over the timescales of the exposure and uptake by plants. Analysis of the NMs transformations was performed to better understand the mechanisms driving the NMs impacts in the environment and to determine in what form the NMs are when they interact with, or enter, plant tissues. We hypothesized that NM co-application with a reduced dose of fertiliser (half of the conventional dose) would be able to maintain lettuce yield with a reduction in N emissions from soil as a result.

4.3. Materials and Methods

4.3.1. Materials

An aqueous dispersion of $Ce_{0.75}Zr_{0.25}O_2$, was obtained from Promethean Particles (UK) via the NanoSolveIT project. Powdered ZSM-5-15 (Si:Al = 15.0) and BEA-19 (Si:Al = 19.0) were obtained from Zeolyst (USA). Hydrodynamic diameter and zeta potential were determined using 500 mg L^{-1} NM

dispersions in deionised water using a dynamic light scattering (DLS) instrument (Zetasizer, Malvern Instruments, UK). NPK treatment comprised of urea (Sigma-Aldrich) and potassium phosphate monobasic (Sigma-Aldrich). Primary particle size information on BEA-19 was sourced from Jendrlin et al. (2022), on ZSM-5 from Song et al. (2004) and on $Ce_{0.75}Zr_{0.25}O_2$ from Dhage et al. (2005).

4.3.2. Greenhouse study, sampling and analysis

The soil used in the study was collected from FarmED (coordinates 51.869981, -1.581136, https://www.farm-ed.co.uk/) where the loam soil had an oolitic limestone bedrock and a 30-year history of conventional wheat and barley planting. The soil was collected in September 2022 with previous cultivation including barley from March – August 2022. Soils were watered to 60% water holding capacity (WHC) with regular water additions of 100-300 mL per 1.5 kg of soil to maintain soil moisture throughout the experiment.

Soils were sieved to 2 mm before 1.5 kg (dry weight) soil was brought back to 60% WHC and left to rest under greenhouse conditions (21˚C, 16:8 light/dark cycle) for one week. After the seven days the soils were treated with either NPK, a combination of half concentration of NPK and NM suspension, or water as a control. In the case of the NM treatments a 25 mg kg^{-1} NM suspension was added to 100 mL of deionised water along with an NPK treatment made from urea and potassium phosphate monobasic. The full NPK treatment consisted of 180 kg ha^{-1} N, 200 kg ha^{-1} of P_2O_5 and K_2O based on the UK DEFRA RB209A fertiliser manual. The application rates used are recommended for a loamy soil with the previous growing season having been used for winter wheat with an average organic matter content of 3-4% (DEFRA, 2011). The reduced fertilisation was half NPK treatment and consisted of 90 kg ha^{-1} N and 100 kg ha^{-1} of P_2O_5 and K_2O. *Lactuca sativa* seeds (“Tom Thumb” variety; Premier Seeds Direct Limited, UK) were sterilised using 1.5% NaClO solution for 10 minutes before rinsing with deionised water until odourless. Five seeds were sown directly in the treated or untreated soils and grown for eight weeks in a greenhouse at 21˚C with 16:8 hour light to dark day cycles. After the first week post-sowing, similarly sized seedlings were maintained (>2 cm tall) and the rest removed from

each pot replicate, to leave one seedling per pot. Lettuce growth was monitored through height and width measurements and leaf counts over the course of the eight-week experiment. The lettuce's fresh biomass was weighed at the end of the eight-week growing period before being snap frozen using liquid nitrogen and stored at -80˚C for future analyses.

4.3.3. Soil characterisation and net nitrogen mineralisation

Soils were characterised before and after the 8-week experiment for gravimetric soil moisture, pH and EC. The soil samples were kept after the experiments and stored in a cold room at 4-7˚C. Gravimetric soil moisture was calculated using a 5g soil subsample that was weighed before and after 24hr drying at 105˚C. Soil extraction for nitrate, ammonium and phosphate analysis was done using 2M KCl with a 1:10 ratio between sieved soil and the KCl solution. The mixture was shaken for one hour at 200 rpm at room temperature before being centrifuged and the supernatant filtered using 0.45 µm syringe filters. The extractant was stored at -20˚C before use. Net nitrogen mineralisation was studied for each biological replicate at the end of the eight-week experiment by incubating 20g of soil at room temperature in the dark for 28 days before extraction as detailed prior. The post incubation soil extractants were then compared to the end of growth period soil extractions to assess how much nitrogen was nitrified. Dried soil samples underwent elemental analysis and were digested for analysis by inductively coupled plasma optical emission spectroscopy (ICP-OES) as described below.

4.3.4. Greenhouse gas fluxes

Static chamber gas sampling with gas chromatography was performed to measure N_2O and CO_2 emissions. Static chambers had dimensions 15 x 20 x 20 cm and were sealed at the base with water to ensure they were airtight. 15 mL of gas samples were taken at 0 hours, 0.5 hours, 1 hour and 2 hours on a weekly basis and stored in 12mL pre-evacuated exetainer vials (Labco Limited, UK). The gas samples were analysed using the Agilent 7890A Gas Chromatograph (GC) interfaced with a PAL3 autosampler

(Agilent Technologies Ltd, USA) following the method used in Comer et al. (2024) and using reference standards as described in Sgouridis and Ullah (2017). Every 20 samples a standard (N_2O = 0.2 ppm, CH_4 = 4 ppm, and CO_2 = 500 ppm) was used to prevent drift with minimum detectable concentration differences of 9 ppb N_2O, 72 ppb CH_4 and 31ppm CO_2. GC analysis of N_2O used a micro electron capture detector (μECD), while a flame ionisation detector (FID) was used to analyse CH_4 and CO_2 methanised into CH_4.

A 1M H_2SO_4 solution with 2% (w/v) glycerol was used as an acid trap for ammonia emissions from the soils. The acid trap was incubated inside the static chambers for two hours during the weekly gas sampling. The acid trap solution was then extracted with deionised water before NH_4^+ analysis via the ISO/DIS 15923-1 standard analysis method on an AQ400 Discrete Analyser (SEAL Analytical, WI, USA).

4.3.5. Soil nutrient analysis

Soils in the pots containing the growing lettuce plants were watered (100-300 mL per pot to reach 60% WHC, and a funnel was used to capture the first 50 mL of resulting leachate on weeks 1, 2, 4 and 8. This leachate was filtered using a 0.45 μm syringe filter and stored at -20˚C until prepared for analysis. Leachate and KCl extracted soil samples were analysed for nitrate, ammonium and orthophosphate concentration using a Tecan Spark microplate reader (Tecan, UK). Ammonium analysis was performed in accordance with the Mulvaney (1996) protocol. Samples and reagents for the ammonium assay were incubated at 40˚C for 15 minutes, returned to room temperature, and absorbance readings were taken at 650 nm. Nitrate concentrations were determined using a VCl_4 based method (Miranda et al., 2001). Microplates underwent a 6-12 hour incubation at 4˚C before an absorbance reading was taken at 540 nm. The phosphate assay was performed as described by Murphy and Riley (1962). The microplate was incubated for 10 minutes at room temperature before taking an absorbance reading at 880 nm. Each assay used their respective standard solutions which were made up in the same extractant background as the samples, KCl or tap water.

4.3.6. Macro- and micronutrients, NM constituent elements and plant stress marker analysis

Samples (lettuce and soil) were digested for inductively coupled plasma optical emission spectroscopy (ICP-OES) according to the protocols for spinach tissue and the US EPA 3052 protocol for soil/sediment as described in the MARS 6 Microwave Acid Digestion Method Note Compendium (CEM, 2019). Digestion details are listed in full in the supplemental information (SI Table S4.1 and S4.2), with digestion program details in SI Table S1 and S2. Resulting digestate was diluted 50-fold before running samples on the Perkin Elmer optima 8000 ICP-OES for analysis (Agilent Technologies Ltd, USA). The elements studied were P, K, Zn, Ca, Mg, Fe and Mn, as well as the NM constituent elements Ce, Zr, Al and Si. Both dried soil samples and freeze-dried lettuce tissue samples underwent EA analysis for C, N, and S. Soil samples were analysed using a FlashSmart Elemental analyser (Thermo Scientific, USA) using a CHNS method with the furnace at 950˚C using vanadium pentoxide as a combustion aid. Lettuce samples were analysed for C and N using a vario PYRO cube (Elementar Analysensysteme GmbH, Hanau, Germany) in combustion mode at 950˚C and then a reduction tube at 600˚C. A thermal conductivity detector was used for signal detection. Frozen lettuce tissues were used for a malondialdehyde (MDA) assay which measures lipid membrane peroxidation as a marker for oxidative stress (Sigma-Aldrich, UK). The assay was performed according to the manufacturer's instructions.

4.3.7. X-ray Absorption Spectroscopy

Soil samples spiked with 3000 mg kg^{-1} $Ce_{0.75}Zr_{0.25}O_2$ NMs were used for X-ray absorption spectroscopy (XAS) analysis. Soils were treated with the NMs dispersion and mixed thoroughly, followed by 8 weeks of incubation at 21˚C. 200 mg soil samples were pelleted for analyses, with XAS spectra collected on beamline B18 (Diaz-Moreno et al., 2018; Dent et al, 2013) at the Diamond Light Source synchrotron radiation facility (Didcot, UK). The energy of the storage ring during the data collection was 3.0 GeV, with the current intensity of 300 mA. A Si(111) double crystal monochromator

was used to select the incident X-ray energy. Pt-coated collimating and focusing mirrors were used to collect the spectra. A pair of dedicated Pt-coated mirrors operated at 7.0 mrad angle was used to eliminate high energy harmonics during the Ce L_{III} - edge spectra measurements. Zr K-edge XAS spectra were measured without harmonic rejection mirrors. Zr K-edge XAS spectra on soil samples were collected in fluorescence mode using a Canberra 36-pixel Monolithic Segmented Hyper Pure Germanium Detector (HPGe) with Xspress4 signal processing (Dennis et al., 2019), while Ce L_{III}-edge spectra were collected in fluorescence mode using Vortex-ME4 silicon drift detector partnered with the Xspress3 digital pulse processor. A set of reference compounds, consisting of cerium and zirconium, including $CePO_4$, $Ce(CH_3COO)_3$, CeO_2, $CeCl_4$, Zr metal, $ZrCl_4$ and $ZrO(NO_3)_2$ were measured in transmission mode using three consecutive ionization chambers, where the reference samples were placed between the first and second ionization chambers. In addition, a range of different ratios of Ce/Zr mixed metal oxide NMs and ZrO_2 reference compounds were measured in fluorescence mode using a Vortex-ME7 silicon drift detector with the Xspress3X digital pulse processor. Powdered reference compounds ($CePO_4$, $Ce(CH_3COO)_3$, $ZrCl_4$ and $ZrO(NO_3)_2$) were mixed with boron nitride (BN) and pressed into pellets. 3000 mg L^{-1} NMs dispersed in water reference compounds (different ratios of Ce/Zr mixed metal oxide NMs, ZrO_2 and CeO_2) were measured in liquid cells with thickness of 1 mm. Energy calibration of collected spectra was achieved by simultaneous measurements of Zr K-edge and Cr K – edge XAS spectra on zirconium and chromium reference foils for Zr K-edge and Ce L_{III} -edge measurements, correspondingly. Spectra on reference foils were measured in transmission mode. The reference foils were placed between the second and third ionization chambers. Demeter software package was used to perform the data analysis, including energy calibration, normalisation and linear combination fitting (LCF) analysis (Ravel and Newville, 2005). Spectra from two to six repetitions for each sample were merged to improve signal-to-noise ratio.

4.3.8. Statistics

R Statistical Software was used for all analyses (v4.0.2; R Core Team, 2023). Data was initially assessed for normality using Shapiro-Wilk tests, Q-Q plots and homogeneity of variance testing. Where

normality was breached, non-parametric statistical analyses were performed. Kruskal-Wallis tests, followed by Dunn's post-hoc test for pairwise comparison were performed for the soil samples. Normally distributed data were analysed with one-way ANOVA, followed by post-hoc Tukey HSD (honest significant difference) tests. GC calculated N_2O and CO_2 concentrations, and leachate nutrient concentrations, were assessed using linear mixed models to interrogate treatment and time effects on emissions. Post-hoc comparisons of linear mixed model results were evaluated using Tukey tests. Lettuce biomass comparisons were performed using Bonferroni corrected two-sample t-tests comparing control lettuce with all other treatments. The threshold for statistical significance was set at $p = 0.05$.

4.4. Results

500 mg L^{-1} NMs dispersed in water showed both zeolites as negatively charged (Table 4.1) with BEA-19 having a more negative zeta potential than ZSM-5-15. The $Ce_{0.75}Zr_{0.25}O_2$, however, was positively charged. The three pristine NMs also had varying agglomerate sizes as determined via DLS, with BEA-19 agglomerates the largest and $Ce_{0.75}Zr_{0.25}O_2$ NMs the smallest.

Table 4.1. Nanomaterial characterisation using dynamic light scattering (DLS) before exposure to soil. Data are means ± standard deviation.

Nanomaterial	Mean hydrodynamic size (nm) (n=3)	Mean zeta potential (mV) (n=3)
BEA-19	997.8 (±196.8)	-39.5 (±0.95)
ZSM-5-15	631.3 (±12.7)	-28.0 (±0.66)
$Ce_{0.75}Zr_{0.25}O_2$	104.5 (±4.37)	+45.2 (±0.75)

BEA-19 primary particle size was found to be 0.05 µm, as measured by SEM or TEM (Jendrlin et al., 2022). According to Jendrlin et al. (2022), ZSM-5 particles were 0.2 µm. Another paper found Zeolyst sourced ZSM-5-15 particles to be 32 nm, with larger aggregates found between 700-1000 nm (Song et al., 2004). $Ce_{0.75}Zr_{0.25}O_2$ primary particle size was found to be 5 nm using TEM (Dhage et al., 2005). The SEM and TEM derived particle sizes makes it clear that the NMs are agglomerated, and that the hydrodynamic size values are thus for the NM aggregates.

Soil moisture varied across treatments, with the control soil having greater moisture levels than BEA-19 ($p=0.02$), $Ce_{0.75}Zr_{0.25}O_2$ ($p=0.0041$), and ZSM-5-15 ($p=0.00061$) treated soils. Additionally, soil moisture was significantly lower in ZSM-5-15-treated soils than that of NPK full ($p=0.01$) (Table 4.2). Soil pH varied across treatments, with NPK full soil pH being significantly lower than in $Ce_{0.75}Zr_{0.25}O_2$ treated soil ($p=0.0052$) or NPK half treated soil ($p=0.01$). The positively charged $Ce_{0.75}Zr_{0.25}O_2$ NMs had a particularly alkalinizing effect on the soil, producing a significantly higher soil pH than in the control ($p=0.032$). Electrical conductivity (EC) of the soil was also affected by the various treatments. The EC of NPK full treated soil was significantly higher than that of the control soil ($p=0.028$) or ZSM-5-15 treated soil ($p=0.0057$).

No meaningful differences were found between soil NO_3^- or PO_4^{3-} concentrations across treatments, with control soil having an undetectable PO_4^{3-} concentration (Table 4.2). There was a disparity between the concentrations of NO_3^- and post-incubation NO_3^- under NPK full treatment, indicating that N was nitrified in this treatment only. The full NPK treatment resulted in significantly more mineralised NO_3^- compared to all other treatments (see SI Table S4.3 for p values). C:N ratio varies across treatments, with no statistically significant deviation from the control across treatments for C:N ratio, or C and N content alone.

Comparing the elemental concentrations for macro- and micronutrients across the treatments reflects broadly similar nutrient profiles (Table 4.2). The only element to have significantly different elemental concentrations was Cu. ZSM-5-15 treated soils had much higher Cu concentrations, with more than 5x the amount of Cu present in soil as compared to the NPK full treated soil ($p=0.007$). The Cu content of soil in the BEA-19 treatment was also significantly different to NPK full ($p=0.26$). Soil nanomaterial constituent concentrations were uniform across treatments other than for Al. BEA-19 Al soil content was significantly lower than that of the control soil ($p=0.0084$).

Table 4.2. Soil properties in the six different soil treatments after the eight-week growth period. Data are means ± standard error. Absent data is due to values being below the limit of detection of the specific method.

Soil properties	Control	NPK full	NPK half	BEA-19 + NPK half	$Ce_{0.75}Zr_{0.25}O_2$ + NPK half	ZSM-5-15 + NPK half
Gravimetric soil moisture (%) (n=4)	73.9 (± 1.1)	69.9 (± 2.9)	66.3 (± 1.6)	63.1 (± 1.5)	60.9 (± 1.2)	58.2 (± 3.2)
pH (n=4)	8.31 (± 0.06)	6.84 (± 0.18)	8.82 (± 0.05)	8.65 (± 0.07)	8.86 (± 0.04)	8.60 (± 0.09)
EC ($\mu S\ cm^{-1}$) (n=4)	49.5 (± 3.3)	76.4 (±8.5)	52.1 (±2.6)	60.0 (±10.5)	46.2 (±4.9)	39.5 (±2.0)
NO_3^- (mg kg^{-1} dry soil) (n=4)	2.81 (± 0.43)	9.14 (± 2.59)	4.02 (± 1.15)	5.70 (± 2.73)	3.29 (± 1.09)	1.82 (± 0.39)
Post-incubation NO_3^- (mg kg^{-1} dry soil) (n=4)	0.789 (± 0.33)	11.7 (± 1.85)	3.28 (± 1.54)	4.36 (± 2.06)	1.80 (± 0.68)	0.934 (± 0.056)
PO_4^{3-} (mg kg^{-1} dry soil) (n=4)	-	0.01 (± 0.0041)	0.0017 (± 0.0007)	0.00081 (± 0.0002)	0.00065 (± 0.00024)	0.0012 (± 0.00026)
N (%) (n=4)	0.26 (± 0.01)	0.28 (± 0.02)	0.28 (± 0.01)	0.28 (± 0.01)	0.27 (± 0.004)	0.28 (± 0.01)
C (%) (n=4)	5.89 (± 0.34)	5.89 (± 0.41)	6.28 (± 0.02)	5.98 (± 0.13)	6.07 (0 ±.02)	6.02 (± 0.21)
C:N (n=4)	22.8 (± 0.3)	20.9 (± 0.7)	22.3 (± 1.0)	21.8 (± 0.7)	22.5 (± 0.6)	21.4 (± 0.8)
K (mg kg^{-1} dry soil) (n=4)	8469 (± 311)	8396 (± 368)	7913 (± 257)	7838 (± 254)	9734 (± 1,147)	8497 (± 268)
P (mg kg^{-1} dry soil) (n=4)	1170 (± 85)	1270 (± 93)	1158 (± 39)	1105 (± 26)	1364 (± 93)	1095 (± 55)
Cu (mg kg^{-1} dry soil) (n=4)	26.0 (±6.7)	15.8 (±1.9)	25.7 (±6.7)	55.4 (±3.7)	43.4 (±1.5)	84.8 (±7.3)
Al (mg kg^{-1} dry soil) (n=4)	18,916 (± 416)	17,482 (± 339)	17,962 (± 6 ± 13)	15,010 (± 585)	21,291 (± 4,932)	16,687 (± 291)
Si (mg kg^{-1} dry soil) (n=4)	170,418 (± 7,860)	160,528 (± 13,517)	151,159 (± 8,819)	146,620 (± 5,459)	156,984 (7,853)	173,300 (± 11,333)
Ce (mg kg^{-1} dry soil) (n=4)	15.7 (± 3.8)	15.5 (± 3.9)	10.3 (± 1.0)	12.0 (± 2.6)	14.4 (± 2.5)	13.3 (± 3.0)
Zr (mg kg^{-1} dry soil) (n=4)	30.4 (± 2.7)	22.9 (± 4.1)	22.2 (± 2.6)	23.3 (± 3.8)	33.6 (± 10.8)	39.2 (± 5.9)

NPK full treatment produced the greatest N_2O emissions in week 2 (Figure 4.1A), but also cumulatively (SI Figure S4.1A). The NPK half combination treatments were consistently low producers of N_2O with one notable exception. Co-addition of ZSM-5-15 NM with NPK half produced 42% more N_2O over the course of the 8-week period as compared to NPK half addition alone. This is most pronounced in week 2, as with the NPK full N_2O emissions. N_2O emissions are significantly different across exposure weeks ($p=2.58 \times 10^{-10}$). NPK full N_2O emissions are significantly different to all treatments ($p<0.05$) other than ZSM-5-15 ($p=0.793$). ZSM-5-15 produces elevated emissions, producing significantly more N_2O emissions than the control soil ($p=0.0165$).

CO_2 evolution was used as a proxy for soil respiration (Figure 4.1B), with cumulative CO_2 produced from each treatment also calculated (SI Figure S4.1B). Initially, CO_2 evolution reflects a similar trend to N_2O emissions, with NPK full treatment having the greatest emissions at weeks 1 and 2, as seen in Figure 4.1B. Towards the end of the 8-week growing period CO_2 emissions are elevated above week 1 CO_2 emissions, with an associated increase in respiratory activity, from ZSM-5-15, $Ce_{0.75}Zr_{0.25}O_2$ and NPK half treatments. Week of exposure had a significant effect on CO_2 emissions captured ($p=1.47 \times 10^{-8}$). Control CO_2 emissions were significantly different compared to all other treatments (SI Table S4.4), other than NPK full application ($p=0.0785$).

Analysis of NH_3 gas emissions was performed for all 8 weeks of growing, however, results greater than the limit of detection were only found for week 1 of the experiment (Figure 4.1C). Comparison of NH_3 gas emissions between treatments showed that NPK full and control soil were statistically significantly different ($p=0.0000323$). Emission factors of NH_3 and N_2O emissions are available in SI Figure S4.2.

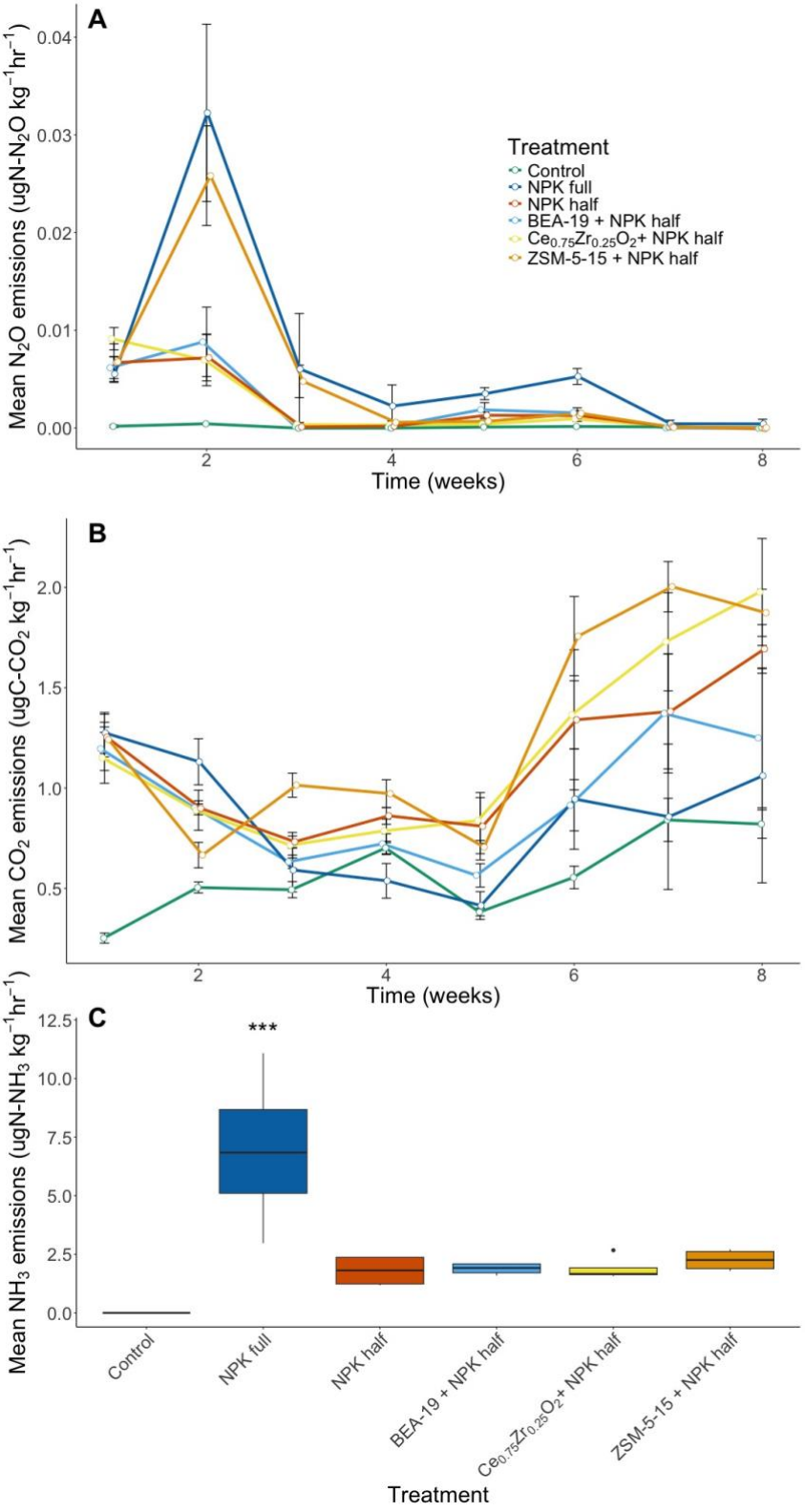


Figure 4.1. (A) Weekly time course of soil N_2O emissions across the five different treatments and control. Error bars indicate standard error from the mean (SEM) based on 4 replicates. (B) Weekly time course of soil CO_2 emissions across the five different treatments and control. Error bars indicate SEM of 4 replicates. (C) Soil NH_3 gas emissions in week 1 of the experiment. Error bars indicate SEM from 4 replicates. "***" is used to denote a statistically significant result as compared to the control of $p < 0.001$.

NO_3^- losses in leachate peaked for all treatments at week 4, as shown in Figure 4.2A, other than for the ZSM-5-15 treated soil, which peaked in week 8 with 12.9 mg L^{-1} of NO_3^- in the leachate. This is not the highest NO_3^- leachate concentration overall, which is found at week 4 in the control soil (16.6 mg L^{-1}). NPK full has the lowest NO_3^- emissions overall. All treatments, other than BEA-19, generated lower NO_3^- leachate concentrations than the control (SI Table S4.5). Exposure duration (week) and treatment have a significant effect on the NO_3^- emissions arising from the $Ce_{0.75}Zr_{0.25}O_2$ NM treatment (*p=0.013*), with exposure duration (week) also proving significant for NPK half (*p=0.034*) and ZSM-5-15 (*p=0.046*) treated soil NO_3^- concentrations.

The PO_4^{3-} concentration in the soil was much higher for NPK full than for all the other treatments (0.099mg L^{-1}), as seen in Figure 4.2B. A statistically significant difference was found between the PO_4 soil concentration of NPK full and control treatments (*p=0.00633*). There was a minor reduction in PO_4 emissions from $Ce_{0.75}Zr_{0.25}O_2$ and ZSM-5-15 treatments relative to the half NPK treatment, this difference, however, was not statistically significant. ZSM-5-15 treatment is significantly correlated with exposure duration (week) (*p=0.0053*).

NH_4^+ concentration in leachate peaked in week 1 before rapidly decreasing, with NPK full emissions reducing by 1mg L^{-1} per week until levels stabilise from week 4 (Figure 2C). NH_4^+ emissions from the NPK full treated soil are significantly higher than the control across all timepoints (*p=2.48x10-6*) and are significantly correlated with treatment duration (week) (*p=0.00075*), as is evident from Figure 4.2C. NPK full treatment NH_4^+ emissions are also significantly different to BEA-19 (*p=0.0036*), NPK half (*p=0.0048*) and ZSM-5-15 treatment emissions (*p=0.0079*). The lack of significant differences between $Ce_{0.75}Zr_{0.25}O_2$ and NPK full treatments is indicative that while the increase in emissions under $Ce_{0.75}Zr_{0.25}O_2$ treatment is not different to the other treatments, it is still elevated.

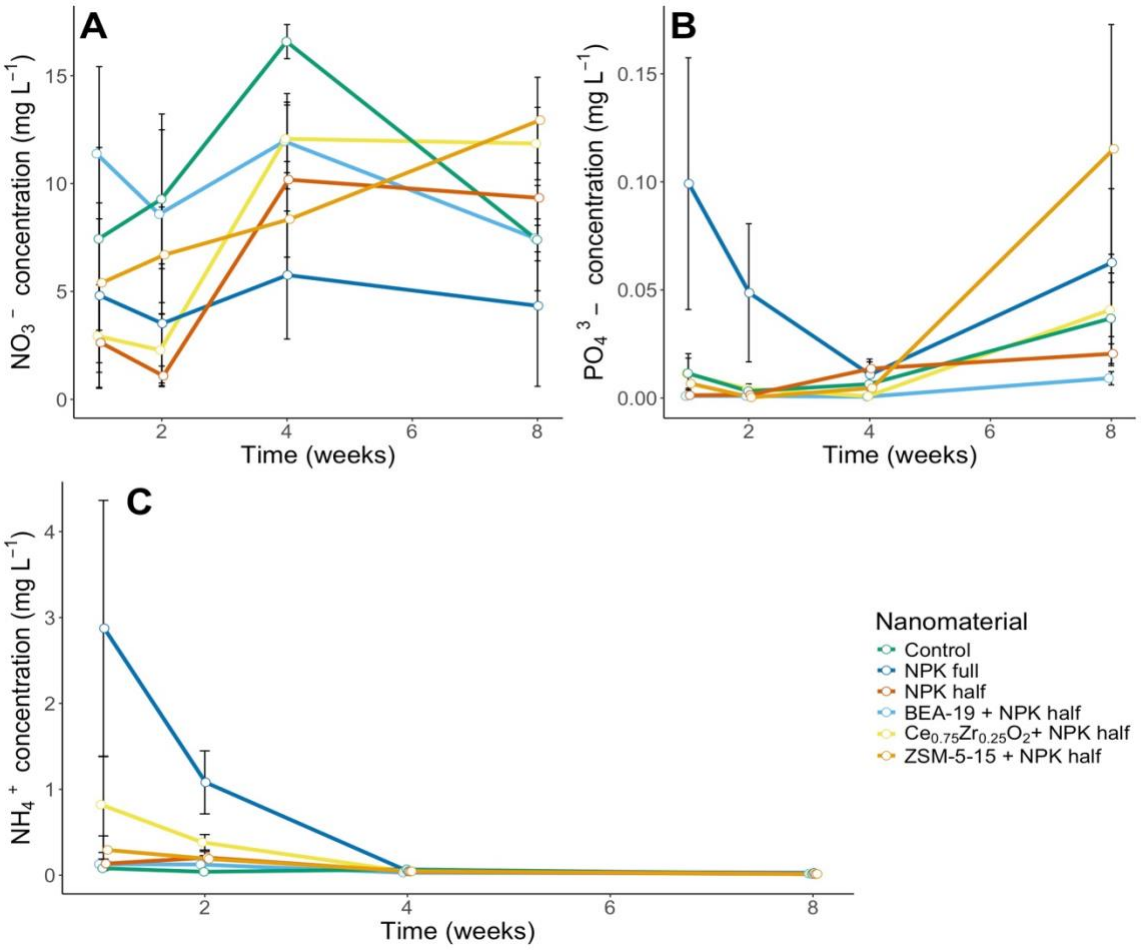


Figure 4.2. (A) NO_3^- concentration in leachate emissions recorded at weeks 1, 2, 4, and 8 across the six treatments. (B) PO_4^{3-} concentration in leachate across weeks 1, 2, 4 and 8. (C) NH_4^+ concentration in leachate recorded at weeks 1, 2, 4 and 8. Error bars reflect SEM based on 4 replicates.

The highest lettuce yields were produced under $Ce_{0.75}Zr_{0.25}O_2$ (40.8g) and ZSM-5-15 (43.5g) treatments, with NPK half treatment alone producing on average 38g lettuce, as shown in Figure 4.3A. Significant increases compared to the control lettuce yield were found under ZSM-5-15 ($p=0.027$) and $Ce_{0.75}Zr_{0.25}O_2$ treatment ($p=0.017$).

MDA concentration is a measure of lipid peroxidation, or the effect of ROS on cell membranes. Control lettuce had the lowest MDA concentration of 0.0073 nmol mg^{-1} of lettuce tissue (Figure 4.3B). Similarly, NPK half, BEA-19 and $Ce_{0.75}Zr_{0.25}O_2$ treated lettuces didn't show the presence of the stress marker, although variability in the BEA-19 data was large. MDA levels were elevated under NPK full and ZSM-5-15 treatments, but these were not found to be statistically significant increases in MDA concentration relative to the control lettuce.

The micronutrient tissue concentrations, apart from Zn, appear to show similar trends (Figure 4.3C). Control tissues have higher concentrations of Cu, Mn and Mg ($p<0.05$) compared to all other treatments. BEA-19 treated lettuce had a lower yield than controls and it can be seen to have higher micronutrient concentrations of Ca, Cu, Fe, Mn and Mg. There were no statistically significant differences found between treatments for any other micronutrients other than Zn. N content of ZSM-5-15 grown lettuce was significantly greater than that in the control lettuce ($p=0.0067$). The P content of NPK full treated lettuce was greater than that in control ($p=0.022$), BEA-19 ($p=0.012$), or $Ce_{0.75}Zr_{0.25}O_2$ lettuce ($p=0.043$). $Ce_{0.75}Zr_{0.25}O_2$ lettuce had significantly lower K content than the control ($p=0.038$) or NPK full ($p=0.013$) lettuce. Differences in elemental concentrations of NM constituent elements in lettuce tissues can be found in SI Figure S4.3.

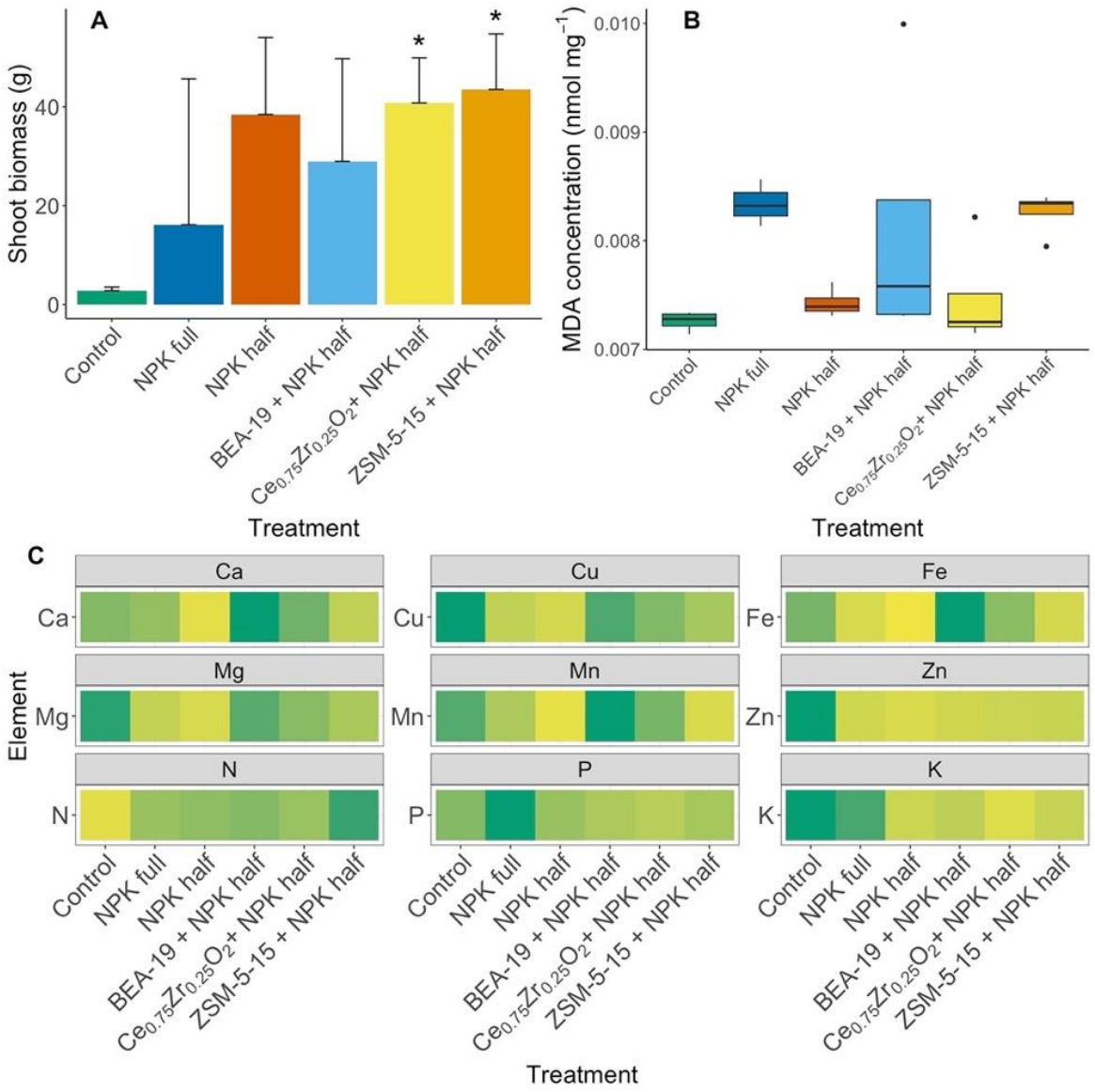


Figure 4.3. (A) Lettuce aboveground biomass after destructive sampling at week 8. Error bars indicate standard deviation (n=4). Significantly different means compared to the control are denoted using '*' where $p<0.05$. (B) Malondialdehyde (MDA) concentration in lettuce shoot tissue including mean and SEM (n=4). Black dots signify outliers. (C) Relative concentration of macro- and micronutrient elements of interest in lettuce tissue compared across the six treatments (n=4), numerical element concentration data is available in SI Table S4.6. N content was determined via elemental analysis, all other nutrients were determined via ICP-OES.

The Ce fraction of the NM is completely transformed from the original $Ce_{0.75}Zr_{0.25}O_2$ in the soil. The linear combination fit (Figure 4.4A) is able to fully describe the transformation of the NM in soil using the X-ray absorption near edge structure (XANES) spectra of CeO_2 (19.6% ± 0.8 %) and $Ce_{0.9}Zr_{0.1}O_2$ (80.4% ± 0.8 %). The results of the linear combination fit were not able to fully reproduce the Zr K-edge experimental spectra for the $Ce_{0.75}Zr_{0.25}O_2$ treated soil, however the Zr K-edge XANES spectrum for the $Ce_{0.75}Zr_{0.25}O_2$ grown lettuce tissue shows that $Ce_{0.75}Zr_{0.25}O_2$ is translocated into aboveground tissues as well as Zr metal and $ZrCl_4$. Reference standards and experimental spectra are presented in SI Figure S4.4.

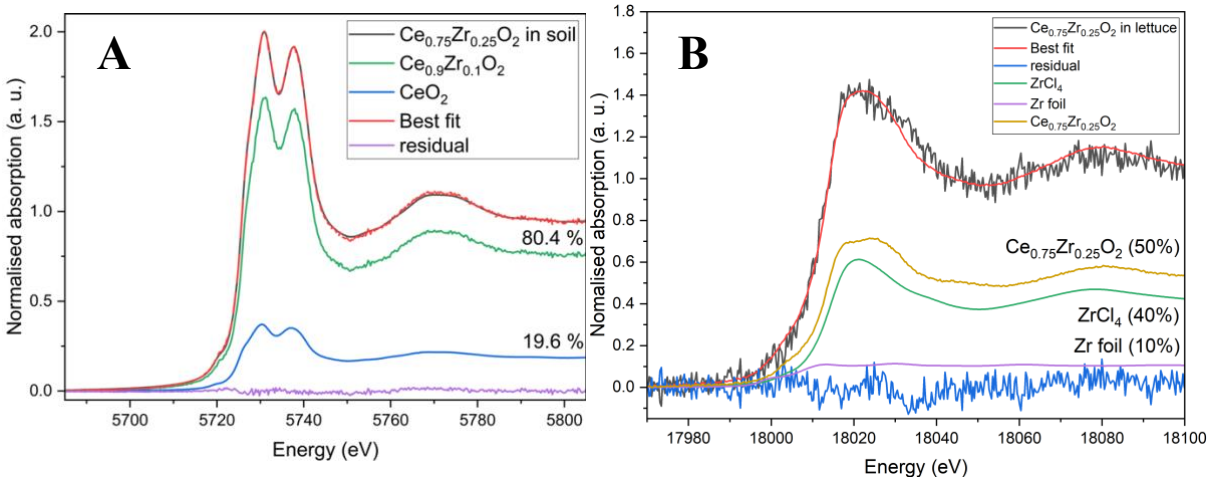


Figure 4.4. (A) Ce L3-edge normalised XANES spectrum of $Ce_{0.75}Zr_{0.25}O_2$ treated soil samples and best linear combination fit of XANES profiles of Ce0.9Zr0.1O2 and CeO_2. (B) Zr K-edge normalised XANES spectrum of $Ce_{0.75}Zr_{0.25}O_2$ grown lettuce tissue and best linear combination fit of XANES profiles of pristine $Ce_{0.75}Zr_{0.25}O_2$ and $ZrCl_4$.

4.5. Discussion

4.5.1. N_2O emissions and soil respiration are elevated under ZSM-5-15 treatment

ZSM-5-15 treatment both elevates N_2O emissions and increases the soil respiration rate. The observed peak in N_2O emissions at week-2 is due to a lag in microbial gas production after the immediate addition of nutrients. N was added to soil in the form of urea which is hydrolysed to NH_4^+ via the enzyme urease, which is then utilised in nitrification, producing N_2O. Nitrate can also be denitrified into N_2O in addition to nitrification as a source of N_2O. Zeolite application has been shown to increase the abundance of ammonia-oxidising archaea and to increase ammonia monooxygenase enzyme activity in agricultural waste (Wu et al., 2020). ZSM-5-15 may therefore be impacting nitrifying microbes and elevating N_2O emissions either through increasing nitrifying community size, or directly impacting on enzymatic activity. Soil pH was reduced under the NPK full treatment due to the increased addition of N fertiliser triggering subsequent nitrification, producing H^+ ions, as seen in Equation 4.1. This correlates with the reduction in NH_3 gas emissions and NH_4^+ in the leachate. However, there is no reduction in soil pH under the ZSM-5-15 treatment. If the theorised mechanism is that ZSM-5-15 is able to upregulate nitrification, then, as with the NPK full treatment, there should be a corresponding drop in soil pH. The absence of a pH change may mean that ZSM-5-15 has a buffering capacity, potentially through its extra-framework ion (NH_4^+) being released, leaving binding sites for H^+ ions through a process of ion exchange (Ahmed et al., 2010; Leinonen and Letho, 2001). Extra-framework ions are held in the pore spaces of the zeolites' 3D structure and are not chemically bound to the NM, allowing ion exchange.

$$2NH_4^+ + 4O_2 + 4e^- \rightarrow 2NO_3 + 4H^+ + 2H_2O + 12e^-$$

Equation 4.1. Nitrosomonas catalysed reduction of ammonium (NH_4^+) in soil.

Alternatively, the ZSM-5-15 triggered N_2O emissions could be through an effect on the final stage of denitrification. This might be through ZSM-5-15 having a toxic effect on soil microbes that are responsible for reducing N_2O to N_2, causing there to be a proportional increase of N_2O. Nitrous oxide reductase (*NOS*) is the only enzyme found to reduce N_2O to N_2 in the N cycle (Kuypers et al., 2018). It may be that ZSM-5-15 has an inhibitory effect on this enzyme, producing elevated N_2O emissions, however, this theory doesn't align with the soil respiration data or the leachate emissions data.

The increase in soil respiration, as determined via CO_2 production, cannot definitively be determined to be produced through either an increase in lettuce root biomass, impacts on the soil microbial community, or both. Previous research shows that the metabolic quotient of soil increased under zeolite application although no impact on respiratory activity was seen (Mulbachova and Simon, 2003). Due to the sampling procedure utilised, no accurate data for root biomass was found in this study, leaving the mechanism unclear.

ZSM-5-15, nor either of the other NM treatments produced any impact on NH_3 emissions, with the highest emissions being from NPK full application. Zeolite addition to poultry manure has been shown to reduce NH_3 volatilisation by up to 44% (Kithome et al., 1999). While the organic matter content of manure is much higher than that of soil, the ability to reduce emissions is relevant. The low NH_3 emissions may be due to the rate of nitrification in the ZSM-5-15 treated soil, whereby NH_3 is being converted rather than emitted as a gas.

Rather than promoting microbial community shifts, ZSM-5-15 may have nanozyme activity and could be directly involved in conversion of NH_4^+ to N_2O. Other zeolite nanozymes have been developed previously, but were functionalised with Zn (Fu et al., 2021; Chen et al., 2019). As ZSM-5-15 has no transition metal functionalisation, these findings are indicative that ZSM-5-15 is able to produce a shift in typical terrestrial N cycling, as compared to control or NPK half treatment alone, likely by promoting nitrifying microbe abundance or enzymatic activity.

4.5.2. Leaching loss dynamics over time and with NM treatment

The timing and magnitude of nutrient emissions in leachate is consistent with the gas emissions data for ZSM-5-15 treatment and its effect on nitrification sourced N_2O emissions. In week 1, the lowest NO_3^- concentration in the leachate was for $Ce_{0.75}Zr_{0.25}O_2$ treatment, whilst NO_3^- concentrations were highest in the control soil. An explanation for this could be due to the NPK half addition producing a lag in emissions as seen with N_2O, due to urea's conversion by urease to NH_4^+ before conversion to NO_3^-. The peak in ammonium concentration in week 1, and decline by week 4, coincides with the peak in nitrate emissions in leachate. This general trend of increasing leachate concentrations over time was true for all the treatments, with peaks in emissions seen at week 4 for all treatments other than ZSM-5-15, which peaked at week 8. The control soil had the lowest N_2O emissions, as compared to the NPK full and all NM with half NPK treatments. This could be due to nitrification of NH_4^+ to NO_3^- occurring more completely, with reduced nitrifier sources of N_2O. Both zeolites used in this experiment had NH_4^+ as their extra-framework ions. This binding capacity for NH_4^+ means that there may be a delay in nitrification under this treatment due to slow release of the NH_4^+. Overall, this will lower the amount of nitrification in the soil at later stages due to the binding of NH_4^+. The increase in leachate concentration of NO_3^- over time for the zeolites indicates a slow release of these extra-framework ions, with BEA-19 potentially having a stronger affinity for NH_4^+ than ZSM-5-15. BEA and ZSM-5 type zeolites have been compared for ion exchange application in catalytic converter exhaust gas adsorption, reflecting the fact that both have catalytic and adsorptive effects across applications (Toops et al., 2021). This also has a further impact on denitrification, due to low nitrification later in the growth period limiting the supply of NO_3^- to denitrifying microbes.

There were three NO_3^- leaching trends across the treatments. NO_3^- leachate emissions are highest for the control group, peaking in week 4, this is partnered with the lowest rate of CO_2 evolution, indicating that denitrification is stunted in the control soils through a lack of soil microbial activity. This reduced microbial activity, combined with the lack of NPK input to the soil, causes the low N_2O emissions. The NO_3^- emissions for NPK full treatment are likely so low due to the soil pH reduction impacting on soil microbial activity, as displayed through the reduced CO_2 emissions data. This lack of

activity slows the N cycle, with reduced NH_4^+ and NO_3^- emissions. NPK half and $Ce_{0.75}Zr_{0.25}O_2$ treatments follow the same trend for NO_3^- emissions; $Ce_{0.75}Zr_{0.25}O_2$ produces slightly elevated emissions but this is coupled with greater soil respiration. NO_3^- emissions for ZSM-5-15 are unique, peaking in week 8, reflecting the time period needed for conversion of NH_4^+ to NO_3^-, further indicating that the earlier (week 2) N_2O emissions peak is nitrification sourced rather than arising from denitrification.

Leachate losses over time reflect changing adsorption dynamics and local conditions for the NMs, with the highest PO_4 emissions occurring in ZSM-5-15 treated soil at week 8. ZSM-5-15 is negatively charged and so, unlike $Ce_{0.75}Zr_{0.25}O_2$, there are no binding dynamics between it and PO_4^{3-}, thus increasing PO_4^{3-} emissions. BEA-19 however has an even more negative zeta potential. Zeolites have previously been utilised for simultaneous removal of NH_4^+ and PO_4^{3-} in water purification, using Ca^{2+} ions to remove PO_4^{3-} (Karapınar, 2009). As the extra-framework ion, NH_4^+, is slowly released over time, pore spaces in the structure of the zeolite will become available, permitting ion exchange. This may happen with H^+ ions as mentioned previously but also other cations, for example Ca^{2+}, K^+ and Na^+. As ion exchange continues to occur this may result in formation of $Ca_3(PO_4)_2$, minimising PO_4^{3-} leaching under BEA-19 treatment. While both BEA-19 and ZSM-5-15 are negatively charged nano-zeolites with relatively similar Si:Al ratios (19 and 15, respectively), pore sizes (6.8Å and 5.5Å) and primary particle sizes, they have very different impacts on gaseous and leachate emissions, and final soil concentrations of NO_3^- and PO_4^{3-}, however the physical basis for these differences is currently unknown.

The leachate emissions data, combined with the N_2O and CO_2 emissions in particular, have a shared narrative around the impact of ZSM-5-15 NMs on soil nitrification. Differences between the NMs, both in terms of constituent elements and hydrodynamic size, zeta potential and other properties, are likely significant in understanding the mechanisms that impact their leachate emissions.

4.5.3. NM zeta potential, ion exchange capacity, and transformations within the soil matrix, influence NM-soil component interactions

Comparing SEM/TEM derived particle sizes and water-dispersed hydrodynamic sizes it is clear that the NMs exist as aggregates under the exposure conditions. Further agglomeration and transformation will then have altered the NMs before interaction with plant roots, altering their capacity for translocation into other plant tissues. The XANES data reflects that the NMs are undergoing transformations within the soil environment. Ce and Zr were below the limit of detection for ICP-OES in lettuce tissue, while this has meant a high quality XANES spectra was not able to be generated for Ce, indicating limited bioaccumulation. In order to understand if the small amounts of translocated NMs undergo further transformations in plant tissues, studies at higher, less environmentally realistic, concentrations are required. The LCF for Ce L3-edge XANES spectra of $Ce_{0.75}Zr_{0.25}O_2$ in soil clearly shows Zr^{4+} ions may leach from the mixed metal oxide, leaving $Ce_{0.9}Zr_{0.1}O_2$ and CeO_2 in the soil (Figure 4.5). Previous study shows that CeO_2 has limited effect on soil microbial biomass, however there may be uptake of Ce by soil microbes (Antisari et al., 2013). This indicates one of the ways in which CeO_2 can interact with the biotic components of soil. $Ce_{0.75}Zr_{0.25}O_2$, $ZrCl_4$ and Zr metal were the primary forms of Zr found in the lettuce samples after the 8 weeks of incubation. Whether the leached Zr^{4+} ions are forming $ZrCl_4$ in the soil or inside the plant roots/shoots is unclear due to low quality soil spectra. $ZrCl_4$ is used industrially and as a catalyst, however ZrO_2 is the more popular nano-form for application. $ZrCl_4$ is not a particularly stable form of Zr and reacts with water indicating that this is perhaps a transient Zr form.

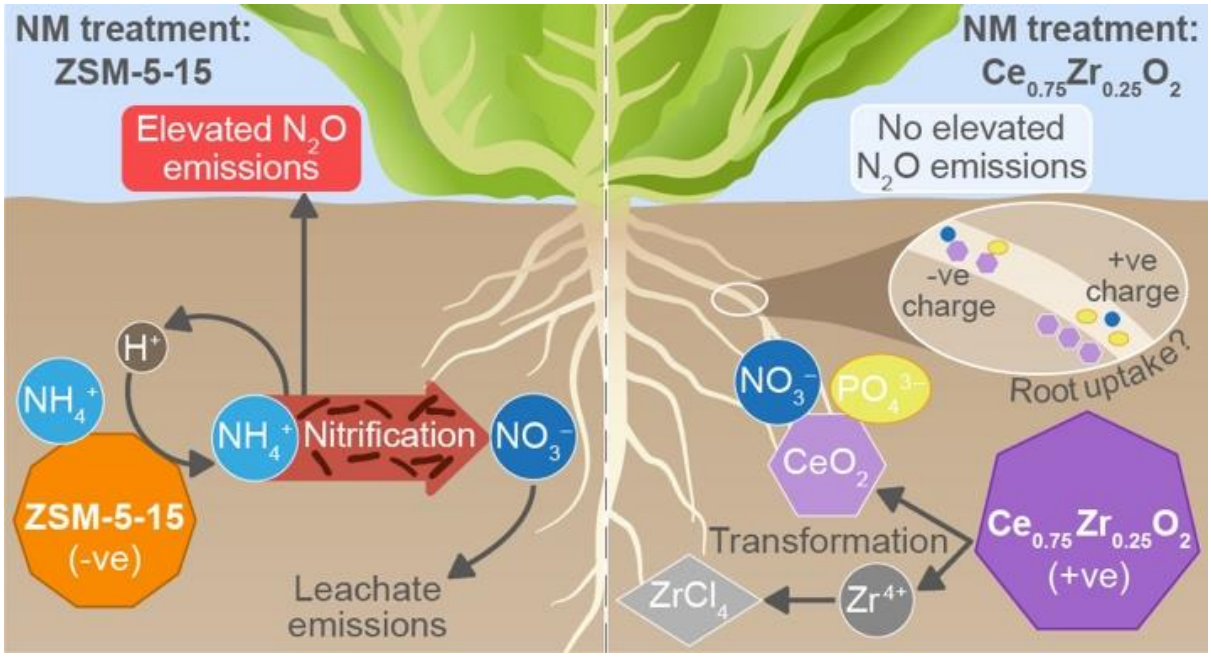


Figure 4.5. Summary image of proposed mechanisms of ZSM-5-15 and $Ce_{0.75}Zr_{0.25}O_2$ activity in agricultural soil and lettuce.

Of the NM properties, zeta potential and in turn, ion exchange capacity, play the most significant role in NM-soil interactions. Clay and organic matter are negatively charged so the positively charged $Ce_{0.75}Zr_{0.25}O_2$ is likely to have been held in the soil matrix, potentially forming interactions with PO_4^{3-} and NO_3^-. This could form part of its mechanism, improving lettuce biomass through slow release of essential nutrients like PO_4^{3-} and NO_3^-, without increasing N emissions. This is particularly relevant post transformation, as CeO_2 has been shown to heteroaggregate with soil clay particles and other natural soil colloids (Cornelis et al., 2011). There is a lack of $CePO_4$ seen in the experimental soil samples, which indicates that any CeO_2-PO_4^{3-} interaction would be through weaker forces such as van der Waal forces in larger agglomerates rather than via chemical bonding. Positively charged NMs also interact differently with plant roots than negatively charged ones, typically remaining on the outside of root surfaces (Spielman-Sun et al., 2017; Li et al., 2019; Parkinson et al., 2022). CeO_2 NMs surface charge can be modulated through application of PO_4^{3-} ions, acting to neutralise and change the zeta potential of the NMs, encouraging translocation into aboveground plant tissues (Zhang et al., 2019, Sharifan et al., 2020). The negatively charged ZSM-5-15 is capable of forming interactions with soil

cations, using ion exchange to prevent soil pH reduction while promoting nitrification through release of NH_4^+. The binding dynamics between ZSM-5-15 and BEA-19 are clearly different, despite the similarities in their compositions, Si:Al ratio, zeta potential and agglomerate size. Both zeolites are bound to NH_4^+ and have similar pore sizes, of 6.8 and 5.5Å for BEA-19 and ZSM-5-15, respectively. With two zeolites of such great similarity, it is hard to determine how they have such different effects on soil N cycling, leachate emissions and lettuce growth on the basis of this dataset alone.

4.5.4. $Ce_{0.75}Zr_{0.25}O_2$ and ZSM-5-15 positively impact lettuce growth with maintained crop quality

ZSM-5-15 is able to increase both lettuce biomass and N content, however the impact of ZSM-5-15 on N_2O emissions means that it cannot be considered as a sustainable alternative to conventional fertilisation. BEA-19 improves the micronutrient status of lettuce but has a negative impact on lettuce biomass accumulation. This is suggested to be due to the very low lettuce growth seen under BEA-19 treatment, which may be the result of a deficiency in Zn (de Almeida et al., 2020). The Zn concentration is much higher in the control lettuce, with the other treatments producing lettuces all within a similar range for Zn concentration in shoot tissue (0.00011-0.00021 mg g^{-1}). Control lettuce biomass was much lower than all other treatments, indicating that the control lettuces' stunted growth was due to a lack of available nitrogen and phosphate in particular, which led to a greater but still deficient Zn concentration (USDA, 2019). $Ce_{0.75}Zr_{0.25}O_2$ treatment promotes lettuce biomass accumulation, without impacting on soil N emissions. However, the NM fails to improve the crop's quality, with no significant differences to any other treatments for macro- or micronutrient tissue concentrations. Therefore, the ratio of nutrients to biomass remains consistent and there is greater lettuce biomass under NM treatments, leading to maintenance of lettuce's quality in terms of nutritive content, partnered with improved yield. Under alkaline conditions, as in all treatments other than NPK full, the increased N content of soil is linked to increased Zn, Cu, Fe and Mn uptake. However, increased P fertiliser additions may have a

negative effect on micronutrient uptake, having been shown to affect Zn among others (Dhaliwal et al., 2019).

None of the lettuce tissues measured displayed high MDA content, a key marker of lipid peroxidation in response to reactive oxygen species production during oxidative stress. MDA concentration was only recorded after destructive sampling so transient changes in MDA concentration over the plants' growing period were not studied. Slightly elevated MDA concentrations were found for NPK full and ZSM-5-15 grown lettuce. This may be due to the more acidic soil found under NPK full treatment, while the effect of ZSM-5-15 on lettuce MDA levels may be due to the action of the NM itself, i.e., a physical effect. It could be through this minor stress that greater biomass accumulation was seen, as many nanofertilisers act to improve crop growth through initiation of minor stress, triggering improved crop stress tolerance through prior activation of stress signalling pathways (Ghosh and Bera, 2021).

Nano-CeO_2 has been shown to have an antioxidative effect, mimicking the antioxidative enzymes catalase (CAT) and superoxide dismutase (SOD) until binding with phosphate (Singh et al., 2011; Li et al., 2015). From the Ce L3-edge XANES spectra linear combination fitting it is clear that there is very limited binding of Ce to PO_4^{3-} in the soil environment, indicating that there is potential for CeO_2 to be acting as a nanozyme, promoting lettuce growth and improving crop stress resilience. However, how the heteroagglomerates of CeO_2 with associated soil anions, clay particles and colloids behave, and how these other compounds are able to influence nanozyme activity is currently unknown. Zeolite nanozymes that are functionalised with a metal group or used in the formation of metal organic frameworks have been shown to also mimic enzymatic activities (Chen et al., 2019, Jiang et al., 2019, Fu et al., 2021). ZSM-5-15 has no transition metal group, limiting the ability of this zeolite to replicate the necessary active sites and microenvironments found in enzymes. ZSM-5-15 grown lettuce may show improved growth through more direct entry of the NM into the plant tissue, allowing ion exchange within the plant to occur and more localised release of NH_4^+ inside the plant.

4.5.5. Outlook

ZSM-5-15 treatment drives changes in the soil N cycling, most notably through increasing N_2O emissions. This is theorised to be through the action of ZSM-5-15 NMs on nitrifying microbes, likely be aided through its supplementation of NH_4^+ ions as part of its structure. This theory is supported by the soil respiration and leachate nutrient emissions data, in particular NH_4^+ and NO_3^- emissions. Disentangling the mechanism of ZSM-5-15 action on N_2O emissions requires further study. Stable isotope 15N labelling of urea and NH_4^+ would be required to determine whether N_2O is being produced via nitrification or denitrification pathways. If the increase in N_2O from ZSM-5-15 is through nitrification then qPCR analysis of relevant N-cycling genes in bacteria, but also archaeal and fungal groups, would elucidate how ZSM-5-15 may be affecting the soil microbial community. Additionally, deciphering what zeolite characteristics trigger the effect would enable improved design and agricultural application of other zeolites also. There are undetermined factors that also influence the differences in NM effect, for example the most significant differences between BEA-19 and ZSM-5-15 zeolite NMs remains unclear in terms of their effect on crop growth and soil N cycling dynamics.

$Ce_{0.75}Zr_{0.25}O_2$ NMs provide a promising avenue for future research, with increased biomass accumulation without triggering increased gaseous or leachate emissions, or soil acidification, whilst also maintaining the lettuce's micronutrient content with this increased biomass accumulation. The mixed metal oxide is likely leaching Zr^{4+} ions, leading to the formation of $ZrCl_4$, $Ce_{0.9}Zr_{0.1}O_2$ and CeO_2, which then act independently in the soil and on the plant. The NM zeta potential, particularly relating to ion exchange capacity, interaction with soil colloids, anions and cations, are all important factors in NM activity in soils.

Understanding the impacts to N cycling and related emissions triggered by NM application to soil is only one component of understanding NM application implications to agroecosystems. Broader understanding of how the zeolites and $Ce_{0.75}Zr_{0.25}O_2$ NMs, both pristine and transformed, are impact soil microbial diversity is essential for improved agricultural sustainability. NM charge triggers differential impacts on the biotic components of soil, with positively charged NMs impacting bacteria more, while negatively charged particles are more toxic to earthworms (Wang et al., 2017; Adeel et al.,

2021). $ZrCl_4$ negatively effects the oligochaete *Enchytraeus crypticus'* reproduction at >500 mg kg^{-1} (Gomes et al., 2015). This concentration is much higher than the experimental concentrations used here, however, impacts on soil fauna remain understudied at lower concentrations.

NMs transform as they enter the soil, with further transformations inside plant tissues (Zhang et al., 2020). Understanding how the transformed NMs go on to interact with plant roots and if further transformations occur at the plant root surface due to root exudates or inside plant tissues is yet to be understood for $Ce_{0.75}Zr_{0.25}O_2$, ZSM-5-15 and BEA-19. Just as these NMs are transforming, understanding how these changes alter their agglomeration and binding dynamics is important to reveal how they behave in natural systems. For example, visualising heteroagglomerates would aid in developing more detailed knowledge around NM kinetics, realistic agglomerate size and interactions with biotic soil components. NM heteroaggregates have been studied under lab conditions using scanning transmission electron microscopy (STEM), but methods for complex environmental sample heteroagglomerates and compound identification is lacking (Mahr et al., 2024, Wang et al., 2015, Praetorius et al., 2020). To understand how Zr compounds and CeO_2 act in the soil post transformation from $Ce_{0.75}Zr_{0.25}O_2$, these visualisations or other characterisation methods in complex samples are required.

References

Abu-Zied, B.M., Schwieger, W., Unger, A., 2008. Nitrous oxide decomposition over transition metal exchanged ZSM-5 zeolites prepared by the solid-state ion-exchange method. Applied Catalysis B: Environmental 84, 277–288. https://doi.org/10.1016/j.apcatb.2008.04.004

Adeel, M., Shakoor, N., Shafiq, M., Pavlicek, A., Part, F., Zafiu, C., Raza, A., Ahmad, M.A., Jilani, G., White, J.C., Ehmoser, E.-K., Lynch, I., Ming, X., Rui, Y., 2021. A critical review of the environmental impacts of manufactured nano-objects on earthworm species. Environmental Pollution 290, 118041. https://doi.org/10.1016/j.envpol.2021.118041

Ahmed, O.H., Sumalatha, G., Muhamad, A.M.N., 2010. Use of zeolite in maize (Zea mays) cultivation on nitrogen, potassium and phosphorus uptake and use efficiency.

Avellan, A., Simonin, M., McGivney, E., Bossa, N., Spielman-Sun, E., Rocca, J.D., Bernhardt, E.S., Geitner, N.K., Unrine, J.M., Wiesner, M.R., Lowry, G.V., 2018. Gold nanoparticle biodissolution by a freshwater macrophyte and its associated microbiome. Nature Nanotech 13, 1072–1077. https://doi.org/10.1038/s41565-018-0231-y

Calvin, K., Dasgupta, D., Krinner, G., Mukherji, A., Thorne, P.W., Trisos, C., Romero, J., Aldunce, P., Barrett, K., Blanco, G., Cheung, W.W.L., Connors, S., Denton, F., Diongue-Niang, A., Dodman, D., Garschagen, M., Geden, O., Hayward, B., Jones, C., Jotzo, F., Krug, T., Lasco, R., Lee, Y.-Y., Masson-Delmotte, V., Meinshausen, M., Mintenbeck, K., Mokssit, A., Otto, F.E.L., Pathak, M., Pirani, A., Poloczanska, E., Pörtner, H.-O., Revi, A., Roberts, D.C., Roy, J., Ruane, A.C., Skea, J., Shukla, P.R., Slade, R., Slangen, A., Sokona, Y., Sörensson, A.A., Tignor, M., Van Vuuren, D., Wei, Y.-M., Winkler, H., Zhai, P., Zommers, Z., Hourcade, J.-C., Johnson, F.X., Pachauri, S., Simpson, N.P., Singh, C., Thomas, A., Totin, E., Arias, P., Bustamante, M., Elgizouli, I., Flato, G., Howden, M., Méndez-Vallejo, C., Pereira, J.J., Pichs-Madruga, R., Rose, S.K., Saheb, Y., Sánchez Rodríguez, R., Ürge-Vorsatz, D., Xiao, C., Yassaa, N., Alegría, A., Armour, K., Bednar-Friedl, B., Blok, K., Cissé, G., Dentener, F., Eriksen, S., Fischer, E., Garner, G., Guivarch, C., Haasnoot, M., Hansen, G., Hauser, M., Hawkins, E., Hermans, T., Kopp, R., Leprince-Ringuet, N., Lewis, J., Ley, D., Ludden, C., Niamir, L., Nicholls, Z., Some, S., Szopa, S., Trewin, B., Van Der Wijst, K.-I., Winter, G., Witting, M., Birt, A., Ha, M., Romero, J., Kim, J., Haites, E.F., Jung, Y., Stavins, R., Birt, A., Ha, M., Orendain, D.J.A., Ignon, L., Park, S., Park, Y., Reisinger, A., Cammaramo, D., Fischlin, A., Fuglestvedt, J.S., Hansen, G., Ludden, C., Masson-Delmotte, V., Matthews, J.B.R., Mintenbeck, K., Pirani, A., Poloczanska, E., Leprince-Ringuet, N., Péan, C., 2023. IPCC, 2023: Climate Change 2023: Synthesis Report. Contribution of Working Groups I, II and III to the Sixth Assessment Report of the Intergovernmental Panel on Climate Change [Core Writing Team, H. Lee and J. Romero (eds.)]. IPCC, Geneva, Switzerland. Intergovernmental Panel on Climate Change (IPCC). https://doi.org/10.59327/IPCC/AR6-9789291691647

CEM, 2019. Mars 6 Microwave Acid Digestion Method Note Compendium.

Chen, C., Hu, Z., Ren, J., Zhang, S., Wang, Z., Yuan, Z.-Y., 2019. ZnO Nanoclusters Supported on Dealuminated Zeolite β as a Novel Catalyst for Direct Dehydrogenation of Propane to Propylene. ChemCatChem 11, 868–877. https://doi.org/10.1002/cctc.201801708

Comer-Warner, S.A., Ullah, S., Dey, A., Stagg, C.L., Elsey-Quirk, T., Swarzenski, C.M., Sgouridis, F., Krause, S., Chmura, G.L., 2024. Elevated temperature and nutrients lead to increased N2O emissions from salt marsh soils from cold and warm climates. Biogeochemistry 167, 21–37. https://doi.org/10.1007/s10533-023-01104-0

Cornelis, G., Ryan, B., McLaughlin, M.J., Kirby, J.K., Beak, D., Chittleborough, D., 2011a. Solubility and Batch Retention of CeO 2 Nanoparticles in Soils. Environ. Sci. Technol. 45, 2777–2782. https://doi.org/10.1021/es103769k

Cornelis, G., Ryan, B., McLaughlin, M.J., Kirby, J.K., Beak, D., Chittleborough, D., 2011b. Solubility and Batch Retention of CeO2 Nanoparticles in Soils. Environ. Sci. Technol. 45, 2777–2782. https://doi.org/10.1021/es103769k

de Almeida, H.J., Vergara Carmona, V.M., Ferreira Inocêncio, M., Furtini Neto, A.E., Cecílio Filho, A.B., Mauad, M., 2020. Soil Type and Zinc Doses in Agronomic Biofortification of Lettuce Genotypes. Agronomy 10, 124. https://doi.org/10.3390/agronomy10010124

Dennis, G., Helsby, W., Omar, D., Horswell, I., Tartoni, N., Hayama, S., Mikulska, I., Diaz-Moreno, S., 2019. First results using the new DLS Xspress4 digital pulse processor with monolithic segmented HPGe detectors on XAS beamlines. AIP Conference Proceedings 2054, 060065. https://doi.org/10.1063/1.5084696

Dent, A.J., Cibin, G., Ramos, S., Parry, S.A., Gianolio, D., Smith, A.D., Scott, S.M., Varandas, L., Patel, S., Pearson, M.R., Hudson, L., Krumpa, N.A., Marsch, A.S., Robbins, P.E., 2013. Performance of B18, the Core EXAFS Bending Magnet beamline at Diamond. J. Phys.: Conf. Ser. 430, 012023. https://doi.org/10.1088/1742-6596/430/1/012023

Dhage, S.R., Gaikwad, S.P., Muthukumar, P., Ravi, V., 2005. Synthesis of Ce0.75Zr0.25O2 at 100 °C. Ceramics International 31, 211–213. https://doi.org/10.1016/j.ceramint.2004.04.009

Dhaliwal, S.S., Naresh, R.K., Mandal, A., Singh, R., Dhaliwal, M.K., 2019. Dynamics and transformations of micronutrients in agricultural soils as influenced by organic matter build-up: A review. Environmental and Sustainability Indicators 1–2, 100007. https://doi.org/10.1016/j.indic.2019.100007

Diaz-Moreno, S., Amboage, M., Basham, M., Boada, R., Bricknell, N.E., Cibin, G., Cobb, T.M., Filik, J., Freeman, A., Geraki, K., Gianolio, D., Hayama, S., Ignatyev, K., Keenan, L., Mikulska, I., Mosselmans, J.F.W., Mudd, J.J., Parry, S.A., 2018. The Spectroscopy Village at Diamond Light Source. J Synchrotron Radiat 25, 998–1009. https://doi.org/10.1107/S1600577518006173

Ditta, A., Arshad, M., 2016. Applications and perspectives of using nanomaterials for sustainable plant nutrition. Nanotechnology Reviews 5, 209–229. https://doi.org/10.1515/ntrev-2015-0060

FoodData Central [WWW Document], n.d. URL https://fdc.nal.usda.gov/fdc-app.html#/food-details/169248/nutrients (accessed 8.14.24).

Fu, T., Xu, C., Guo, R., Lin, C., Huang, Y., Tang, Y., Wang, H., Zhou, Q., Lin, Y., 2021. Zeolitic Imidazolate Framework-90 Nanoparticles as Nanozymes to Mimic Organophosphorus Hydrolase. ACS Appl. Nano Mater. 4, 3345–3350. https://doi.org/10.1021/acsanm.1c00540

Galloway, J.N., Cowling, E.B., 2002. Reactive Nitrogen and The World: 200 Years of Change. AMBIO: A Journal of the Human Environment 31, 64–71. https://doi.org/10.1579/0044-7447-31.2.64

Ghosh, S.K., Bera, T., 2021. 22 - Molecular mechanism of nano-fertilizer in plant growth and development: A recent account, in: Jogaiah, S., Singh, H.B., Fraceto, L.F., Lima, R. de (Eds.), Advances in Nano-Fertilizers and Nano-Pesticides in Agriculture, Woodhead Publishing Series in Food Science, Technology and Nutrition. Woodhead Publishing, pp. 535–560. https://doi.org/10.1016/B978-0-12-820092-6.00022-7

Gomes, S.I.L., Caputo, G., Pinna, N., Scott-Fordsmand, J.J., Amorim, M.J.B., 2015. Effect of 10 different TiO2 and ZrO2 (nano)materials on the soil invertebrate Enchytraeus crypticus. Environmental Toxicology and Chemistry 34, 2409–2416. https://doi.org/10.1002/etc.3080

Gui, X., Zhang, Z., Liu, S., Ma, Y., Zhang, P., He, X., Li, Y., Zhang, J., Li, H., Rui, Y., Liu, L., Cao, W., 2015. Fate and Phytotoxicity of CeO2 Nanoparticles on Lettuce Cultured in the Potting Soil Environment. PLoS ONE 10, e0134261. https://doi.org/10.1371/journal.pone.0134261

Jendrlin, M., Radu, A., Zholobenko, V., Kirsanov, D., 2022. Performance modelling of zeolite-based potentiometric sensors. Sensors and Actuators B: Chemical 356, 131343. https://doi.org/10.1016/j.snb.2021.131343

Jiang, D., Ni, D., Rosenkrans, Z.T., Huang, P., Yan, X., Cai, W., 2019. Nanozyme: new horizons for responsive biomedical applications. Chem. Soc. Rev. 48, 3683–3704. https://doi.org/10.1039/C8CS00718G

Karapınar, N., 2009. Application of natural zeolite for phosphorus and ammonium removal from aqueous solutions. Journal of Hazardous Materials 170, 1186–1191. https://doi.org/10.1016/j.jhazmat.2009.05.094

Kithome, M., Paul, J.W., Bomke, A.A., 1999. Reducing Nitrogen Losses during Simulated Composting of Poultry Manure using Adsorbents or Chemical Amendments. Journal of Environmental Quality 28, 194–201. https://doi.org/10.2134/jeq1999.00472425002800010023x

Kuypers, M.M.M., Marchant, H.K., Kartal, B., 2018. The microbial nitrogen-cycling network. Nat Rev Microbiol 16, 263–276. https://doi.org/10.1038/nrmicro.2018.9

Leinonen, H., Lehto, J., 2001. Purification of metal finishing waste waters with zeolites and activated carbons. Waste Manag Res 19, 45–57. https://doi.org/10.1177/0734242X0101900106

Li, H., Guo, Y., Liang, A., Xu, X., Hao, Y., Shang, H., Li, C., Cai, Z., Han, L., Zhao, J., Jia, W., White, J.C., Ma, C., Xing, B., 2024. Commonly Used Engineered Nanomaterials Improve Soil Health via Suppressing Soil-Borne Fusarium and Positively Altering Soil Microbiome. ACS EST Eng. 4, 915–927. https://doi.org/10.1021/acsestengg.3c00501

Li, J., Tappero, R.V., Acerbo, A.S., Yan, H., Chu, Y., Lowry, G.V., Unrine, J.M., 2019. Effect of CeO_2 nanomaterial surface functional groups on tissue and subcellular distribution of Ce in tomato (*Solanum lycopersicum*). Environ. Sci.: Nano 6, 273–285. https://doi.org/10.1039/C8EN01287C

Li, Y., He, X., Yin, J.-J., Ma, Y., Zhang, P., Li, J., Ding, Y., Zhang, J., Zhao, Y., Chai, Z., Zhang, Z., 2015. Acquired Superoxide-Scavenging Ability of Ceria Nanoparticles. Angewandte Chemie International Edition 54, 1832–1835. https://doi.org/10.1002/anie.201410398

Lowry, G.V., Avellan, A., Gilbertson, L.M., 2019. Opportunities and challenges for nanotechnology in the agri-tech revolution. Nat. Nanotechnol. 14, 517–522. https://doi.org/10.1038/s41565-019-0461-7

Ma, D., Wang, J., Xue, J., Yue, Z., Xia, S., Song, L., Gao, H., 2021. Effects of Soil pH on Gaseous Nitrogen Loss Pathway via Feammox Process. Sustainability 13, 10393. https://doi.org/10.3390/su131810393

Mahr, C., Stahl, J., Gerken, B., Baric, V., Frei, M., Krause, F.F., Grieb, T., Schowalter, M., Mehrtens, T., Kruis, E., Mädler, L., Rosenauer, A., 2024. Characterization of mixing in nanoparticle hetero-

aggregates by convolutional neural networks. Nano Select 5, 2300128. https://doi.org/10.1002/nano.202300128

Miranda, K.M., Espey, M.G., Wink, D.A., 2001. A Rapid, Simple Spectrophotometric Method for Simultaneous Detection of Nitrate and Nitrite. Nitric Oxide 5, 62–71. https://doi.org/10.1006/niox.2000.0319

Mudalige, T., Qu, H., Van Haute, D., Ansar, S.M., Paredes, A., Ingle, T., 2019. Chapter 11 - Characterization of Nanomaterials: Tools and Challenges, in: López Rubio, A., Fabra Rovira, M.J., martínez Sanz, M., Gómez-Mascaraque, L.G. (Eds.), Nanomaterials for Food Applications, Micro and Nano Technologies. Elsevier, pp. 313–353. https://doi.org/10.1016/B978-0-12-814130-4.00011-7

Mühlbachová, G., Šimon, T., 2003. Effects of zeolite amendment on microbial biomass and respiratory activity in heavy metal contaminated soils. Plant Soil Environ. 49, 536–541. https://doi.org/10.17221/4190-PSE

Mulvaney, R.L., 1996. Nitrogen—Inorganic Forms, in: Methods of Soil Analysis. John Wiley & Sons, Ltd, pp. 1123–1184. https://doi.org/10.2136/sssabookser5.3.c38

Murphy, J., Riley, J.P., 1962. A modified single solution method for the determination of phosphate in natural waters. Analytica Chimica Acta 27, 31–36. https://doi.org/10.1016/S0003-2670(00)88444-5

Narasaiah, B.P., Koppala, S., Kar, P., Lokesh, B., Mandal, B.K., 2022. Photocatalytic and Antioxidant Studies of Bioinspired ZrO2 Nanoparticles Using Agriculture Waste Durva Grass Aqueous Extracts. Journal of Hazardous Materials Advances 7, 100112. https://doi.org/10.1016/j.hazadv.2022.100112

Pagano, L., Rossi, R., White, J.C., Marmiroli, N., Marmiroli, M., 2023. Nanomaterials biotransformation: In planta mechanisms of action. Environmental Pollution 318, 120834. https://doi.org/10.1016/j.envpol.2022.120834

Parkinson, S.J., Tungsirisurp, S., Joshi, C., Richmond, B.L., Gifford, M.L., Sikder, A., Lynch, I., O'Reilly, R.K., Napier, R.M., 2022. Polymer nanoparticles pass the plant interface. Nat Commun 13, 7385. https://doi.org/10.1038/s41467-022-35066-y

Praetorius, A., Badetti, E., Brunelli, A., Clavier, A., Alberto Gallego-Urrea, J., Gondikas, A., Hassellöv, M., Hofmann, T., Mackevica, A., Marcomini, A., Peijnenburg, W., K. Quik, J.T., Seijo, M., Stoll, S., Tepe, N., Walch, H., Kammer, F. von der, 2020. Strategies for determining heteroaggregation attachment efficiencies of engineered nanoparticles in aquatic environments. Environmental Science: Nano 7, 351–367. https://doi.org/10.1039/C9EN01016E

Ravel, B., Newville, M., 2005. ATHENA, ARTEMIS, HEPHAESTUS: data analysis for X-ray absorption spectroscopy using IFEFFIT. J Synchrotron Rad 12, 537–541. https://doi.org/10.1107/S0909049505012719

RB209 2021 Section 6 Vegetables and bulbs | AHDB [WWW Document], n.d. URL https://ahdb.org.uk/knowledge-library/rb209-2021-section-6-vegetables-and-bulbs (accessed 8.19.24).

R Core Team (2023). R: A language and environment for statistical computing. R Foundation for Statistical Computing, Vienna, Austria. URL https://www.R-project.org/.

Rizwan, M., Ali, S., Qayyum, M.F., Ok, Y.S., Adrees, M., Ibrahim, M., Zia-ur-Rehman, M., Farid, M., Abbas, F., 2017. Effect of metal and metal oxide nanoparticles on growth and physiology of globally important food crops: A critical review. Journal of Hazardous Materials, SI:Environmental Nanotechnol 322, 2–16. https://doi.org/10.1016/j.jhazmat.2016.05.061

Rodrigues, E.S., Montanha, G.S., de Almeida, E., Fantucci, H., Santos, R.M., de Carvalho, H.W.P., 2021. Effect of nano cerium oxide on soybean (*Glycine max* L. Merrill) crop exposed to environmentally relevant concentrations. Chemosphere 273, 128492. https://doi.org/10.1016/j.chemosphere.2020.128492

Sgouridis, F., Ullah, S., 2017. Soil Greenhouse Gas Fluxes, Environmental Controls, and the Partitioning of N2O Sources in UK Natural and Seminatural Land Use Types. Journal of Geophysical Research: Biogeosciences 122, 2617–2633. https://doi.org/10.1002/2017JG003783

Sharifan, H., Wang, X., Ma, X., 2020. Impact of nanoparticle surface charge and phosphate on the uptake of coexisting cerium oxide nanoparticles and cadmium by soybean (Glycine max. (L.) merr.). International Journal of Phytoremediation 22, 305–312. https://doi.org/10.1080/15226514.2019.1658713

Simonin, M., Cantarel, A.A.M., Crouzet, A., Gervaix, J., Martins, J.M.F., Richaume, A., 2018. Negative Effects of Copper Oxide Nanoparticles on Carbon and Nitrogen Cycle Microbial Activities in Contrasting Agricultural Soils and in Presence of Plants. Front. Microbiol. 9, 3102. https://doi.org/10.3389/fmicb.2018.03102

Singh, S., Dosani, T., Karakoti, A.S., Kumar, A., Seal, S., Self, W.T., 2011. A phosphate-dependent shift in redox state of cerium oxide nanoparticles and its effects on catalytic properties. Biomaterials 32, 6745–6753. https://doi.org/10.1016/j.biomaterials.2011.05.073

Smil, V., 2000. Enriching the Earth: Fritz Haber, Carl Bosch, and the Transformation of World Food Production. The MIT Press. https://doi.org/10.7551/mitpress/2767.001.0001

Song, W., Justice, R.E., Jones, C.A., Grassian, V.H., Larsen, S.C., 2004. Synthesis, Characterization, and Adsorption Properties of Nanocrystalline ZSM-5. Langmuir 20, 8301–8306. https://doi.org/10.1021/la049516c

Spielman-Sun, E., Lombi, E., Donner, E., Howard, D., Unrine, J.M., Lowry, G.V., 2017. Impact of Surface Charge on Cerium Oxide Nanoparticle Uptake and Translocation by Wheat (Triticum aestivum). Environ. Sci. Technol. 51, 7361–7368. https://doi.org/10.1021/acs.est.7b00813

Stark, W.J., Maciejewski, M., Mädler, L., Pratsinis, S.E., Baiker, A., 2003. Flame-made nanocrystalline ceria/zirconia: structural properties and dynamic oxygen exchange capacity. Journal of Catalysis 220, 35–43. https://doi.org/10.1016/S0021-9517(03)00235-5

Svendsen, C., Walker, L.A., Matzke, M., Lahive, E., Harrison, S., Crossley, A., Park, B., Lofts, S., Lynch, I., Vázquez-Campos, S., Kaegi, R., Gogos, A., Asbach, C., Cornelis, G., von der Kammer, F., van den Brink, N.W., Mays, C., Spurgeon, D.J., 2020. Key principles and operational practices for improved nanotechnology environmental exposure assessment. Nat. Nanotechnol. 15, 731–742. https://doi.org/10.1038/s41565-020-0742-1

Toops, T.J., Binder, A.J., Kunal, P., Kyriakidou, E.A., Choi, J.-S., 2021. Analysis of Ion-Exchanged ZSM-5, BEA, and SSZ-13 Zeolite Trapping Materials under Realistic Exhaust Conditions. Catalysts 11, 449. https://doi.org/10.3390/catal11040449

Vittori Antisari, L., Carbone, S., Gatti, A., Vianello, G., Nannipieri, P., 2013. Toxicity of metal oxide (CeO2, Fe3O4, SnO2) engineered nanoparticles on soil microbial biomass and their distribution in soil. Soil Biology and Biochemistry 60, 87–94. https://doi.org/10.1016/j.soilbio.2013.01.016

Wang, H., Adeleye, A.S., Huang, Y., Li, F., Keller, A.A., 2015. Heteroaggregation of nanoparticles with biocolloids and geocolloids. Advances in Colloid and Interface Science, Colloid and Polymer Interfaces in Bio-resources and Environments 226, 24–36. https://doi.org/10.1016/j.cis.2015.07.002

Wang, L., Hu, C., Shao, L., 2017. The antimicrobial activity of nanoparticles: present situation and prospects for the future. Int J Nanomedicine 12, 1227–1249. https://doi.org/10.2147/IJN.S121956

Wu, X., Ren, L., Zhang, J., Peng, H., 2020. Effects of Zeolite and Biochar Addition on Ammonia-Oxidizing Bacteria and Ammonia-Oxidizing Archaea Communities during Agricultural Waste Composting. Sustainability 12, 6336. https://doi.org/10.3390/su12166336

Xu, C., Peng, C., Sun, L., Zhang, S., Huang, H., Chen, Y., Shi, J., 2015. Distinctive effects of TiO2 and CuO nanoparticles on soil microbes and their community structures in flooded paddy soil. Soil Biology and Biochemistry 86, 24–33. https://doi.org/10.1016/j.soilbio.2015.03.011

Zhang, P., Guo, Z., Zhang, Z., Fu, H., White, J.C., Lynch, I., 2020. Nanomaterial Transformation in the Soil–Plant System: Implications for Food Safety and Application in Agriculture. Small 16, 2000705. https://doi.org/10.1002/smll.202000705

Zhang, P., Ma, Y., Xie, C., Guo, Z., He, X., Valsami-Jones, E., Lynch, I., Luo, W., Zheng, L., Zhang, Z., 2019. Plant species-dependent transformation and translocation of ceria nanoparticles. Environ. Sci.: Nano 6, 60–67. https://doi.org/10.1039/C8EN01089G

Zhang, Z., He, X., Zhang, H., Ma, Y., Zhang, P., Ding, Y., Zhao, Y., 2011. Uptake and distribution of ceria nanoparticles in cucumber plants†. Metallomics 3, 816–822. https://doi.org/10.1039/c1mt00049g

Zheng, Y., Hu, Z., Huang, H., Ji, W., Sun, M., Chen, C., 2011. Synthesis and Characterization of Nanometer $Ce_{0.75}Zr_{0.25}O_2$ Powders by Solid-State Chemical Reaction Method. Journal of Nanomaterials 2011, 1–7. https://doi.org/10.1155/2011/657516

Zhu, G., Zhang, P., Zhao, W., Shakoor, N., Sun, Y., Wang, Qibin, Wang, Quanlong, Li, M., Jiang, Y., Tan, Z., Rui, Y., Lynch, I., 2024. Toxicity of metal-based nanomaterials in different organisms. Toxin Reviews 43, 236–254. https://doi.org/10.1080/15569543.2024.2317296

Chapter 5. Greenhouse Gas Emissions from Hydroponically Grown Lettuce Under Nano-Metal Oxide Treatment Monitored Using Stable ^{15}N Isotope Tracing

J. J. Chadwick[1]*, Arnoud Witteveen[2], Iuliia Mikulska[3], Swaroop Chakraborty[1], Peng Zhang[1], Sami Ullah[1], Iseult Lynch[1]*

[1] School of Geography, Earth and Environmental Sciences, University of Birmingham, Edgbaston, Birmingham B15 2TT, UK

[2] Saturn Bioponics, Birmingham, B17 0JL, UK

[3] Diamond Light Source Diamond Light Source Ltd, Diamond House, Harwell Science & Innovation Campus, Didcot, Oxfordshire OX11 0DE, UK

* Corresponding authors: Jessica J. Chadwick jxc1326@student.bham.ac.uk; Iseult Lynch, i.lynch@bham.ac.uk

Acknowledgements

This work was supported by the Biotechnology and Biological Sciences Research Council (BBSRC) and University of Birmingham funded Midlands Integrative Biosciences Training Partnership (MIBTP) grant number BB/T00746X/1. Gas chromatography and ^{15}N tracer gas flux analysis was undertaken by Fotis Sgouridis at University of Bristol (UK). Titanium dioxide polyvinylpyrrolidone and cobalt ferrous oxide nanomaterials were obtained from Promethean Particles via the EU-funded NanoSolveIT project (Grant Agreement Nº 814572). Funding for XANES/XAS analysis was won by Jessica Chadwick, Swaroop Chakraborty, and Iseult Lynch and was provided via the University of Birmingham and Diamond Light Source collaboration.

CReDIT statement

Jessica Chadwick: Writing – Original Draft, Investigation, Formal analysis, Visualisation, Conceptualisation, Funding acquisition. Arnoud Witteveen: Supervision, Methodology, Resources. Iuliia Mikulska: Formal analysis, Funding acquisition, Writing – Review and Editing. Swaroop Chakraborty: Funding acquisition, Writing – Review and Editing. Peng Zhang: Supervision, Funding acquisition. Sami Ullah: Supervision, Writing – Review and Editing, Funding acquisition. Iseult Lynch: Supervision, Writing – Review and Editing, Funding acquisition.

5.1. Abstract

Hydroponics presents opportunities for crop production with improved land and water usage as compared to conventional agriculture, using nutrient media to grow crops without the use of soil. By tailoring nutrient mixes to the crop grown this is aimed to improve overall system efficiency. One of the ways this may be achieved is through the addition of nanomaterials to the nutrient media, enabling even greater improvements in nutrient use efficiency. The nano metal oxides TiO_2 PVP and $Co_{2.25}Fe_{0.75}O_4$ were added to hydroponic nutrient media to grow lettuce crops using a vertical, recirculating hydroponic setup. N_2O emission sources were monitored using ^{15}N stable isotope tracing. The hydroponic system used had an aerated rootzone with the majority of the N_2O emissions derived from nitrifying microbes that populate the inert rockwool substrate that the lettuce roots are held in. There was little difference between NM treatments and the nutrient media control. This is likely due to the action of both NMs being on denitrification, which makes up a minority of the total N_2O emissions, resulting in minimal net N_2O reduction. TiO_2 PVP may be toxic to denitrifying bacteria, reducing denitrifier sourced N_2O. $Co_{2.25}Fe_{0.75}O_4$ transforms in hydroponic media to form Co_3O_4 and Fe_2O_3, both of which may act to cause more complete denitrification, minimising denitrifier sourced N_2O also. Further study is required to fully understand NM mechanisms that impact N_2O production and NM hetero- and homoagglomeration, translocation and bioaccumulation in crop residues.

5.2. Introduction

Precision agriculture focuses on the use of new technology to improve the efficiency of crop growth. This can include nanotechnological advances to enhance nutrient delivery and reduce pollution associated with agriculture, use of stacked or hydroponic systems to minimise water usage, in addition to application of computational approaches such as normalised difference vegetation index (NDVI) data and image-based technologies to indicate nutrient deficiencies and instigate corrective actions automatically (Zhang et al., 2021; Chadwick et al., 2023). Hydroponics is the use of nutrient media to grow crops in a soilless system, allowing nutrient needs to be tailored precisely to the crop being grown. Hydroponics is also able to increase crop yield in a smaller area as compared to conventional agriculture due to its vertical arrangement that maximises space utilisation. Therefore, hydroponics has considerable commercial appeal due to the cleanliness of the end product, with improved yields using less water and land area than conventional agriculture, and minimising pollution of surrounding water sources due to the lack of surface run-off or groundwater contamination (Carmassi et al., 2005; Verdoliva et al., 2021). There are a range of different hydroponic systems, as summarised by McKeil (2019), with recirculating hydroponic systems using continuously circulating aqueous media enriched with essential macro- and micronutrients for maximal water and nutrient use efficiency (NUE). Reduced land and water usage mean that hydroponics is considered a more efficient way to produce crops that have high water requirements but require minimal space, like lettuce, tomatoes and strawberries than conventional greenhouse approaches.

Agriculture is the primary anthropogenic source of nitrous oxide (N_2O), a potent GHG that contributes to global warming. N_2O is produced from different microbial communities involved in the N cycle, with different clades contributing to N_2O production via denitrification, nitrification or nitrifier denitrification (Figure 5.1). Improved understanding of N_2O emissions from crops grown hydroponically, and the different pathways that lead to its production, can aid in making hydroponics an even more sustainable option for crop growth. Determining the microbial source of N_2O requires use of the ^{15}N tracer gas flux method, whereby N_2O emissions can be tracked back to which biological pathway is being utilised in its production (Stevens and Laughlin, 1998). The source of hydroponic N_2O

emissions may depend on root growth substrate, with peat substrate causing greater denitrification and coir substrate causing a greater proportion of N_2O to be produced via nitrification (Lin et al., 2023).

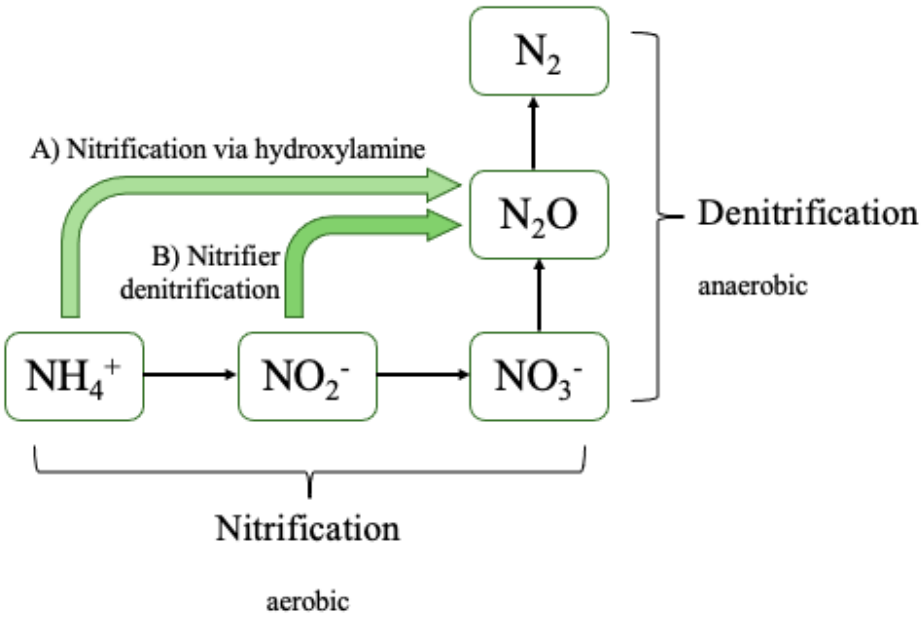


Figure 5.1. Summary of microbial pathways of N_2O production adapted from Rapson and Dacres (2013).

Engineered nanomaterials (NM) have at least one dimension between 1 and 100 nm and are man-made particles with high surface area to volume ratios and complex surface chemistries, enabling their use in a wide range of industrial, medical and agricultural applications (Regulation (EU) 2015/2283, 2021; Piccinno et al., 2012). NMs can be applied as sensors to monitor changes in aqueous media, e.g., pH or EC, or can be applied to improve nutrient use efficiency as part of the hydroponic media or a foliar spray (Chadwick et al., 2023). Utilising NMs within hydroponics has the potential to combine the benefits of both approaches, aiding in nutrient uptake and maximising yield while minimising environmental impacts of agriculture. TiO_2 based NMs are the most produced NM, commonly used in a range of cosmetic, medical and industrial applications, thus potentially entering aquatic and terrestrial environments during use and at end of life (Menard et al., 2011). The addition of the water-soluble polymer polyvinylpyrrolidine (PVP) to nano-TiO_2 can aid in NM dispersion and

stability (Zheng et al., 2001). $Co_{2.25}Fe_{0.75}O_4$ NMs are a form of spinel structure transition metal ferrites, which follow the structure $Co_XFe_{3-X}O_4$. Spinel ferrites have magnetic properties and their application in biomedical, industrial and environmental applications is well researched (Amiri et al., 2019; Qin et al., 2021; Kefeni et al., 2017). NM transformations and mobility in aquatic media depend on both the NMs properties and the medium composition, and thus safe and sustainable NM application in hydroponic systems require dedicated study to understand the potential for NM toxicity and efficacy in this context. Understanding how NMs function and transform in hydroponic media, as well as the NM effects on nutrient cycling, and nutrient uptake by the plants, is essential in determining the viability of combined NM-hydroponic systems as part of a sustainable agricultural approach.

The experiments presented here applied two nanoscale metal oxides (TiO_2 PVP and $Co_{2.25}Fe_{0.75}O_{4)}$ to a vertical, recirculating hydroponic setup with a rockwool substrate for the crop rootzone that underwent intermittent wetting with the hydroponic media. The NMs were applied to the nutrient media, and impacts on lettuce growth and quality, as well as the impact on N cycling were determined. Lettuce is a popular crop for hydroponic systems, due to its fast growth period, with improved yield and nitrate contents when grown hydroponically compared to traditional soil-grown lettuce (Sharma et al., 2018). To interrogate the effects of NM treatment on GHG emissions from the hydroponic system and lettuce growth, a range of endpoints were studied in order to assess how the NM addition impacted on lettuce productivity and quality, including the NM bioaccumulation risk. Lettuce quality was assessed through elemental analysis of nutrients, with additional monitoring for the presence of the constituent elements of the NMs in order to understand the potential for NM bioaccumulation in the edible lettuce tissues. N cycling was assessed utilising ^{15}N labelled tracers added to the rockwool substrate in the hydroponic setup, to determine the relative sources of N_2O production in the system, e.g., nitrification or denitrification derived N_2O emissions. Helium incubation to directly determine N_2 emissions from soil, as the endpoint of complete denitrification, is better suited to soil cores than hydroponic setups using chamber-based gas flux methods, and as such only N_2O was directly studied (Micucci et al., 2024). The rockwool substrate acted as a rootzone region which was studied separately to the bulk aqueous medium to determine nutrient accumulation in the hydroponic system's

rhizosphere equivalent. To explore how the NMs responded to the aqueous hydroponic medium solution, NM transformations were studied to improve understanding of NM interactions with the lettuce roots and potential translocation and/or transformation within the hydroponic medium and lettuce tissues. We hypothesised that NMs would transform within the hydroponic medium, resulting in altered surface chemistry, and associated changes in NM physiochemical properties. NMs were further hypothesised to bind with essential nutrients, such as nitrate (NO_3^-) or phosphate (PO_4^{3-}), aiding in their uptake into lettuce tissues. Application of NM treatments to the hydroponic system was hypothesised to improve lettuce biomass accumulation and nutritive quality, enhancing the productive output possible from the hydroponic system, with minimal N losses to the atmosphere.

5.3. Methodology

5.3.1. Materials

Aqueous dispersion of TiO_2 PVP and $Co_{2.25}Fe_{0.75}O_4$ were each obtained from Promethean Particles (UK) via the NanoSolveIT project (Grant Agreement No. 814572). The two nano metal oxides were characterised at 12.5mg L^{-1} deionised (dI) water before the experiment and in hydroponic medium at week 6, the end of the lettuce growth period. The nutrients added and their proportions for the hydroponic medium are listed in supplementary information (SI) Table S5.1. Characterisation was performed to determine the hydrodynamic diameter and zeta potential using the dynamic light scattering (DLS) instrument (Zetasizer, Malvern Instruments, UK). NM samples underwent 15 minutes of continuous sonication in a sonic Elmasonic S 10 H sonic bath at <30˚C at 37kHz (Elma Schmidbauer GmbH, Singen, Germany) prior to measurements. Primary particle size information on TiO_2 PVP and $Co_{2.25}Fe_{0.75}O_4$ were sourced from Khan et al. (2020) and Bhowmik et al. (2015).

5.3.2. Hydroponic experimental setup

Lactuca sativa seeds (Rijk Zwaan, The Netherlands) were grown in hydrated rock wool plugs and covered for 7 days to germinate. Lettuce seedlings greater than 2 cm tall were then transplanted with their rock wool plug into the central reservation of the vertical hydroponic setup consisting of a 13.5 mL/hour pump. The experimental setup is detailed in full in SI Figure S5.1. Each hydroponic stack consisted of four lettuce plugs and each treatment type was done in triplicate. The treatments were a negative control containing the hydroponic medium solution unaltered and the hydroponic medium with 12.5mg L^{-1} of either TiO_2 PVP or $Co_{2.25}Fe_{0.75}O_4$. Bulk nutrient media was monitored for pH and electrical conductivity (EC) across the six-week period, with potable soft water additions as needed to keep the medium between the bounds of pH 5.2-7 and 2-4 mS, respectively.

5.3.3. Greenhouse gas fluxes and partitioning of N_2O emissions

$K^{15}NO_3$ (98 at. % ^{15}N, Sigma Aldrich) tracer was added to the rockwool substrate to investigate what proportion of the produced N_2O was denitrification sourced. The hydroponic stacks were removed from their reserve tanks and incubated in a 10 L airtight gas sampling chamber (30 x 29 x 29 cm) for 1 hour with 15 mL gas samples taken every 20 minutes into 12 mL pre-evacuated exetainer vials (Labco Limited, UK). ^{15}N labelling occurred in weeks 1, 3 and 6, with gas sampling of CH_4, CO_2 and N_2O occurring for the other weeks. The target enrichment using the ^{15}N-NO_3 tracer was 20% based on Mulvaney (1984). However, this enrichment is based on soil sampling rather than a hydroponic medium system, and as such the rockwool moisture level and denitrifying community component may have been sub-optimal. The tracer was dissolved in deionised water and 20 mL was directly applied to the rockwool substrate, with the sampling timings as listed above. CH_4, CO_2 and N_2O samples were analysed as described in Comer et al. (2023) using an Agilent 7890A Gas Chromatograph (GC) using a PAL3 autosampler (Agilent Technologies Ltd, USA) and was performed at the University of Bristol. CO_2 was converted into CH_4 for analysis using the GC's flame ionisation detector (FID). The reference standards utilised were as those used in Sgouridis and Ullah (2017), with every 20 samples a mixed gas

standard (N_2O = 0.2 ppm, CH_4 = 4 ppm, and CO_2 = 500 ppm) used to prevent drift. The ^{15}N content of the N_2O in the 12 mL exetainers was analysed using a continuous flow isotope ratio mass spectrometer ((Elementar Isoprime Precision; Elementar Analysensysteme GmbH, Hanau, Germany) coupled with a trace-gas pre-concentrator inlet with autosampler (isoFLOW GHG; Elementar Analysensysteme GmbH, Hanau, Germany) as described in Sgouridis et al. (2023) and detailed further in the SI. Flux rates were determined using linear regression across the time points (0, 20, 40 and 60 minutes), multiplied by the volume of the gas sampling chamber and divided by liquid volume stored in the rockwool substrate and adjusted for incubation time.

5.3.4. Hydroponic medium nutrient analyses

10 mL subsamples of hydroponic medium were taken from the main medium tanks and analysed for nitrate, ammonium and phosphate concentration using a Tecan Spark microplate reader (Tecan, UK). The ammonium detection method utilised was that of Mulvaney (1996) and involved a 15 minute 40˚C incubation of the samples and standards (0-20 mg L^{-1}) before returning them to room temperature with absorbance readings taken at 650 nm. Nitrate analysis was via a VCl_4 based method from Miranda et al. (2001) using standards from 0-10 mg L^{-1}. This method incubates microplates for 6-12 hours at 4˚C with absorbance readings taken at 540 nm. Phosphate analyses were performed using the method of Murphy and Riley (1962). This involved a 10 minute incubation at room temperature and absorbance readings taken at 880 nm. Standards were made up for each assay using deionised (dI) water and ranged from 0 to 20 mg L^{-1}. For total organic carbon (TOC) and total dissolved nitrogen (TDN) analyses of the hydroponic medium, samples were diluted 3-fold and run following either the TOC-L or TNM-L procedure on the TOC-L CPH/CPN analyser (Shimadzu, Kyoto, Japan) with an ASI-L autosampler (Shimadzu, Kyoto, Japan). The values were base-corrected using the same potable water as used in the hydroponic medium. Standards were made using dI water at concentrations of 2-25ppm for TDN and TOC analyses, with quality control standards of 10ppm used every 15 samples.

5.3.5. Macro- and micronutrient and nanomaterial constituent elements analysis

Lettuce tissue digestion for inductively coupled plasma optimal emission spectroscopy (ICP-OES) was performed in accordance with the method described in the MARS 6 Microwave Acid Digestion method Note Compendium (CEM, 2019). Briefly, 0.5g of dry lettuce tissue was dissolved in 10 mL of HNO_3; the lettuce tissue digestion program is detailed in SI Table S5.2. The resulting digestate was filtered through a 0.35 µm syringe filter and diluted 50-fold before running on the Perkin Elmer optima 8000 ICP-OES (Agilent Technologies Ltd., USA). Hydroponic medium was acidified to 2% using HNO_3, filtered as described for the digestate above and diluted 10-fold before ICP-OES analysis. Standards were made up in 2% HNO_3 for all analysed samples with standard concentrations from 0 to 10 ppm. Translocation indices (TI) were calculated for NM constituent elements Co, Fe and Ti using Equation 5.1 derived from Puga et al. (2015).

$$TI\ (\%) = shoot\ (\mu g/g) \times \frac{100}{root\ (\mu g/g)}$$

[Equation 5.1]

5.3.6. X-ray Absorption Spectroscopy analysis of NMs bioaccumulation and transformation

TiO_2 PVP and $Co_{2.25}Fe_{0.75}O_4$ exposed lettuce samples were oven dried at 70˚C for 72 hours before being ground and pelleted for analysis, with near-edge fine structure x-ray spectroscopy (XANES) spectra collected on beamline B18 (Diaz-Moreno et al., 2018; Dent et al., 2013) at the Diamond Light Source synchrotron radiation facility (Didcot, UK). The energy of the storage ring during the data collection was 3.0 GeV, with the current intensity of 300 mA. A Si(111) double crystal monochromator was used to select the incident X-ray energy. Pt-coated collimating and focusing mirrors were used to collect the spectra. Co, Ti and Fe K-edge XAS spectra on soil samples were collected in fluorescence mode using a Canberra 36-pixel Monolithic Segmented Hyper Pure Germanium Detector (HPGe) with Xspress4 signal processing (Dennis et al., 2019). Hydroponic

medium samples containing the NMs were also studied by Fe K-edge, Co K-edge and Ti K-edge XANES spectra, however, due to the low NMs concentrations used experimentally, higher concentration of NMs were applied and aged in the hydroponic medium in the same ratio as was used in the lettuce experiment. The higher concentration of TiO_2 PVP and $Co_{2.25}Fe_{0.75}O_4$ used for the ageing experiment was 3000 mg L^{-1}, with NMs added to the nutrient medium solution and aged for six weeks before XANES analysis. For $Co_{2.25}Fe_{0.75}O_4$ treated media, XANES spectra of pristine $Co_{2.25}Fe_{0.75}O_4$, Co_3O_4, and $CoCO_3$ were collected as reference standards for Co, and Fe_2O_3 and FeO_4 for Fe. Reference standard samples were ground before being mixed and pelleted with BN (boron nitride). Measurements were taken in transmission mode using three consecutive ionization chambers, where the reference samples were placed between first and second ionization chambers. XANES spectra of pristine TiO_2 PVP and TiO_2 rutile were collected as standards for TiO_2 PVP, with measurements taken in transmission mode as with Co and Fe. Reference foils' spectra were measured in transmission mode and placed between the second and third ionization chambers. The Demeter software package was used to perform the data analysis, including normalization, energy calibration, and linear combination fitting (LCF) analysis (Ravel and Newville, 2005).

5.3.7. Statistics

All statistical testing was performed in R (v4.0.1; R Core Team, 2023). Data was tested for normality using Shapiro-Wilk tests, Q-Q plots and homogeneity of variance testing. If the assumptions of normality were breached, then non-parametric statistical analyses were performed instead. For normally distributed data one-way analysis of variance (ANOVA) were performed, followed by post-hoc Tukey honest significant difference (HSD) tests. Non-normally distributed data was instead analysed using Kruskal-Wallis tests, with significant results analysed using Dunn's post-hoc test for pairwise comparisons. Comparisons of data across time e.g., pH and EC of the hydroponic medium between weeks 1 and 6, were analysed using two-way repeated measures ANOVA. Significant results were then analysed using Bonferroni corrected pairwise comparisons. GC produced data was analysed using linear mixed models, to assess the importance of both week and treatment on N_2O, CO_2 and CH_4

production. Fixed effect results with t values > 2 were deemed significant. Post-hoc comparisons of linear mixed model results were also evaluated using Tukey tests. The threshold for statistical significance was set at $p = 0.05$.

5.4. Results

NMs were dispersed in deionised water for pre-exposure characterisation at 25 mg L^{-1} with week 6 characterisation taking place in hydroponic medium, including all added nutrient constituents. Both metal oxide NMs had negative zeta potentials after the 6-week experiment. However, $Co_{2.25}Fe_{0.75}O_4$ changed from positively to negatively charged, with TiO_2 PVP NMs becoming less negatively charged over time. Pre-exposure NMs both had similarly sized agglomerates. $Co_{2.25}Fe_{0.75}O_4$ agglomerates were on average slightly smaller after the experiment, this may be due to sedimentation of NMs or preferential binding of the NMs to other compounds in the medium altering the agglomerate size. The hydrodynamic size of TiO_2 PVP reduced by 3.9 times, this is likely due to sedimentation of larger NM agglomerates resulting in an apparent reduction in agglomerate size.

The primary particle size of TiO_2 PVP is reported to be ~10nm (Khan et al., 2020). $Co_{2.25}Fe_{0.75}O_4$ particles were reported to vary in size based on the annealing conditions, ranging from 15-47 nm (Bhowmik et al., 2015).

Table 5.1. NM characterisation summary for pre-exposure NMs and NMs in hydroponic medium at week 6. Data are for 25 mg L^{-1} NM dispersions in either deionised water (pre-exposure) or in hydroponic medium (week 6). Data presented are means ± standard deviation.

	$Co_{2.25}Fe_{0.75}O_4$		TiO_2 PVP	
	Pre-exposure	Week 6	Pre-exposure	Week 6
Hydrodynamic size (nm) (n=3)	511.6 (± 7.31)	414.6 (± 1.39)	742.8 (± 14.2)	189.9 (± 5.81)
Zeta potential (mV) (n=3)	+34.2 (± 0.91)	-34.6 (± 0.4)	-14.2 (± 1.5)	-3.12 (± 1.5)

Table 5.2. Hydroponic medium characterisation from week 1 and week 6 for the three treatments. Rockwool hydroponic medium was only tested at week 6. Data presented are means ± standard deviation.

	Control		$Co_{2.25}Fe_{0.75}O_4$		TiO_2 PVP	
	Week 1	Week 6	Week 1	Week 6	Week 1	Week 6
pH (n=3)	6.17 (± <0.01)	5.64 (± 0.05)	6.13 (± 0.03)	5.63 (± 0.04)	6.14 (± 0.01)	5.65 (± 0.16)
EC (mS) (n=3)	2203 (± 10)	2843 (± 207)	2209 (± 15)	3344 (± 306)	2209 (± 13)	3399 (± 319)
NH_4^+ (mg L^{-1} bulk medium) (n=3)	25.5 (± 2.63)	18.6 (± 0.82)	26.7 (± 6.82)	17.3 (± 0.47)	42.6 (± 12.4)	17.5 (± 0.95)
NO_3^- (mg L^{-1} bulk medium) (n=3)	18.8 (± 13.9)	0.957 (± 0.278)	14.7 (± 12.4)	0.758 (± 0.063)	28.0 (± 8.36)	0.768 (± 0.048)
PO_4^{3-} (mg L^{-1} bulk medium) (n=3)	72.3 (± 12.2)	15.3 (± 0.82)	69.6 (± 1.53)	19.2 (± 1.30)	62.5 (± 6.10)	17.9 (± 0.04)
Bulk TOC (mg L^{-1}) (n=3)	13.6 (± 5.43)	13.6 (± 0.86)	16.7 (± 6.76)	17.9 (± 2.11)	9.81 (± 4.55)	15.5 (± 1.30)
Bulk TN (mg L^{-1}) (n=3)	96.4 (± 34.5)	197.9 (± 15.8)	113.5 (± 33.5)	228.2 (± 23.6)	77.3 (± 24.1)	236.7 (± 21.8)
NH_4^+ (mg L^{-1} rockwool medium) (n=3)		18.5 (± 0.63)		17.4 (± 1.04)		17.5 (± 0.50)
NO_3^- (mg L^{-1} rockwool medium) (n=3)		20.4 (± 4.70)		3.30 (± 2.51)		9.83 (± 10.9)
PO_4^{3-} (mg L^{-1} rockwool medium) (n=3)		18.7 (± 0.86)		16.2 (± 1.45)		17.6 (± 1.16)
Rockwool TOC (mg L^{-1}) (n=3)		7.81 (± 1.99)		14.95 (± 7.08)		5.87 (± 5.37)
Rockwool TN (mg L^{-1}) (n=3)		113.5 (± 14.7)		198.1 (± 50.1)		96.8 (± 88.2)

Over the course of the six weeks the pH decreased, and EC increased (Table 5.2), with week having a significant effect on both parameters (*t=-6.6; t=4.51*). EC may have also been influenced by the presence of the NMs, with $Co_{2.25}Fe_{0.75}O_4$ and TiO_2 PVP treatments both producing higher EC values than the control at week 6, but these were not significant (*p=0.058; p=0.218, respectively*). The pH and

EC of the hydroponic medium was monitored over the course of the experiment, with full weekly changes in both pH and EC for each treatment detailed in SI Figure S5.2.

The bulk hydroponic medium was depleted in NO_3^- following all treatments. Both control and $Co_{2.25}Fe_{0.75}O_4$ treatments reduced the NO_3^- content of bulk hydroponic medium by ~19 times, while TiO_2 PVP treatment showed a reduction of ~36 times. PO_4^{3+} was also reduced, as was NH_4^+. However, total organic carbon (TOC) varied significantly across treatments. Control TOC was maintained while both NM treatments increased TOC. Total nitrogen (TN) increased under all treatments over the six weeks, with a 3-fold change in bulk medium TN under TiO_2 PVP treatment. These changes in TOC and TN may help to explain the increases in EC seen over time, and particularly under $Co_{2.25}Fe_{0.75}O_4$ and TiO_2 PVP treatments.

Rockwool medium assessments were only possible at the end of the experiment, due to effect on lettuce root growth if sampling was performed mid-growth period. NH_4^+ content in bulk and rockwool media were similar across treatments. NO_3^- accumulated in the rockwool medium, with more NO_3^- in rockwool medium than in the bulk medium, however this difference was not found to be statistically significant. Significant differences were found in PO_4^{3+} concentration across treatments and between the two hydroponic medium compartments. $Co_{2.25}Fe_{0.75}O_4$ bulk medium had a significantly higher concentration of PO_4^{3+} than that of the control ($p=0.00684$). PO_4^{3+} concentration differed between bulk and rockwool hydroponic media for $Co_{2.25}Fe_{0.75}O_4$ treatment ($p=0.0401$) and the control ($p=0.018$).

TOC concentration was consistent across all media sampled at week 6. Rockwool medium TN at week 6 was much lower than that for bulk medium at the same timepoint. Significantly different TN concentrations were found between TiO_2 PVP treatment in the bulk and rockwool hydroponic media ($p=0.0228$). Differences in bulk hydroponic medium and rockwool medium for NM constituent elements and macro- and micronutrients are detailed in full in SI Table S5.3.

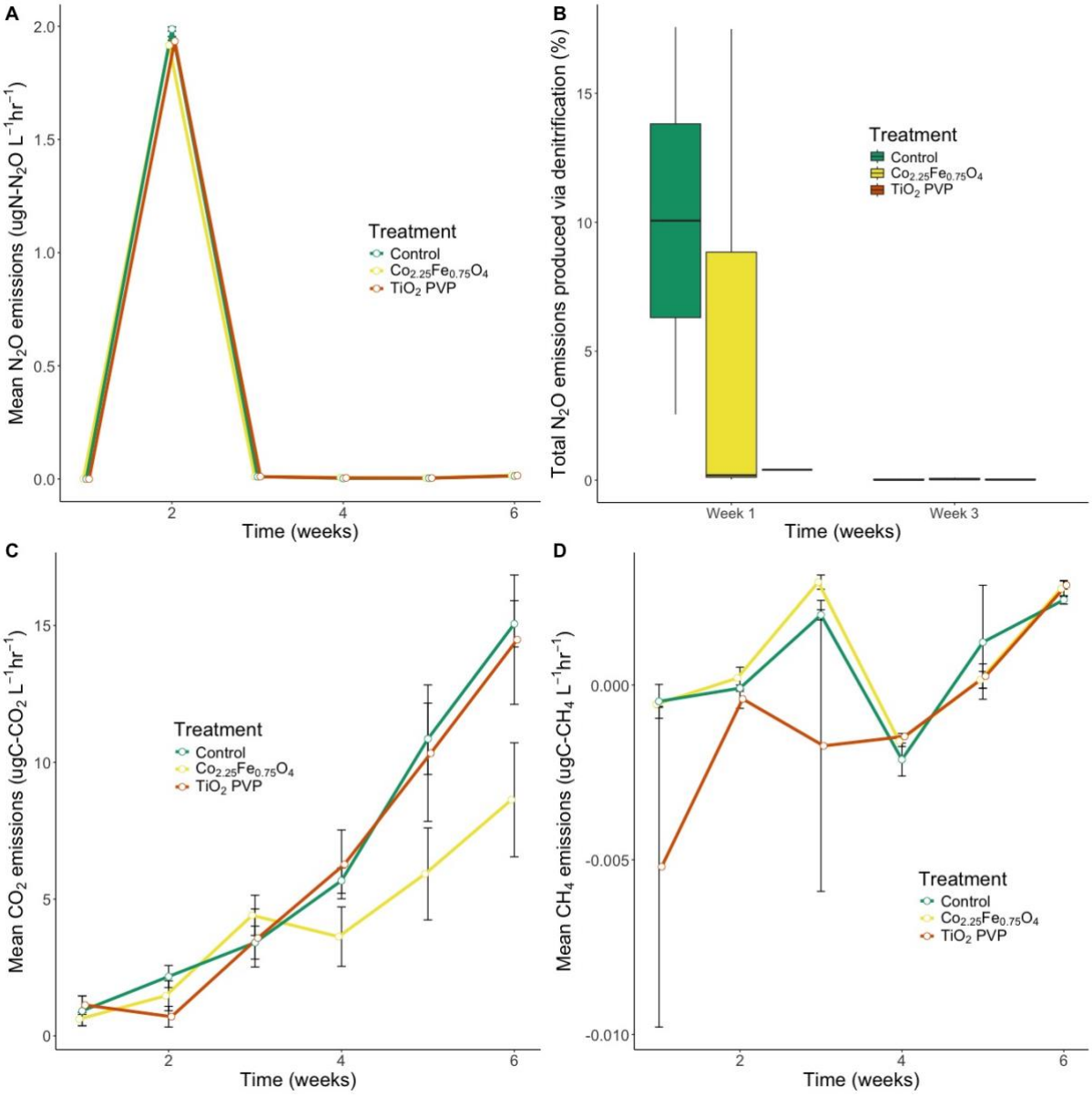


Figure 5.2. (A) Weekly time course of hydroponic N_2O emissions across the two NM treatments and control. Error bars indicate standard error from the mean (SEM) based on 3 replicates. (B) Proportion of denitrification derived N_2O emissions across the two NM treatments and control at weeks 1 and 3 of the experiment. (C) Weekly time course of hydroponic CO_2 emissions across the two NM treatments and control. Error bars indicate SEM of 3 replicates. (D) Weekly time course of hydroponic CH_4 emissions across the two NM treatments and control. Error bars indicate SEM of 3 replicates.

N_2O emissions peak in week 2 (Figure 5.2A), with negligible production of N_2O by comparison in weeks 1, and 3 through 6. All three treatments produced a similar peak in N_2O emissions, with *week* having a significant interaction with $Co_{2.25}Fe_{0.75}O_4$ (*t=2.03*). The N_2O emissions between the three treatments appear similar, yet there is a significant difference seen between $Co_{2.25}Fe_{0.75}O_4$ emissions as

compared to the control (*t=-2.67*), with a slightly less significant difference seen between TiO_2 PVP and control N_2O emissions (*t=-2.03*). Cumulative N_2O emissions are depicted in SI Figure S5.3. The pathway via which these N_2O emissions are produced was studied at weeks 1, 3 and 6, with week 6 emissions showing significant deviations in data quality and as such were discounted. Denitrification sourced N_2O emissions were higher in week 1 than in week 3, as seen in Figure 5.2B. The control treatment at week 1 produced ~10% of N_2O emissions via denitrification. This indicates that the remaining ~90% of N_2O emissions at week 1 are primarily released through nitrification pathways. While ^{15}N tracer gas data was not recorded for week 2, it is likely that this large spike in N_2O emissions is also nitrification sourced.

CO_2 emissions (Figure 5.2C) from the lettuce and rockwool substrate increase over time under all treatments, peaking at week 6. The trend of CO_2 emissions for TiO_2 PVP and control treatments are highly similar, with a deviation from this pattern, and a much lower final CO_2 production rate seen under $Co_{2.25}Fe_{0.75}O_4$ treatment. CO_2 emissions are studied as a proxy for plant and microbial respiration. The increase in respiration is likely due to an increase in root biomass over the course of the six weeks (Figure 5.3), with increases in the microbial biomass in the rockwool substrate also. *Week* had a highly significant effect on CO_2 emissions (*t=7.51*), with a significant interaction between $Co_{2.25}Fe_{0.75}O_4$ and *week* also (*t=-3.293*), reflecting the time-based impact on gaseous emissions.

CH_4 emissions peaked for the control and TiO_2 PVP treatments at week 6, with $Co_{2.25}Fe_{0.75}O_4$ peaking at week 3 instead, as displayed in Figure 5.2D. CH_4 emissions were also negative under TiO_2 PVP treatment until week 5, with three weeks producing negative CH_4 emissions under control conditions and two for $Co_{2.25}Fe_{0.75}O_4$. None of the treatments showed linear increases in CH_4 emissions over time, with minor peaks seen at week 2 and week 3 for TiO_2 PVP and control treatments, respectively. *Week* had a significant effect on CH_4 emissions (*t=2.96*), however *treatment* appeared to have no effect.

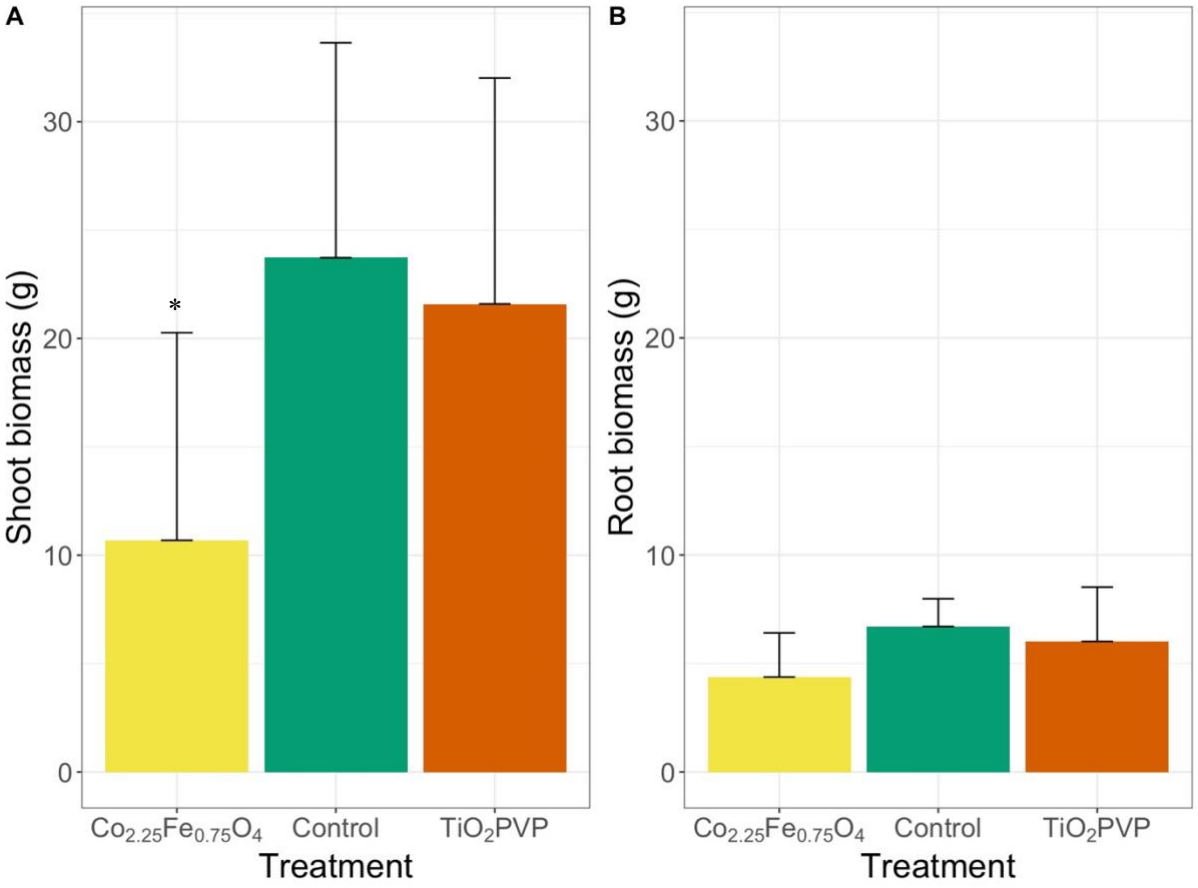


Figure 5.3. Lettuce fresh biomass for shoot (A) and root (B) tissues for each of the treatments (control or NM treated). Error bars indicate standard deviation from the mean. Statistical significance of $p < 0.05$ is denoted by '*'.

Far greater biomass accumulation occurred in the lettuce shoot tissues as opposed to the root tissues, as seen when comparing Figure 5.3A and 5.3B. Control treated lettuce had the greatest mean biomass accumulation for both shoots and roots. $Co_{2.25}Fe_{0.75}O_4$ grown lettuce was significantly smaller than those for control and TiO_2 PVP ($p=0.0083$; $p=0.03$). None of the root biomass differences between treatments were found to be statistically significant ($p=0.40$).

Comparing the Co content of the hydroponic medium and different compartments of the lettuce tissue produced shows very different concentrations of the NM constituent element (Figure 5.4). The greatest concentration of Co was found in the lettuce root tissues, with $Co_{2.25}Fe_{0.75}O_4$ treated lettuce having >2000 mg Co per kg of lettuce tissue. Due to wide variation in Co concentrations found in lettuce root tissues under $Co_{2.25}Fe_{0.75}O_4$ treatment, this difference was not significant (*p=0.091*). Lettuce shoot tissue Co concentration was much lower at ~10 mg kg^{-1}, but this was still significantly more than for the control (*p=0.0295*) and TiO_2 PVP treatment (*p=0.0075*). Both of the lettuce tissue concentrations were greater than those found in the bulk hydroponic medium and rockwool medium. There were significant differences between Co concentration in the bulk hydroponic medium compared to the control and TiO_2 PVP treatments (*p=0.0000018; p=0.0000048*). This difference was also seen in the rockwool medium where $Co_{2.25}Fe_{0.75}O_4$ had greater Co contents than control or TiO_2 PVP (*p=0.033; p=0.049*). These results are as expected, with no Co featuring in the standard hydroponic media nor in the TiO_2 PVP NM treatment.

Neither Fe nor Ti, the other NM constituent elements, showed significant differences in concentration in lettuce or hydroponic medium between treatments. NM translocation index values for the NM constituent elements, and macro- and micronutrient concentrations in both medium compartments and lettuce tissues can be seen in SI Table S5.4. Significantly higher concentrations of Cu (*p = 0.038*), Mo (*p = 0.035*) and Ni (*p = 0.013*) were found in $Co_{2.25}Fe_{0.75}O_4$ grown lettuces as compared to TiO_2 PVP grown lettuce.

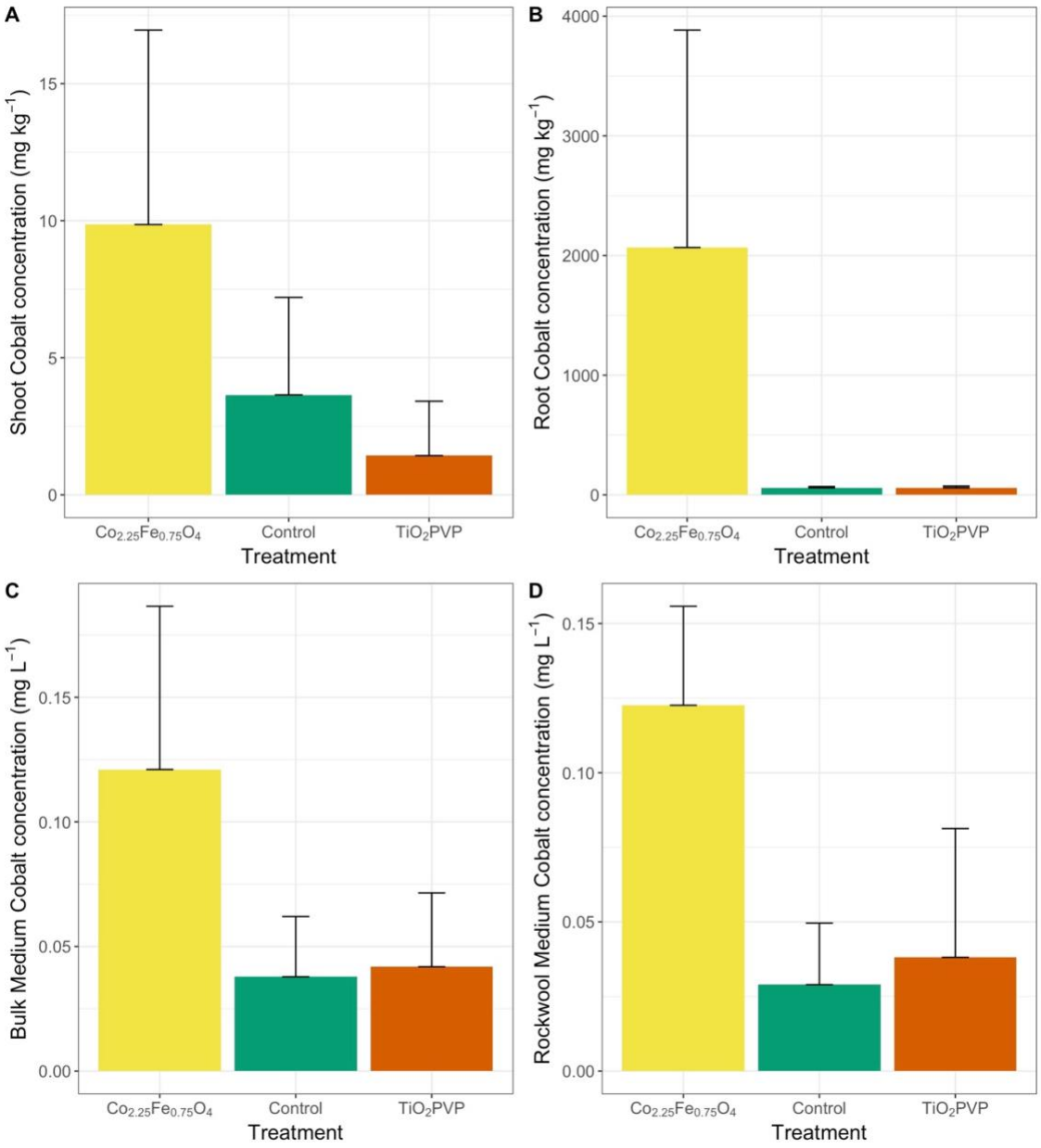


Figure 5.4. Comparison of Co concentration for shoot (A) and root (B) tissues, and between the bulk hydroponic medium (C) and medium stored in the rockwool root zone (D). Error bars indicate standard deviation from the mean.

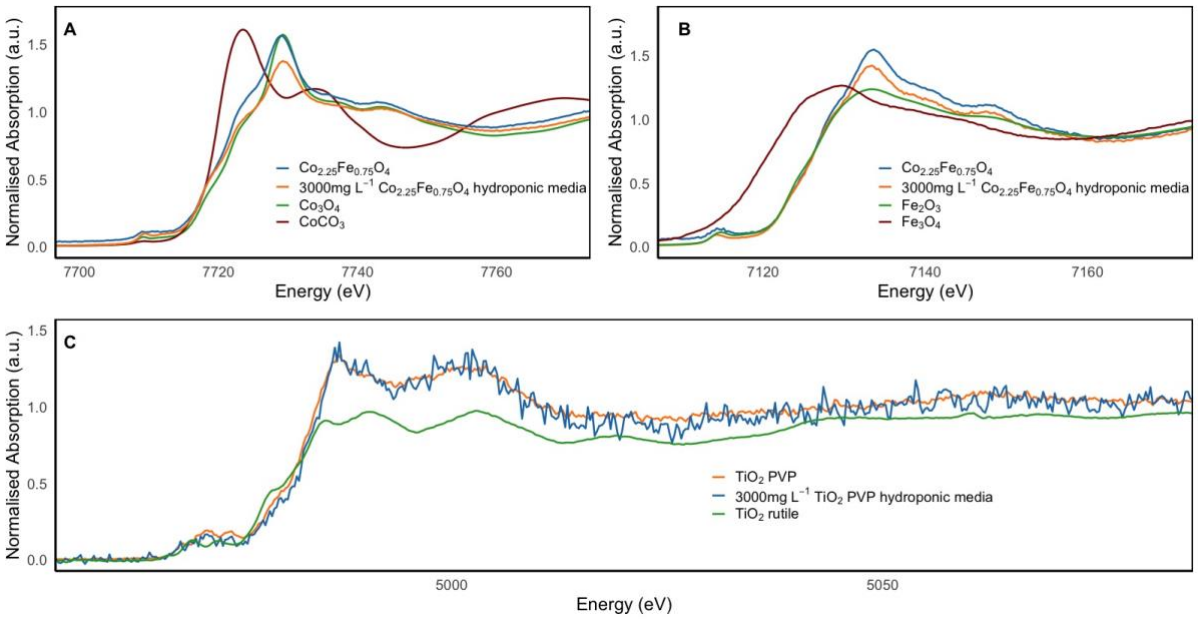


Figure 5.5. (A) Co K-edge XANES spectrum measured in hydroponic medium sample with 3000 mg L^{-1} added $Co_{2.25}Fe_{0.75}O_4$ NMs as compared to XANES spectra for $Co_{2.25}Fe_{0.75}O_4$, Co_3O_4 and $CoCO_3$. (B) Fe K-edge XANES spectrum measured on hydroponic media sample with 3000 mg L^{-1} added $Co_{2.25}Fe_{0.75}O_4$ NMs, compared to XANES profiles of pristine $Co_{2.25}Fe_{0.75}O_4$ NMs, Fe_2O_3 and Fe_3O_4. (C) Ti K-edge XANES spectrum measured on soil sample with added TiO_2 PVP NMs, compared to XANES profiles of pristine TiO_2 PVP and TiO_2 rutile.

Linear combination fitting for $Co_{2.25}Fe_{0.75}O_4$ hydroponic medium at 3000 mg L^{-1} showed that the sample's XANES profile could be completely described by two Co compounds, $CoCO_3$ (14%) and Co_3O_4 (86%) (Figure 5.5A). Co is in a 2+ valence state in $CoCO_3$ and in a +2.667 state when in Co_3O_4 NMs, with the valence state of the medium sample finding Co to be in a +2.578 valence state with an error margin of 0.012. Details of the linear combination fit are found in SI Table S5.5. Measurements on lettuce grown in soils with a lower (more environmentally realistic) concentration of nano metal oxides (25 mg L^{-1}) didn't produce high quality signals, however a XANES profile could still be detected indicating potential bioaccumulation of the NMs.

The highest concentration of $Co_{2.25}Fe_{0.75}O_4$ NMs in hydroponic medium had the clearest XANES signal, however, merging the spectra for the experimentally used concentration of 25 mg L^{-1} produced a sufficiently clear signal for linear combination fitting, as seen in SI Figure S5.4. The

hydroponic medium with 3000 mg L^{-1} $Co_{2.25}Fe_{0.75}O_4$, could be completely described in terms of the Fe content by a linear combination of the XANES spectra of $Co_{2.25}Fe_{0.75}O_4$ (44.5%) and Fe_2O_3 (55.5%).

The 3000 mg L^{-1} hydroponic medium sample of TiO_2 PVP was completely described by a linear combination of the XANES spectra of pristine TiO_2 PVP (96.2%), with a very small portion indicated to be TiO_2 rutile (3.8%), as seen in Figure 5.5C. The margin of error for TiO_2 rutile was 0.022 and, from Figure 5.5C, it seems highly likely that the TiO_2 PVP undergoes little to no transformation in the hydroponic medium.

5.5. Discussion

5.5.1. Impacts of TiO_2 PVP and $Co_{2.25}Fe_{0.75}O_4$ NMs on N-cycling are different but with similar outcomes

Emissions of N_2O in this hydroponic system showed a similar pattern across the three treatments, with significant reductions seen under $Co_{2.25}Fe_{0.75}O_4$ and TiO_2 PVP NM treatments. In many agricultural systems nitrification sourced N_2O is a minor source of N_2O, relative to other sources, such as denitrification, (Liang and Robertson, 2021). N_2O emissions at weeks 1 and 3 were predominantly nitrifier sourced, either through nitrifier denitrification or nitrification, as shown through the $^{15}N_2O$ data. While data for the N_2O emissions peak at week 2 is lacking, the data at week 3 is potentially similar to the pattern for week 2. The nitrifier sourced N_2O indicates that the hydroponic system is much more aerated than expected. The recirculating nature of the hydroponic setup with the intermittent wetting of the rockwool substrate that the lettuce roots grow in means that the anaerobic conditions that denitrifiers thrive in are avoided, therefore minimising denitrification sourced N_2O emissions. Karlowsky et al. (2023) found that hydroponically grown tomatoes produced the majority of their N_2O emissions via bacterial denitrification or nitrifier denitrification. This result instead follows the theory proposed by Lin et al. (2023), that N_2O emissions from soilless culture is largely dependent on growth substrate, with the microbial communities that populated the substrate determining the N_2O emission source.

The significant difference between the control and NM treatments impact on N_2O emissions suggests that NM addition must have some effect on the N_2O producing bacterial communities in the rockwool substrate. TiO_2 NMs have been shown to have little impact on nitrifying bacteria in soil, neither inhibiting nor promoting their activity, with ROS production due to TiO_2 NM presence having no correlation to nitrification inhibition (Choi and Hu, 2009). TiO_2 PVP NMs were not studied in the Choi and Hu paper but significant differences in ROS production were found between different TiO_2 nanoforms. The presence of the PVP polymer may therefore have an impact on the nitrifying bacteria, acting to immobilise nitrifying bacteria or increasing intracellular ROS production and changing bacterial growth strategy to reduce N_2O emissions. Alternatively, TiO_2 PVP may be acting on the smaller component of denitrification sourced N_2O, given that the difference between TiO_2 PVP treatment to the control was also small. TiO_2 NMs have been shown to be toxic to aerobic denitrifying bacteria in sewage sludge at 5-25mg L^{-1} (Li et al., 2016). This toxic effect was determined to be via ROS production, with TiO_2 NMs impacting on the microbial diversity of the sludge. These effects may be paralleled in this study with TiO_2 PVP NMs reducing net N_2O emissions not through impact on nitrifying bacteria, but on denitrifying bacteria, thus impacting only a small proportion of the total N_2O emissions. Lower NM concentrations agglomerate less, increasing the chance of contact with denitrifying bacteria due to the greater available surface area, therefore increasing toxicity risk, as theorised by Liu et al. (2020) with TiO_2 NMs and *Pseudomonas stutzeri*. TiO_2 PVP NMs don't appear to undergo significant transformation while in the hydroponic medium. This is likely due to the stabilising capabilities of PVP encapsulating the TiO_2 nanoparticles. PVP has been shown to reduce the activity of Au/TiO_2 catalysts, more than other polymers used for encapsulation (Yang et al., 2021). This may be another reason such a small change is seen in N_2O emissions, with PVP reducing the effect of TiO_2 NM on denitrifiers.

The transformed $Co_{2.25}Fe_{0.75}O_4$ compounds, Co_3O_4 and Fe_2O_3, as found in the XANES spectra linear combination fitting may act on the microbial community independently of one another. Co_3O_4 is applied in electrochemical denitrification, reducing NO_3 (Fu et al., 2021; Chen et al., 2024). In the context of soil, Co_3O_4 NMs have been used in NO_2^- detectors, reducing NO_2^- to NO_3^- (Puspalak et al., 2022). Here, the nano-Co_3O_4 may act to bind NO_2^- or NO_3^- ions in the soil, corroborated by the change

in $Co_{2.25}Fe_{0.75}O_4$ zeta potential from positive to negative over the 6-weeks, enabling cation interaction. Co_3O_4 may then reduce denitrification sourced N_2O emissions due to promoting ion exchange with NO_2^-/NO_3^-, forcing more efficient denitrification to produce N_2 rather than N_2O. Fe_2O_3 has been shown to function similarly, with nano-Fe_2O_3 used to promote more complete denitrification in a denitrifier biofilm-electrode (Yin et al., 2022). Nano-Fe_2O_3 however has been shown to have insignificant impact on N_2O emissions and de/nitrification gene abundance in soil (Wang et al., 2024). This indicates that the effect on N_2O emissions may primarily be through the action of Co_3O_4, or the combined effect of the two NMs may be required for N_2O emission impact. Further work should compare the mixed metal oxide's effect on N_2O emissions from a hydroponic system with each transformation product in isolation.

The microbial and root respiration, as measured by proxy of CO_2 evolution from the system, indicate increased respiring biomass with time. The CO_2 source is unknown, but the increasing lettuce biomass indicates that it may be at least partially lettuce root sourced. Lettuce growth is reduced under $Co_{2.25}Fe_{0.75}O_4$ NM treatment, with the lowest CO_2 emissions seen for this treatment also. If CO_2 emissions are primarily from root respiration, then little difference between NM impacts on microbes can be seen in this way, and more direct study of NM impacts on denitrifying enzymes is required.

This recirculating hydroponic system, being aerated, nutrient rich and freshwater, is closer to a rice field or wetland than to conventional soil agriculture, with hydroponic systems being used previously to represent paddy soils experimentally (Wang et al., 2018). In particular, the rockwool substrate and roots parallel the shallow oxygenated water of the rice paddy, with lettuce roots able to release O_2, providing a habitat for aerobic microbes. Methanogenesis is an anaerobic process whereby specialist microbes (methanogens) produce CH_4 gas, with methanotrophic bacteria oxidising CH_4 to consume it under oxic conditions. Methane (CH_4) emissions alter over the course of the experiment, with NM treatment not significantly modifying the emissions produced. Several of the weeks show negative CH_4 flux, indicating greater methanotroph activity, with increasing CH_4 emissions over time. The lack of $^{15}N_2O$ data for the later weeks of the experiment means that claims about the water balance of the system cannot be accurately made, although a consistent recirculation schedule was maintained

across the 6-week experiment. Denitrification may increase or decrease over time with lettuce roots either holding greater water in the rockwool substrate or increased demand from lettuce biomass accumulation causing greater drying. The change in CH_4 emissions from negative to positive flux indicates a potential shift towards more anaerobic conditions, with more methanogen activity. However, there are aerobic methanotrophs also, but these are found in aerated upland soils which have very different conditions than those found in the hydroponic system utilised here (Knief et al., 2003). If the rockwool substrate becomes more anaerobic with time due to enhanced lettuce root growth preventing free draining of the hydroponic media, the N_2O emissions, while still low from week 3 onwards of the experiment, may become more denitrification sourced. The NMs are theorised to be able to either inhibit or promote denitrification, with both pathways reducing N_2O emissions, explaining why there is sustained low N_2O production over the rest of the experiment.

5.5.2. NM transformations and lettuce growth and quality

The ICP-OES data clearly shows Co entering the lettuce tissues at a higher rate than Fe, as if the NMs were entering the plant tissue as intact particles there would be an expected ratio of 3:1 for Co:Fe, however, only Co tissue concentration was found to be significantly increased relative to the control, with no difference found for Fe concentration. $Co_{2.25}Fe_{0.75}O_4$ transforms in the hydroponic media, leaching Fe^{3+} ions which go on to form Fe_2O_3 and Co_3O_4 NMs. These two compounds were applied as NMs independently in previous research, with concentrations of <100 mg L^{-1} Co_3O_4 having a positive effect on *Brassica napus* growth (Jahani et al., 2020). Fe_2O_3 NMs have been used to replace Fe-EDTA for hydroponically grown radishes (*Raphanus sativus*) to increase crop yield and nutritive quality (Garza-Alonso et al., 2023). However, in this experiment $Co_{2.25}Fe_{0.75}O_4$ application reduced lettuce shoot biomass, the economically significant part of the crop. This may be due similar to results from Jurkow et al. (2020) where Fe_2O_3 application reduced lettuce fresh weigh but increased lettuce dry weight. Dry weight was not recorded in this study so the whether the NM's effect is on water uptake or genuine biomass cannot be clearly understood from the data. There was also significant uptake and translocation of Co, with high values found in both lettuce roots and shoots relative to the hydroponic

medium. Co has been shown to be toxic to lettuce at higher concentrations, which may also be the result of bioaccumulation of Co compounds, reducing biomass accumulation (Akeel and Jahan, 2020). Due to the concentrations used however, XANES spectra from lettuce shoot samples were not of sufficient quality for comparison. Fe lettuce tissue content is much higher generally as it is present in the NM Fe_2O_3, but also is an essential plant micronutrient. Fe K-edge XANES spectra for $Co_{2.25}Fe_{0.75}O_4$ grown lettuce did not produce high quality data, as seen in SI Figure S5.4. A linear combination fit for the lettuce tissue indicated that XANES spectra of $Co_{2.25}Fe_{0.75}O_4$ (49.8%), Fe_2O_3 (30.7%) and Fe_3O4 (19.6%) could completely describe the sample. This indicates that perhaps $Co_{2.25}Fe_{0.75}O_4$ is the main source of Co in the lettuce tissues, with fewer of the Co transformation products found in the medium being taken up. There is also an additional transformation of Fe inside the lettuce tissue, forming Fe_3O_4., which was not found to be present in the medium. Whether this is a true transformation from $Co_{2.25}Fe_{0.75}O_4$ to Fe_3O_4 or if this is a further transformation from one of the Fe transformation compounds (Fe_2O_3) from the medium that are converted to Fe_3O_4 in the shoot tissue is unknown based on the data presented here. To explore this further, synthesising $Co_{2.25}Fe_{0.75}O_4$ NMs with stable isotope labelled Fe could aid in tracing the Fe directly from the NM and the transformations it undergoes in different compartments.

The spectra quality of TiO_2 PVP for both pristine NMs and experimental samples is much lower than that for the reference standard, TiO_2 rutile. Whether this is due to the interaction between the stabilising PVP and the NM is unknown and requires further study. Previous research has not indicated that TiO_2 NMs undergo transformation after uptake into plants (Cox et al., 2017). Additionally, higher concentrations of NMs are needed for more accurate study of XANES spectra in lettuce tissues under the assumption that the transformations recorded will be the same as those at lower, more feasible, concentrations.

5.5.3. The rootzone has an important effect on nutrient accumulation and NM transformation

There are significant differences between rockwool substrate derived hydroponic medium and bulk hydroponic medium. This reflects the significance of the rhizosphere in this study, with greater NO_3^- and PO_4^{3-} contents in the rockwool at week 6. TN content was greater in the bulk medium, showing the active role the roots play in partitioning the hydroponic system. These differences occur in large part through the localised action of the roots in the rockwool substrate, triggering accumulation of different microbial species as well as inorganic nutrients. TN content in the bulk medium was also altered by NM addition, increasing under TiO_2 PVP application. Rockwool concentrations of Zn and S were reduced under $Co_{2.25}Fe_{0.75}O_4$ treatment. It may be that $Co_{2.25}Fe_{0.75}O_4$, or the transformation products $CoCO_3$ and Co_3O_4, interact directly with macro- and micronutrient compounds and ions, with the decrease in zeta potential of the NM over the growth period indicative that interactions between the positively charged NM and anions may be forming a corona around the NM or negatively charged heteroagglomerates (Lundqvist et al., 2011; Liu et al., 2013). Changes in agglomeration or corona formation can have big impacts on NM mobility and uptake, especially in aqueous environments (Liu et al., 2023). Additionally, NM interaction with the plant roots may be triggering changes in root exudate composition and concentration, further changing the possible interactions occurring in the rootzone of the hydroponic setup. The role of plant root exudates in NM transformation is particularly pertinent in hydroponics due to media recirculation and increased exudate mobility as compared to the soil environment (Cervantes-Avilés et al., 2021). Due to time constraints and scope of the study no root exudate studies were performed, however, future work should interrogate interactions between $CoCO_3$, Co_3O_4 and TiO_2 PVP NMs with inorganic nutrient compounds and root exudates, like organic acids and proteins.

Nutrient inputs were consistent across treatments however uptake of Cu, Mo and Ni in lettuce shoot tissues was lower in TiO_2 PVP grown lettuce, perhaps indicative of a negative impact on lettuce root active transport capabilities. This may be occurring due to agglomeration of TiO_2 PVP on the outside of the roots, blocking root pores, with TiO_2 NMs shown to aggregate on wheat root surfaces

and reduce root pore size in corn (Wild and Jones, 2009; Asli and Neumann, 2009). This could partially explain the reduction in TiO_2 PVP hydrodynamic size over time, with larger agglomerates interacting with root tissues (Larue et al., 2012).

5.5.4. Conclusion

The two NMs (TiO_2 PVP versus $Co_{2.25}Fe_{0.75}O_4$) have opposing effects on denitrifying bacteria with similar results. TiO_2 PVP likely inhibits denitrification to reduce N_2O emissions, potentially due to NM toxicity on denitrifying bacteria. The transformation products of $Co_{2.25}Fe_{0.75}O_4$, namely Co_3O_4 and Fe_2O_3, promote more complete denitrification to N_2 thus reducing denitrifier sourced N_2O emissions. However, neither NM applied had a significant effect on the total N_2O evolved from the hydroponic medium, due to most N_2O emissions being nitrifier sourced.

Bioaccumulation of Co compounds in lettuce tissue could be triggering toxicity due to limited biomass accumulation under $Co_{2.25}Fe_{0.75}O_4$ treatment and evidence of Co accumulation in lettuce shoot and root tissues. TiO_2 PVP application may impact on lettuce root's capacity for active transport, blocking root cell pores due to agglomeration of the NM on root surfaces, with visualisation required for evidence of this mechanism. The NMs also likely interact with the nutrients present in the medium, altering their zeta potential over the course of the growth period, and, along with plant roots, changing the nutrient concentrations found in the rockwool medium as opposed to the bulk medium.

Utilising ^{15}N tracers for both denitrification and nitrification pathways are essential to elucidating the underpinning mechanism of $Co_{2.25}Fe_{0.75}O_4$ NM's effect on N_2O emissions. This work would aid in determining whether the hypothesised Co_3O_4/Fe_2O_3 mechanism is accurate. Other work including study of de/nitrification gene abundance and qPCR of N cycling genes, more weeks studied using ^{15}N labelled tracers, with higher concentrations needed for accurate study in lettuce tissues using XANES to inform about risks of bioaccumulation. Changing NM concentration would likely have a large effect on N_2O and bacteria, resulting in the need for dose-response studies using the NMs.

References

Akeel, A., Jahan, A., 2020. Role of Cobalt in Plants: Its Stress and Alleviation, in: Naeem, M., Ansari, A.A., Gill, S.S. (Eds.), Contaminants in Agriculture: Sources, Impacts and Management. Springer International Publishing, Cham, pp. 339–357. https://doi.org/10.1007/978-3-030-41552-5_17

Amiri, M., Salavati-Niasari, M., Akbari, A., 2019. Magnetic nanocarriers: Evolution of spinel ferrites for medical applications. Advances in Colloid and Interface Science 265, 29–44. https://doi.org/10.1016/j.cis.2019.01.003

Asli, S., Neumann, P.M., 2009. Colloidal suspensions of clay or titanium dioxide nanoparticles can inhibit leaf growth and transpiration via physical effects on root water transport. Plant, Cell & Environment 32, 577–584. https://doi.org/10.1111/j.1365-3040.2009.01952.x

Bhowmik, R.N., Panda, M.R., Yusuf, S.M., Mukadam, M.D., Sinha, A.K., 2015. Structural phase change in Co2.25Fe0.75O4 spinel oxide by vacuum annealing and role of coexisting CoO phase on magnetic properties. Journal of Alloys and Compounds 646, 161–169. https://doi.org/10.1016/j.jallcom.2015.05.276

Carmassi, G., Incrocci, L., Maggini, R., Malorgio, F., Tognoni, F., Pardossi, A., 2005. Modeling Salinity Build-Up in Recirculating Nutrient Solution Culture. Journal of Plant Nutrition 28, 431–445. https://doi.org/10.1081/PLN-200049163

CEM, 2019. Mars 6 Microwave Acid Digestion Method Note Compendium.

Cervantes-Avilés, P., Huang, X., Keller, A.A., 2021. Dissolution and Aggregation of Metal Oxide Nanoparticles in Root Exudates and Soil Leachate: Implications for Nanoagrochemical Application. Environ. Sci. Technol. 55, 13443–13451. https://doi.org/10.1021/acs.est.1c00767

Chadwick, J.J., Witteveen, A., Zhang, P., Lynch, I., 2023. 10 - Hydroponics and alternative forms of agriculture: opportunities from nanotechnology, in: Zhang, P., Lynch, I., White, J.C., Handy, R.D. (Eds.), Nano-Enabled Sustainable and Precision Agriculture. Academic Press, pp. 259–272. https://doi.org/10.1016/B978-0-323-91233-4.00018-1

Chen, Y., He, J., Pang, H., Yu, D., Jiang, P., Hao, X., Zhang, J., 2024. Electrochemical denitrification by a recyclable cobalt oxide cathode: Rapid recovery and selective catalysis. Journal of Hazardous Materials 463, 132870. https://doi.org/10.1016/j.jhazmat.2023.132870

Choi, O., Hu, Z., 2009. Role of Reactive Oxygen Species in Determining Nitrification Inhibition by Metallic/Oxide Nanoparticles. Journal of Environmental Engineering 135, 1365–1370. https://doi.org/10.1061/(ASCE)EE.1943-7870.0000103

Comer-Warner, S.A., Ullah, S., Dey, A., Stagg, C.L., Elsey-Quirk, T., Swarzenski, C.M., Sgouridis, F., Krause, S., Chmura, G.L., 2024. Elevated temperature and nutrients lead to increased N2O emissions from salt marsh soils from cold and warm climates. Biogeochemistry 167, 21–37. https://doi.org/10.1007/s10533-023-01104-0

Cox, A., Venkatachalam, P., Sahi, S., Sharma, N., 2017. Reprint of: Silver and titanium dioxide nanoparticle toxicity in plants: A review of current research. Plant Physiology and Biochemistry, Effects of Nanomaterials in Plants 110, 33–49. https://doi.org/10.1016/j.plaphy.2016.08.007

Dennis, G., Helsby, W., Omar, D., Horswell, I., Tartoni, N., Hayama, S., Mikulska, I., Diaz-Moreno, S., 2019. First results using the new DLS Xspress4 digital pulse processor with monolithic segmented HPGe detectors on XAS beamlines. AIP Conference Proceedings 2054, 060065. https://doi.org/10.1063/1.5084696

Dent, A.J., Cibin, G., Ramos, S., Parry, S.A., Gianolio, D., Smith, A.D., Scott, S.M., Varandas, L., Patel, S., Pearson, M.R., Hudson, L., Krumpa, N.A., Marsch, A.S., Robbins, P.E., 2013. Performance of B18,

the Core EXAFS Bending Magnet beamline at Diamond. J. Phys.: Conf. Ser. 430, 012023. https://doi.org/10.1088/1742-6596/430/1/012023

Diaz-Moreno, S., Amboage, M., Basham, M., Boada, R., Bricknell, N.E., Cibin, G., Cobb, T.M., Filik, J., Freeman, A., Geraki, K., Gianolio, D., Hayama, S., Ignatyev, K., Keenan, L., Mikulska, I., Mosselmans, J.F.W., Mudd, J.J., Parry, S.A., 2018. The Spectroscopy Village at Diamond Light Source. J Synchrotron Radiat 25, 998–1009. https://doi.org/10.1107/S1600577518006173

Fu, T., Xu, C., Guo, R., Lin, C., Huang, Y., Tang, Y., Wang, H., Zhou, Q., Lin, Y., 2021. Zeolitic Imidazolate Framework-90 Nanoparticles as Nanozymes to Mimic Organophosphorus Hydrolase. ACS Appl. Nano Mater. 4, 3345–3350. https://doi.org/10.1021/acsanm.1c00540

Garza-Alonso, C.A., Cadenas-Pliego, G., Juárez-Maldonado, A., González-Fuentes, J.A., Tortella, G., Benavides-Mendoza, A., 2023. Fe2O3 nanoparticles can replace Fe-EDTA fertilizer and boost the productivity and quality of *Raphanus sativus* in a soilless system. Scientia Horticulturae 321, 112261. https://doi.org/10.1016/j.scienta.2023.112261

Jahani, M., Khavari-Nejad, R.A., Mahmoodzadeh, H., Saadatmand, S., 2020. Effects of cobalt oxide nanoparticles (Co3O4 NPs) on ion leakage, total phenol, antioxidant enzymes activities and cobalt accumulation in Brassica napus L. Notulae Botanicae Horti Agrobotanici Cluj-Napoca 48, 1260–1275. https://doi.org/10.15835/nbha48311766

Jurkow, R., Sękara, A., Pokluda, R., Smoleń, S., Kalisz, A., 2020. Biochemical Response of Oakleaf Lettuce Seedlings to Different Concentrations of Some Metal(oid) Oxide Nanoparticles. Agronomy 10, 997. https://doi.org/10.3390/agronomy10070997

Karlowsky, S., Buchen-Tschiskale, C., Odasso, L., Schwarz, D., Well, R., 2023. Sources of nitrous oxide emissions from hydroponic tomato cultivation: Evidence from stable isotope analyses. Front. Microbiol. 13. https://doi.org/10.3389/fmicb.2022.1080847

Kefeni, K.K., Mamba, B.B., Msagati, T.A.M., 2017. Application of spinel ferrite nanoparticles in water and wastewater treatment: A review. Separation and Purification Technology 188, 399–422. https://doi.org/10.1016/j.seppur.2017.07.015

Khan, A., Di Maio, A., Guggenheim, E., Chetwynd, A., Pencross, D., Tang, S., Belinga-Desaunay-Nault, M.-F., Thomas, S., Rappoport, J., Lynch, I., 2020. Surface Chemistry-Dependent Evolution of the Nanomaterial Corona on TiO2 Nanomaterials Following Uptake and Sub-Cellular Localization. Nanomaterials 10, 401. https://doi.org/10.3390/nano10030401

Knief, C., Lipski, A., Dunfield, P.F., 2003. Diversity and Activity of Methanotrophic Bacteria in Different Upland Soils. Applied and Environmental Microbiology 69, 6703–6714. https://doi.org/10.1128/AEM.69.11.6703-6714.2003

Larue, C., Laurette, J., Herlin-Boime, N., Khodja, H., Fayard, B., Flank, A.-M., Brisset, F., Carriere, M., 2012. Accumulation, translocation and impact of TiO2 nanoparticles in wheat (*Triticum aestivum* spp.): Influence of diameter and crystal phase. Science of The Total Environment 431, 197–208. https://doi.org/10.1016/j.scitotenv.2012.04.073

Li, D., Li, B., Wang, Q., Hou, N., Li, C., Cheng, X., 2016. Toxicity of TiO2 nanoparticle to denitrifying strain CFY1 and the impact on microbial community structures in activated sludge. Chemosphere 144, 1334–1341. https://doi.org/10.1016/j.chemosphere.2015.10.002

Liang, D., Robertson, G.P., 2021. Nitrification is a minor source of nitrous oxide (N2O) in an agricultural landscape and declines with increasing management intensity. Glob Chang Biol 27, 5599–5613. https://doi.org/10.1111/gcb.15833

Lin, W., Li, Q., Zhou, W., Yang, R., Zhang, D., Wang, H., Li, Yujia, Qi, Z., Li, Yuzhong, 2023. Insights into production and consumption processes of nitrous oxide emitted from soilless culture systems by

dual isotopocule plot and functional genes. Science of The Total Environment 856, 159046. https://doi.org/10.1016/j.scitotenv.2022.159046

Liu, J., Legros, S., von der Kammer, F., Hofmann, T., 2013. Natural Organic Matter Concentration and Hydrochemistry Influence Aggregation Kinetics of Functionalized Engineered Nanoparticles. Environ. Sci. Technol. 47, 4113–4120. https://doi.org/10.1021/es302447g

Liu, S., Zhang, X., Zeng, K., He, C., Huang, Y., Xin, G., Huang, X., 2023. Insights into eco-corona formation and its role in the biological effects of nanomaterials from a molecular mechanisms perspective. Science of The Total Environment 858, 159867. https://doi.org/10.1016/j.scitotenv.2022.159867

Lundqvist, M., Stigler, J., Cedervall, T., Berggård, T., Flanagan, M.B., Lynch, I., Elia, G., Dawson, K., 2011. The Evolution of the Protein Corona around Nanoparticles: A Test Study. ACS Nano 5, 7503–7509. https://doi.org/10.1021/nn202458g

McKeil, J., 2018. Best Types Of Hydroponics Systems and How They Work In 2019 [WWW Document]. Happy Hydro. URL https://www.happyhydro.com/blogs/news/best-types-of-hydroponics-systems-and-how-they-work-in-2019 (accessed 3.1.22).

Menard, A., Drobne, D., Jemec, A., 2011. Ecotoxicity of nanosized TiO2. Review of in vivo data. Environmental Pollution 159, 677–684. https://doi.org/10.1016/j.envpol.2010.11.027

Micucci, G., Lewicka-Szczebak, D., Sgouridis, F., Well, R., Buchen-Tschiskale, C., McNamara, N.P., Krause, S., Lynch, I., Roos, F., Ulla, S., 2024. Combining the 15N Gas flux method and N2O isotopocule data for the determination of soil microbial N2O sources.

Miranda, K.M., Espey, M.G., Wink, D.A., 2001. A Rapid, Simple Spectrophotometric Method for Simultaneous Detection of Nitrate and Nitrite. Nitric Oxide 5, 62–71. https://doi.org/10.1006/niox.2000.0319

Mulvaney, R.L., 1996. Nitrogen—Inorganic Forms, in: Methods of Soil Analysis. John Wiley & Sons, Ltd, pp. 1123–1184. https://doi.org/10.2136/sssabookser5.3.c38

Mulvaney, R.L., 1984. Determination of 15N-Labeled Dinitrogen and Nitrous Oxide with Triple-Collector Mass Spectrometers. Soil Science Society of America Journal 48, 690–692. https://doi.org/10.2136/sssaj1984.03615995004800030045x

Murphy, J., Riley, J.P., 1962. A modified single solution method for the determination of phosphate in natural waters. Analytica Chimica Acta 27, 31–36. https://doi.org/10.1016/S0003-2670(00)88444-5

Piccinno, F., Gottschalk, F., Seeger, S., Nowack, B., 2012. Industrial production quantities and uses of ten engineered nanomaterials in Europe and the world. J Nanopart Res 14, 1109. https://doi.org/10.1007/s11051-012-1109-9

Puga, A.P., Abreu, C.A., Melo, L.C.A., Beesley, L., 2015. Biochar application to a contaminated soil reduces the availability and plant uptake of zinc, lead and cadmium. Journal of Environmental Management 159, 86–93. https://doi.org/10.1016/j.jenvman.2015.05.036

Puspalak, A., Chinnadurai, P., Prathibha, R., Kumar, M.P., Manjushree, S.G., UdayaKumar, V., S. Adarakatti, P., 2023. Cobalt oxide nanoparticles based carbon electrode for the detection of residual nitrite in the soil of agricultural fields. Materials Research Innovations 27, 100–109. https://doi.org/10.1080/14328917.2022.2085909

Qin, J.-Y., Wang, S., Zhou, S., Liu, T., Yin, Y., Yang, J., 2021. Dominating Role of Interfacial N–Ni Coordination in Spinel Nickel Ferrite/N-Doped Graphene Hybrids for Boosting Reversible Oxygen Electrocatalysis. Adv Energy and Sustain Res 2, 2000106. https://doi.org/10.1002/aesr.202000106

Rapson, T.D., Dacres, H., 2014. Analytical techniques for measuring nitrous oxide. TrAC Trends in Analytical Chemistry 54, 65–74. https://doi.org/10.1016/j.trac.2013.11.004

Ravel, B., Newville, M., 2005. ATHENA, ARTEMIS, HEPHAESTUS: data analysis for X-ray absorption spectroscopy using IFEFFIT. J Synchrotron Rad 12, 537–541. https://doi.org/10.1107/S0909049505012719

R Core Team (2023). R: A language and environment for statistical computing. R Foundation for Statistical Computing, Vienna, Austria. URL https://www.R-project.org/.

Regulation (EU) 2015/2283 of the European Parliament and of the Council of 25 November 2015 on novel foods, amending Regulation (EU) No 1169/2011 of the European Parliament and of the Council and repealing Regulation (EC) No 258/97 of the European Parliament and of the Council and Commission Regulation (EC) No 1852/2001, 2021.

Sgouridis, F., Reay, M., Cotchim, S., Ma, J., Radu, A., Ullah, S., 2023. Stimulation of soil gross nitrogen transformations and nitrous oxide emission under Free air CO2 enrichment in a mature temperate oak forest at BIFoR-FACE. Soil Biology and Biochemistry 184, 109072. https://doi.org/10.1016/j.soilbio.2023.109072

Sgouridis, F., Ullah, S., 2017. Soil Greenhouse Gas Fluxes, Environmental Controls, and the Partitioning of N2O Sources in UK Natural and Seminatural Land Use Types. Journal of Geophysical Research: Biogeosciences 122, 2617–2633. https://doi.org/10.1002/2017JG003783

Sharma, N., Acharya, S., Kumar, K., Singh, N., Chaurasia, O.P., 2018. Hydroponics as an advanced technique for vegetable production: An overview. Jour. of Soi. and Wat. Conser. 17, 364. https://doi.org/10.5958/2455-7145.2018.00056.5

Stevens, R.J., Laughlin, R.J., 1998. Measurement of nitrous oxide and di-nitrogen emissions from agricultural soils. Nutrient Cycling in Agroecosystems 52, 131–139. https://doi.org/10.1023/A:1009715807023

Verdoliva, S.G., Gwyn-Jones, D., Detheridge, A., Robson, P., 2021. Controlled comparisons between soil and hydroponic systems reveal increased water use efficiency and higher lycopene and β-carotene contents in hydroponically grown tomatoes. Sci Hortic 279, 109896. https://doi.org/10.1016/j.scienta.2021.109896

Wang, J., Guo, L., Yang, F., Xiang, J., Long, L., Ni, K., 2024. Nanoparticles of Zinc Oxides Mitigated N2O Emissions in Tea Plantation Soil. Agronomy 14, 1113. https://doi.org/10.3390/agronomy14061113

Wang, Y., Lv, N., Mao, X., Yan, Z., Wang, J., Tan, W., Li, X., Liu, H., Wang, L., Xi, B., 2018. Cadmium tolerance and accumulation characteristics of wetland emergent plants under hydroponic conditions. RSC Advances 8, 33383–33390. https://doi.org/10.1039/C8RA04015J

Wild, E., Jones, K.C., 2009. Novel Method for the Direct Visualization of in Vivo Nanomaterials and Chemical Interactions in Plants. Environ. Sci. Technol. 43, 5290–5294. https://doi.org/10.1021/es900065h

Yang, N., Pattisson, S., Douthwaite, M., Zeng, G., Zhang, H., Ma, J., Hutchings, G.J., 2021. Influence of Stabilizers on the Performance of Au/TiO2 Catalysts for CO Oxidation. ACS Catal. 11, 11607–11615. https://doi.org/10.1021/acscatal.1c02820

Yin, H., Lin, X., Zhao, F., Pu, Y., Chen, Y., Tang, X., 2022. Nano-α-Fe2O3 for enhanced denitrification in a heterotrophic/biofilm-electrode autotrophic denitrification reactor. Water Environment Research 94, e10814. https://doi.org/10.1002/wer.10814

Zhang, P., Guo, Z., Ullah, S., Melagraki, G., Afantitis, A., Lynch, I., 2021. Nanotechnology and artificial intelligence to enable sustainable and precision agriculture. Nat. Plants 7, 864–876. https://doi.org/10.1038/s41477-021-00946-6

Zheng, M., Gu, M., Jin, Y., Wang, H., Zu, P., Tao, P., He, J., 2001. Effects of PVP on structure of TiO2 prepared by the sol-gel process. Materials Science and Engineering: B 87, 197–201. https://doi.org/10.1016/S0921-5107(01)00743-7

Chapter 6. Nanomaterial Interactions with Nitrogen Cycling Soil Microbial Communities and Ecotoxicological Implications for *Eisenia fetida*

Jessica. J. Chadwick[1,2], Sami Ullah[1], Iseult Lynch[1], Cynthia Kallenbach[2]

[1] School of Geography, Earth and Environmental Sciences, University of Birmingham, B17, UK

[2] Department of Natural Resource Sciences, McGill University, Quebec, Canada

Acknowledgements

Thanks go to Joann Whalen, Noura Alsawari, and Mohammed Antari (McGill University, QC, Canada) for gas chromatography analysis and *Eisenia fetida* ecotoxicology assay advice. ICP-OES/MS work was assisted by Chris Stark (University of Birmingham, UK). Zeolite nanomaterials were provided by Aleksandar Radu (University of Lincoln, UK) with $Co_{2.25}Fe_{0.75}O_4$ obtained from Promethean Particles via the EU-funded NanoSolveIT project (Grant Agreement Nº 814572). This work was primarily funded through the Mitacs Globalink Research Award, with Birmingham based work (ICP-OES/MS) supported by the Biotechnology and Biological Sciences Research Council (BBSRC) and University of Birmingham funded Midlands Integrative Biosciences Training Partnership (MIBTP) grant number BB/T00746X/1.

CReDIT statement

Jessica Chadwick: Writing – Original Draft, Investigation, Formal analysis, Visualisation, Conceptualization, Funding acquisition. Sami Ullah: Supervision, Writing – Review and Editing, Funding acquisition. Iseult Lynch: Supervision, Writing – Review and Editing, Conceptualization, Funding acquisition. Cynthia Kallenbach: Supervision, Conceptualization, Writing – Review and Editing, Funding acquisition.

6.1. Abstract

Nanomaterial (NM) entry to the soil environment occurs through direct pathways, including the rising use of nano-enabled fertilisers and pesticides as part of a sustainable agriculture strategy, and indirectly through NMs presence in sewage sludge and effluent that end up in soils. Understanding how NMs accumulated in the soil impacts soil microbial communities and soil fauna is essential for sustainable use of NMs in agriculture. Drivers for NM utilisation in agriculture include the potential for reduced synthetic fertiliser application and reduced pollution due to increased efficiency of nitrogen utilisation. NM co-application with reduced doses of fertiliser may alter reactive nitrogen (Nr) emissions, largely through microbial-mediated activity. This experiment was designed to explore both abiotic and biotic impacts on NM and reduced fertilisation amendments on soils' N cycling. We compared lettuce grown in soil treated with four different NMs or conventional fertilizer, with and without a microbial community. BEA-150, a zeolite NM, increases microbial nitrous oxide (N_2O) emissions and nitrate concentrations in leachate, potentially also increasing abiotically derived N_2O emissions. Nr losses were least affected by ZSM-5-15, instead being influenced more by abiotic factors, such as soil moisture. The effect of the $Ce_{0.75}Zr_{0.25}O_2$ NM was also highly impacted by microbial presence, increasing N_2O emissions and nitrate leachate concentrations from autoclaved soils. Lettuce growth was increased in autoclaved soil due to release of N from soil and dead microbes. Earthworms (*Eisenia fetida)* exposed to low concentrations of ZSM-5-15 experienced sub-lethal responses, potentially with NM uptake being agglomerate size dependent. The importance of microbial interactions and abiotic soil factors on NM efficacy for lettuce growth and in minimising Nr losses in soil indicates that NM impacts are not only plant species and NM dependent, but very likely also soil type dependent, with potential for sublethal ecotoxicological impacts at environmentally relevant concentrations.

6.2. Introduction

Nanomaterials' (NM) unique characteristics, derived from their large surface area to volume ratio, surface chemistry and adsorption abilities, have made them a common target for research in a wide range of industrial sectors (Schodek et al., 2009). NMs can be designed with specific properties or functions in mind, for example magnetic or catalytic functionality (Falinksi et al., 2018). NM usage in agricultural contexts is increasing due to the ability of NMs to permit slow release of their nutritive or pesticide load (Khot et al., 2012). This can increase the efficiency of synthetic fertiliser and pesticide additions, minimising agricultural pollution through nutrient run-off or inadvertent effects of pesticides on soil biota. Applying NMs in agriculture as fertiliser or pesticides directly introduces NMs to the soil environment, however NMs applied in other industries can also enter soil, for example due to effluent disposal or sewage sludge application of agricultural fields, with soil acting as a major NM sink (Dror et al., 2015). NM impacts on soil, whether through direct or indirect application, is of major interest in terms of soil biology and biogeochemistry. The soil biological community, including soil microbes and fauna like the earthworm *Eisenia fetida,* are instrumental in soil nitrogen (N) cycling, affecting plant available N as well as N losses to air and groundwater. Thus, the interaction between NMs and the soil biological community and the potential ecotoxicology consequences need to be better understood given the increasing application and accumulation of NMs in the soil.

The global N cycle is largely regulated through the action of terrestrial microbes that control N cycling. Additional N inputs to soil causes reactive N (Nr) compounds to pollute waterways through surface run-off and groundwater leaching, as well as volatilisation of N compounds, including formation of the greenhouse gas N_2O. The concentration of Nr is partly mediated by microbial activity through their production of extracellular enzymes. Extracellular enzymes are secreted by soil microbes which breakdown organic matter into smaller compounds and mineral nutrients. Microbes can then assimilate these smaller compounds, promoting microbial growth but also increasing the N mineralisation rate and thus Nr concentrations. Secretion of extracellular enzymes is energetically costly to the microbe and occurs under situations of high nutrient availability, allowing extracellular enzyme activity (EEA) to

act as an indicator of nutrient cycling (Jian et al., 2016). Extracellular enzymes with particular relevance to N cycling include urease and peptidases enzymes that aid in protein digestion and enzymes involved in oligosaccharide breakdown.

Just as EEA is a good indicator of soil nutrient status and microbial function, earthworm responses are a good indicator of compound toxicity to soil fauna. Earthworms are known as ecosystem engineers, with essential roles in organic matter incorporation into soil and soil aeration (Jänsch et al., 2005). *Eisenia fetida* are a commonly used model organism for terrestrial ecotoxicology studies, due to their direct interaction with the soil and significance as a primary consumer in multiple food chains. Looking at both toxic and sub-lethal impacts of NMs on earthworms is a crucial aspect of determining the sustainable use of NMs in the broader agroecosystem context.

Ecotoxicological studies frequently focus on aquatic organisms, like the filter feeder *Daphnia*, as indicators of a compound's toxic effects on biota, to understand the environmental fate and exposure routes to organisms. Terrestrial ecotoxicology is more complex, with the soil matrix being a highly heterogeneous environment, with the additional potential for NM interactions with soil colloids, organic matter and cations (Garcia-Velasco et al., 2016). These NM interactions with soil colloids could, for instance, alter both the NM and soil properties, with NMs shown to impact on soil sorption capacity (Dror et al., 2015). NMs may therefore be able to affect N cycling through binding to organic and inorganic solutes, catalysing N transformation independently of any microbial activity.

NM interactions with microbes may vary significantly depending on the NM properties, with NM characteristics such as composition, size and shape all impacting on NM effects (Suresh et al., 2013). The NMs studied in this experiment were two zeolites of differing Si:Al ratios, ZSM-5-15 and BEA-150, and the mixed metal oxide $Ce_{0.75}Zr_{0.25}O_2$. Zeolites have been shown to use the pores that occur as part of their 3D structure in ion exchange, making them good candidates for nutrient delivery, with existing applications as industrial catalysts (Colella, 1996). Both zeolites utilised in this study featured NH_4^+ as their extra-framework ion, associating with pore spaces of both zeolites. Ion exchange of NH_4^+ using zeolites has been used in wastewater amendment, making them particularly promising as slow-release fertilisers that could reduce Nr losses to the environment by increasing plant N-use efficiency

(Hedström, 2001). Cerium zirconium oxides have also been used industrially as catalysts, in particular in vehicle catalytic converters, reflecting their catalytic and redox activity which may be of relevance in mitigating N emissions (Ozawa, 1998; Bulfin et al., 2016).

Our objective was to examine two core aspects of soil biological and biogeochemical responses to soil application of engineered NMs while growing lettuce (*Lactuca sativa*): the microbial and abiotic impacts of NMs on N cycling and the potential toxic effects on the earthworm *Eisenia fetida*. In the first part of the study, we used three NMs (ZSM-5-15 and BEA-150, and $Ce_{0.75}Zr_{0.25}O_2$) with a reduced dose of N, phosphorus and potassium (NPK) fertiliser in comparison to reduced dose fertiliser alone and a negative control. To determine the extent of NMs abiotic versus microbial-mediated impacts on N cycling we included a comparison between sterilised and unsterilised natural soil. In response to these amendments, we measured EEA as an indicator of microbial activity and soil N status, lettuce yield and nutritive quality, and inorganic N cycling through leachate inorganic N concentrations and N_2O gaseous emissions. In the second part of the study we performed an adapted standard test for *Eisenia fetida* reproduction (OECD 222) using the same natural soil as in the lettuce experiment and a range of zeolite NM doses. Together these experiments aimed to inform how significantly microbes and NM interactions impact N cycling and soil N losses, while also examining the potential implications of nano-enabled fertiliser application on soil microbial and earthworm activity.

6.3. Materials and Methods

6.3.1. Materials

A 5% aqueous dispersion of $Ce_{0.75}Zr_{0.25}O_2$, was obtained from Promethean Particles (UK) via the NanoSolveIT project. Powdered ZSM-5-15 (Si:Al = 15.0) and BEA-19 (Si:Al = 19.0) were obtained from Zeolyst (USA). Hydrodynamic diameter and zeta potential were recorded using 500 mg L^{-1} deionised water dispersed NMs with a dynamic light scattering (DLS) instrument (Zetasizer, Malvern Instruments, UK). Nitrogen, phosphorus and potassium (NPK) amendment of the soil comprised of urea (Sigma-Aldrich) and potassium phosphate monobasic (Sigma-Aldrich).

6.3.2. Greenhouse study: experimental set up and sampling

We conducted a greenhouse study with lettuce to test the effect of NM on lettuce growth, N cycling and extracellular enzyme activity (EEA). The soil used for the greenhouse lettuce growth is a Courval sandy loam and has a history of maize, forage, and soybean conventional cultivation. Over the past decade, soil pH is on average 6.5. After sampling, soils were stored for two weeks in sealed containers at room temperature in the dark prior to the start of the experiment. Soils were sieved to 2 mm before half of the total soil volume was autoclaved (121˚C, 30 minutes) and the rest was left as natural soil stored at room temperature.

For each experimental unit, 1kg (dry weight) soil of either autoclaved or natural soil was added to a pot and adjusted to 60% water holding capacity (WHC) and left to rest under greenhouse conditions (21˚C, 16:8 light/dark cycle) for seven days before applying the amendments. Three NM amendments were used per soil condition (autoclaved versus natural), as summarised in Table 6.1. The three NMs were BEA-150, ZSM-5-15 and $Ce_{0.75}Zr_{0.25}O_2$ applied at a rate of 25 mg kg^{-1} of dry soil in a 100 mL water suspension plus an additional 35 kg ha^{-1} urea and 60 kg ha^{-1} P_2O_5 and K_2O, which was 50% of the recommended dose according to the Guide de Référence en Fertilisation (CRAAQ, 2013). Two non-NM amendments were also used: an NPK amendment alone at the same rate as used in the NM

amendments (i.e., half of the recommended dose) and a negative control where neither NPK nor NMs were added to the soil. Each amendment combination (soil condition and NMs plus controls) was replicated three times. To control for the effect of added water when applying the NM suspensions, the same volume of water was added to the control amendment. Regular water additions occurred weekly to maintain soil moisture at ~60% WHC throughout the experiment. Soil moisture and pH were monitored over the course of the experiment (Supplementary Information; SI Figure S6.1).

Three *Lactuca sativa* seeds ("Black Seeded Simpson" variety; OSC Seeds, ON, Canada) were sown directly in the soil for all amendment/condition combinations and grown for seven weeks in a greenhouse at 18-25˚C with 16:8 light to dark day cycles. After the first week post-sowing, similarly sized seedlings were maintained (>2 cm tall) and the rest were removed from each pot replicate, leaving one seedling per pot. The lettuce's fresh biomass was weighed at the end of the seven-week growing period before drying at 70˚C for 48 hours and stored at room temperature for future analysis.

Table 6.1. Experimental amendments to study NM abiotic and biotic effects on lettuce growth, N cycling and extracellular enzyme activity.

Soil Condition	Amendment	NPK application rate	NM application rate	Biological Replicates
Autoclaved	Control (water)	-	-	3
Autoclaved	NPK	35 kg ha^{-1} N, 60 kg ha^{-1} P_2O_5	-	3
Autoclaved	BEA-150 + NPK	35 kg ha^{-1} N, 60 kg ha^{-1} P_2O_5	25 mg kg^{-1}	3
Autoclaved	$Ce_{0.75}Zr_{0.25}O_2$ + NPK	35 kg ha^{-1} N, 60 kg ha^{-1} P_2O_5	25 mg kg^{-1}	3
Autoclaved	ZSM-5-15 + NPK	35 kg ha^{-1} N, 60 kg ha^{-1} P_2O_5	25 mg kg^{-1}	3
Natural	Control (water)	-	-	3
Natural	NPK	35 kg ha^{-1} N, 60 kg ha^{-1} P_2O_5	-	3
Natural	BEA-150 + NPK	35 kg ha^{-1} N, 60 kg ha^{-1} P_2O_5	25 mg kg^{-1}	3
Natural	$Ce_{0.75}Zr_{0.25}O_2$ + NPK	35 kg ha^{-1} N, 60 kg ha^{-1} P_2O_5	25 mg kg^{-1}	3
Natural	ZSM-5-15 + NPK	35 kg ha^{-1} N, 60 kg ha^{-1} P_2O_5	25 mg kg^{-1}	3

6.3.3. Greenhouse gas flux sampling

Gas sampling of CH_4, CO_2 and N_2O was performed weekly using 15x15 cm cylindrical gas sampling chambers. Gas samples were taken at regular intervals, including a zero hour blank, and at 20, 40 and 60 minutes. Samples were analysed using Bruker 450 Gas Chromatograph (GC), equipped with an electron capture detector (ECD) and a flame ionization detector (FID) and a PAL3 autosampler (Bruker Corporation, USA) at McGill University (Ejack and Whalen, 2021). Gas flux rates were calculated using the change in gas concentrations in parts per million (ppm) across the time points, multiplied by the volume of the sampling chamber and divided by both dry soil mass and incubation time ($\mu g\ N_2O\text{-}N\ kg^{-1}\ h^{-1}$). Due to technical difficulties only gas data for weeks 1, 2, 6 and 7 was used in the analysis.

6.3.4. Soil and leachate characterisation and nutrient analysis

Soils and leachates were analysed for nitrate (NO_3^-) and ammonium (NH_4^+) content on weeks 1, 3, 5 and 7 of the experiment with subsamples taken from each pot over the experimental period before destructive sampling at the final timepoint. Soil was subsampled and homogenized from each pot and extracted using 0.5 M KCl at a ratio of 1:5. Leachate samples were collected immediately following water additions to the pots to adjust for soil moisture, by collecting of the first 50 mL of leached water. Soil and leachate samples were stored at 4-7˚C and analysed within 48 hours of collection. Gravimetric soil moisture and pH were also measured at weeks 1, 3, 5 and 7. Soil samples for gravimetric soil moisture and pH were taken before watering and so reflect the driest the soils reached. Gravimetric soil moisture analysis was performed on 5g of soil, with mass measurements taken at the time of sampling and after 48 hours of drying at 70˚C. Measurements for soil pH were done using a ratio of 1:5 of soil and 0.01M $CaCl_2$. Nutrient analysis was performed on KCl extracted soil and leachate samples for NH_4^+ and NO_3^-, using protocols from Mulvaney (1996) and Miranda et al. (2001), respectively. Both compounds were analysed using a microplate reader (BioTek Instruments, USA). Soil and leachate NO_3^- samples had absorbances read at 540 nm and NH_4^+ samples were read at 650 nm.

6.3.5. Macro- and micronutrient and NM constituent element analysis

Nutrient and NM constituent elements were analysed in soil and lettuce shoots. The analysis was performed on heat-assisted acid digested samples, as described in the MARS 6 Microwave Acid Digestion Method Note Compendium (CEM, 2019), using a MARS 6 microwave digestion system with details per sample type available in SI Table S6.1. Once digested, samples were diluted 50-fold with deionised water. Diluted samples were then run using inductively coupled plasma optical emission spectroscopy (ICP-OES) on a Perkin Elmer optima 8000 ICP-OES (Agilent Technologies Ltd, USA) using mixed element standards for each element of interest (Ce, Zr, Si, Al, Mn, Mg, Na, Fe, P, Ni, K, Zn, Ca, Cu) that ranged from 0.05 to 10 ppm.

6.3.6. Extracellular microbial enzyme activity assays

Potential extracellular enzyme activity (EEA) was determined for four hydrolytic N-cycling enzymes: β-1,4-N-acetylglucosaminidase (NAG), leucine aminopeptidase (LAP), tyrosine aminopeptidase (TAP) and amidohydrolase (urease) with their respective substrate compounds detailed in Table 6.2. Soil extracellular enzyme activities were assessed pre-experiment (week 0) and at 1, 3, 5 and 7 weeks using the fluorescence-based assay for NAG, LAP and TAP (Saiya-Cork et al., 2002), and an absorbance-based assay for urease (Sinsabaugh.et al., 2000) within 5 days of sampling. Briefly, a soil slurry was made with 1 g dry soil homogenized with 100 mL of 50 mM sodium acetate buffer adjusted to the average soil pH as monitored separately at each week's sampling point (SI Figure S6.1). The potential activity of NAG, LAP, and TAP were determined fluorometrically using black, 96-well microplates and compound-specific fluorescing substrates bound to 4-methylumbelliferone or 7-amino-4-methyl coumarin. For each enzyme, 200 µL of soil slurry was combined with 50 µL of 200 µm substrate and incubated at 13-15˚C for ~5 hours. Plates were read at an excitation of 365 nm and 450 nm emission. Full details on microplate layout and incubation times for each enzyme are detailed in SI Table S6.2. Urease activity was determined colorimetrically through a 20-hour incubation period at

room temperature followed by pipetting of the reaction mix into a clear microplate and NH_4^+ was quantified in the same way as for the soil and leachate samples, described above.

Table 6.2. Summary of extracellular microbial enzymes of interest with their respective roles in N-cycling and substrates.

	β-1,4-N-acetylglucosaminidase (NAG)	**Leucine aminopeptidase** (LAP)	**Tyrosine aminopeptidase** (TAP)	**Amidohydrolase** (Urease)
N-cycling function	Hydrolyses glucosamine	Hydrolyses leucine and other hydrophobic amino acids	Hydrolyses tyrosine	Urea $(CONH_2)_2$ breakdown
Substrate	4-Methylumbelliferyl-N-acetyl-β-D-glucosaminide	L-Leucine-7-amido-4-methylcoumarin hydrochloride	L-Tyrosine 7-amido-4-methylcoumarin	Urea

6.3.7. Earthworm *Eisenia fetida* toxicology experiment

Eisenia fetida reproduction test and NM constituent element analysis

An earthworm reproduction test was performed with slight adjustments from the OECD Test No. 222: Earthworm Reproduction Test (*Eisenia fetida*/*Eisenia andrei*), with an outline of the procedure detailed below (OECD, 2016). Peat moss (Premier Horticulture Inc., Canada) was sieved to 2 mm and watered until damp. Juvenile worms (Merlan Scientific Limited, Canada) were then added and fed using worm food (Magic Products Inc., USA) on a 2-3 day schedule for 7 days. After 7 days, all worms were isolated from their peat moss growth medium to obtain their initial weight. During the isolation process, worms were placed on filter paper dampened with deionized water for 24 hours to allow the worms to empty their gut contents, prior to recording their initial weight. Sexually mature worms were then identified by visual inspection to confirm full clitellum development. 10 sexually mature worms were added to each 500 g soil (dry weight) experimental unit, with four biological replicates per NM

amendment or control. The soil used was that detailed in 6.2.2, but this reproduction test was separate to the previously described set of experiments. Soil and worms were kept in 1 L glass mason jars. Two NMs were studied, BEA-150 and ZSM-5-15, at concentrations of 25 mg kg^{-1}, 50 mg kg^{-1} and 100 mg kg^{-1} for BEA-150 and 25 mg kg^{-1} and 100 mg kg^{-1} for ZSM-5-15. There was also a negative (water) control where there were no chemical additions to the field soil. Throughout the test duration, the worms were fed with 5 g of worm food every 5 days. The soil and worms were then incubated on a 12:12 light:dark schedule kept between 18-21˚C, with the soil maintained at 60% of WHC over the experimental duration based on soil weight. After 28 days the mature worms were removed from the soil and the 24 hour isolation process was repeated before weighing. After final mature worm biomass was recorded, the worms were frozen at -20˚C for later ICP-OES analysis of NM contents. Details of ICP-OES and relevant standards, as well as the worm tissue digestion procedure, are detailed in the SI, with details of the acid digestion protocol presented in SI Table S6.1. Juvenile worms that hatched within the 28 days were left in the amended soils and returned to their original containers. The soils were then incubated for a further 28 days, with a single feed of 5 g at the start of the 28-day period. At the end of the second 28-day incubation, juvenile worms and worm eggs were hand-sorted and counted to measure juvenile production and cocoon hatchability.

6.3.8. Statistics

All analyses were conducted in R Studio (v.4.3.1; R Core Team, 2023). Data was assessed for normality using Shapiro-Wilk tests with homogeneity of variance assessed using Levene's test. Normally distributed data was analysed using ANOVA, followed by Tukey's post-hoc test if the ANOVA was found to be significant. If the data was not normally distributed a Kruskal-Wallis test and its accompanying post-hoc Dunn's test were performed. These tests were performed on soil and lettuce ICP-OES results. Lettuce height and biomass were analysed using two-way ANOVAs, a synergistic model was used for biomass and an additive model for lettuce height. Soil and leachate NH_4^+ and NO_3^- concentrations were modelled using generalised estimating equations models. Linear mixed effect models were performed on N_2O and CO_2 data. Enzyme activity data was analysed using a range of

methods: a generalised linear model with gamma distribution was used for logarithmically transformed LAP enzyme activity, a generalised linear model with Gaussian distribution for NAG, a fixed effects linear mixed model for logarithmically transformed TAP enzyme activity, and a generalised estimating equations model for urease activity.

6.4. Results and Discussion

NMs were characterised using dynamic light scattering (DLS) prior to their addition to the soil (Table 6.3). Both zeolite NMs were negatively charged, with the metal oxide, $Ce_{0.75}Zr_{0.25}O_2$, having a positive zeta potential. NM agglomerate sizes, as detected via DLS, also varied, with the largest agglomerates seen for BEA-150, then smaller agglomerates for ZSM-5-15, and the least agglomeration was found for the $Ce_{0.75}Zr_{0.25}O_2$ NMs.

The hydrodynamic sizes shown in Table 6.3 are of agglomerates rather than primary particles based on TEM study of these materials. BEA-150 and ZSM-5-15 were found to have primary particle sizes of 0.1µm and 0.2 µm, respectively, via scanning electron microscopy (Jendrlin et al., 2022). $Ce_{0.75}Zr_{0.25}O_2$ NMs were found to have an average size of 10 nm using X-ray diffraction (Dhage et al., 2005).

Table 6.3. NM characterisation by DLS before exposure to soil. Data are means ± standard deviation.

Nanomaterial	Mean hydrodynamic size (nm) and standard deviation (SD) (n=3)	Mean zeta potential (mV) and SD (n=3)
BEA-150	704.4 (± 2.71)	-42.5 (± 0.64)
ZSM-5-15	631.3 (± 12.7)	-28.0 (± 0.66)
$Ce_{0.75}Zr_{0.25}O_2$	104.5 (± 4.37)	+45.2 (± 0.75)

6.4.1. Lettuce growth experiment comparing soil condition and NM amendments over time

Soil element concentrations and nitrate and ammonium concentrations

Analysis of soil nutritive elements and NM constituent elements showed no significant difference between soil conditions or soil amendments ($p > 0.05$). However, we did observe significant effects on soil N between the autoclaved and natural soils (SI Table S6.3). Week 1 average NH_4^+ concentrations of autoclaved soil were higher than this in natural soil (Table 6.4), with 9.33 mg kg^{-1} in autoclaved soil averaged across NM amendments as opposed to 4.40 mg kg^{-1} in natural soil. The opposite was true for NO_3^- concentration, with higher concentrations in natural soil at week 1 (8.56 mg kg^{-1} versus 0.55 mg kg^{-1}). Across the experimental time period average NO_3^- and NH_4^+ in the natural soil were lower compared to those in the autoclaved soils, with very little change in the NH_4^+ concentration of the autoclaved soils over time but with a significant decrease occurring in the natural soils by week 7 (SI Table S6.4).

Soil moisture was lower than 60% WHC due to sampling before watering (SI Figure S6.1). Soil pH was consistent across amendments, with autoclaved soil being slightly more neutral at week 1. Over time all soils became more alkaline, with natural soils undergoing greater increases in alkalinity (SI Figure S6.1).

Table 6.4. Soil properties across the five different soil amendments in both the natural and autoclaved soil conditions before and after the seven-week growth period. Data are means ± standard error of the mean (SEM). Absent data is due to values being below the limit of detection of the specific method.

	Natural					**Autoclaved**				
	Control	NPK half	BEA-150 + NPK half	$Ce_{0.75}Zr_{0.25}O_2$ + NPK half	ZSM-5-15 + NPK half	Control	NPK half	BEA-150 + NPK half	$Ce_{0.75}Zr_{0.25}O_2$ + NPK half	ZSM-5-15 + NPK half
Week 1										
pH (n=3)	6.28 (± 0.05)	6.09 (±0.16)	6.11 (±0.1)	6.14 (±0.17)	6.14 (±0.18)	6.48 (±0.14)	6.82 (±0.11)	6.78 (±0.22)	6.69 (±0.24)	6.72 (±0.17)
Gravimetric soil moisture (%) (n=3)	28.0 (±4.66)	25.5 (±7.34)	22.6 (±8.77)	29.6 (±6.12)	23.6 (±2.24)	26.9 (±9.4)	15.3 (±2.64))	28.0 (±5.28)	18.7 (±2.84)	24.2 (±9.84)
NH_4^+ (mg kg^{-1} dry soil) (n=3)	1.77 (±0.21)	9.94 (±3.53)	4.37 (±1.39)	3.5 (±0.82)	2.41 (±0.93)	9.32 (±2.34)	12.9 (±1.39)	5.88 (±0.24)	13.7 (±1.49)	4.91 (±0.75)
NO_3^- (mg kg^{-1} dry soil) (n=3)	6.58 (±2.3)	8.91 (±0.44)	8.75 (±0.77)	9.39 (±0.87)	9.16 (±0.31)	0.31 (±0.34)	0.46 (±0.15)	0.76 (±1.25)	0.66 (±0.69)	0.57 (±0.27)
Week 7										
pH (n=1)	6.65	6.99	6.97	6.91	6.93	6.77	6.94	6.92	6.91	7.08
Gravimetric soil moisture (%) (n=3)	41.6 (±3.08)	38.6 (±3.32)	39.9 (±1.61)	37.9 (±3.92)	39.1 (±2.47)	38.0 (±1.15)	38.1 (±0.7)	38.4 (±0.66)	35.6 (±0.86)	37.0 (±1.73)
NH_4^+ (mg kg^{-1} dry soil) (n=3)	0.82 (±12)	0.83 (±0.2)	0.81 (±0.07)	0.86 (±0.06)	0.86 (±0.12)	0.93 (±0.07)	1.16 (±0.37)	0.9 (±0.18)	1.23 (±0.3)	1.04 (±0.47)
NO_3^- (mg kg^{-1} dry soil) (n=3)	0.07 (±0.03)	0.17 (±0.03)	0.12 (±0.02)	0.23 (±0.04)	0.10 (±0.02)	-	0.26 (±0.31)	0.42 (±0.44)	0.06 (±0.03)	0.22 (±0.3)

Leachate nitrate and ammonium concentrations

Overall, when averaged across time natural soil had lower NH_4^+ losses compared to autoclaved soil ($p < 0.001$). Within the natural soils, NM amendment generally resulted in lower NH_4^+ leachate concentrations compared to NPK half application alone. However, this was not the case for the autoclaved soils, where some of the highest NH_4^+ losses occurred in NM treated soils. NPK half addition increased NH_4^+ concentration in the leachate ($p = 0.01$), as did BEA-150 and ZSM-5-15 (both $p < 0.001$), the two zeolite amendments.

NM amended soils mostly responded similarly to the NPK half application in terms of NO_3^- leachate, all peaking at week 5 in the natural soils. However, in autoclaved soil, differences in the NM treatments emerge. NO_3^- losses peak at week 5 under the $Ce_{0.75}Zr_{0.25}O_2$ and NPK half amendment, and peaks at week 3 in the control soil, as in natural soil. However, NO_3^- leachate concentrations were reduced in autoclaved soil treated with ZSM-5-15 and BEA-150 as compared to control ($p < 0.001$ for both). NPK half amendment in autoclaved soil produced consistently high NO_3^- emissions in weeks 3 and 5 (SI Table S6.4).

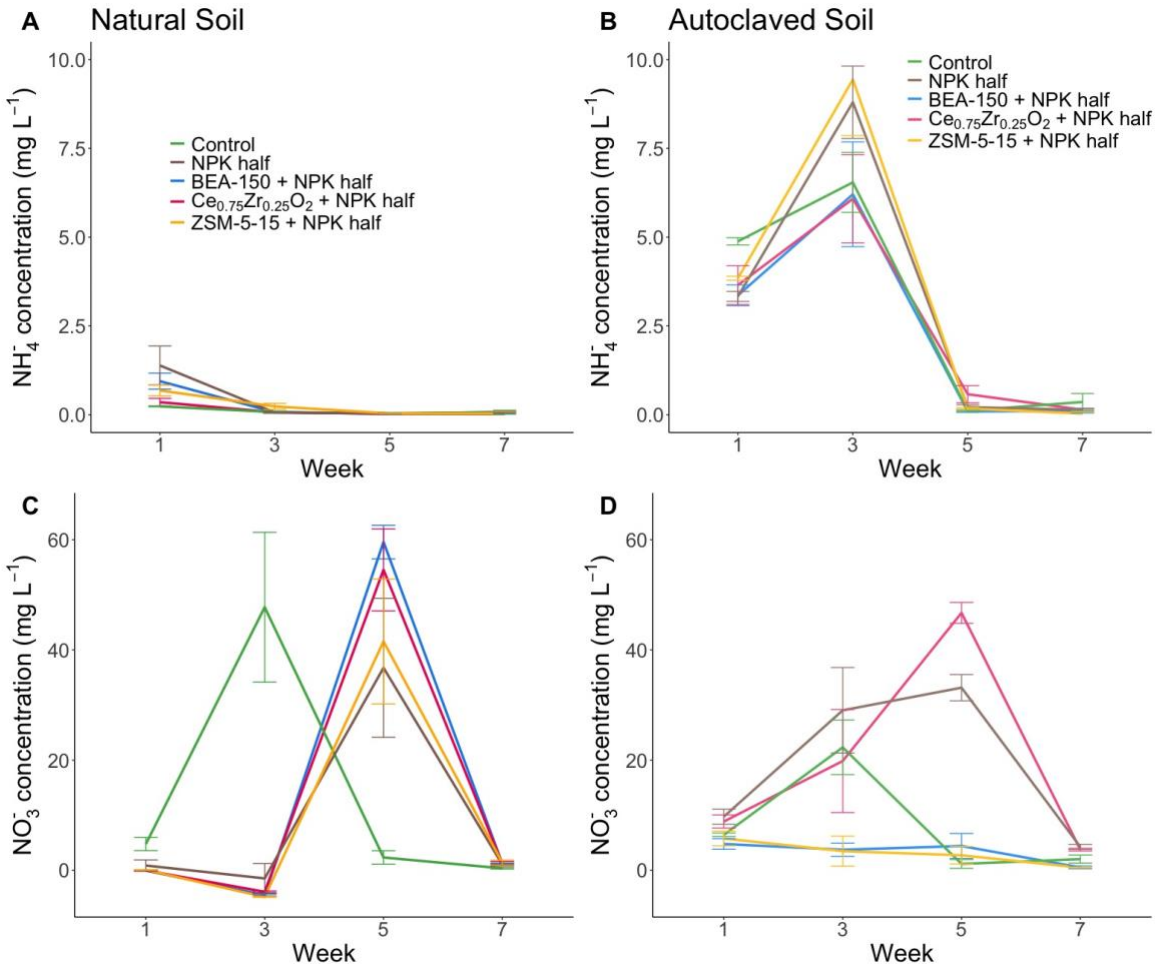


Figure 6.1. Concentration of ammonium (NH_4^+) in soil leachate from natural and autoclaved soil across the lettuce growth period of the experiment for different NM amendments (A and B); Concentration of nitrate (NO_3^-) in the leachate from natural and autoclaved soils across lettuce growth period of the experiment for different NM amendments (C and D). Error bars are standard error of the mean (SEM); n=3.

Soil N_2O and CO_2 emissions

We observed that NPK addition alone produced some of the greatest N_2O emissions compared to the control and NM treated soils, regardless of soil sterilisation. Soil N_2O emissions peaked at week 2 for across all soils and amendments, however $Ce_{0.75}Zr_{0.25}O_2$ and ZSM-5-15 had the lowest emissions in natural soil, and BEA-150 and ZSM-5-15 had the lowest emissions in autoclaved soil. In natural soil, BEA-150 amendment produced similar N_2O emissions as NPK half amendment alone, with BEA-150 producing significantly lower N_2O emissions in autoclaved soil as compared to NPK half alone in autoclaved soil ($p = 0.009$). In autoclaved soil, $Ce_{0.75}Zr_{0.25}O_2$ was more similar to NPK half amendment. ZSM-5-15 N_2O emissions increased under autoclaved soil compared to natural soil also.

Unlike N_2O emission, CO_2 emissions occur later during lettuce growth, peaking at week 6. CO_2 emissions were significantly affected by week ($p = 3.7 \times 10^{-7}$), with neither amendment nor soil condition having any significant effect. However, non-significant differences in the NM amendments were observed, where ZSM-5-15 had the greatest CO_2 emissions, used to indicate soil and autotroph (plant) respiration, under natural soil, while producing the lowest CO_2 emissions in autoclaved soil. Soil sterilisation increased CO_2 emissions when in combination with $Ce_{0.75}Zr_{0.25}O_2$ and BEA-150 amendments, compared to the natural soils. NPK half amendment and the control soils were similar for both autoclaved and natural soils indicating that the differential effect is occurring through NM application rather than being a facet of NPK addition.

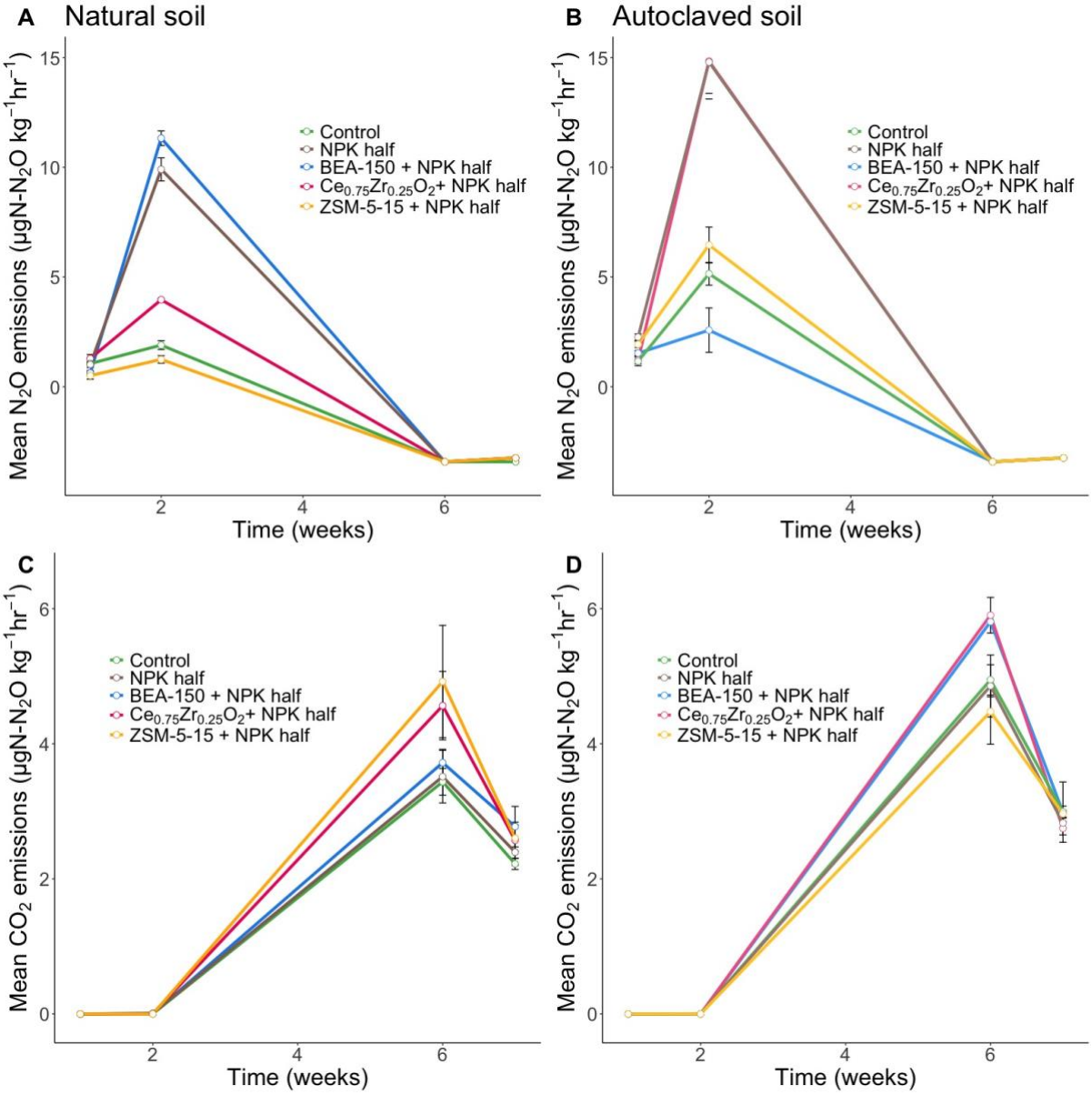


Figure 6.2. N_2O emissions from natural and autoclaved soils treated with different combinations of NM and NPK amendments over the lettuce growth period with gas sampling occurring at weeks 1, 2, 6 and 7 (A and B). CO_2 emissions from natural and autoclaved soils treated with different combinations of NMs and NPK amendment over the lettuce growth period with gas sampling occurring at weeks 1, 2, 6 and 7 (C and D). Error bars are standard error of the mean; n=3.

Soil potential extracellular enzyme activity

Peptidase enzyme activity (LAP and TAP) was elevated in natural soil as compared to autoclaved soil (Figure 6.3A and 6.3B). NPK half amendment produced significantly different LAP activity to the control, with lower activity seen in weeks 1, 3, and 7 in natural soil, and higher activity in weeks 3, 5 and 7 in autoclaved soil ($p = 5.71 \times 10^{-6}$). Elevated activity was seen across all NM and NPK half amendments for TAP in natural soil relative to autoclaved soil. *Week* played a significant role in TAP activity, increasing in week 5 and 7 in natural soil ($p = 0.16$; $p = 0.0083$). ZSM-5-15 amendment produced significantly different TAP enzyme activity across soil types and weeks as compared to the control, ($p = 0.00058$), with elevated activity relative to the control in autoclaved soil and reduced activity in natural soil. β-1,4-N-acetylglucosaminidase (NAG) activity peaks in both autoclaved and natural soil at week 1 before activity reduces across all amendments other than BEA-150 ($p > 0.05$). There were also significant interactions seen between week, soil condition and amendment (SI Table S6.5). Urease activity was variable in both autoclaved and natural soils across amendments. Urease activity was highest under BEA-150 amendment in week 5 ($p = 0.00037$), with a significant increase in BEA-150 activity in autoclaved soil at week 5 ($p = 0.00026$). Urease activity peaked in week 5 for the natural soil, with control soils having the greatest activity across all four timepoints studied. Urease activity was significantly different under BEA-150 amendment, between all weeks and by soil amendment ($p < 0.001$). Weeks 3 and 5 showed significantly different urease activity for NPK half amendment compared to the control ($p = 0.0085$; $p = 0.36$).

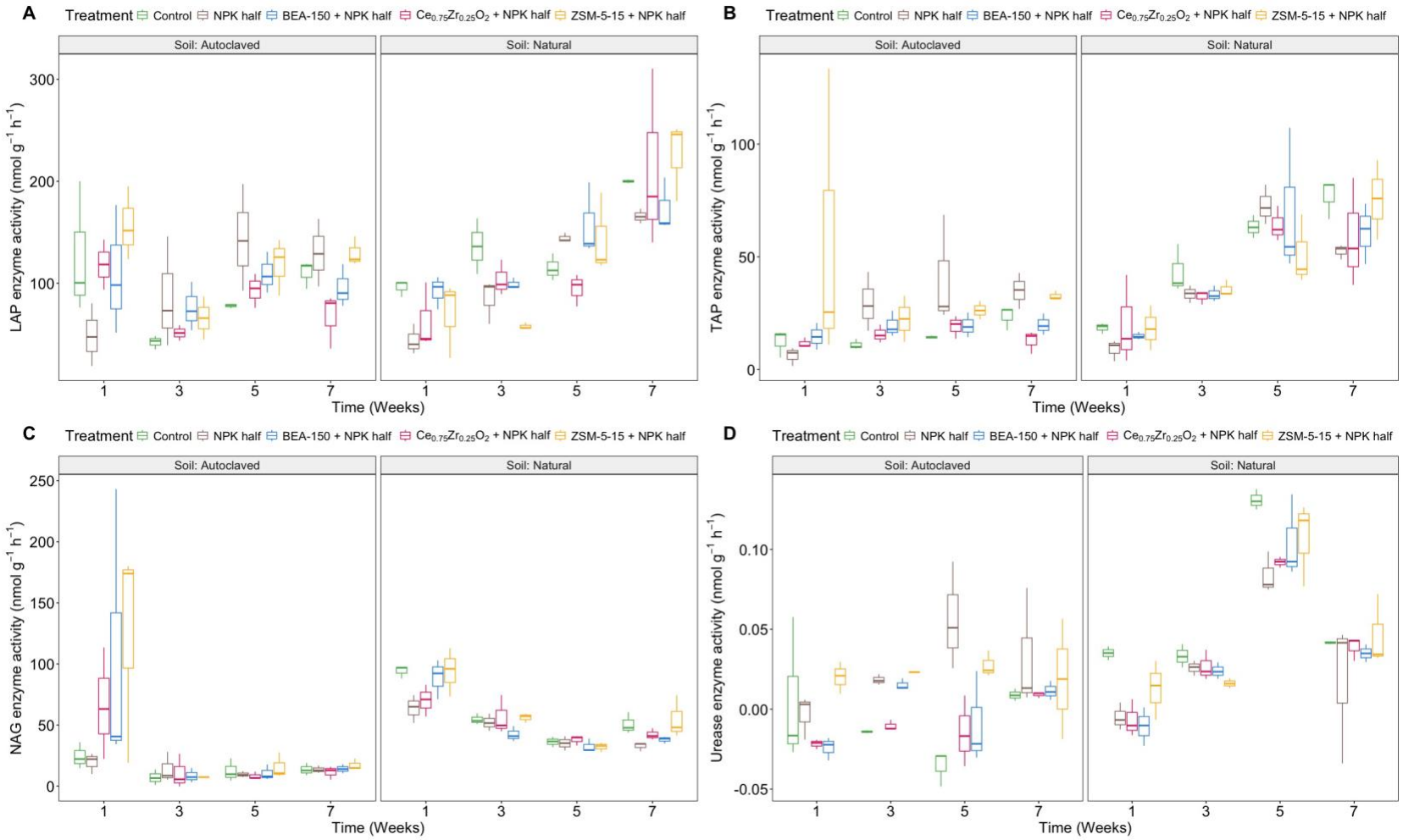


Figure 6.3. (A) Leucine aminopeptidase enzyme activity in autoclaved and natural soil under each of the amendments across the lettuce growth period. (B) Tyrosine aminopeptidase enzyme activity in autoclaved and natural soil under each of the amendments across the lettuce growth period. (C) NAG enzyme activity in autoclaved and natural soil under each of the amendments across the lettuce growth period. (D) Urease enzyme activity in autoclaved and natural soil under each of the amendments across the lettuce growth period. Error bars are standard error of the mean (SEM); n=3.

Lettuce growth and shoot tissue element concentrations

Soil condition had a significant effect on biomass ($p = 0.00074$), with soil amendment and soil condition interacting to produce an effect on biomass accumulation ($p = 0.042$). Lettuce height was lowest in the control natural soil. NPK half amendment caused significantly taller lettuce compared to the control ($p = 0.03$), and soil sterilisation significantly increased lettuce height ($p = 0.0002$). $Ce_{0.75}Zr_{0.25}O_2$ treated natural soil improved lettuce biomass accumulation compared to the control, but due to wide variation in lettue biomass this result was not statistically significant. NM application in natural soil did not significantly reduce lettuce biomass or height as compared to NPK half treatment alone.

Lettuce tissues nutrient and NM element concentrations were significantly different for two analysed elements (Si and Cu) (SI Table S6.6). Lettuce Si concentrations were significantly higher in the control grown lettuces as compared to the $Ce_{0.75}Zr_{0.25}O_2$ ($p = 0.0164$) and ZSM-5-15 ($p = 0.0137$) grown lettuces. Cu content was highest in the natural control soil, with control grown lettuce having 0.0031 mg kg^{-1} Cu on average. This result was significantly greater than the Cu content of NPK half grown lettuce in both natural and autoclaved soil ($p = 0.046$; $p = 0.0389$).

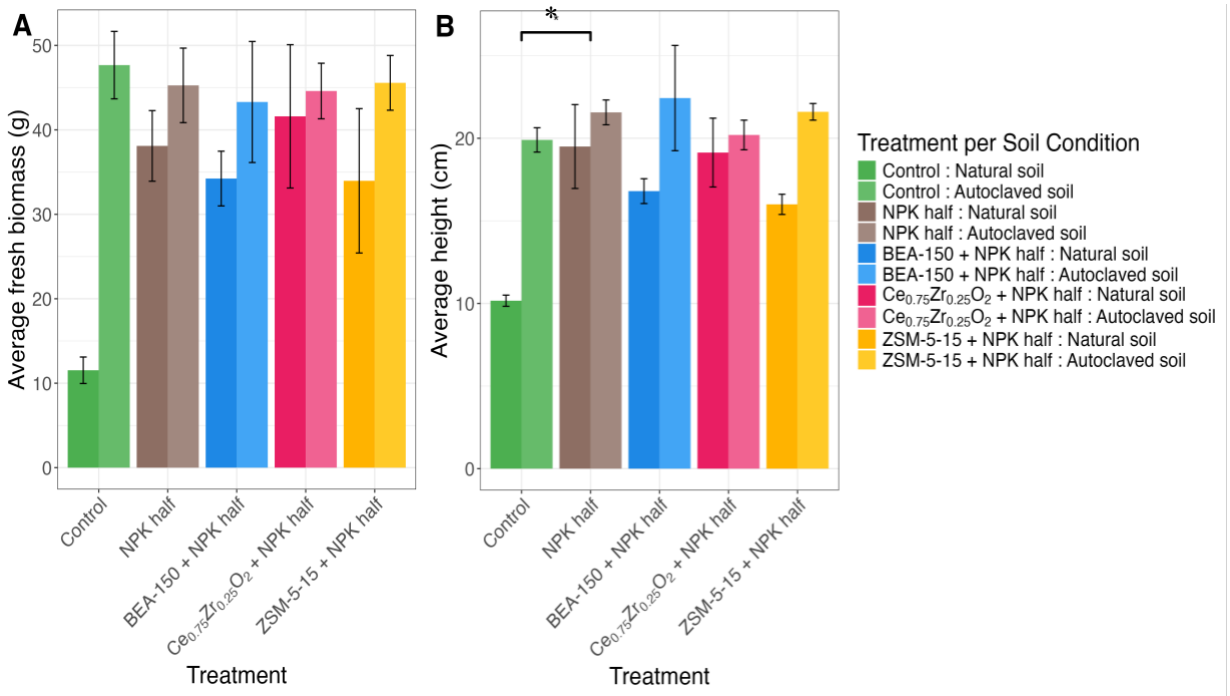


Figure 6.4. (A) Average fresh biomass of lettuce shoot tissue per amendment per soil condition at week 7 of the experiment. (B) Average lettuce height per amendment per soil condition at week 7 of the experiment. Error bars are standard error of the mean (SEM). Statistically significant differences as compared to the negative control (Control) amendment are denoted with '*' ($p < 0.05$).

6.4.2. *Eisenia fetida* dose response to zeolite application

The earthworm reproduction test passed the validation criteria overall, with the coefficient of variation of reproduction, the number of juveniles produced and adult mortality over four weeks all considered. However, both tested concentrations of ZSM-5-15 failed to meet the validation criteria, although the differences in juvenile production identified were not statistically significant ($p > 0.05$). The effect of BEA-150 and ZSM-5-15 on earthworms was different with increasing concentration across several of the studied parameters (Figure 6.5). As BEA-150 concentration increased there was no statistically significant effect on weight change, mortality, juvenile production, unhatched cocoons or concentration of the two NM constituent elements, Si and Al. The only result approaching significance was that ZSM-5-15 application at the rate of 25 mg kg^{-1} soil reduced the total number of unhatched cocoons as compared to the control ($p = 0.052$). Though BEA-150 and ZSM-5-15 have very different Si:Al ratios the final Si and Al contents of the worm tissue remained similar across amendments and amendment concentrations ($p > 0.05$). There was some indication that Si tissue concentration increased with higher BEA-150 concentration while ZSM-5-15 decreased slightly with increasing concentration. There was no pattern deciphered from Al contents.

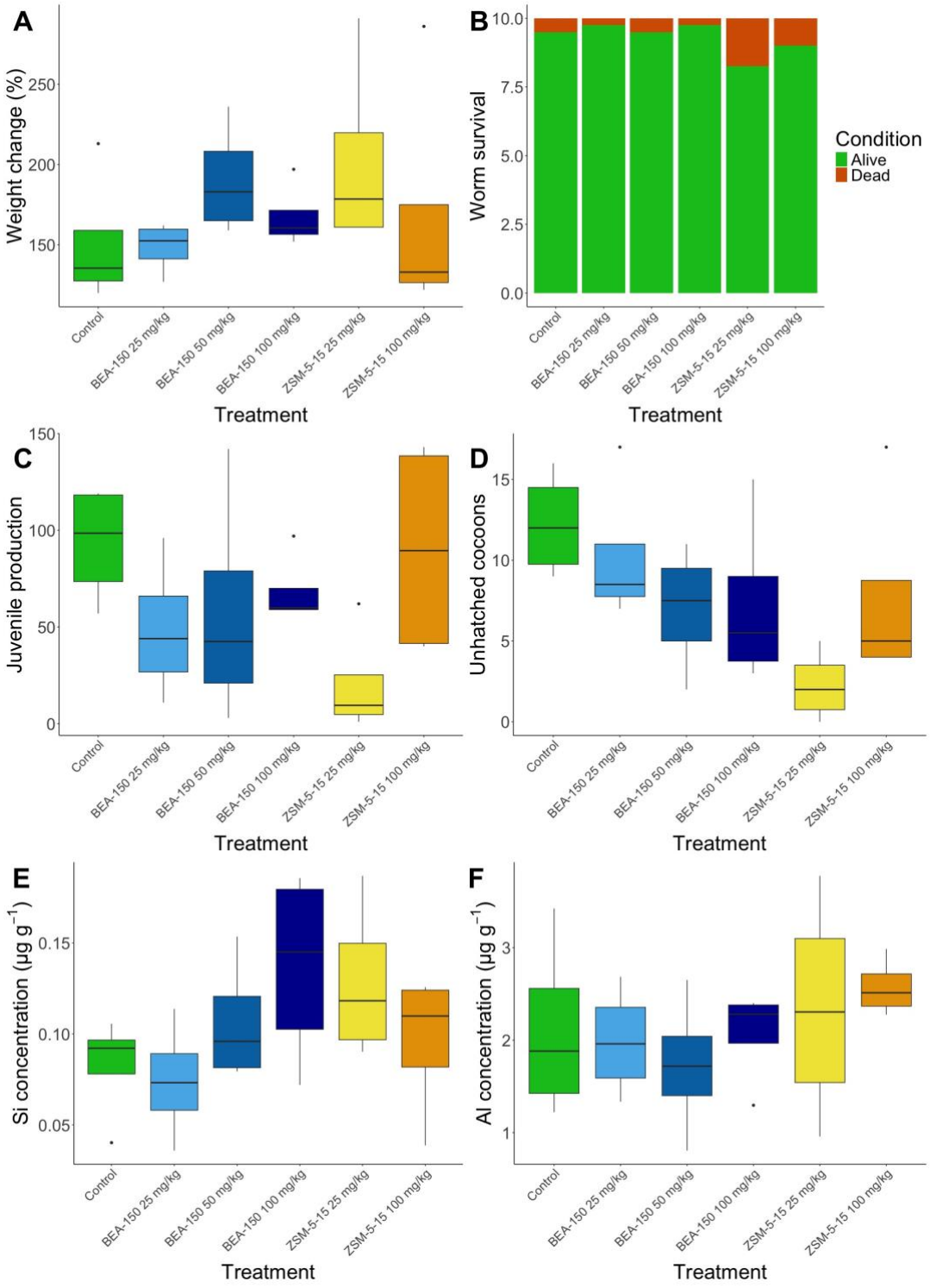


Figure 6.5. (A) Average percentage change in *Eisenia fetida* worm body mass compared between day 0 and day 28. (B) Average proportion of survived versus dead worms after 28 days in each of the amendment soils. (C) Average number of juvenile worms produced per amendment as counted at day 56. (D) Average number of unhatched cocoons produced per amendment as counted at day 56. (E) Average Si concentration of each living worm at day 28. (F) Average Al concentration of each living worm at day 28.

6.5. Discussion

6.5.1. N_2O emissions are modulated by the interaction between NMs and soil microbes

BEA-150 N_2O emissions are elevated in the presence of a natural microbial community, with N_2O emissions reduced by more than four times when soil is sterilized through autoclaving. BEA-150 also increases NO_3^- concentration in leachate from natural soil, with no effect on NO_3^- leachate in autoclaved soil. N_2O emissions are largely produced through the action of nitrifying and denitrifying soil microbial communities (Bremner, 1997). BEA-150 may therefore be promoting depolymerisation and increase nitrification derived N_2O emissions through production of NH_3 and NO_3^-. NH_3 volatilisation was not studied in this paper but would be of interest in future studies due to N addition in the form of urea. BEA-150 amendment also impacts CO_2 emissions from the soil, used here to represent soil respiration, with higher respiratory activity found under autoclaved rather than natural soil. This may be a facet of several factors; soil respiration includes both microbial and plant root activity, and lettuce growth (biomass and height) were improved under autoclaved soils due to the increase in Nr and P availability (Skipper and Westerman, 1972). While we do not expect that the autoclaved soils were fully sterilized nor remained sterile over the course of the experiment, microbial biomass would have been reduced relative to the natural soils. This indicates that while BEA-150 clearly interacts with the microbial community to elevate N_2O emissions, part of these emissions may not be biotically derived, with low CO_2 emissions indicating low soil respiration. Sterile soils, such as those that have been autoclaved, are able to produce N_2O emissions abiotically, through three main pathways; chemodenitrification, abiotic decomposition of ammonium nitrate and the abiotic-biotic coupled formation of the N_2O intermediary hydroxylamine (NH_2OH) (Chalk and Smith, 1983; Rubasinghege et al., 2011; Heil et al., 2015). BEA-150 may be acting to increase production of hydroxylamine or may be involved in the oxidation of hydroxylamine to produce N_2O emissions through a mixture of biotic and abiotic factors. Elucidating the mechanism by which BEA-150 is triggering these increased emissions requires further study, utilising ^{15}N stable isotope tracing of de/nitrification derived N_2O. To determine if BEA-150 is triggering N_2O production via chemodenitrification, which occurs in NO_2^- rich environments, soil NO_2^- concentrations would need to be examined (Wei et al., 2019). Alternatively, the

increased N_2O emissions may be through ion exchange of soil cations (e.g. H^+) with NH_4^+, the extra-framework ion carried by BEA-150. ZSM-5-15 has the same extra-framework ion but a very different Si:Al ratio, 15 as compared to BEA-150 at 150. BEA-150 also has slightly larger pores, of 6.8Å rather than 5.5Å, and its primary particle size is larger (Jendrlin et al., 2022). These physical differences between the zeolite NMs may partly explain the difference in effect on N emissions.

Control soils produced greater N_2O emissions when sterilised compared to natural soil, but N_2O emissions increased further in the presence of ZSM-5-15, indicating an abiotic impact in ZSM-5-15 treated soil. Previous work indicates that ZSM-5-15 promotes N_2O production in natural soil is likely via nitrification pathways, utilising ion exchanged NH_4^+ (Chadwick et al., *Chapter 4*). Emissions from ZSM-5-15 treated UK soil in the previous study are far lower, reduced below the NPK half amendment alone. This indicates that ZSM-5-15 emissions are dependent on abiotic soil factors and may also be impacted by soil microbial community differences, with all ZSM-5-15 treated soils producing less N_2O emissions in Canadian agricultural soil as compared to UK agricultural soil (Chadwick et al., *Chapter 4*). Synthetic fertiliser and biochar, a similar soil amendment to the zeolites studied here, have both been shown to impact microbial communities, in turn altering N_2O emissions (Harter et al., 2014; Lazcano et al., 2021). ZSM-5-15 treatment resulted in greater NH_4^+ concentrations in leachate, indicating that while the NH_4^+ ions were able to be utilised by microbes in the UK agricultural soil, they were perhaps instead released into the leachate in the Canadian soil context.

$Ce_{0.75}Zr_{0.25}O_2$ NM N_2O emissions are the same as NPK half emissions alone in autoclaved soil but the N_2O emissions in the presence of $Ce_{0.75}Zr_{0.25}O_2$ NMs are reduced in natural soils. This is paired with $Ce_{0.75}Zr_{0.25}O_2$ amendment increasing NO_3^- concentration in leachate in both natural and autoclaved soils. Together these results indicate that there is an interaction occurring between $Ce_{0.75}Zr_{0.25}O_2$ NMs and soil microbes. Additionally, the mixed metal oxide $Ce_{0.75}Zr_{0.25}O_2$ has been shown to transform in soil, leaching Zr^{4+} ions and forming $Ce_{0.9}Zr_{0.1}O_2$ and CeO_2 NMs, with Zr found in lettuce tissues as $Ce_{0.75}Zr_{0.25}O_2$, Zr metal (Zr^{4+}) and $ZrCl_4$ (Chadwick et al., *Chapter 4*).

N_2O emissions reduced below zero at weeks 6 and 7 of the growth period. This is indicative of consumption and is likely caused by excessive soil drying in between watering over this time (Chapuis-Lardy et al., 2007). This is coupled with peak NO_3^- emissions in leachate at week 5, reducing the

available substrate for nitrification derived N_2O emissions. The similarity in magnitude between the natural and autoclaved soils indicates that the majority of the CO_2 emitted from soil respiration is root derived or potentially that autoclaving was unsuccessful, and the soil microbes are more thermostable than expected or are repopulating post sterilisation. Studying soil microbial biomass at timepoints across the experiment in future would help to determine if effects in autoclaved soil are solely through abiotic interactions or are through recovery of, and changes in, the soil microbiome (Marschner and Rumberger, 2004; Li et al., 2019). Previous data has shown ZSM-5-15 amendment increasing N_2O emissions from natural soil when applied with a reduced rate of NPK (Chadwick et al., Chapter 4), while this study shows ZSM-5-15 reducing N_2O emissions in both natural and autoclaved soils. This reflects the extent to which N_2O emissions and NM effects are dependent on soil factors, both biotic and abiotic, including soil microbial community makeup, pH, surface chemistry of clays and colloids, and micronutrient availability (Zhu-Barker et al., 2015).

6.5.2. NM and autoclaving impacts on extracellular activity and lettuce growth

Lettuce growth was not particularly impacted by NM presence and was stimulated by NPK addition and also by the expected nutrient release in autoclaved soils. Autoclaved soil results in improved lettuce biomass accumulation and height (Figure 6.4). This is likely through a nutrient burst as a result of the autoclaving process whereby nutrients like N, P, Mn and S become more extractable (Wolf and Skipper, 1994; Berns et al., 2008). As well as the release of nutrients post autoclaving, microbial biomass is killed and decomposes, increasing the nutrients available to plants as a result of lower competition for finite nutrients (Berns et al., 2008). The greenhouse used in the lettuce growth experiments was subject to higher than expected temperatures with the soil gravimetric moisture content reflecting that the soils dried to ~24% of WHC in week one. Due to this extreme drying in between watering back to 60% WHC, the Birch effect, whereby rewetting of soil triggers release of CO_2 and inorganic N as well as increasing decomposition and mineralisation, may also have impacted microbial activity (Jarvis et al., 2007). Soils were sampled prior to adjustment of the moisture levels (based on the gravimetric analysis) and thus EEA was measured at these lower moisture levels but this may not be the clearest display of what is happening in soil, with the water addition likely causing an increase in microbial respiration, permitting

greater enzyme production in the natural soils. Due to missing datapoints from weeks 3-5, whether the Birch effect was occurring, as monitored by CO_2 emissions from soil, is unknown. However, with the potential soil drying, in between watering as indicated by N_2O consumption at weeks 6 and 7, there is a likelihood for this to have occurred.

Both aminopeptidases increased over time in the natural soil but not in the autoclaved soil. There was limited effect on NAG activity with NM amendment and soil condition, in both autoclaved and natural soils. Urease activity was higher in natural soils, showing an interaction between autoclaved soil and BEA-150 and time (week 5). This could be indicative of a direct effect of BEA-150 on urease that is minimised by microbial activity, which could contribute to the lower N_2O emissions seen under BEA-150 amendment in autoclaved soil. As urea was the applied form of N, it may be that this primed urease enzyme activity over time, leading to effects in both autoclaved and natural soil. BEA-150 amendment increased LAP and TAP EEA activity relative to the control in autoclaved soils, indicating that there may be a positive feedback loop where BEA-150 enhances aminopeptidase activity, permitting greater depolymerisation of cleaved amino acids by BEA-150 to increase N_2O emissions. Other zeolite NMs have depolymerisation activity, although these act on the organic polymer lignin (Nandiwale et al., 2017). LAP and TAP activity decrease in natural soils amended with BEA-150, with the NM potentially preferentially interacting with other microbes and enzymes. It would appear that the majority of the effects seen are due to whether the soil had living microbial biomass, with NPK addition but regardless of NM, impacting aminopeptidase activity. Some extracellular enzymes are able to remain stable after autoclaving the soil, e.g., phosphodiesterase, and killing of soil microbial biomass through the heating process (Carter et al., 2007). This study reflects that aminopeptidases and urease are also likely to be quite thermally stable. Autoclaving combines heat, humidity and pressure to kill soil biota, generaing a reduced microbial biomass, not studied directly in this experiment, and also limiting microbial metabolism, such as enzyme activity, as seen in the impact on extracellular enzyme activity, with no time based effect being observed in autoclaved soil (Carter et al., 2007). Soil characteristics are likely to influence extracellular enzyme stability, with properties like pH, soil moisture, cation exchange capacity and soil organic matter all likely to alter enzyme functioning (Tate, 2002).

6.5.3. ZSM-5-15 shows sublethal effects on *Eisenia fetida* at lower concentrations

BEA-150 agglomerates in water are slightly larger than those for ZSM-5-15, with BEA-150 also having a more negative zeta potential. Concentration dependent agglomerate size was not studied, but primary particle size for both zeolites have been found to be similar via SEM, 0.1µm for BEA-150 and 0.2µm for ZSM-5-15 (Jendrlin et al., 2022). Agglomerate size has been found to be more significant for NM transport in soil than primary particle size when studying aluminium NMs (Darlington et al., 2009). As ZSM-5-15 agglomerates are slightly smaller they may be more able to enter worm tissues or dissociate from the soil matrix as it is ingested by the worms, allowing a higher proportion of the particles to enter the worm tissues and have impacts on reproduction. This could explain the impact on the number of unhatched cocoons being lower in the 25 mg kg^{-1} ZSM-5-15 amendment. The total number of juveniles was not significantly lower than the control with the ZSM-5-15 amendment, however, the fewest juveniles found were under the 25 mg kg^{-1} amendment of ZSM-5-15. BEA-150 was not found to have any sub-lethal effects at the studied concentrations. The Si and Al concentrations are derived from whole worm tissue digestions so there is limited resolution regarding whether the zeolites accumulated in any specific tissues of the worms. Future work should feature partitioning of internal and external tissues and NM transformations studied in the different tissues, for example by synchrotron experiments such as XANES, in order to better understand the bioaccumulation risk. Additionally, comparing the NMs with bulk versions at a broader range of concentrations would similarly increase contextual understanding of NM agrochemical application. Differences in size and charge will have significant impacts on the NMs ability to enter organisms like earthworms and plants and to interact with microbes to affect N-cycling.

6.5.4. Conclusion

BEA-150 and $Ce_{0.75}Zr_{0.25}O_2$ interact with soil microbes to increase N_2O emissions and Nr contents of leachate, with ZSM-5-15 more influenced by abiotic factors, such as soil colloid and clay contents. Sensitivity of NMs to biotic and abiotic factors is different across NMs, occurring even between two zeolites. The different ratio of Si to Al could be a potential source of this difference in the microbial interaction with the zeolites, but sophisticated structures like pore size may also be the cause of the different impacts observed. Further research is required to elucidate the validity of any links between physical characteristics and zeolite effects in soil. NM addition with half dose NPK did not appear to alter the lettuce biomass accumulation but had minor impacts on lettuce nutritive quality. Both aminopeptidases studied were influenced by time in the natural soils and retained activity in microbially sterile soils indicating their thermal stability. Urease activity varied across soil condition and time, likely due to N addition in the form of urea, with BEA-150 increasing urease activity in autoclaved soil. *Eisenia fetida* potentially undergo sub-lethal impacts from environmentally realistic concentrations of ZSM-5-15, however, whether bioaccumulation occurs in the NM form or via transformation product is unknown, with higher resolution data of NM constituent element localisation and transformation in worm tissues required to clarify this. Earthworms are only one species of many that are affected by agrochemical application - future work should look at a broader range of soil invertebrate species (e.g., Collembola) and increase the concentrations tested to get an idea of lethal as well as sub-lethal impacts, in addition to performing repeat exposure studies at lower exposure doses. Other future work could include ^{15}N stable isotope tracing through the system, assessment of phosphate extracellular enzymes activity, as well as stress response signalling in plant and animal tissues in response to NM application.

References

Berns, A.E., Philipp, H., Narres, H.-D., Burauel, P., Vereecken, H., Tappe, W., 2008. Effect of gamma-sterilization and autoclaving on soil organic matter structure as studied by solid state NMR, UV and fluorescence spectroscopy. European Journal of Soil Science 59, 540–550. https://doi.org/10.1111/j.1365-2389.2008.01016.x

Bremner, J.M., 1997. Sources of nitrous oxide in soils. Nutrient Cycling in Agroecosystems 49, 7–16. https://doi.org/10.1023/A:1009798022569

Bulfin, B., Call, F., Vieten, J., Roeb, M., Sattler, C., Shvets, I.V., 2016. Oxidation and Reduction Reaction Kinetics of Mixed Cerium Zirconium Oxides. J. Phys. Chem. C 120, 2027–2035. https://doi.org/10.1021/acs.jpcc.5b08729

Carter, D.O., Yellowlees, D., Tibbett, M., 2007. Autoclaving kills soil microbes yet soil enzymes remain active. Pedobiologia 51, 295–299. https://doi.org/10.1016/j.pedobi.2007.05.002

CEM, 2019. Mars 6 Microwave Acid Digestion Method Note Compendium.

Chalk, P.M., Smith, C.J., 1983. Chemodenitrification, in: Freney, J.R., Simpson, J.R. (Eds.), Gaseous Loss of Nitrogen from Plant-Soil Systems. Springer Netherlands, Dordrecht, pp. 65–89. https://doi.org/10.1007/978-94-017-1662-8_3

Chapuis-Lardy, L., Wrage, N., Metay, A., Chotte, J.-L., Bernoux, M., 2007. Soils, a sink for N2O? A review. Global Change Biology 13, 1–17. https://doi.org/10.1111/j.1365-2486.2006.01280.x

Colella, C., 1996. Ion exchange equilibria in zeolite minerals. Mineral. Deposita 31, 554–562. https://doi.org/10.1007/BF00196136

CRAAQ, 2013. Guide de référence en fertilisation 2e edition.

Darlington, T.K., Neigh, A.M., Spencer, M.T., Guyen, O.T.N., Oldenburg, S.J., 2009. Nanoparticle characteristics affecting environmental fate and transport through soil. Environmental Toxicology and Chemistry 28, 1191–1199. https://doi.org/10.1897/08-341.1

Dhage, S.R., Gaikwad, S.P., Muthukumar, P., Ravi, V., 2005. Synthesis of Ce0.75Zr0.25O2 at 100 °C. Ceramics International 31, 211–213. https://doi.org/10.1016/j.ceramint.2004.04.009

Dror, I., Yaron, B., Berkowitz, B., 2015. Abiotic soil changes induced by engineered nanomaterials: A critical review. Journal of Contaminant Hydrology, Fate and Transport of Biocolloids and Nanoparticles in Soil and Groundwater Systems 181, 3–16. https://doi.org/10.1016/j.jconhyd.2015.04.004

Ejack, L., Whalen, J.K., 2021. Freeze-thaw cycles release nitrous oxide produced in frozen agricultural soils. Biol Fertil Soils 57, 389–398. https://doi.org/10.1007/s00374-020-01537-x

Falinski, M.M., Plata, D.L., Chopra, S.S., Theis, T.L., Gilbertson, L.M., Zimmerman, J.B., 2018. A framework for sustainable nanomaterial selection and design based on performance, hazard, and economic considerations. Nature Nanotech 13, 708–714. https://doi.org/10.1038/s41565-018-0120-4

Garcia-Velasco, N., Gandariasbeitia, M., Irizar, A., Soto, M., 2016. Uptake route and resulting toxicity of silver nanoparticles in Eisenia fetida earthworm exposed through Standard OECD Tests. Ecotoxicology 25, 1543–1555. https://doi.org/10.1007/s10646-016-1710-2

Harter, J., Krause, H.-M., Schuettler, S., Ruser, R., Fromme, M., Scholten, T., Kappler, A., Behrens, S., 2014. Linking N2O emissions from biochar-amended soil to the structure and function of the N-cycling microbial community. The ISME Journal 8, 660–674. https://doi.org/10.1038/ismej.2013.160

Hedström, A., 2001. Ion Exchange of Ammonium in Zeolites: A Literature Review [WWW Document]. URL https://ascelibrary.org/doi/epdf/10.1061/%28ASCE%290733-9372%282001%29127%3A8%28673%29 (accessed 10.4.24).

Heil, J., Liu, S., Vereecken, H., Brüggemann, N., 2015. Abiotic nitrous oxide production from hydroxylamine in soils and their dependence on soil properties. Soil Biology and Biochemistry 84, 107–115. https://doi.org/10.1016/j.soilbio.2015.02.022

Jänsch, S., Amorim, M.J., Römbke, J., 2005. Identification of the ecological requirements of important terrestrial ecotoxicological test species. Environ. Rev. 13, 51–83. https://doi.org/10.1139/a05-007

Jarvis, P., Rey, A., Petsikos, C., Wingate, L., Rayment, M., Pereira, J., Banza, J., David, J., Miglietta, F., Borghetti, M., Manca, G., Valentini, R., 2007. Drying and wetting of Mediterranean soils stimulates decomposition and carbon dioxide emission: the "Birch effect"†. Tree Physiology 27, 929–940. https://doi.org/10.1093/treephys/27.7.929

Jendrlin, M., Radu, A., Zholobenko, V., Kirsanov, D., 2022. Performance modelling of zeolite-based potentiometric sensors. Sensors and Actuators B: Chemical 356, 131343. https://doi.org/10.1016/j.snb.2021.131343

Khot, L.R., Sankaran, S., Maja, J.M., Ehsani, R., Schuster, E.W., 2012. Applications of nanomaterials in agricultural production and crop protection: A review. Crop Protection 35, 64–70. https://doi.org/10.1016/j.cropro.2012.01.007

Lazcano, C., Zhu-Barker, X., Decock, C., 2021. Effects of Organic Fertilizers on the Soil Microorganisms Responsible for N2O Emissions: A Review. Microorganisms 9, 983. https://doi.org/10.3390/microorganisms9050983

Li, K., DiLegge, M.J., Minas, I.S., Hamm, A., Manter, D., Vivanco, J.M., 2019. Soil sterilization leads to re-colonization of a healthier rhizosphere microbiome. Rhizosphere 12, 100176. https://doi.org/10.1016/j.rhisph.2019.100176

Marschner, P., Rumberger, A., 2004. Rapid changes in the rhizosphere bacterial community structure during re-colonization of sterilized soil. Biol Fertil Soils 40, 1–6. https://doi.org/10.1007/s00374-004-0736-4

Miranda, K.M., Espey, M.G., Wink, D.A., 2001. A Rapid, Simple Spectrophotometric Method for Simultaneous Detection of Nitrate and Nitrite. Nitric Oxide 5, 62–71. https://doi.org/10.1006/niox.2000.0319

Mulvaney, R.L., 1996. Nitrogen—Inorganic Forms, in: Methods of Soil Analysis. John Wiley & Sons, Ltd, pp. 1123–1184. https://doi.org/10.2136/sssabookser5.3.c38

Nandiwale, K.Y., Danby, A.M., Ramanathan, A., Chaudhari, R.V., Subramaniam, B., 2017. Zirconium-Incorporated Mesoporous Silicates Show Remarkable Lignin Depolymerization Activity. ACS Sustainable Chem. Eng. 5, 7155–7164. https://doi.org/10.1021/acssuschemeng.7b01344

OECD, 2016. Test No. 222: Earthworm Reproduction Test (Eisenia fetida/Eisenia andrei). Organisation for Economic Co-operation and Development, Paris.

Ozawa, M., 1998. Role of cerium–zirconium mixed oxides as catalysts for car pollution: A short review1. Journal of Alloys and Compounds 275–277, 886–890. https://doi.org/10.1016/S0925-8388(98)00477-0

R Core Team (2023). R: A language and environment for statistical computing. R Foundation for Statistical Computing, Vienna, Austria. URL https://www.R-project.org/.

Rubasinghege, G., Spak, S.N., Stanier, C.O., Carmichael, G.R., Grassian, V.H., 2011. Abiotic Mechanism for the Formation of Atmospheric Nitrous Oxide from Ammonium Nitrate. Environ. Sci. Technol. 45, 2691–2697. https://doi.org/10.1021/es103295v

Saiya-Cork, K.R., Sinsabaugh, R.L., Zak, D.R., 2002. The effects of long term nitrogen deposition on extracellular enzyme activity in an *Acer saccharum* forest soil. Soil Biology and Biochemistry 34, 1309–1315. https://doi.org/10.1016/S0038-0717(02)00074-3

Schodek, D.L., Ferreira, P., Ashby, M.F., 2009. Nanomaterials, Nanotechnologies and Design: An Introduction for Engineers and Architects. Butterworth-Heinemann.

Sinsabaugh, R.L., Reynolds, H., Long, T.M., 2000. Rapid assay for amidohydrolase (urease) activity in environmental samples. Soil Biology and Biochemistry 32, 2095–2097. https://doi.org/10.1016/S0038-0717(00)00102-4

Skipper, H.D., Westermann, D.T., 1973. Comparative effects of propylene oxide, sodium azide, and autoclaving on selected soil properties. Soil Biology and Biochemistry 5, 409–414. https://doi.org/10.1016/0038-0717(73)90067-9

Suresh, A.K., Pelletier, D.A., Doktycz, M.J., 2013. Relating nanomaterial properties and microbial toxicity. Nanoscale 5, 463–474. https://doi.org/10.1039/C2NR32447D

Tate, R., 2002. 8. Microbiology and Enzymology of Carbon and Nitrogen Cycling. Enzymes in the Environment: Activity, Ecology, and Applications. CRC Press.

Wei, J., Ibraim, E., Brüggemann, N., Vereecken, H., Mohn, J., 2019. First real-time isotopic characterisation of N2O from chemodenitrification. Geochimica et Cosmochimica Acta 267, 17–32. https://doi.org/10.1016/j.gca.2019.09.018

Wolf, D.C., Skipper, H.D., 1994. Soil Sterilization, in: Methods of Soil Analysis. John Wiley & Sons, Ltd, pp. 41–51. https://doi.org/10.2136/sssabookser5.2.c3

Zhu-Barker, X., Cavazos, A.R., Ostrom, N.E., Horwath, W.R., Glass, J.B., 2015. The importance of abiotic reactions for nitrous oxide production. Biogeochemistry 126, 251–267. https://doi.org/10.1007/s10533-015-0166-4

Chapter 7. Urea-Doped Amorphous Calcium Phosphate Application During Lettuce Growth Decreases N Losses Compared to Conventional Fertilisation

Jessica Chadwick[1,2], Peng Zhang[1], Sami Ullah[1], Iseult Lynch[1], Ryan Mushinski[2]

[1] School of Geography, Earth and Environmental Sciences, University of Birmingham, Edgbaston, Birmingham B15 2TT, UK

[2]School of Life Sciences, University of Warwick, Warwick, Coventry, CV4 7AL, UK

[*] Corresponding authors: Jessica J. Chadwick, jxc1326@student.bham.ac.uk; Ryan Mushinski, Ryan.Mushinski@warwick.ac.uk

Acknowledgements

This work was supported by the Biotechnology and Biological Sciences Research Council (BBSRC) and University of Birmingham funded Midlands Integrative Biosciences Training Partnership (MIBTP) grant number BB/T00746X/1.

CReDIT statement

Jessica Chadwick: Writing – Original Draft, Investigation, Formal analysis, Visualisation, Conceptualisation. Peng Zhang: Formal analysis, Supervision, Funding acquisition. Sami Ullah: Supervision, Funding acquisition. Iseult Lynch: Supervision, Writing – Review and Editing, Funding acquisition. Ryan Mushinski: Conceptualization, Supervision, Writing – Review and Editing.

7.1. Abstract

Finding alternatives to synthetic fertilisers is a priority in order to improve global food security whilst also improving the sustainability of agriculture. Nanoparticles are nanoscale materials that have unique qualities due to their size, large surface area and ability to transform as they enter new environments. This enables them to adsorb biomolecules to their surface, changing their reactivity and stability. This study directly compared the application of urea and the nanofertiliser, urea-doped amorphous calcium phosphate (U-ACP), on glasshouse-grown lettuce, assessing soil microbial group sizes (nitrifiers and denitrifiers) to infer impacts of the hydroxyapatite nanomaterial on microbial communities. To gauge wider impacts of the different treatments on N cycling, reactive N emissions, including both gaseous emissions, with NO_Y gases focussed on in this study, and also losses of NO_2^-, NO_3^- and NH_4^+ in surface run-off and groundwater leaching, were studied. Nitrifying bacterial group abundance decreased over the course of the experiment, while denitrifiers, specifically those expressing *qnorB*, were more prevalent in U-ACP treated soils at the end of the lettuce growth period. Urea treated soils had significantly higher concentrations of ammonia and nitrate as well as greater NO emissions. Overall, the conventional urea treatment caused greater amounts of N to be volatilized or lost through leaching than U-ACP, with urea also triggering soil acidification (~30% pH reduction) that stunted lettuce yield. U-ACP treatment was able to increase lettuce yield by 77% as compared to the negative control and reduce NO and NO_Y emissions to the same level as the control. U-ACP has clear potential to be an effective nanofertiliser, promoting lettuce biomass accumulation while minimising N losses to the environment.

7.2. Introduction

With the world's population predicted to continue increasing, peaking at 11 billion around 2100 (UN, 2015), the required amount of high quality, nutritional food must also increase in order to fulfil demand and maximise global food security. As extreme weather events like droughts and floods become more frequent with the onset of climate change, available agricultural land will face growing pressure. Total agricultural production is predicted to require an increase of 60% by 2050 in order to match global needs (Alexandratos and Bruinsma, 2012). Soil degradation is a by-product of this intensive farming, with the quality of soils globally decreasing, driving a need for further fertilisation (Beretta-Blanco et al., 2019). Fertiliser is an essential part of modern agriculture, enabling the necessary input of nutrients for farmers to produce crops of sufficient yield and quality annually. Conventional synthetic fertilisers have poor use efficiency with a study in China indicating that up to 60% of the nitrogen applied is lost through volatilization or leaching (FAO, 2002). Environmental concerns around excess fertiliser use are significant, with run-off into waterways and eutrophication of water sources common (Yang et al., 2008). Regions with the greatest levels of arable farming have the highest excess nitrate levels in their rivers (DEFRA, 2007). This is due to fertiliser sourced N leaching more than naturally occurring nitrogen sources (Crews & Peoples, 2004). The need to develop sustainable options for fertilisation in agriculture is crucial, not just for biodiversity but also for future food security in an increasingly uncertain world.

Fertilisation affects the natural soil nitrogen (N) budget, thus leading to high levels of aqueous and gaseous (volatile) losses. N cycling in the soil is controlled primarily through the action of the microbial community, allowing nitrogen fixation, nitrification and denitrification all to occur. Human inputs of N, such as fertiliser, require N to be fixed using the Haber-Bosch process, an energetically costly industrial technique that produces ammonia. Once N is present in the soil as ammonia it undergoes a series of microbe-mediated reactions, whereby the ammonia is processed into different forms, some of which are accessible to plants. The diversity and health of these microbial groups is essential for functioning soils that are able to have high productivity in agriculture and continue biogeochemical cycling (Philippot et al., 2013). Soil microbes are also responsible for later transformations of N compounds, including those that are damaging to the environment when produced in excess due to

inefficient fertiliser application (Kuypers et al., 2018). Nitrogen emissions from agriculture contribute to global warming, with nitric oxide (NO) and reactive N emissions (HONO, NO_2), collectively known as NO_Y, produced during nitrification and denitrification by soil microbes (Figure 7.1), as well as through abiotic reactions on soil surfaces. NO_Y is a less commonly studied group of reactive N gas, with N_2O frequently focussed on (Bouwman et al., 2002). N_2O has major global warming potential but the effects of NO_Y gases on ground level ozone and hydroxyl radical production, acid rain and climate change are still significant, with NO_Y also being linked to respiratory diseases in humans (Tang et al., 2020; van Strien et al., 2004).

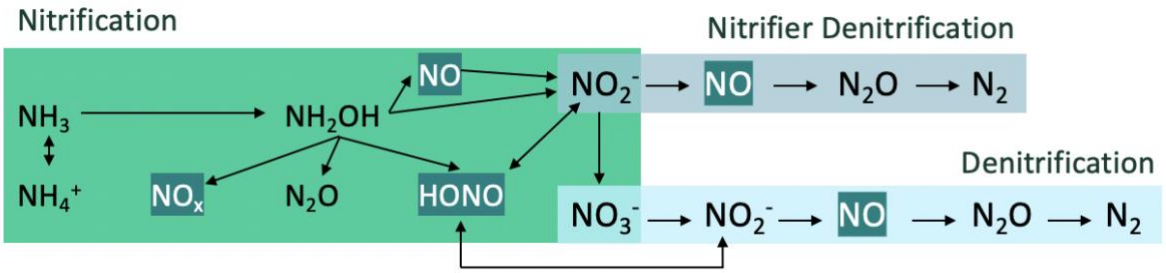


Figure 7.1. Outline of N compounds that occur throughout the nitrogen cycle, with NO_Y species highlighted in teal. NO_X refers to NO and NO_2. U-ACP may be acting to limit microbial access to N, reducing production of NO_Y. Sourced from Chadwick et al. (2023).

Nanomaterials (NMs) have at least one dimension between 1 and 100 nm, with high surface area to volume ratios and reactivity making them suitable for application as catalysts and as carriers of other molecules, including macronutrients like N (Khan et al., 2019). Within agriculture NMs have been applied as nanopesticides, nanoadditives, and nanofertilisers. Nanofertilisers are able to interact with the soil matrix, microbes and plants differently as compared to conventional synthetic fertilisers, either aiding in slow-release dynamics of essential nutrients, helping in targeted delivery of nutrients to plants, or having other micronutrients form part of their structure (Liu and Lal, 2015). Nanofertilisers have been shown to be able to deliver nutrients through plasmodesmata, cellular channels that also exist on the nano scale, reducing the energetic cost associated with nutrient uptake (Ditta and Arshad, 2016). Hydroxyapatites are mineral compounds primarily composed of phosphorus and calcium, nanoparticle

versions of this naturally occurring compound can act as a macronutrient nanofertiliser (Carmona et al., 2022). Calcium phosphate is present biologically in soils, acting to harden calcified tissues like collagen (Cui et al., 2008). Amorphous calcium phosphate (ACP) has been used in medical applications and more recently in agriculture as a method to deliver N and P, with the NM acting as a N carrier, making it a better option than other synthetic NMs (Sun et al., 2020; Liu and Lal, 2014). Ramírez-Rodríguez et al., (2020) identified urea-doped amorphous calcium phosphate (U-ACP) nanoparticles as maintaining yield and quality of wheat with reduced amounts of nitrogen needed as compared to plants grown using the conventional urea formulation. The nanoparticles uptake by roots was faster than that of conventional urea, indicating an improvement in nitrogen uptake efficiency. The positive effect of nanoparticles on nutrient use efficiency has been corroborated in other agricultural settings, including in viticulture (Pérez-Álvarez et al., 2021; Gaiotti et al., 2021), and hydroponically grown cucumbers (Carmona et al., 2021), providing evidence that nanofertilisers with embedded macronutrients, like N, are effective at improving nitrogen use efficiency. The wider environmental effects of nanofertiliser use are yet to be fully elucidated, including impacts on gaseous and leachate emissions of N and impacts on soil microbial communities.

To study soil microbial communities, representative genes core to different aspects of the N cycle were targeted to understand the activity of their respective chemical processes. Nitrifying genes, like ammonia monooxygenase, oxidise ammonia (NH_3) into different intermediates before becoming nitrite (NO_2^-). Bacterial *AmoA* is the A subunit of the first enzyme in ammonia oxidation and is responsible for oxidising ammonia into hydroxylamine, the primary step of nitrification. However, the clade that bacterial *AmoA* is sourced from also participates in nitrifier denitrification, with N_2O production via hydroxylamine (Wrage et al., 2001). Nitrite oxidoreductase (*NxrB*) is another nitrifying gene, used in the second step of nitrification where it oxidises nitrite and is a major source of nitrate in the environment. The other genes originally identified are involved in denitrification, including *NirK* and *qNorB*. One of the genes involved in denitrification is *NorB* (nitric oxide reductase), for which there is a quinol-oxidising subunit (*qNorB*) and a cytochrome c-oxidising complex (*cNorB*). *NirK* is the essential denitrifying enzyme in reducing NO_2^- to NO, with two distinct clades responsible for this step of the N cycle (Helen et al., 2016).

In this study, we compared N-cycle community sizes, volatile and aqueous N losses, and plant (*Lactuca sativa*) growth in soils treated with urea versus U-ACP. Based on previous work (Ramírez-Rodríguez et al., 2020), the U-ACP is predicted to reduce NO and NO_Y emissions, with less ammonia and nitrates leaching through the soil, as compared to the urea treatment. Understanding the effect that the U-ACP has on soil microbes is important in order to develop truly sustainable options for farmers, that not only maintain yields and reduce pollution, but also prevent further losses in soil quality and help propagate healthy N cycling. This study aimed to determine the effect of U-ACP on N cycling soil microbial communities, N cycling, in particular relating to NOY emissions, and effect on core soil parameters and lettuce growth. The working hypothesis is that U-ACP is more resilient to microbial attack, and that the reduced availability of N causes a shift in the microbial community structure. Due to the N being part of the NMs structure, there is also predicted to be lower leaching due to strong adsorption. If these hypotheses are proven correct, and the lettuces grown were of comparable size and quality between treatments, it would indicate that U-ACP enabled a more efficient delivery of N to the plants, minimising environment losses.

7.3. Methods and Materials

7.3.1. U-ACP synthesis and characterisation

U-ACP was synthesised based on Ramírez-Rodríguez et al. (2020). Briefly this involved the creation of the U-ACP precipitate by mixing two solutions, one containing calcium, citrate and urea with another containing phosphate, and incubating them together at 37°C. Rather than freeze-drying the samples, after washing the precipitates with pure water several times in a centrifuge (5000 rpm for 15 min), the samples were left under a fume hood to dry overnight. Characterisation of the pristine U-ACP nanoparticles was achieved using transmission electron microscopy (TEM) by dispersing a small amount of the particles in ethanol, add a drop to carbon-coated copper grids and blotting with a tissue. The TEM instrument used was JEOL 1400 TEM (JEOL, Japan) and three particles were analysed for average size and size distribution with only one agglomerate studied.

7.3.2. Soil characterisation

Soil from the Warwick Crop Centre (coordinates 52.2062, -1.6116) was processed by sieving through a 2mm sieve which removed stones and larger organic matter. Soil characterisation shows a sandy loam was used with 2.1% organic matter. Field soil was found to be pH 6.61 with a conductivity of 78.9 mS cm^{-1} and bulk density of 1.486 g cm^{-3}. Previous planting of the area included cereals, leguminous crops and oilseed rape with conventional synthetic fertiliser application of ~98 kg ha-1 yr-1 in 2021 and 2022 (Purchase et al., 2023).

7.3.3. Lettuce pot experiment

Experimental pots (18cm diameter) were filled to contain between 1.5 and 1.6kg of the 2mm sieved soil. These pots were left for three days before each was treated with a different source of N. Five pots were kept as controls (no added source of nutrients), five were treated with 140 kg ha^{-1} of urea and 40 kg ha^{-1} of potassium phosphate (K_2HPO_4) and five with urea-doped ACP as adjusted from fertilisation recommendations in UK DEFRA RB209A fertiliser manual (2017). The amount of N applied was the same between the urea and U-ACP containers, adjusted for N content by weight. While the urea and potassium phosphate were water soluble and applied in a 300 mL solution, the U-ACP was insoluble, applied as a solid, with the treated soils watered with 300 mL Millipore water (Merck, Germany) afterwards. To condition the soil the pots were left for five days at room temperature before the lettuce seeds (*Lactuca sativa*) were sown. Three seeds were sown per pot, with only one seedling >1cm tall permitted to remain per pot after week 1. The plants were grown under long-day conditions (16:8 hours light to dark) at 20°C. The plants were watered with 100 mL Millipore water daily, with leachate sampled pots receiving 200 mL on sampling days. At the end of the experiment the lettuce plants fresh weights were recorded, with total biomass, above-ground biomass and below-ground biomass all recorded.

7.3.4. Quantification of soil N gas fluxes

NOx and NO_Y analysis were performed using a Teledyne T200U-NOy analyser (Teledyne, Thousand Oaks, CA, U.S.A.), with the same method as detailed in Purchase et al. (2023). Ozone (O_3) free air was used as the carrier gas and was scrubbed of nitrogen gases using a molecular sieve, this allowed estimation of net potential from soil and excluded O_3 converted NO to NO_2. Both NO and molybdenum converted NO_Y were measured. NO and NO_Y emissions were recorded for each plant chamber, with NO recorded directly and values for NO_Y derived from NO_Y - NO. The lower detectable limit was < 50 ppt and the flow rate averaged 3.14 L min^{-1} over the sampling period. There were several outlier values seen in the NO gas dataset, with extreme outliers in the U-ACP treatment group in week 1 and in the urea treatment group during weeks 2 through 4. Extreme outliers were not visualised in Figure 7.3A, with an upper limit of 1000ppb m^{-2} h^{-1} of NO. Potted samples were watered with 100 mL Millipore water before measurements were taken. Flow rate through the sealed chamber was recorded before and after gas sampling. Samples underwent 80 minutes of analysis each, with 20 minutes for the empty (no soil) control chamber. For statistical comparison an average was taken for the middle hour of each chamber measured. In order to provide a reliable baseline, the average from the empty sealed chamber on non-sampling days and overnight was used.

7.3.5. Leachate sampling and analysis

Leachate was collected whenever the 50 mL falcon tubes used to collect it were filled more than 25 mL. These samples were filtered and stored at 4°C until analysis. Leachate was analysed using the ammonia (method no. G-102-93 rev. 10 (multitest MT7/MT8)), NOx, and nitrate (method no. G-109-94 rev. 10 (Multitest MT7/MT8)) protocols for the SEAL AutoAnalyzer 3 (AA3) HR Segmented Flow Analyser (SEAL Analytical). The limit of detection was 0.1µg/L for each of the studied nutrients and MilliPore water blanks were used to ensure accuracy. The reagents for the analysis were all created according to the AA3 protocols using MilliPore water. Due to the high N concentrations present in some of the samples a range of different dilutions were used, including 4-fold, 10-fold and 32-fold dilutions.

In order to get the values for nitrate (NO_3^-) content the concentration of the nitrite (NO_2^-) analysis was subtracted from the NOx concentration values.

7.3.6. Soil sampling and pH testing

Soil was sampled at three time points, before conditioning with N treatments, after 5 days of N treatments and at the end of the lettuce experiment (end of week 5). At the end of the lettuce experiment (week 5) three soil samples were taken from the bulk soil of each pot. These three technical replicates were mixed before storage. Soil samples were kept at -80°C. Topsoil pH was tested using a 2:1 mass ratio of 0.01M calcium chloride ($CaCl_2 \cdot 2H_2O$) solution to 10g of air-dried soil.

7.3.7. Soil microbial community analysis

DNA was extracted from the soil samples stored at -20˚C using the DNeasy PowerLyzer PowerSoil Kit (Qiagen). The protocol was followed for the full extraction and samples were stored at -20°C. When extracting the DNA from the soils the SLS Lab Pro VelociRuptor was used to homogenise the soil samples. DNA was quantified using a Qubit, with 1x dsDNA HS Working Solution (Invitrogen) in accordance with the manufacturer's protocol. The protocol, including timings, concentrations and relative proportions, used for the bulk PCR of the DNA samples was derived from the Earth Microbiome Project's 16S rRNA Illumina Amplicon Protocol. The protocol was altered in order to better fit the annealing temperatures of the primers for the genes chosen and to allow 15 minutes for the enzyme to activate. HotStar Taq (Qiagen) was used for PCR, with resulting PCR products run on a 1.5% agarose gel made with Tris/Borate/EDTA (TBE) buffer. Samples were run with a 1kb Plus DNA ladder (New England Biolabs (NEB)) and 6x purple gel loading dye (NEB). Primers were derived from past papers, most notably Ma et al. (2019) and Keeley et al. (2020). The genes chosen are core functional genes for their bacterial or archaeal taxa/clades and are frequently used to infer abundance of N-cycling microbes.

N cycling and bacterial 16S rRNA gene abundance was assessed by quantitative polymerase chain reaction (qPCR) of extracted DNA. The primers used are shown in full in Supplementary Table

S7.1. Quantitative PCR was conducted on a Stratagene Mx3005P qPCR machine (Agilent Technologies, USA) with a 10 µL volume involving 1 µL of DNA extract, 0.5 µL of each primer (100 mM), 5 µL of the SYBR Green universal master mix (ThermoFisher Scientific, UK) and 3 µL of sterile water. The gBlock sequences used per gene were the same as the primers, in addition to 16S rRNA, with complete sequences and amplicon lengths shown in full in SI Table S7.1. Quantitative PCR reactions, including timings, for each gene of interest are also detailed in full in SI Table S7.2. Standards were made up using each gene's respective gBlock between 1 x 10^{-2} and 1 x 10^{-9} ng/µL. Melting curves were used to verify the amplification specificity of each of the studied genes. Threshold cycles (Ct) values were converted to gene copies g^{-1} of wet soil. Relative abundance of each gene of interest was calculated by dividing the abundance of each gene of interest by the abundance of the total 16S rRNA gene abundance.

7.3.8. Statistical analyses

For the lettuce pot experiment, each treatment was replicated five times. This carried forward for the gas sampling, leachate analysis experiments and soil DNA extractions. Three soil sample replicates were taken at the end of the five-week period and compiled. R Studio (v4.0.2; R Core Team, 2023) was used for statistical analyses, with data checked for assumptions of normality, which, if parametric, were then analysed using two-way repeated measures analysis of variance (ANOVA). Post-hoc testing for significant results used Tukey pairwise comparison test. Non-parametric data was tested using a Friedman test, with significant results undergoing Wilcoxon rank sum pairwise comparisons. Linear models were performed for lettuce growth parameters with Bonferroni corrected pairwise t-tests performed on linear model outputs. Kruskal-Wallis tests were performed for qPCR data to compare between treatment effects. The significance level was set at $p < 0.05$ for all statistical tests.

7.4. Results

The simple batch method used to generate the urea-doped amorphous calcium phosphate nanoparticles created irregularly shaped nanoparticle agglomerates as seen in Figure 7.2. The agglomerate pictured is around 166 x 150 nm, with individual NPs measuring ~2 nm in diameter based off of three particles measured.

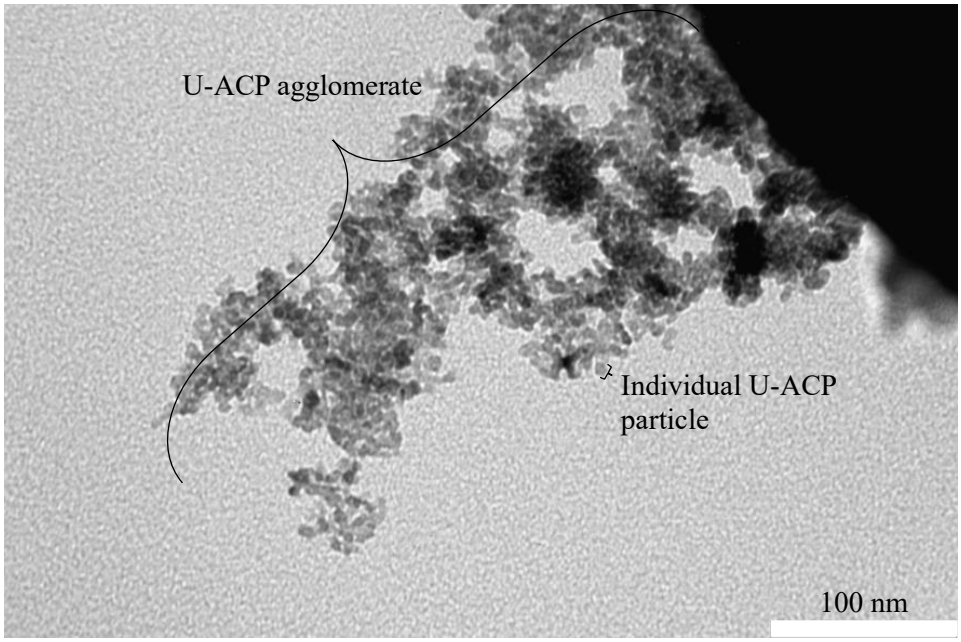


Figure 7.2. TEM generated micrograph of pristine U-ACP nanocomposites. The pictured agglomerate was calculated to be 166 x 150 nm, with individual particles measuring ~2 nm.

Table 7.1. Soil pH of pre-conditioned (week 0) soil as compared to soil in week 5 of the experiment under each of the three treatments.

	Control		U-ACP		Urea	
	Week 0 (n=4)	Week 5 (n=4)	Week 0 (n=4)	Week 5 (n=5)	Week 0 (n=4)	Week 5 (n=5)
Soil pH	5.22 (± 0.12)	5.27 (± 0.16)	5.19 (± 0.09)	5.53 (± 0.05)	5.20 (± 0.10)	4.38 (± 0.11)

The pH of the urea treated soils (Table 7.1) was significantly lower by week 5 than the other two sample conditions, with an average of pH 4.38 ($p = 1.24 \times 10^{-8}$). The other soil samples had means around pH 5, with the U-ACP treated soil having the highest average of pH 5.53, this difference was

significantly different to the control ($p = 0.0016$). The urea treatment was also statistically different to both the control ($p = 1.7 \times 10^{-8}$) and the U-ACP ($p = 3.8 \times 10^{-9}$) treatments.

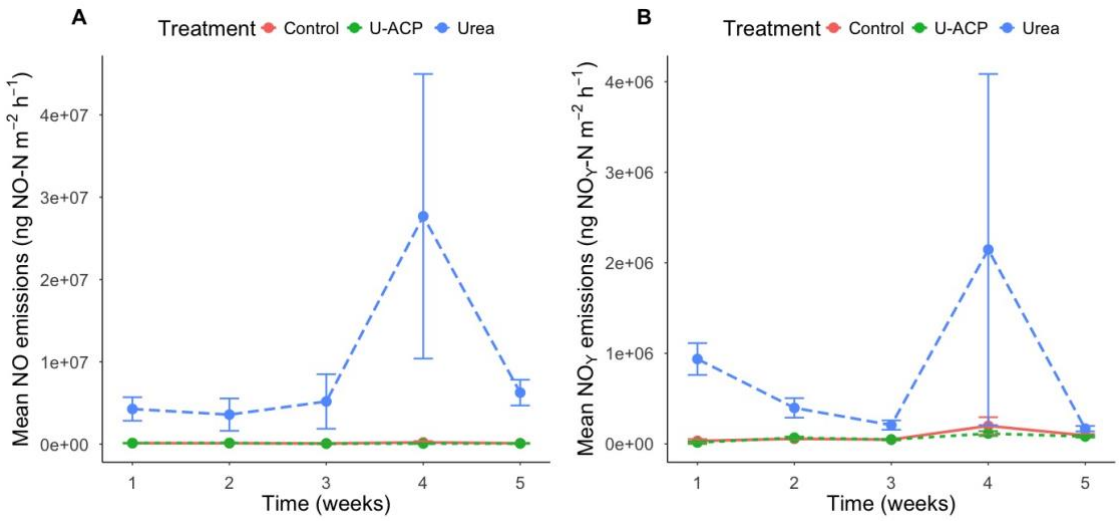


Figure 7.3. (A) NO and (B) NO_Y-NO gas emissions from control, U-ACP and urea treated soils over a five-week period. Weeks 1 and 2 all had n = 5 per treatment, with weeks 3 to 5 having n = 4 for the control group, and n = 5 for the other two treatments. Error bars show the standard error of the mean (SEM).

For the urea treated soils the release of NO gas is greater than that for the control and U-ACP treated soils at several timepoints, as seen in Figure 7.3A. Overall, NO emissions were found to be non-normally distributed. NO emission measurements were significantly different across the treatments over the course of the lettuce experiment ($p=0.022$) with a large effect size found ($W=0.76$). Urea treatment caused significantly different NO emissions to both control and U-ACP treatments, ($p=0.024$ for both).

NO_Y emissions were greatest in the urea treatment, with the control and U-ACP soil treatments having consistently low parts per billion across the five week growth period. Outliers were identified for the NO_Y-NO datapoints across all weeks and soil treatments. From this analysis, extreme outliers were not visualised in Figure 7.3B, with an upper limit of 150ppb/m^2/h NO_Y-NO used. Week 4 had the most significant differences, with both the control treatment and the urea treatment having $p < 0.05$. There were no statistically significant differences between any of the treatment groups or weeks for the NO_Y dataset.

NH_4^+ concentration in leachate was greatest under urea treatment, with control and U-ACP treatment having consistently low concentrations across all six weeks, as seen in Figure 7.4A. NH_4^+ concentration was significantly different across both the different weeks ($p = 2.55 \times 10^{-5}$), different treatments ($p = 4.28 \times 10^{-11}$), and the p-value for the interaction between *week* and *treatment* was also significant ($p = 4.49 \times 10^{-7}$). This indicates that *week*, *treatment*, and the interaction between the two, are all associated with significant differences in the NH_4^+ concentration of leachate. Pairwise comparisons of urea treatment with both control and U-ACP treatment were significant (for both, $p = 1.4 \times 10^{-5}$). Urea treatment generated significantly different ammonium and nitrate concentrations in soil leachate as compared to both the control and U-ACP treatments.

NO_2^- concentration in leachate was low at the start of the experiment, before peaking in week 2 (Figure 7.4B). Exposure duration (*Week*) had a significant effect on leachate nitrite concentration ($p = 2.46 \times 10^{-7}$). U-ACP treatment had higher NO_2^- concentrations than its control and urea counterparts, but this result was not statistically significant.

NO_3^- concentration was initially high across the three treatments, before decreasing in control and U-ACP for the rest of the weeks. NO_3^- peaked after NO_2^-, with NO_2^- being transformed into NO_3^- by soil microbes. Urea treated soils however, had high concentrations of NO_3^- across all timepoints, ranging from 155 to 300 mg L^{-1}. A similar pattern to that seen for NH_3 was found for leachate NO_3 concentrations. *Week* ($p = 3.16 \times 10^{-6}$), *treatment* ($p = 3.02 \times 10^{-13}$), and the interaction of the two factors ($p = 3.79 \times 10^{-5}$) all had a significant effect on NO_3^- concentration of leachate. Significant differences in leachate NO_3^- concentration were found between urea and control ($p = 3.7 \times 10\text{-}8$) and urea and U-ACP ($p = 2.8 \times 10\text{-}8$) treatments.

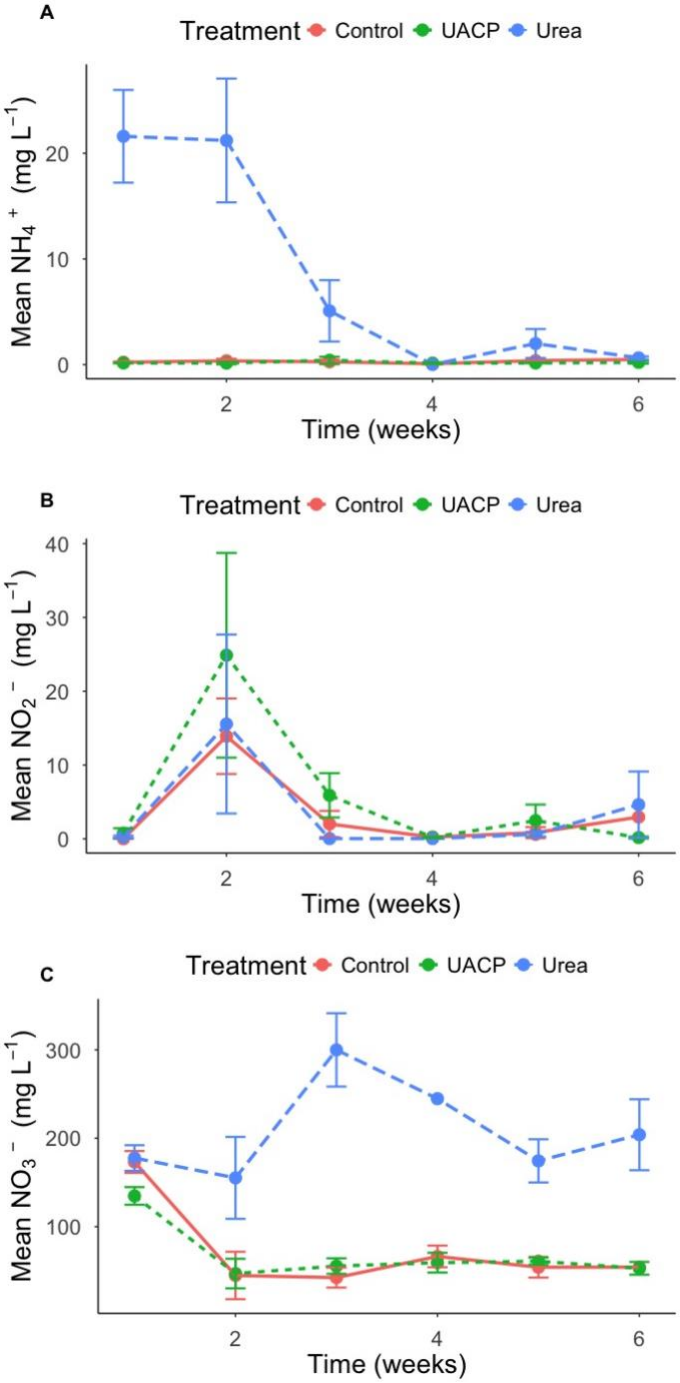


Figure 7.4. (A) Mean NH_4^+ concentration in soil leachate across the 6-week experiment from the three different soil treatments. (B) Mean NO_2^- concentration in soil leachate across the 6-week experiment from the three different soil treatments. (C) Mean NO_3^- concentration in soil leachate across the 6-week experiment from the three different soil treatments. Error bars show the standard error of the mean (SEM).

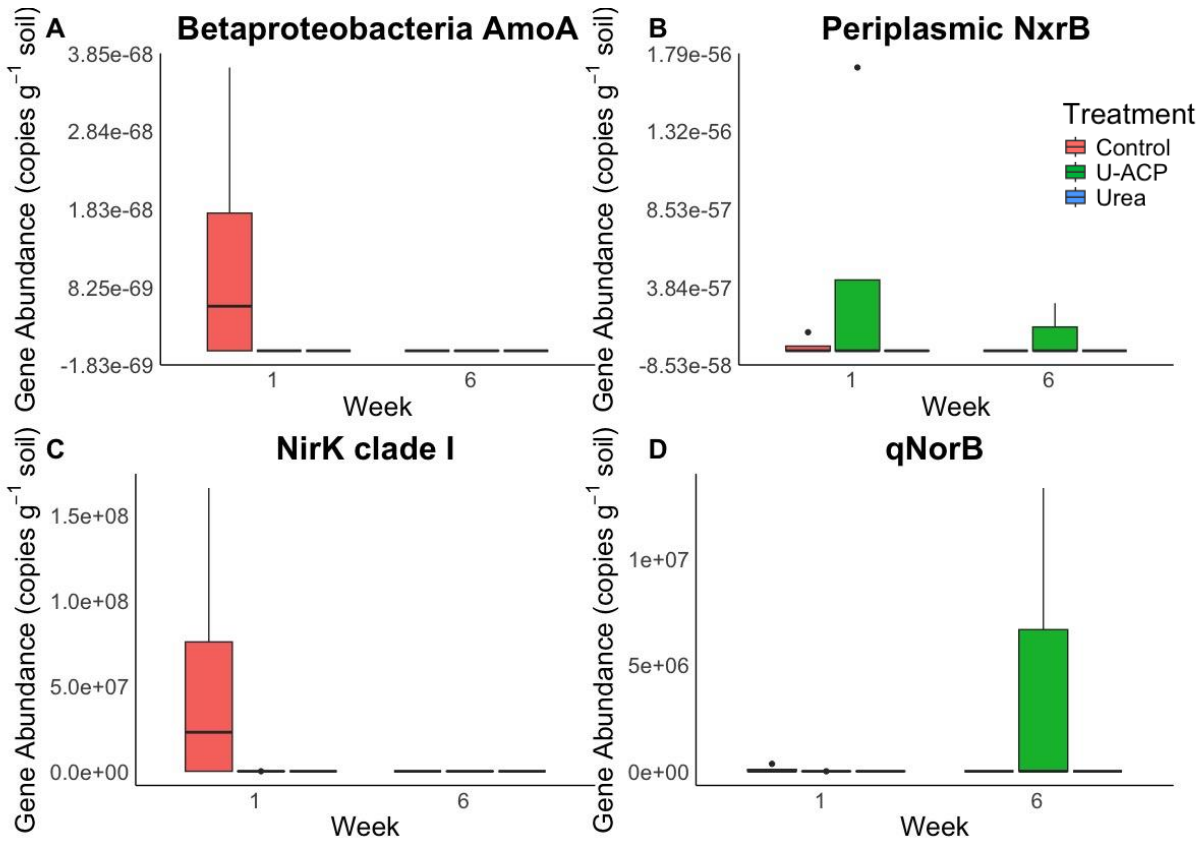


Figure 7.5. (A) Abundance of betaproteobacteria AmoA relative to 16S rRNA bacterial gene abundance. (B) Abundance of periplasmic NxrB relative to 16S rRNA bacterial gene abundance. (C) Abundance of NirK clade I relative to 16S rRNA bacterial gene abundance. (D) Abundance of qNorB relative to 16S rRNA bacterial gene abundance. Outliers greater than 1.5 times the mean were excluded, as were 0 values.

The four genes used as primers on the soil microbial DNA samples were betaproteobacteria *amoA*, periplasmic *nxrB*, *nirK* clade I and *qnorB*, as seen in Figure 7.5. No statistically significant differences were found between gene abundances of any of the treatments studied. Bacterial *amoA* and periplasmic *nxrB* both showed less abundance relative to bacterial 16S rRNA, while *nirK* clade I and *qNorB* both had greater abundance than bacterial 16S rRNA. Bacterial *amoA* and *nirK* had the most copies per gram of control soil at week 1 of the experiment, however these abundances decreased over the course of the experiment. Control and U-ACP treated soils showed the presence of periplasmic *nxrB* at week 1, with abundance for both treatments decreasing over time. This pattern of decreasing abundance was bucked for *qnorB*, with increased presence in U-ACP treated soil at the end of the lettuce growth period. A further gene presence/absence study was performed using PCR as seen in SI Figure S7.1.

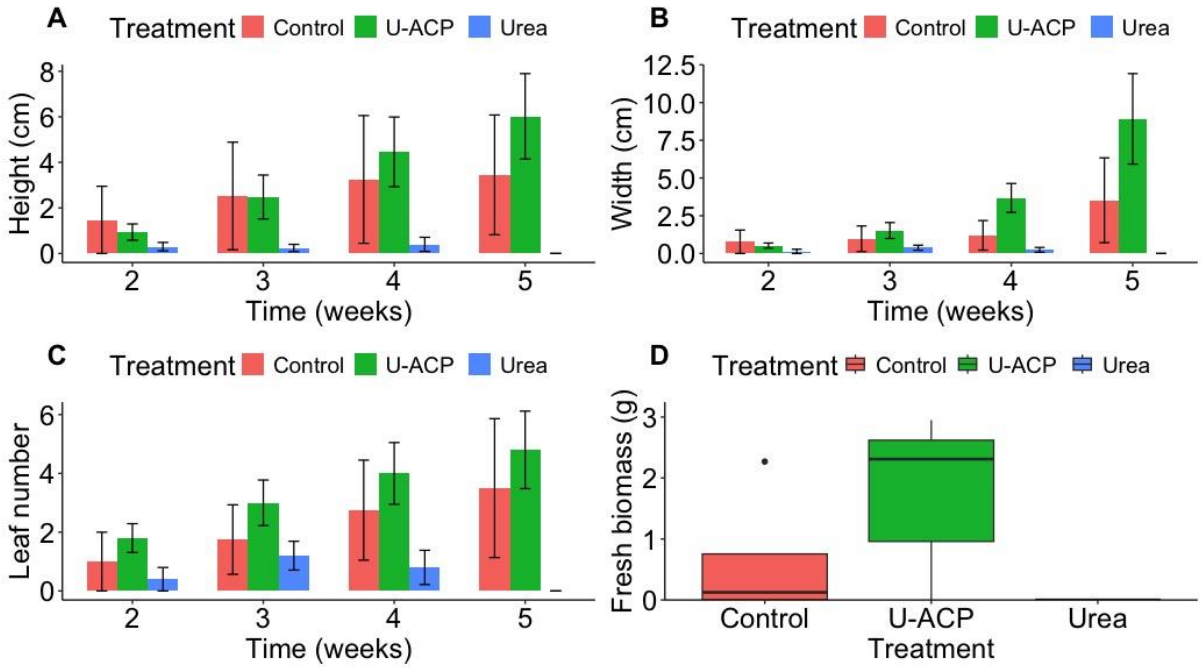


Figure 7.6. (A) Mean lettuce height from weeks 2 to 5 for all three treatments. (B) Mean lettuce width from weeks 2 to 5 for all three treatments. (C) Mean lettuce leaf number from weeks 2 to 5 for all three treatments. Error bars indicate standard error. (D) Mean fresh biomass of lettuce week 5 for all three treatments. Black dots indicate outliers.

Plant growth data, as shown in Figure 7.6A-D, clearly reflects that there is more lettuce growth in the control and U-ACP treated chambers than for the urea treated soils. All three metrics for plant growth that were measured are higher in the control and U-ACP treatments. The control group has greater number of mean leaves and are taller than U-ACP, but U-ACP grown lettuces are wider. Treatment was found to have a significant effect on height ($p = 0.0049$), width ($p = 0.00097$) and number of leaves ($p = 0.0011$). Exposure time indicated as Week (of growth) was also found to have a significant effect on lettuce width ($p = 0.0038$). Urea treatment produced significantly different lettuce heights compared to control ($p = 0.037$) and U-ACP ($p = 0.0059$). Width was also significantly different under urea treatment compared to U-ACP treatment ($p = 0.0041$). Significant differences were found when comparing the leaf numbers between urea and control treatments ($p = 0.037$), and urea and U-ACP treatments ($p = 0.0059$). There is no statistically significant difference between the mean mass of the control and U-ACP grown lettuces ($p > 0.05$).

7.5. Discussion

U-ACP treated soils were able to increase fresh lettuce yield by 77%, while also maintaining the same NO and NO_Y-NO emissions as the control even with the same N content as the urea treatment. U-ACP soil also produced lower concentrations of NH_3 and NO_3^- in leachate. Slightly elevated NO_2^- levels were found in the U-ACP leachate, however, it appears that the net N losses are reduced as compared to urea treatment. This provides evidence that U-ACP is also a suitable avenue for further research in sustainable nanofertiliser application, producing better lettuce crops with minimal N losses. Comparing different concentrations of U-ACP treatment would help in further optimising the use of U-ACP in arable agriculture, as in viticulture Pérez-Álvarez et al. (2020). Interrogating N content of the lettuce tissues, and other forms of N losses, like N_2O and NH_3 gas emissions, would prove useful in definitively concluding improved NUE for U-ACP treatments. Additionally, elemental analysis of the lettuce tissues produced should be done for effective understanding of how U-ACP may influence lettuce quality as well as yield.

Urea treated soils had the greatest NO, NO_Y, NH_3 and NO_3^- emissions, either as gas or in the soil leachate. The urea treated soils also produced the worst lettuce yield, with the highly available form of N causing soil acidification through the process of nitrification releasing H^+ ions into the soil matrix. However, the gene abundance data clearly shows that nitrifying bacteria are barely present in the urea treated soils by week 5. This indicates that the soil pH is so extreme under urea treatment, as seen in Table 7.1, that the pH sensitive autotrophic nitrifying bacteria are negatively affected, reducing their abundance. However, evidence of heterotrophic nitrifiers driving ammonification and hence NO_3 supply cannot be excluded. Urea addition is known to accelerate nitrification and trigger greater soil acidification and N losses (Tong and Xu, 2012).

U-ACP, as a nanocomposite, has urea as part of its structure, limiting N losses by reducing microbial access to the N source through adsorption to urea (Carmona et a., 2021). Reducing the access to the N source limits the rate of N cycling, which, coupled with U-ACP's relatively fast entry into roots, minimises N losses (Ramírez-Rodríguez et al., 2020). NO is produced as a result of incomplete denitrification, with complete denitrification catalysing the change of NO into N_2O and then N_2. This process can be acted out by denitrifying microbes, or by nitrifiers that are able to perform denitrification.

The genes assessed via qPCR were bacterial *amoA*, *nxrB*, *nirK* and *qnorB*. Other genes considered via PCR were archaeal *AmoA*, COMAMMOX *AmoA*, *NirS*, *NorB* and *cNorB*, however these could not successfully be replicated. The experimental conditions were optimised for lettuce growth and so the soil remained aerobic, making it unlikely to find some of the listed genes that prefer anaerobic environments (Francis et al., 2007). Other genes, like COMAMMOX, however, are not typically found in agricultural soils (Shi et al., 2020). The qPCR results showed reductions in the abundance of nitrifying taxa across control and U-ACP conditions, with close to no clades found under urea treatment due to the effect of urea on soil pH. Previous research shows that ammonia-oxidising bacterial diversity is reduced by N fertilisation, a result that is corroborated here (Sun et al., 2024). Gene abundance of the denitrifying *qnorB* expressing taxa was more prevalent in the U-ACP treated soils at the end of the lettuce experiment. This indicates that there may be greater levels of denitrification under this treatment condition, however, this doesn't appear to translate into increased NO_Y emissions. The gene *qnorB* is an aerobic denitrifier that catalyses the reaction of NO to N_2O (Ji et al., 2015). This experiment focussed on NO_Y emissions, but future research should include N_2O emissions also. This would increase clarity on whether U-ACP is genuinely producing fewer reactive N emissions or if the N is simply being volatilized in a different form. It is essential that all alternatives to conventional fertilisers that are intended to improve the sustainability of agriculture are effective at reducing total N emissions. As U-ACP also largely consists of calcium phosphate it is important to consider the potential effects this part of the nanofertiliser may be having on the soil microbial community. Calcium phosphate is a core component of Pikovskaya (PVK) medium which is used to identify phosphate-solubilising bacteria (Joe et al., 2018). Phosphate solubilising bacteria are core to making soluble phosphorus available to plants and may be another line of enquiry when considering U-ACP as it has sources of both N and P in the nanocomposite. Additionally, not all of the originally identified functional genes were able to be amplified, with p450nor, a fungal nitric oxide reductase gene missing from this set of experimental data. Future work should definitely include fungal nitrogen cycling functional genes in order to assess whether the calcium phosphate part of the nanocomposite has any effect on the soil microbial community.

Although the soils in this experiment were treated with dry, solid U-ACP, the regular watering of the chambers and the presence of water in the soil and plant environments makes this study essential

to understanding how the size and stability of the nanoparticle is altered by entering a biological context. Further research into how the nanofertiliser may transform and aggregate in the soil matrix and intracellular plant environments would be of interest. As the NM constituents are all essential plant nutrients, seeing how U-ACP treatment impacts on nutrient balance and quality of the lettuce yield could provide further positive evidence for the sustainable use of this NM in agriculture.

7.5.1. Optimisation of the U-ACP

Time constraints prevented further characterisation, but future work will include study of the nanoparticles zeta potential, their size and appearance in water, and dynamic light scattering (DLS), otherwise known as photon correlation spectroscopy. A more efficient U-ACP synthesis method as developed by Carmona et al. (2021), which increases the N-doping level of the NM has been developed. This increase in N may improve the cost-effectiveness of the NM (Carmona et al., 2021). Deeper understanding of the binding dynamics of the urea and ACP is needed to understand what triggers desorption of the urea from the NM, and whether there are environmentally realistic soil conditions that could cause rapid losses of N that could then potentially impact on soil pH, affecting crop yields. Future research should involve dose responses of different N-content U-ACP in order to understand how the U-ACP can best be developed as a sustainable nanofertiliser. In addition, U-ACP should be compared to a range of different N fertiliser options, not just urea, for more realistic comparisons that don't trigger such extreme soil acidification. Studying effects on other clades of soil microbes, including fungal N-cycling genes as well as effects on broader soil microbial communities, protists and fauna like earthworms and collembola is essential for understanding how U-ACP would impact agroecosystems more broadly. Measuring N contents of the lettuce tissue, N_2O and NH_3 gaseous emissions in addition to NO_Y emissions using ^{15}N stable isotope tracing would allow further elucidation of how the U-ACP interacts with de/nitrifiers in the soil and partitioning of the available N in the system.

7.5.2. Conclusion

Soil degradation has a significant effect on agriculture, with reduction of effective agricultural land and increase in required yield, having an accumulative effect. Finding sustainable solutions to nurture global soils back to health and solve food insecurity are essential. Nanofertilisers, like U-ACP, could provide a viable option for farmers to maintain crop yields and quality cost effectively while minimising harm to the environment. This study adds evidence that U-ACP is an efficient source of N for plants, with significantly less leachate and N gas emissions compared to the conventional synthetic urea when applied at a constant N mass. Additionally, soil properties (pH) and soil microbial communities remained closer to those of the untreated controls with U-ACP than with conventional urea fertilizer. Finally, the lettuce quality was significantly higher with U-ACP compared to urea, confirming that in all 3 aspects – reduced N emissions / pollution, improved soil quality post growth, lettuce size and quality- the U-ACP performed significantly better than the conventional urea. U-ACP NMs have a relatively "green" synthesis process, making it a good candidate for commercialisation in future (Carmona et al., 2021). In order for U-ACP, and other similar nanofertilisers, to be viable for future commercial use, additional research into their transformations and subsequent interactions in intracellular plant environments is needed, for example through the use of x-ray absorption spectroscopy.

References

Alexandratos, N., Bruinsma, J., 2012. World Agriculture towards 2030/2050: the 2012 revision.

Beretta-Blanco, A., Pérez, O., Carrasco-Letelier, L., 2019. Soil quality decrease over 13 years of agricultural production. Nutr Cycl Agroecosyst 114, 45–55. https://doi.org/10.1007/s10705-019-09990-3

Bouwman, A.F., Boumans, L.J.M., Batjes, N.H., 2002. Emissions of N2O and NO from fertilized fields: Summary of available measurement data. Global Biogeochemical Cycles 16, 6-1-6–13. https://doi.org/10.1029/2001GB001811

Carmona, F.J., Dal Sasso, G., Ramírez-Rodríguez, G.B., Pii, Y., Delgado-López, J.M., Guagliardi, A., Masciocchi, N., 2021. Urea-functionalized amorphous calcium phosphate nanofertilizers: optimizing the synthetic strategy towards environmental sustainability and manufacturing costs. Sci Rep 11, 3419. https://doi.org/10.1038/s41598-021-83048-9

Carmona, F.J., Guagliardi, A., Masciocchi, N., 2022. Nanosized Calcium Phosphates as Novel Macronutrient Nano-Fertilizers. Nanomaterials (Basel) 12, 2709. https://doi.org/10.3390/nano12152709

Chadwick, J.J., Zhang, P., Ullah, S., Lynch, I., 2023. 2 - Use of nanotechnology to increase nutrient use efficiency, enhance crop nutrition, and reduce agrochemical pollution, in: Zhang, P., Lynch, I., White, J.C., Handy, R.D. (Eds.), Nano-Enabled Sustainable and Precision Agriculture. Academic Press, pp. 17–41. https://doi.org/10.1016/B978-0-323-91233-4.00010-7

Crews, T.E., Peoples, M.B., 2004. Legume versus fertilizer sources of nitrogen: ecological tradeoffs and human needs. Agriculture, Ecosystems & Environment 102, 279–297. https://doi.org/10.1016/j.agee.2003.09.018

Cui, F.Z., Wang, Y., Cai, Q., Zhang, W., 2008. Conformation change of collagen during the initial stage of biomineralization of calcium phosphate. J. Mater. Chem. 18, 3835. https://doi.org/10.1039/b805467c

DEFRA, 2007. Nitrates in water – the current status in England (2006).

Ditta, A., Arshad, M., 2016. Applications and perspectives of using nanomaterials for sustainable plant nutrition. Nanotechnology Reviews 5, 209–229. https://doi.org/10.1515/ntrev-2015-0060

Food and Agriculture Organization of the United Nations, 2002. The State of Food and Agriculture 2002: Agriculture and Global Public Goods Ten Years after the Earth Summit, The State of Food and Agriculture. UN. https://doi.org/10.18356/7c6c1b96-en

Francis, C.A., Beman, J.M., Kuypers, M.M.M., 2007. New processes and players in the nitrogen cycle: the microbial ecology of anaerobic and archaeal ammonia oxidation. The ISME Journal 1, 19–27. https://doi.org/10.1038/ismej.2007.8

Gaiotti, F., Lucchetta, M., Rodegher, G., Lorenzoni, D., Longo, E., Boselli, E., Cesco, S., Belfiore, N., Lovat, L., Delgado-López, J.M., Carmona, F.J., Guagliardi, A., Masciocchi, N., Pii, Y., 2021. Urea-Doped Calcium Phosphate Nanoparticles as Sustainable Nitrogen Nanofertilizers for Viticulture: Implications on Yield and Quality of Pinot Gris Grapevines. Agronomy 11, 1026. https://doi.org/10.3390/agronomy11061026

Galazzo, G., van Best, N., Benedikter, B.J., Janssen, K., Bervoets, L., Driessen, C., Oomen, M., Lucchesi, M., van Eijck, P.H., Becker, H.E.F., Hornef, M.W., Savelkoul, P.H., Stassen, F.R.M., Wolffs, P.F., Penders, J., 2020. How to Count Our Microbes? The Effect of Different Quantitative Microbiome Profiling Approaches. Frontiers in Cellular and Infection Microbiology 10.

Helen, D., Kim, H., Tytgat, B., Anne, W., 2016. Highly diverse nirK genes comprise two major clades that harbour ammonium-producing denitrifiers. BMC Genomics 17, 155. https://doi.org/10.1186/s12864-016-2465-0

Ji, B., Yang, K., Zhu, L., Jiang, Y., Wang, H., Zhou, J., Zhang, H., 2015. Aerobic denitrification: A review of important advances of the last 30 years. Biotechnol Bioproc E 20, 643–651. https://doi.org/10.1007/s12257-015-0009-0

Joe, M.M., Deivaraj, S., Benson, A., Henry, A.J., Narendrakumar, G., 2018. Soil extract calcium phosphate media for screening of phosphate-solubilizing bacteria. Agriculture and Natural Resources 52, 305–308. https://doi.org/10.1016/j.anres.2018.09.014

Keeley, R.F., Rodriguez-Gonzalez, L., Class, U.S.F.G., Briggs, G.E., Frazier, V.E., Mancera, P.A., Manzer, H.S., Ergas, S.J., Scott, K.M., 2020. Degenerate PCR primers for assays to track steps of nitrogen metabolism by taxonomically diverse microorganisms in a variety of environments. Journal of Microbiological Methods 175, 105990. https://doi.org/10.1016/j.mimet.2020.105990

Khan, Ibrahim, Saeed, K., Khan, Idrees, 2019. Nanoparticles: Properties, applications and toxicities. Arabian Journal of Chemistry 12, 908–931. https://doi.org/10.1016/j.arabjc.2017.05.011

Kuypers, M.M.M., Marchant, H.K., Kartal, B., 2018. The microbial nitrogen-cycling network. Nat Rev Microbiol 16, 263–276. https://doi.org/10.1038/nrmicro.2018.9

Liu, R., Lal, R., 2015. Potentials of engineered nanoparticles as fertilizers for increasing agronomic productions. Science of The Total Environment 514, 131–139. https://doi.org/10.1016/j.scitotenv.2015.01.104

Liu, R., Lal, R., 2014. Synthetic apatite nanoparticles as a phosphorus fertilizer for soybean (Glycine max). Sci Rep 4, 5686. https://doi.org/10.1038/srep05686

Ma, Y., Zilles, J.L., Kent, A.D., 2019. An evaluation of primers for detecting denitrifiers via their functional genes. Environmental Microbiology.

Pérez-Álvarez, E.P., Ramírez-Rodríguez, G.B., Carmona, F.J., Martínez-Vidaurre, J.M., Masciocchi, N., Guagliardi, A., Garde-Cerdán, T., Delgado-López, J.M., 2021. Towards a more sustainable viticulture: foliar application of N-doped calcium phosphate nanoparticles on Tempranillo grapes. Journal of the Science of Food and Agriculture 101, 1307–1313. https://doi.org/10.1002/jsfa.10738

Philippot, L., Spor, A., Hénault, C., Bru, D., Bizouard, F., Jones, C.M., Sarr, A., Maron, P.-A., 2013. Loss in microbial diversity affects nitrogen cycling in soil. ISME J 7, 1609–1619. https://doi.org/10.1038/ismej.2013.34

Purchase, M.L., Bending, G.D., Mushinski, R.M., 2023. Spatiotemporal Variations of Soil Reactive Nitrogen Oxide Fluxes across the Anthropogenic Landscape. Environ. Sci. Technol. 57, 16348–16360. https://doi.org/10.1021/acs.est.3c05849

Ramírez-Rodríguez, G.B., Miguel-Rojas, C., Montanha, G.S., Carmona, F.J., Dal Sasso, G., Sillero, J.C., Skov Pedersen, J., Masciocchi, N., Guagliardi, A., Pérez-de-Luque, A., Delgado-López, J.M., 2020. Reducing Nitrogen Dosage in Triticum durum Plants with Urea-Doped Nanofertilizers. Nanomaterials 10, 1043. https://doi.org/10.3390/nano10061043

RB209 2021 Section 6 Vegetables and bulbs | AHDB [WWW Document], 2017. URL https://ahdb.org.uk/knowledge-library/rb209-2021-section-6-vegetables-and-bulbs (accessed 8.19.24).

R Core Team (2023). R: A language and environment for statistical computing. R Foundation for Statistical Computing, Vienna, Austria. URL https://www.R-project.org/.

Shi, Y., Jiang, Y., Wang, S., Wang, X., Zhu, G., 2020. Biogeographic distribution of comammox bacteria in diverse terrestrial habitats. Science of The Total Environment 717, 137257. https://doi.org/10.1016/j.scitotenv.2020.137257

Sun, H., Liu, C., Li, X., Liu, H., Zhang, W., Yang, H., Li, C., Yang, L., 2020. A novel calcium phosphate–based nanocomposite for the augmentation of cement-injectable cannulated pedicle screws fixation: A cadaver and biomechanical study. Journal of Orthopaedic Translation, The Role of FEA and Other Imaging-based Assessment in Orthopaedics 20, 56–66. https://doi.org/10.1016/j.jot.2019.08.001

Tang, K., Qin, M., Fang, W., Duan, J., Meng, F., Ye, K., Zhang, H., Xie, P., Liu, J., Liu, W., Feng, Y., Huang, Y., Ni, T., 2020. An automated dynamic chamber system for exchange flux measurement of reactive nitrogen oxides (HONO and NOX) in farmland ecosystems of the Huaihe River Basin, China. Science of The Total Environment 745, 140867. https://doi.org/10.1016/j.scitotenv.2020.140867

Tong, D., Xu, R., 2012. Effects of urea and (NH4)2SO4 on nitrification and acidification of Ultisols from Southern China. Journal of Environmental Sciences 24, 682–689. https://doi.org/10.1016/S1001-0742(11)60832-2

United Nations, 2015. World Population Prospects 2022: Summary of Results, Statistical Papers - United Nations (Ser. A), Population and Vital Statistics Report. United Nations. https://doi.org/10.18356/9789210014380

Usman, M., Farooq, M., Wakeel, A., Nawaz, A., Cheema, S.A., Rehman, H. ur, Ashraf, I., Sanaullah, M., 2020. Nanotechnology in agriculture: Current status, challenges and future opportunities. Science of The Total Environment 721, 137778. https://doi.org/10.1016/j.scitotenv.2020.137778

van Strien, R.T., Gent, J.F., Belanger, K., Triche, E., Bracken, M.B., Leaderer, B.P., 2004. Exposure to NO2 and Nitrous Acid and Respiratory Symptoms in the First Year of Life. Epidemiology 15, 471. https://doi.org/10.1097/01.ede.0000129511.61698.d8

Wrage, N., Velthof, G.L., van Beusichem, M.L., Oenema, O., 2001. Role of nitrifier denitrification in the production of nitrous oxide. Soil Biology and Biochemistry 33, 1723–1732. https://doi.org/10.1016/S0038-0717(01)00096-7

Yang, X., Wu, X., Hao, H., He, Z., 2008. Mechanisms and assessment of water eutrophication. Journal of Zhejiang University. Science. B 9, 197. https://doi.org/10.1631/jzus.B0710626

Chapter 8. General Discussion and Conclusion

This thesis aimed to identify engineered nanomaterials with the potential to enhance nitrogen use efficiency without compromising on crop yield and quality. This began with a screening experiment (Chapter 3) where 54 NMs of different constituent elements and structures were used for priming wheat and lettuce seeds. Seed responses varied by NM type, with varying improvements in germination seen within and between NM types, e.g., zeolites and metal oxides. Additionally, seed species often responded differently to the application of the same NM, with lettuce seeds frequently being more sensitive to NMs than the physiologically larger wheat seeds. The NMs were characterised before and after exposure to the seeds, with some correlation tests indicating that the pre-exposure characteristics of the NMs were more closely linked to wheat root growth and the post-exposure characteristics more correlated with shoot growth. Seed exudates were determined to be an important factor in altering the NM characteristics, although more research is required to elucidate the interactions between NMs and amino acids, proteins and organic acids.

A selection of three NMs from the screening experiment were then used in soil-based application and compared to addition of a reduced dose of synthetic fertiliser in terms of efficacy to grow lettuce and soil N-cycling impacts with conventional fertilisation (Chapter 4). Two of the zeolite NMs added were very similar across all of the physicochemical characteristics, including composition, Si:Al ratio, extra-framework ion and pore size. However, ZSM-5-15 actively increased N_2O emissions from the soil, likely through a process of ion exchange causing H^+ ions to replace NH_4^+ ions in the zeolite's pores, enabling NH_4^+ ions to be accessible to nitrifying bacteria, causing an increase in nitrifier derived N_2O emissions. BEA-19 has very similar properties in terms of Si:Al ratio, pore size, extra-framework ion and overall particle size to ZSM-5-15, however this zeolite had no effect on N_2O emissions nor on lettuce growth. $Ce_{0.75}Zr_{0.25}O_2$, a mixed metal oxide, had limited effect on N_2O emissions and Nr concentration in leachate. It was able to maintain the nutritive quality of the lettuce grown and to enhance yield, making this NM a good target for future research in sustainable agriculture. The transformation study showed that the Zr^{4+} ions were partially leached from the mixed metal oxide structure in the soil by week 8 of the growth period, with both $Ce_{0.75}Zr_{0.25}O_2$ NMs and $ZrCl_4$ formed from leached Zr^{4+} ions found in the

lettuce tissues. ICP-OES data didn't indicate bioaccumulation of Zr in the lettuce but future research into the broader impacts of $Ce_{0.75}Zr_{0.25}O_2$ on non-target organisms is required.

Soil-based application focuses on root uptake pathways of NMs with N_2O emissions primarily being nitrification driven. Similarly, N_2O emissions from recirculating vertical hydroponic systems followed this trend, with N_2O emissions from the nitrifier pathways more prevalent at all studied weeks (as seen in Chapter 5). This indicates that the root area of the hydroponic setup was more aerated and had greater microbial activity than expected in the biologically inert rockwool environment. NM addition in the context of hydroponics had little effect on Nr emissions, at least with the three NMs utilised herein.

Some of the same NMs as studied in Chapter 4 were used in Chapter 6, focussed now around impacts on soil biology, specifically microbial extracellular enzyme activity and ecotoxicological impacts on *Eisenia fetida* earthworms. The extracellular N-cycling enzymes were thermally stable, and activity was still present in autoclaved soil. The main source of differences in enzyme activity was from any addition of N, with or without accompanying NM. BEA-150, another zeolite NM, increased N_2O emissions in natural soil but not autoclaved soil, indicating an important biotically controlled aspect to BEA-150's effect on N cycling. NM characteristics play a significant role, with both BEA NMs (BEA-19 and BEA-150) having very different effects on N_2O production, with the ratio of Si:Al being the main difference between them. Similar characteristics between BEA-19 and ZSM-5-15 also resulted in very different impacts on soil, highlighting the importance of further research on which NM characteristics are most significant. It does also indicate the importance of abiotic soil parameters (e.g., soil moisture, colloids and clays) and soil microbial community composition, however, the exact ways in which these a/biotic factors alter NM soil effects also appears to be NM dependent. The ZSM-5-15 that was previously found to increase N_2O emissions (Chapter 4) was found to also have an impact on earthworm reproduction, reducing the total number of cocoons produced. This effect was only seen at the lower, more environmentally relevant NM concentration (25 mg kg^{-1}) indicating that there may be an impact from increased agglomerate size with increasing NM concentration that reduces the NM bioavailability and thus its apparent toxicity. ZSM-5-15 may be absorbed or bioaccumulate in worm tissues based on

the concentration of Si in the worms, however only whole tissue digestions were performed so NM localisation is unknown and requires future study.

The final chapter (Chapter 7) utilised a NM where the N was physically part of the nanostructure rather than synthetic fertiliser and NM co-application to soil. The urea-doped hydroxyapatite was able to reduce NO_Y emissions from soil as compared to soils in which the same amount of N was applied in the form of urea. However, N_2O emissions were not monitored over the growth period and so it cannot be determined from this data alone if a true reduction in N emissions occurred or if the NM changed the dynamic flux of the N cycle to produce greater N_2O emissions. This work highlighted the importance of looking at as many N endpoints as possible, including N_2O, NH_3 and NO_Y gases, as well as NH_4^+ and NO_3^- in leachate and soils, and plant tissue N content in order to fully identify changes in nitrogen use efficiency.

NM addition to soil, whether as a co-additive or with nutrients embedded in their structure, do not result in a single trend in Nr emissions from soils and no clear pattern emerged from the small set of NMs utilised here. Using NM characteristics such as constituent elements, agglomerate size or zeta potential is not sufficient to accurately predict how NMs will transform or affect biota, nor what their effects on N cycling will be. These findings are significant when considering the importance of NMs that are safe and sustainable by design especially in applications such as agriculture and food production where the NMs may be intentionally added to the environment. The safe by design approach should consider the NM synthesis route, broader impacts of the NMs in soils, for example NM persistence and influence on soil microbial communities and soil fauna, and in crop plants, in terms of bioaccumulation and potential risks posed to human health from NMs or their degradation/transformation products in the edible parts of plants. It is essential to consider all of these factors as NMs are taken forward for further study and/or rolled out for widespread use in crop production, in order to prevent regrettable substitutions as so often have happened in the past with agrochemicals, for example neonicotinoid insecticide impact on non-target populations, such as bees (Blacquière et al., 2012). The mixed metal oxide $Ce_{0.75}Zr_{0.25}O_2$ was identified as being a good avenue for further research due to its maintenance of nutritive quality and enhanced lettuce yield without impact on Nr emissions. NM application may cause elevated levels of heavy metal ions to leach from NMs into soils, with current risk and implications

unclear at present. A critical question to be addressed is whether there is potential for these heavy metal ions to biomagnify either in human or wildlife populations. Studying where NMs are transferred to in plant tissues and indirect targets, like earthworms and other terrestrial ecotoxicological model organisms, like Collembola, and in what forms these NMs are translocated in (i.e., untransformed or following some environmental transformations or changes in speciation) will help improve understanding of NM persistence and toxicology. More N cycling endpoints need to be considered in NM studies to effectively look at microbial responses and wider, climatic impacts, with agricultural N_2O emissions especially being targeted by international policy to reduce anthropogenic N_2O emissions (Kanter et al., 2020). The studies presented here focussed on engineered NMs and N cycling but other, naturally occurring or green synthesised NMs may also be of interest, as would endpoints of P compounds in leachate, including more N endpoints in terms of gas, leachate, soil and plant tissue, and NM impacts on soil C cycling.

Future work should aim to utilise different crops, as the seed priming study showed that different crops can have varying responses to the same NM treatment and with the added complexity of the soil environment these differences are likely to be exacerbated in full life cycle studies. These results were all found for lettuce in soils from temperate climates and were conducted under greenhouse conditions. Field trials including a broader range of biotic and abiotic stresses as well as studying interactions of soil fauna and NMs are needed. While many studies have looked at how NM application impacts crop stress responses, having a clear lab-based understanding of ecotoxicological responses is essential before performing field trials in order to minimise environmental risks. Deeper analysis of soil microbial community shifts and responses to NMs, including looking beyond bacterial clades to fungi and archaea, would enhance comprehension of how NMs effect metrics for soil health. Developing quality models using experimental data for NM impacts on N cycling, ecotoxicological responses and crop effects would also be a significant area of further research to ensure safety is at the forefront of nanotechnological applications. While many of the tested NMs have been determined to be unsuitable for future use in agriculture, results from soil-based studies are still relevant, with soils being a major sink for NMs used in industry, as a result of sewage sludge application to soil for example (Dror et al., 2015).

NMs have huge potential to maintain or improve crop yields to meet the demands of a growing population whilst mitigating some of the problems synthetic fertiliser has caused to the natural environment and agroecosystems. Implementing studies that aim to look holistically at crop impacts, N cycling, soil microbes and fauna will be more environmentally protective overall, as they are less likely to miss critical impacts or currently unknown adverse NM effects, allowing informed choices for future farming. As with conventional fertilisation, nanofertilisers are subject to the same considerations and NM usage must comply with the principles of the right source, rate, time and place for genuine improvements in the sustainability of agriculture to be possible.

"In nature, nothing exists alone."

Rachel Carson, Silent Spring

References

Blacquière, T., Smagghe, G., van Gestel, C.A.M., Mommaerts, V., 2012. Neonicotinoids in bees: a review on concentrations, side-effects and risk assessment. Ecotoxicology 21, 973–992. https://doi.org/10.1007/s10646-012-0863-x

Carson, R., 1962. Silent Spring.

Dror, I., Yaron, B., Berkowitz, B., 2015. Abiotic soil changes induced by engineered nanomaterials: A critical review. Journal of Contaminant Hydrology, Fate and Transport of Biocolloids and Nanoparticles in Soil and Groundwater Systems 181, 3–16. https://doi.org/10.1016/j.jconhyd.2015.04.004

Kanter, D.R., Ogle, S.M., Winiwarter, W., 2020. Building on Paris: integrating nitrous oxide mitigation into future climate policy. Current Opinion in Environmental Sustainability, Climate Change, Reactive Nitrogen, Food Security and Sustainable Agriculture 47, 7–12. https://doi.org/10.1016/j.cosust.2020.04.005

Appendices

Supplementary Information for: Chapter 3 – Differential impacts on wheat and lettuce seedling outcomes from nano-zeolite and metal oxide seed priming – a comparative study

Jessica J Chadwick[1], Peng Zhang[1], Aleksandar Radu[2], Sam Parkinson[3], Ify Leonard Ugbomeh[1], Sami Ullah[1], Iseult Lynch[1]

[1] School of Geography, Earth and Environmental Sciences, University of Birmingham, Edgbaston, B15 2TT Birmingham, United Kingdom

[2] School of Chemistry, University of Lincoln, Lincoln LN6 7TS, UK

[3] School of Chemistry, University of Birmingham, Edgbaston, B15 2TT Birmingham, United Kingdom

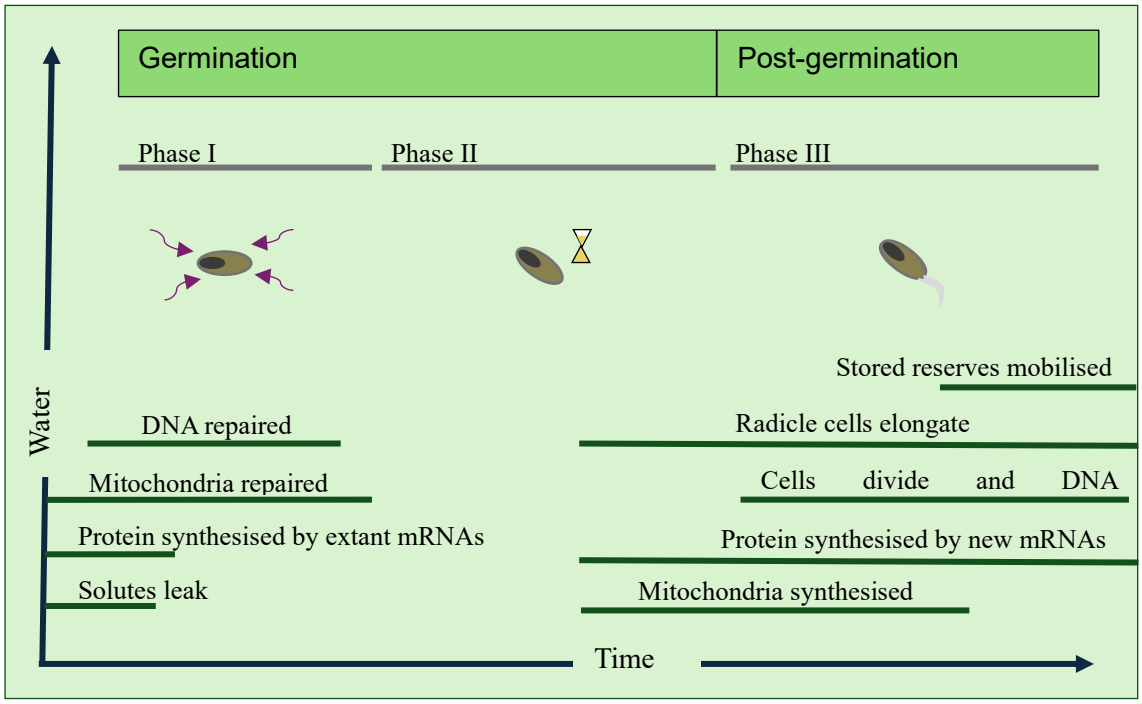
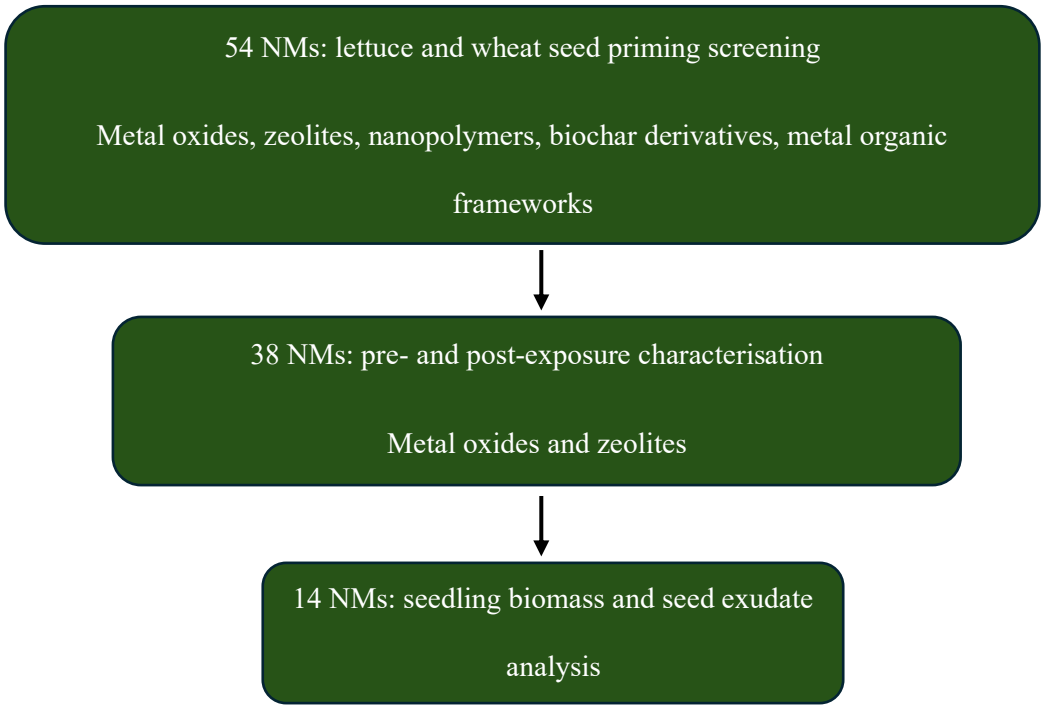


Figure S3.1. Time course of physiological events in germination and post-germination growth as adapted from Bewley, 1997.



Scheme S3.1. Schematic of selection process and NMs screened at each stage of experiment.

Table S3.1. Seed priming incubation conditions. Wheat seeds were incubated for 7 days after exposure to 500 mg L^{-1} nanomaterial suspensions, while lettuce seeds were incubated for 5 days after exposure.

	Conditions
Light:Dark	16:8
Light temperature (˚C)	27
Dark temperature (˚C)	18
Light humidity (%)	40
Dark humidity (%)	50

Table S3.2. Wheat and lettuce seed priming outcomes for each tested nanomaterial. Nanomaterials are grouped by type. Data shown are means and standard deviation. There were three biological replicates for each nanomaterial per seed type, each of which included 14 technical replicates.

Nanomaterial	Wheat				Lettuce			
	Shoot length (cm) (n=3)	Root length (cm) (n=3)	Germination rate (%) (n=3)	Seedling vigour (cm %) (n=3)	Shoot length (cm) (n=3)	Root length (cm) (n=3)	Germination rate (%) (n=3)	Seedling vigour (cm %) (n=3)
Metal oxides								
TiO_2	6.7 (± 0.4)	7.5 (± 0.5)	97.6 (± 4.1)	1385.2 (± 54.1)	2.2 (± 0.2)	2.4 (± 0.3)	97.6 (± 4.1)	451.4 (± 66.9)
TiO_2 D540	5.9 (± 1.0)	7.5 (± 2.1)	88.1 (± 14.9)	1204.0 (± 441.2)	2.1 (± 0.2)	2.2 (± 0.3)	97.6 (± 4.1)	425.0 (± 40.7)
$Ce_{0.5}Zr_{0.5}O_2$	6.5 (± 1.4)	5.3 (± 1.3)	81.0 (± 10.9)	949.4 (± 104.3)	1.8 (± 0.1)	2.4 (± 0.3)	95.2 (± 4.1)	403.8 (± 33.0)
ZrO_2	7.0 (± 0.9)	4.0 (± 0.2)	83.3 (± 16.5)	906.4 (± 128.1)	2.2 (± 0.1)	2.5 (± 0.1)	95.2 (± 4.1)	446.0 (± 26.7)
$Ce_{0.1}Zr_{0.9}O_2$	6.7 (± 0.6)	5.1 (± 1.3)	92.9 (± 12.4)	1104.2 (± 273.3)	1.8 (± 0.3)	2.1 (± 0.5)	90.5 (± 8.2)	351.4 (± 99.2)
$Ce_{0.75}Zr_{0.25}O_2$	5.8 (± 0.2)	4.3 (± 1.2)	78.6 (± 21.4)	802.8 (± 294.6)	2.0 (± 0.2)	2.8 (± 0.2)	100.0 (± 0.0)	479.3 (± 31.9)
$Ce_{0.25}Zr_{0.75}O_2$	6.3 (± 0.4)	5.6 (± 0.7)	92.9 (± 0.0)	1104.9 (± 100.8)	2.2 (± 0.2)	2.3 (± 0.1)	95.2 (± 4.1)	429.5 (± 36.7)
AlOOH	6.6 (± 0.5)	5.4 (± 0.8)	85.7 (± 7.1)	1033.2 (± 94.5)	2.1 (± 0.0)	2.1 (± 0.2)	92.9 (± 12.4)	391.0 (± 66.9)
$Ce_{0.9}Zr_{0.1}O_2$	5.6 (± 0.3)	4.3 (± 0.4)	83.3 (± 14.9)	832.7 (± 168.7)	2.0 (± 0.2)	2.5 (± 0.3)	95.2 (± 4.1)	429.3 (± 34.6)
Fe_3O_4	7.0 (± 0.4)	7.3 (± 0.5)	83.3 (± 10.9)	1182.9 (± 135.0)	2.3 (± 0.1)	2.4 (± 0.4)	95.2 (± 8.2)	444.8 (±81.2)
CeO_2/Co_3O_4	6.3 (± 0.9)	5.6 (± 1.4)	88.1 (± 4.1)	1051.9 (± 180.2)	2.4 (± 0.2)	2.8 (± 0.4)	97.6 (± 4.1)	509.8 (± 76.0)
TiO_2 PVP	7.8 (± 0.2)	3.6 (± 0.8)	61.9 (± 10.9)	706.6 (± 155.3)	2.1 (± 0.2)	2.9 (± 0.5)	97.6 (± 4.1)	492.4 (± 86.6)
$Co_{1.5}Fe_{1.5}O_4$	6.6 (± 1.5)	5.4 (± 1.0)	95.2 (± 8.2)	1130.1 (± 158.1)	2.5 (± 0.3)	2.4 (± 0.0)	92.9 (± 7.1)	455.2 (± 29.8)
$Co_{2.25}Fe_{0.75}O_4$	6.6 (± 1.4)	4.9 (± 1.0)	92.7 (± 0.3)	1064.8 (± 174.4)	2.5 (± 0.3)	2.9 (±0.1)	100.0 (± 0.0)	539.5 (± 25.4)

Nanomaterial	Wheat				Lettuce			
	Shoot length (cm) (n=3)	Root length (cm) (n=3)	Germination rate (%) (n=3)	Seedling vigour (cm %) (n=3)	Shoot length (cm) (n=3)	Root length (cm) (n=3)	Germination rate (%) (n=3)	Seedling vigour (cm %) (n=3)
$Co_{0.75}Fe_{2.25}O_4$	7.7 (± 1.3)	6.1 (± 1.1)	73.1 (± 11.2)	1009.0 (± 167.0)	2.2 (± 0.2)	2.4 (± 0.3)	97.6 (± 4.1)	452.4 (± 57.1)
Fe_2O_3	10.0 (± 4.8)	5.4 (± 2.0)	92.9 (± 7.1)	1416.9 (± 516.8)	2.2 (± 0.6)	2.1 (± 1.0)	85.7 (± 12.4)	379.5 (± 181.8)
Co_3O_4	6.8 (± 1.2)	4.2 (± 0.7)	81.0 (± 8.2)	885.4 (± 49.7)	2.7 (± 0.1)	2.9 (± 0.3)	95.2 (± 4.1)	534.5 (± 16.4)
CeO_2	6.8 (± 1.0)	6.4 (± 0.6)	92.9 (± 12.4)	1223.5 (± 144.0)	1.9 (± 0.4)	2.5 (± 0.7)	97.6 (± 4.1)	425.7 (± 108.7)
Zeolites								
BEA-12	5.5 (± 0.9)	6.3 (± 1.3)	92.9 (± 7.1)	1107.6 (± 263.6)	2.1 (± 0.1)	2.5 (± 0.1)	97.6 (± 4.1)	424.1 (± 14.8)
BEA-19	6.0 (± 0.6)	8.3 (± 1.7)	92.9 (± 7.1)	1338.1 (± 268.4)	1.8 (± 0.1)	2.2 (± 0.2)	81.0 (± 10.9)	336.6 (± 98.9)
MOR-10	6.0 (± 0.6)	6.8 (± 0.9)	95.2 (± 4.1)	1219.2 (± 184.0)	1.8 (± 0.1)	1.9 (± 0.2)	95.2 (± 4.1)	329.9 (± 78.0)
FER	5.4 (± 0.5)	4.8 (± 1.4)	88.1 (± 8.2)	892.8 (± 177.0)	2.0 (± 0.1)	2.2 (± 0.3)	88.1 (± 4.1)	418.8 (± 24.0)
NaX	6.2 (± 1.1)	8.0 (± 2.2)	90.5 (± 16.5)	1319.8 (± 501.3)	2.0 (± 0.2)	2.3 (± 0.5)	90.6 (± 4.3)	432.4 (± 61.2)
NaY	5.1 (± 0.7)	5.3 (± 1.5)	76.2 (± 8.2)	806.7 (± 233.2)	1.9 (± 0.2)	2.4 (± 0.2)	92.9 (± 12.4)	397.7 (± 49.6)
NaA	6.1 (± 0.2)	3.9 (± 1.0)	88.1 (± 4.1)	877.4 (± 107.9)	1.8 (± 0.3)	2.6 (± 0.4)	81.0 (± 8.2)	366.2 (± 131.9)
KX	6.2 (± 0.6)	6.9 (± 1.8)	100.0 (± 0.0)	1311.8 (± 229.4)	2.4 (± 0.1)	2.3 (± 0.4)	95.2 (± 8.2)	441.3 (± 64.3)
KY	7.1 (± 0.7)	8.9 (± 1.8)	95.2 (± 8.2)	1536.1 (± 338.5)	1.9 (± 0.1)	2.1 (± 0.4)	97.6 (± 4.1)	372.9 (± 67.8)
KA	6.3 (± 0.1)	7.9 (± 1.0)	100.0 (± 0.0)	1414.8 (± 96.0)	2.0 (± 0.0)	3.2 (± 0.3)	90.5 (± 4.1)	437.5 (± 20.0)

Nanomaterial	Wheat				Lettuce			
	Shoot length (cm) (n=3)	Root length (cm) (n=3)	Germination rate (%) (n=3)	Seedling vigour (cm %) (n=3)	Shoot length (cm) (n=3)	Root length (cm) (n=3)	Germination rate (%) (n=3)	Seedling vigour (cm %) (n=3)
MAP	6.6 (± 0.5)	8.3 (± 1.1)	92.9 (± 7.1)	1393.8 (± 195.3)	2.1 (± 0.3)	2.9 (± 0.2)	97.6 (± 4.1)	439.2 (± 29.8)
CW	6.4 (± 0.5)	5.3 (± 1.2)	85.7 (± 7.1)	1007.8 (± 220.9)	2.1 (± 0.1)	2.8 (± 0.2)	100.0 (± 0.0)	440.1 (± 4.2)
CVZA	7.0 (± 0.3)	6.7 (± 1.0)	97.6 (± 4.1)	1338.9 (± 142.8)	2.0 (± 0.2)	2.5 (± 0.3)	95.2 (± 4.1)	398.6 (± 22.0)
CVZB	6.3 (± 0.6)	7.4 (± 1.7)	90.5 (± 8.2)	1239.8 (± 222.8)	2.2 (± 0.0)	2.3 (± 0.5)	90.5 (± 4.1)	371.2 (± 77.8)
LTL	5.7 (± 0.8)	6.1 (± 1.1)	90.5 (± 16.5)	1083.5 (± 330.9)	2.1 (± 0.0)	2.3 (± 0.4)	97.6 (± 4.1)	409.1 (± 57.5)
BEA-150	6.4 (± 0.3)	7.9 (± 0.8)	90.5 (± 4.1)	1288.5 (± 98.9)	2.4 (± 0.1)	2.5 (± 0.1)	100.0 (± 0.0)	442.8 (± 47.3)
ZSM-5-40	6.7 (± 1.0)	7.1 (± 1.4)	95.2 (± 4.1)	1300.3 (± 176.4)	2.3 (± 0.1)	2.5 (± 0.2)	88.1 (± 8.2)	442.8 (± 24.4)
ZSM-5-25	6.1 (± 0.9)	8.1 (± 2.3)	85.7 (± 7.1)	1221.3 (± 327.6)	2.1 (± 0.1)	2.7 (± 0.2)	93.0 (± 0.3)	407.7 (± 33.7)
ZSM-5-15	6.6 (± 0.2)	7.9 (± 0.8)	92.9 (± 7.1)	1342.7 (± 168.8)	2.2 (± 0.2)	2.3 (± 0.2)	100.0 (± 0.0)	426.2 (± 18.6)
Metal organic frameworks								
AlFu	6.5 (± 1.6)	5.4 (± 1.5)	85.7 (± 7.1)	1026.3 (± 326.3)	1.3 (± 0.3)	1.6 (± 0.5)	85.7 (± 7.1)	246.7 (± 82.2)
CPO-27 (Ni)	5.8 (± 0.8)	4.4 (± 1.4)	92.9 (± 12.4)	952.4 (± 289.6)	0.2 (± 0.0)	0.0 (± 0.0)	59.5 (± 10.9)	12.5 (± 2.1)
Fe BTC	6.0 (± 1.2)	4.7 (± 1.2)	92.9 (± 7.1)	1003.6 (± 261.2)	1.4 (± 0.1)	1.1 (± 0.2)	85.7 (± 12.4)	214.5 (± 51.2)
HKUST-1	1.3 (± 0.6)	0.1 (± 0.1)	33.3 (± 10.9)	51.6 (± 39.0)	0.4 (± 0.0)	0.1 (± 0.0)	78.6 (± 7.1)	41.5 (± 1.3)

Nanomaterial	Wheat				Lettuce			
	Shoot length (cm) (n=3)	Root length (cm) (n=3)	Germination rate (%) (n=3)	Seedling vigour (cm %) (n=3)	Shoot length (cm) (n=3)	Root length (cm) (n=3)	Germination rate (%) (n=3)	Seedling vigour (cm %) (n=3)
MIL-100	4.4 (± 1.3)	5.1 (± 1.7)	78.6 (± 7.1)	758.3 (± 246.3)	1.4 (± 0.4)	1.5 (± 0.3)	85.7 (± 7.1)	248.1 (± 77.4)
UTSA-16 (Co)	6.7 (± 0.4)	6.5 (± 1.5)	92.9 (± 12.4)	1216.6 (± 76.9)	0.8 (± 0.2)	0.2 (± 0.0)	83.3 (± 10.9)	87.2 (± 5.4)
Nanopolymers								
$PQDMAEMA_{70}$-$P(MMA_{297}$-$MBA_3)$	6.4 (± 0.1)	7.3 (± 1.7)	97.6 (± 4.1)	1326.1 (± 142.9)	0.9 (± 0.1)	0.7 (± 0.2)	76.2 (± 4.1)	123.7 (± 21.8)
$PQDMAEMA_{70}$-$P(MMA_{198}$-$MBA_2)$	6.6 (± 0.3)	6.0 (± 2.2)	85.7 (± 7.1)	1094.7 (± 272.1)	0.7 (± 0.2)	0.6 (± 0.2)	78.6 (± 7.1)	97.0 (± 39.1)
$PQDMAEMA_{70}$-$P(MMA_{99}$-MBA_1	6.6 (± 0.7)	8.7 (± 1.7)	97.6 (± 4.1)	1492.6 (± 272.5)	0.9 (± 0.2)	0.8 (± 0.2)	92.9 (± 0.0)	164.7 (± 36.0)
$PDMAm_{70}$-$P(DAAm_{45}$-$MBA_5)$	6.7 (± 0.4)	8.3 (± 0.8)	92.9 (± 0.0)	1389.8 (± 40.2)	0.7 (± 0.1)	0.6 (± 0.2)	73.8 (± 4.1)	90.3 (± 7.7)
$PDMAm_{70}$-$P(DAAm_{90}$-$MBA_{10})$	7.1 (± 0.5)	7.0 (± 2.5)	90.5 (± 4.1)	1271.4 (± 272.3)	0.9 (± 0.3)	0.7 (± 0.3)	85.7 (± 7.1)	140.0 (± 58.4)
Biochar derivatives								
Beech biochar	6.6 (± 1.0)	5.0 (± 0.9)	92.9 (± 0.0)	1080.9 (± 163.9)	1.4 (± 0.4)	1.2 (± 0.4)	90.5 (± 4.1)	237.6 (± 58.9)
Hydroxyapatite-modified beech biochar	6.2 (± 0.7)	6.0 (± 0.9)	100.0 (± 0.0)	1214.0 (± 26.3)	1.4 (± 0.0)	1.0 (± 0.2)	81.0 (± 4.1)	198.1 (± 25.3)
Magnetite and hydroxyapatite dual functionalised beech biochar	7.1 (± 1.3)	6.5 (± 2.9)	92.9 (± 7.1)	1274.3 (± 483.5)	1.6 (± 0.1)	1.5 (± 0.2)	88.1 (± 8.2)	276.9 (± 48.4)
Magnetite-modified beech biochar	6.6 (± 1.1)	6.0 (± 0.8)	92.9 (± 0.0)	1169.1 (± 177.8)	0.4 (± 0.1)	0.1 (± 0.0)	69.0 (± 10.9)	38.2 (± 9.2)

Nanomaterial	Wheat				Lettuce			
	Shoot length (cm) (n=3)	Root length (cm) (n=3)	Germination rate (%) (n=3)	Seedling vigour (cm %) (n=3)	Shoot length (cm) (n=3)	Root length (cm) (n=3)	Germination rate (%) (n=3)	Seedling vigour (cm %) (n=3)
Magnetite-modified hydroxyapatite	6.2 (± 1.9)	6.0 (± 2.1)	88.1 (± 14.9)	1108.8 (± 518.9)	1.5 (± 0.2)	1.3 (± 0.4)	81.0 (± 14.9)	227.9 (± 79.7)

Table S3.3. Wheat seed biomass and seed exudate protein concentration and lettuce seed exudate protein concentration in response to nanomaterial exposure. If a nanomaterial was not studied for the plant species it is denoted with "-", while if the data produced was below the limit of detection it is denoted with "—". Data presented are mean values and standard deviation.

Nanomaterial	Wheat		Lettuce
	Fresh biomass (g) (n = 3)	Seed exudate protein concentration (µg mL^{-1}) (n = 3)	Seed exudate protein concentration (µg mL^{-1}) (n = 3)
BEA-19	1.84 (± 0.10)	355.5 (± 66.2)	39.6 (± 29.1)
BEA-150	-	-	51.1 (± 17.3)
KA	1.71 (± 0.17)	830.5 (± 5.8)	-
KY	1.88 (± 0.20)	593.7 (± 8.3)	-
MAP	1.56 (± 0.23)	737.2 (± 39.1)	-
CW	-	-	—
NaX	1.93 (± 0.12)	297.4 (± 3.88)	-
ZSM-5-15	1.37 (± 0.17)	831.0 (± 40.2)	24.5 (± 67.8)
$Ce_{0.75}Zr_{0.25}O_2$	-	-	—
$Co_{2.25}Fe_{0.75}O_4$	-	-	3.4 (± 26.8)
Fe_3O_4	1.41 (± 0.06)	1070.3 (± 62.6)	—
TiO_2	1.65 (± 0.11)	852.4 (± 9.55)	-
TiO_2 D540	1.44 (± 0.26)	1127.3 (± 38.4)	-
TiO_2 PVP	-	-	—

Table S3.4. Sophisticated structure details of zeolite nanomaterials used in seed priming experiments.

Zeolite	Si:Al ratio	Pore size (Å)	Extra-framework ion	Particle size as determined by SEM (µm)
BEA 12	12.5	6.8	NH_4^+	0.02
BEA 19	19.0	6.8	NH_4^+	0.1
MOR	10.0	6.7	NH_4^+	0.3
FER	10.0	5.0	Na^+	1
NaX	1.3	7.4	Na^+	2
NaY	2.6	7.4	Na^+	2
NaA	1.0	4.2	Na+	3
KX	1.3	7.4	0.5 Na^+, 0.5 K^+	2
KY	2.6	7.4	0.2 Na^+, 0.8 K^+	2
KA	1.0	4.2	0.5 Na^+, 0.5 K^+	3
MAP	1.0	3.3	Na^+	0.02
CLPT W	5.2	5.0	0.4 K^+, 0.1 Na^+, 0.4 Ca^{2+}, 0.1 Fe^{3+}	0.4
CLPT VZA	4.5	5.0	0.5 Na^+, 0.2 K^+, 0.25 Ca^{2+}, 0.1 Mg^{2+}	100
CLPT VZB	5.5	5.0	0.4 K^+, 0.3 Ca^{2+}, 0.2 Mg^{2+}, 0.1 Fe^{3+}	5
LTL	3.1	7.1	K^+	0.5

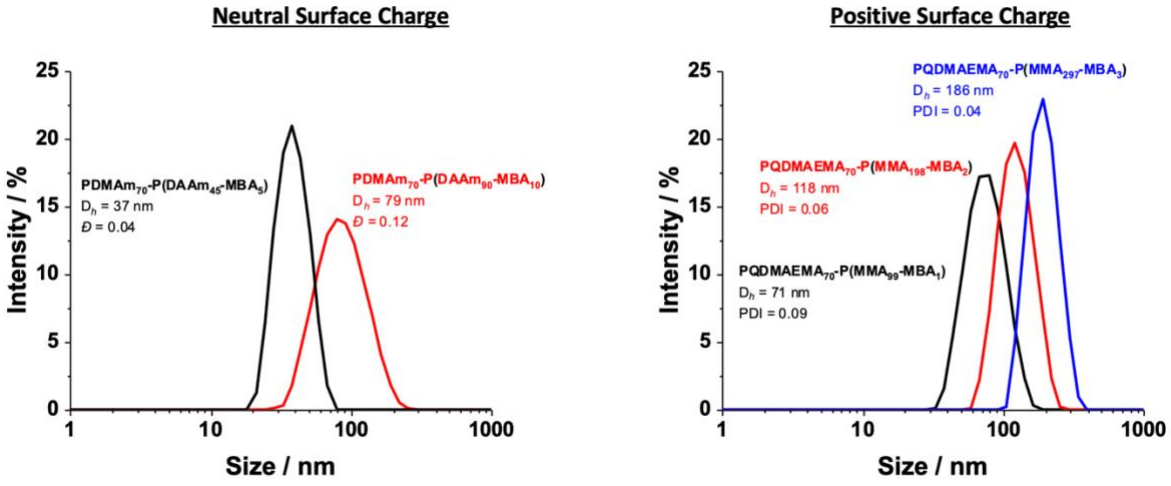


Figure S3.2. Size distribution of the neutral and positively charged nanopolymers used in seed priming experiments.

Supplementary Information for: Chapter 4 – Soil-based zeolite and metal oxide nanomaterial application alters reactive Nitrogen losses and lettuce (Lactuca sativa) growth

Jessica J. Chadwick,[1]* Aleksandar Radu,[2] Iuliia Mikulska,[3] Swaroop Chakraborty,[1] Peng Zhang,[1] Sami Ullah,[1] Iseult Lynch[1]*

[1] School of Geography, Earth and Environmental Sciences, University of Birmingham, Edgbaston, Birmingham B15 2TT, UK

[2] School of Chemistry, University of Lincoln, Lincoln LN6 7TS, UK

[3] Diamond Light Source Ltd, Harwell Science & Innovation Campus, Didcot, Oxfordshire OX11 0DE, UK

* Corresponding authors: Jessica J. Chadwick, jessicajchadwick@gmail.com; Iseult Lynch, i.lynch@bham.ac.uk

Methods

Additional methodological details for acid digestion of lettuce and soil samples

Detection of the uptake of nanomaterials was performed by inductively coupled plasma-optical emission spectroscopy (ICP-OES). For this, 0.5g of dry lettuce tissue or dried soil per treatment was weighed. Lettuce tissue was dissolved in 10 mL of nitric acid (HNO_3), and soils were dissolved with 9 mL HNO_3 and 3 mL hydrofluoric acid (HF). Lettuce digestions occurred at 210˚C for 15 minutes in a MARS 6 microwave digestion system in which iWave temperature sensors were floor-mounted to detect the solution temperature during digestion, while the soils were digested at 180˚C for 10 minutes using the same set-up. The respective digestion program details are available in Table S1 and S2.

Table S4.1. Program details for Mars 6 Microwave Digester heat-assisted digestion of lettuce tissue using 0.5g dry tissue with 10mL HNO3 as sourced from Mars 6 Microwave Acid Digestion Method Note Compendium.

Temperature (˚C)	210
Ramp (mm:ss)	15:00
Hold (mm:ss)	15:00
Pressure (psi)	800
Power (W)	1000

Table S4.2. Program details for Mars6 Microwave Digester heat-assisted digestion of soil using 0.5g dry soil with 9mL HNO3 and 3mL HF as based on US EPA 3052 via Mars 6 Microwave Acid Digestion Method Note Compendium.

Temperature (˚C)	180
Ramp (mm:ss)	05:30
Hold (mm:ss)	09:30
Pressure (psi)	800
Power (W)	1000

Results

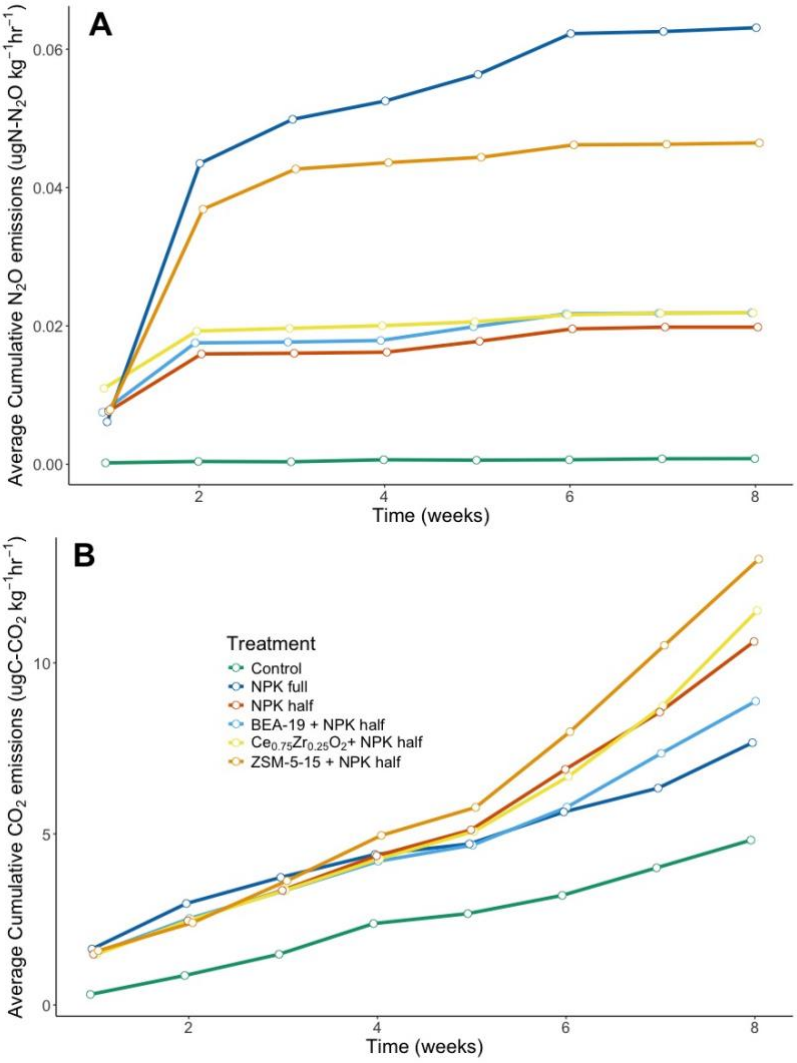


Figure S4.1. Cumulative emissions from soil of N_2O (A) and CO_2 (B) over the course of the 8-week growing period. The details of the treatments and their associated colours (for both panels A and B) are shown as the inset in panel B. NPK full is the standard application of nitrogen, phosphorus and potassium (180kg/ha N in the form of urea and 200kg/ha in the form of potassium phosphate monobasic), while NPK half is a half-dose of each (90kg/ha N and 100kg/ha P_2O_5 and K_2O). Control is no fertiliser at all, and no nanomaterials. The nanomaterial treatments are all with NPK half treatment. Nanomaterial treatments include BEA-19and ZSM-5-15 two nano-zeolites, and $Ce_{0.75}Zr_{0.25}O_2$, a nano-metal oxide.

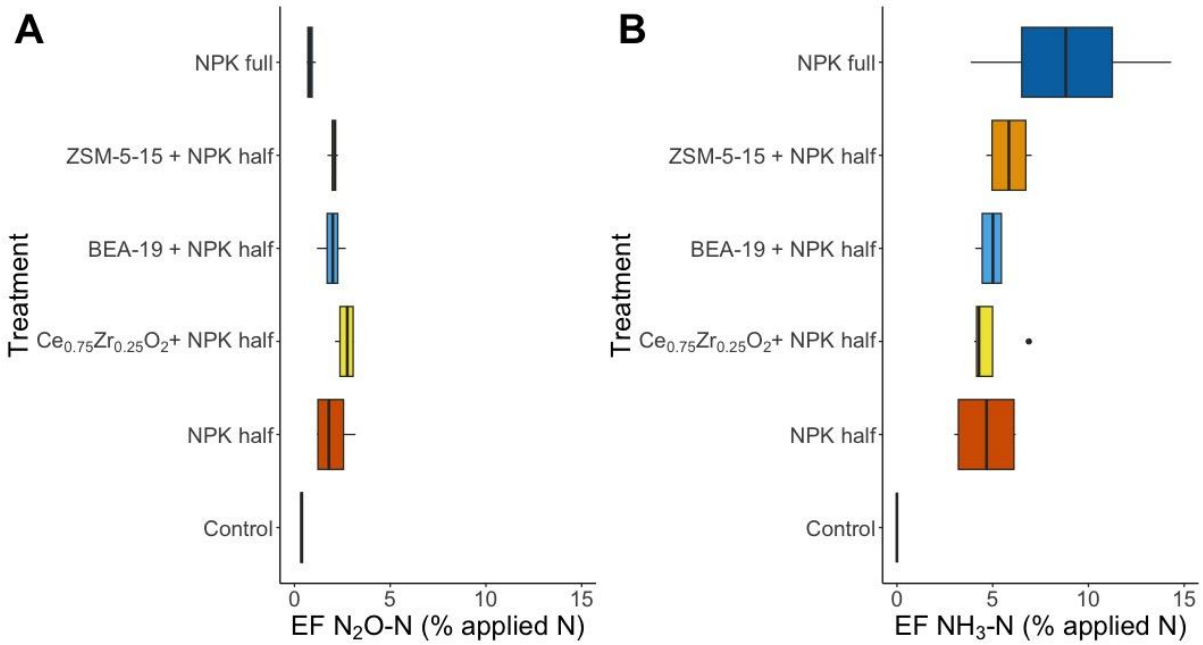


Figure S4.2. Emission factors of N_2O (A) and NH_3 (B) gas emissions as a proportion of the total N added to each treatment. NPK full is the standard application of nitrogen, phosphorus and potassium (180kg/ha N in the form of urea and 200kg/ha in the form of potassium phosphate monobasic), while NPK half is a half-dose of each (90kg/ha N and 100kg/ha P_2O_5 and K_2O). Control is no fertiliser at all, and no nanomaterials. The nanomaterial treatments are all with NPK half treatment. Nanomaterial treatments are BEA-19and ZSM-5-15 two nano-zeolites. $Ce_{0.75}Zr_{0.25}O_2$ is a nano-metal oxide.

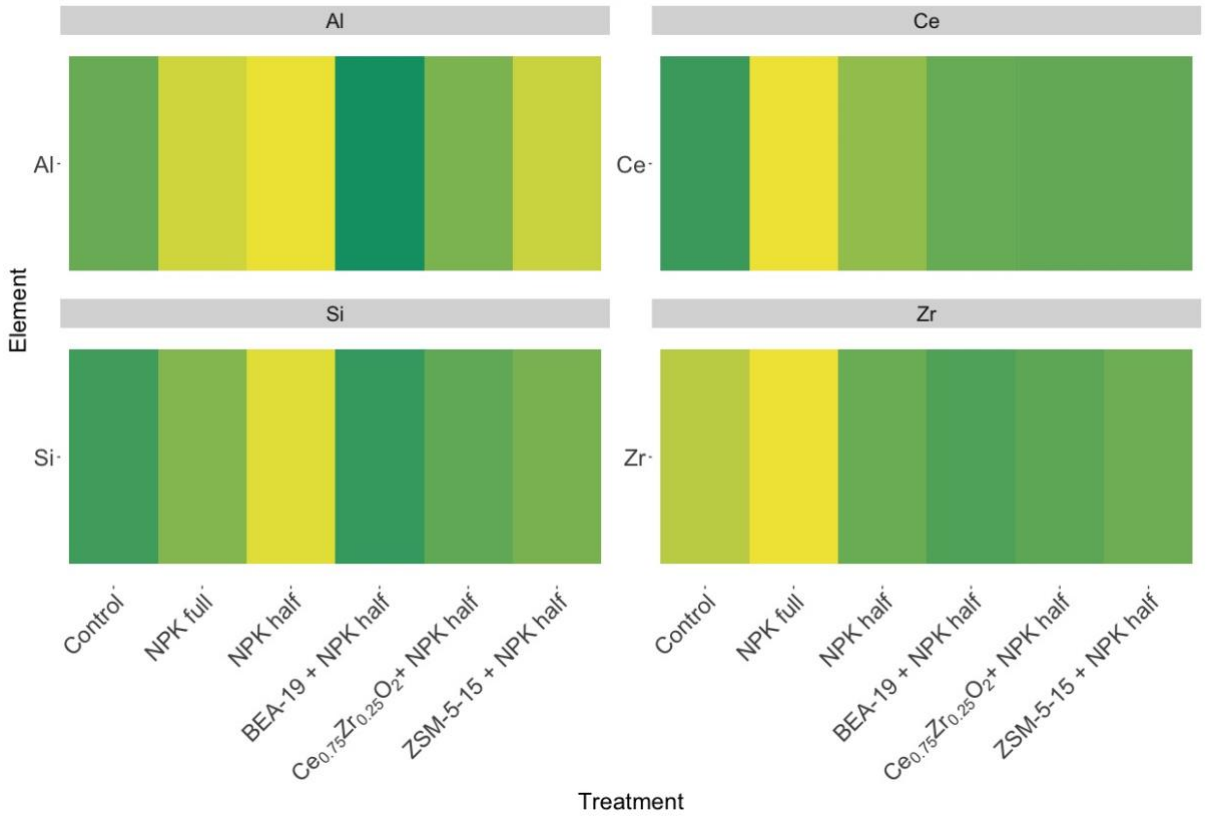


Figure S4.3. Relative concentration of elemental constituents of NMs used in $Ce_{0.75}Zr_{0.25}O_2$, BEA-19 and ZSM-5-15 treatments found in lettuce tissue compared across the six treatments. BEA-19 and ZSM-5-15 are zeolites containing Al and Si. NPK full is the standard application of nitrogen, phosphorus and potassium (180kg/ha N in the form of urea and 200kg/ha in the form of potassium phosphate monobasic), while NPK half is a half-dose of each (90kg/ha N and 100kg/ha P_2O_5 and K_2O). Control is no fertiliser at all, and no nanomaterials. The nanomaterial treatments are all with NPK half treatment.

Table S4.3. P-values of statistically significant differences in mineralised NO_3^- concentration of different treatments in relation to NPK full treated soil. NPK full is the standard application of nitrogen, phosphorus and potassium (180kg/ha N in the form of urea and 200kg/ha in the form of potassium phosphate monobasic), while NPK half is a half-dose of each (90kg/ha N and 100kg/ha P_2O_5 and K_2O). Control is no fertiliser at all, and no nanomaterials. The nanomaterial treatments are all with NPK half treatment.

	Control	NPK full	NPK half	BEA-19 + NPK half	$Ce_{0.75}Zr_{0.25}O_2$ + NPK half	ZSM-5-15 + NPK half
Mineralised NO_3^- (mg kg^{-1} dry soil) (n=4)	0.00021	-	0.0034	0.011	0.00064	0.00025

Table S4.4. P-values of statistically significant differences in mean CO_2 gaseous emissions of different treatments in relation to control soil and lettuce. NPK full is the standard application of nitrogen, phosphorus and potassium (180kg/ha N in the form of urea and 200kg/ha in the form of potassium phosphate monobasic), while NPK half is a half-dose of each (90kg/ha N and 100kg/ha P_2O_5 and K_2O). Control is no fertiliser at all, and no nanomaterials. The nanomaterial treatments are all with NPK half treatment.

	Control	NPK full	NPK half	BEA-19 + NPK half	$Ce_{0.75}Zr_{0.25}O_2$ + NPK half	ZSM-5-15 + NPK half
Mean CO_2 emissions (ug kg^{-1} h^{-1}) (n=4)	-	0.0785	<0.0001	0.0055	<0.0001	<0.0001

Table S4.5. P-values of statistically significant differences in leachate NO_3^- concentration of different treatments in relation to the control soil. NPK full is the standard application of nitrogen, phosphorus and potassium (180kg/ha N in the form of urea and 200kg/ha in the form of potassium phosphate monobasic), while NPK half is a half-dose of each (90kg/ha N and 100kg/ha P_2O_5 and K_2O). Control is no fertiliser at all, and no nanomaterials. The nanomaterial treatments are all with NPK half treatment.

	Control	NPK full	NPK half	BEA-19 + NPK half	$Ce_{0.75}Zr_{0.25}O_2$ + NPK half	ZSM-5-15 + NPK half
NO_3^- (mg L^{-1} leachate) (n=4)	-	0.044	0.00395	-	0.0056	0.0386

Table S4.6. Concentration of elemental nutrients across shoot lettuce tissue grown in the six different treatment soils. NPK full is the standard application of nitrogen, phosphorus and potassium (180kg/ha N in the form of urea and 200kg/ha in the form of potassium phosphate monobasic), while NPK half is a half-dose of each (90kg/ha N and 100kg/ha P_2O_5 and K_2O). Control is no fertiliser at all, and no nanomaterials. The nanomaterial treatments are all with NPK half treatment.

	Control (n=4)	NPK full (n=3)	NPK half (n=4)	BEA-19 + NPK half (n=4)	$Ce_{0.75}Zr_{0.25}O_2$ + NPK half (n=4)	ZSM-5-15 + NPK half (n=4)
Ca (mg/g)	0.15746843	0.18306005	0.18378503	0.15617002	0.16820275	0.15144748
Cu (mg/g)	0.03080826	0.02429536	0.02592205	0.02117193	0.02624364	0.02643565
Fe (mg/g)	0.02605645	0.00946766	0.01781764	0.01873396	0.02013273	0.01119552
Mn (mg/g)	0.00070856	0.00048091	0.00058748	0.00051019	0.00059444	0.00038113
Mg (mg/g)	0.03080826	0.02429536	0.02592205	0.02117193	0.03375122	0.02643565
Zn (mg/g)	0.00056602	0.00015337	0.00011078	0.00012825	0.0001721	0.00020532
P (mg/g)	0.02046859	0.03596641	0.02301406	0.0192665	0.02012262	0.02425014
K (mg/g)	0.44987047	0.49895419	0.37169321	0.30797222	0.27396367	0.297656
Ce (mg/g)	8.8761E-05	3.1517E-06	5.4653E-05	7.3909E-05	0.00016856	5.6479E-05
Zr (mg/g)	1.0457E-05	-	3.8643E-05	2.4673E-05	2.9459E-05	3.4717E-05
Si (mg/g)	0.01307812	0.01017922	0.00985731	0.00858166	0.00987787	0.01204843
Al (mg/g)	0.02370997	0.00900661	0.01746708	0.01797256	0.01906906	0.0108446
N (%)	3.55643	4.06831333	4.807775	4.807695	4.456745	5.2650925

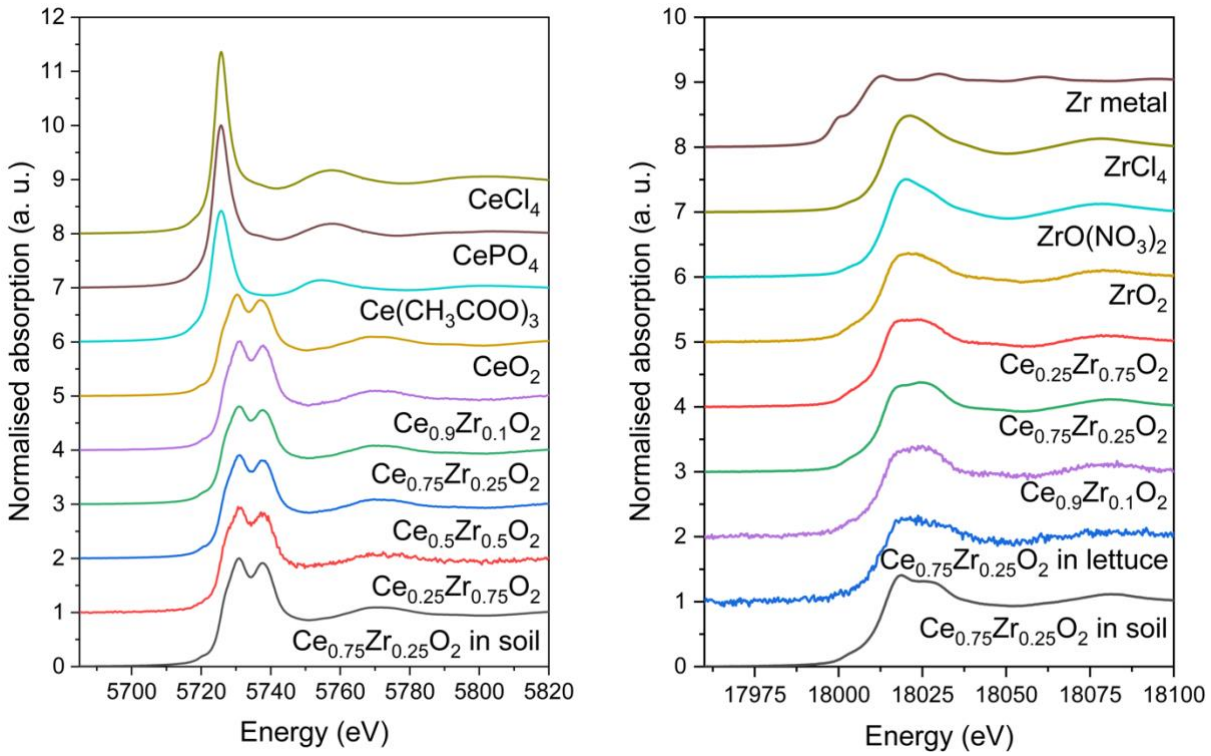


Figure S4.4. (A) Ce L3-edge XANES spectra measured on experimental soil samples with added $Ce_{0.75}Zr_{0.25}O_2$ NMs and NPK half and Ce-containing reference standards. (B) Zr K-edge XANES spectra measured on experimental soil sample with added $Ce_{0.75}Zr_{0.25}O_2$ NMs and NPK half and lettuce grown in soil and Zr-containing reference standards.

Linear combination fitting of Ce L3-edge XANES spectrum of $Ce_{0.75}Zr_{0.25}O_2$ treated soil sample and Zr K-edge XANES profile of $Ce_{0.75}Zr_{0.25}O_2$ grown lettuce tissue have been done in a range from -40 eV to 80 eV relative to the energy position of corresponding absorption edge. Results of LCF are presented in the Table S4.7.

Table S4.7. Results of Linear combination fitting of Ce L3-edge XANES spectrum of $Ce_{0.75}Zr_{0.25}O_2$ treated soil sample and Zr K-edge XANES profile of $Ce_{0.75}Zr_{0.25}O_2$ grown lettuce tissue. The quality of the fit is shown in Figure 4.4.

Sample	Absorption Edge	Standard	Weight %	R-factor
$Ce_{0.75}Zr_{0.25}O_2$ treated soil	Ce L3-edge	$Ce_{0.9}Zr_{0.1}O_2$	80.4 ± 0.8	0.0002283
		CeO_2	19.6 ± 0.8	
$Ce_{0.75}Zr_{0.25}O_2$ grown lettuce tissue	Zr K-edge	$Ce_{0.75}Zr_{0.25}O_2$	49.4 ± 9.1	0.0095713
		$ZrCl_4$	40.8 ± 7.8	
		Zr metal foil	9.8 ± 1	

Supplementary Information for: Chapter 5 – Greenhouse gas emissions from hydroponically grown lettuce under nano-metal oxide treatment using stable 15N isotope tracing and NM transformations in hydroponic media

J. J. Chadwick[1]*, Arnoud Witteveen[2], Iuliia Mikulska[3], Swaroop Chakraborty[1], Peng Zhang[1], Iseult Lynch[1]*, Sami Ullah[1]

[1] School of Geography, Earth and Environmental Sciences, University of Birmingham, Edgbaston, Birmingham B15 2TT, UK

[2] Saturn Bioponics,

[3] Diamond Light Source Diamond Light Source Ltd, Diamond House, Harwell Science & Innovation Campus, Didcot, Oxfordshire OX11 0DE, UK

[*] Corresponding authors: Jessica J. Chadwick jxc1326@student.bham.ac.uk; Iseult Lynch, i.lynch@bham.ac.uk

Methods

Table S5.3. Hydroponic medium constituent compounds and proportions for each master mix, Hydroponic A and Hydroponic B, which were both made to 1L. 40mL of each master mix of Hydroponic A and B was then added to each hydroponic medium tank of 12L.

Hydroponic A	g	Hydroponic B	g
Calcium nitrate	655	Potassium nitrate	400
Magnesium nitrate	225	Magnesium sulfate	180
Potassium nitrate	90	MKP	125
Ammonium nitrate	30	MAP	75
		Potassium sulfate	75
		Urea	75
		Ammonium sulfate	45
		Iron chelate EDDHA	16
		Manganese EDTA	9

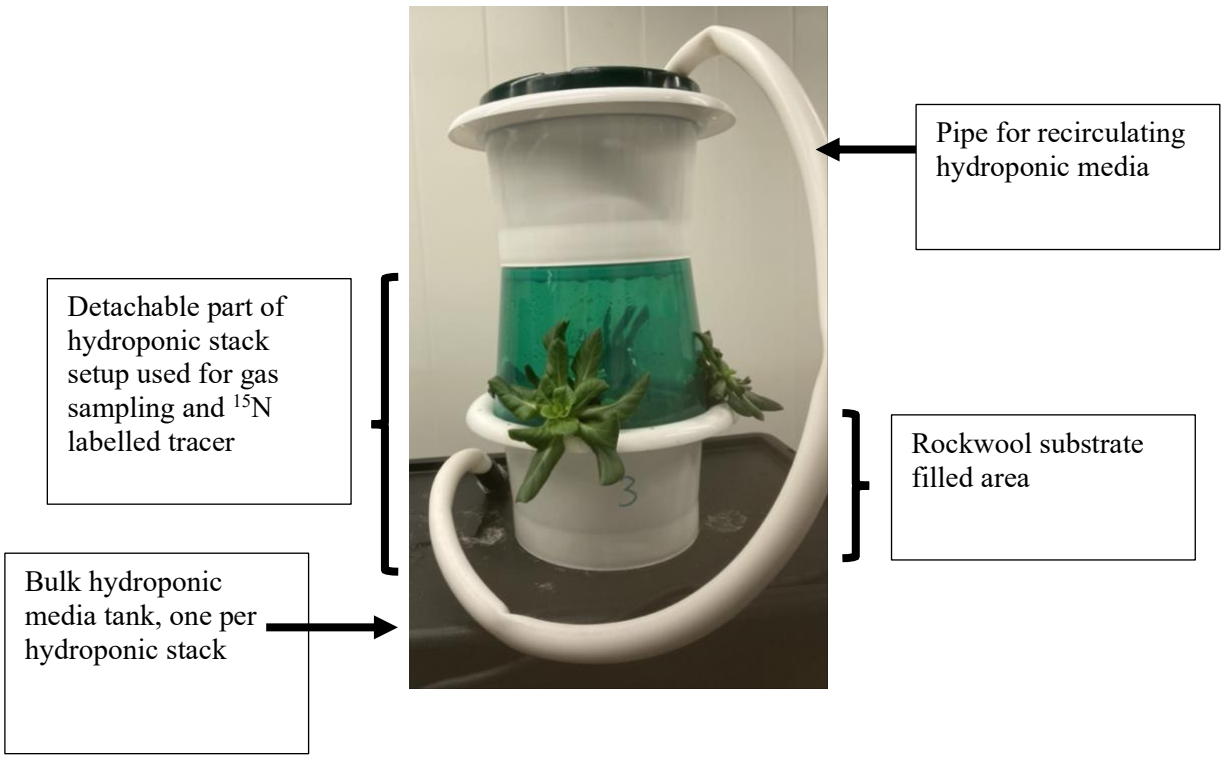


Figure S5.1. Hydroponic setup for lettuce growing and gas sampling including rockwool substrate for lettuce rootzone, storage tank for hydroponic media and pipe to allow recirculation of media through the vertical stack system.

Table S5.4. Program details for Mars 6 Microwave Digester heat-assisted digestion of lettuce tissue using 0.5g dry tissue with 10mL HNO3 as sourced from Mars 6 Microwave Acid Digestion Method Note Compendium.

Temperature (˚C)	210
Ramp (mm:ss)	15:00
Hold (mm:ss)	15:00
Pressure (psi)	800
Power (W)	1000

Results

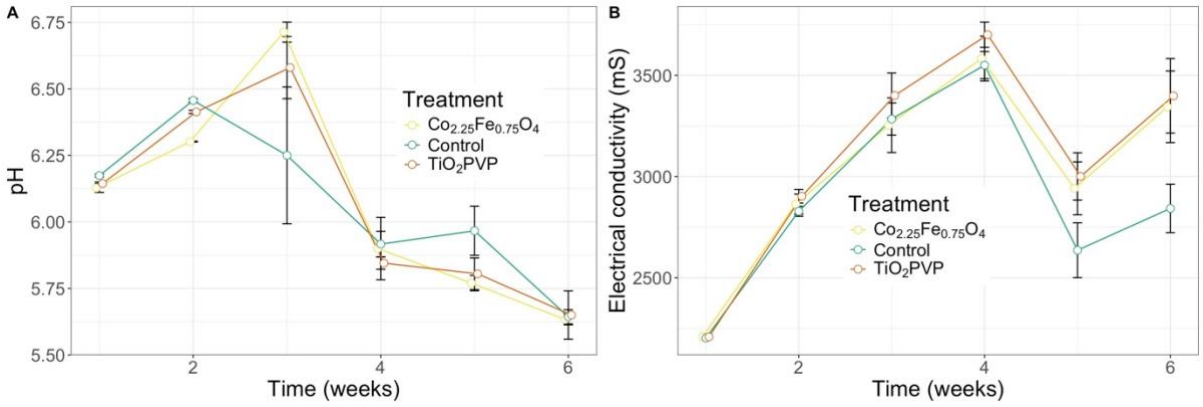


Figure S5.2. Changes in pH (A) and EC (B) over the six week experiment for each of the 12.5mg L^{-1} NM treatments in the nutrient media (TiO_2 PVP and $Co_{2.25}Fe_{0.75}O_4$) and the hydroponic media control. Error bars depict the standard error of the mean (SEM).

Table S5.5. Characterisation of nanomaterial constituent elements, macronutrients and micronutrients in hydroponic medium sourced from either the main hydroponic tank (bulk medium) or from the rockwool medium where the lettuce roots were located. Data presented are means ± standard deviation. Missing values were below the limit of detection.

	Control		$Co_{2.25}Fe_{0.75}O_4$		TiO_2 PVP	
Element	Bulk medium	Rockwool medium	Bulk medium	Rockwool medium	Bulk medium	Rockwool medium
Co (mg L^{-1}) (n=3)	58.9 (± 10.1)	0.03 (± 0.02)	2067 (± 1817)	0.12 (± 0.03)	59.3 (± 14.1)	0.04 (± 0.04)
Fe (mg L^{-1}) (n=3)	166321 (± 48845)	6.94 (± 1.29)	188,478 (± 49,420)	12.7 (± 3.7)	163940 (± 43807)	8.89 (± 2.54)
Ti (mg L^{-1}) (n=3)	3191 (± 1055)	-	3629 (± 1144)	-	3519 (± 1250)	-
P (mg L^{-1}) (n=3)	42876 (± 5055)	271 (± 44.4)	41580 (± 16932)	458 (± 107)	35740 (± 9170)	458 (± 55.5)
K (mg L^{-1}) (n=3)	208429 (± 24929)	1407 (± 237)	197274 (± 93876)	2844 (± 897)	177415 (± 43535)	2042 (± 655)
Ca (mg L^{-1}) (n=3)	531031 (± 166376)	1045 (± 179)	620943 (± 168218)	1533 (±218)	530733 (± 135408)	1359 (± 177)
S (mg L^{-1}) (n=3)	21506 (± 3972)	591 (± 111)	20410 (± 6202)	837 (± 88)	19855 (± 2783)	804 (± 93)
Mg (mg L^{-1}) (n=3)	196019 (± 60502)	302 (± 42)	215405 (± 59650)	538 (± 145)	192842 (± 49978)	378 (± 92)
Mn (mg L^{-1}) (n=3)	19766 (± 6483)	6.82 (± 1.03)	22135 (± 6531)	12.4 (± 3.3)	20033 (± 4942)	8.63 (± 2.19)
Zn (mg L^{-1}) (n=3)	-	1.75 (± 0.42)	-	3.89 (± 1.24)	-	1.91 (± 0.81)

	Control		$Co_{2.25}Fe_{0.75}O_4$		TiO_2 PVP	
Element	Bulk medium	Rockwool medium	Bulk medium	Rockwool medium	Bulk medium	Rockwool medium
Cu (mg L^{-1}) (n=3)	409 (± 120)	-	485 (± 135)	-	411 (± 121)	-
Mo (mg L^{-1}) (n=3)	-	0.16 (± 0.12)	-	0.11 (± 0.04)	-	0.13 (± 0.06)
Ni (mg L^{-1}) (n=3)	151 (± 27.6)	0.36 (± 0.04)	166 (± 37.6)	0.36 (± 0.05)	150 (± 36.4)	0.35 (± 0.05)
B (mg L^{-1}) (n=3)	167 (± 26.9)	-	277 (± 87.4)	-	211 (± 42.9)	-

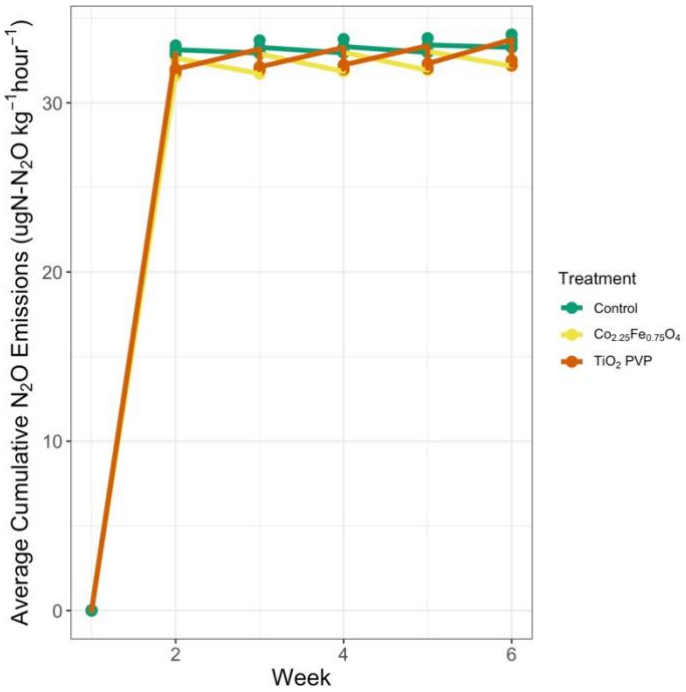


Figure S5.3. Cumulative N_2O emissions from hydroponic medium over the 6 week growth period compared between the three different treatments, control, $Co_{2.25}Fe_{0.75}O_4$ NM addition and TiO_2 PVP NM addition.

Table S5.4. Concentration of nanomaterial constituent elements, macronutrients and micronutrients in dried lettuce shoot tissue grown hydroponically with one of three treatments, $Co_{2.25}Fe_{0.75}O_4$ NM application, TiO_2 PVP or the control hydroponic medium alone. Translocation index was only calculated for NM constituent elements. Data presented are means ± standard deviation. Missing values were below the limit of detection.

Element	Control		$Co_{2.25}Fe_{0.75}O_4$		TiO_2 PVP	
	Concentration (mg kg^{-1}) (n=4)	Translocation index	Concentration (mg kg^{-1}) (n=4)	Translocation index	Concentration (mg kg^{-1}) (n=4)	Translocation index
Co	3.64 (± 3.56)	6.11 (± 2.35)	9.86 (± 7.09)	0.75 (± 0.47)	1.43 (± 1.99)	2.40 (± 1.03)
Fe	1274 (± 707)	0.76 (± 0.08)	1463 (± 631)	0.83 (± 0.32)	1436 (± 685)	0.96 (± 0.49)
Ti	29 (± 33)	0.75 (± 0.73)	49.2 (± 33.9)	1.52 (± 0.78)	46.1 (± 34.9)	1.59 (± 1.26)
P	69133 (± 32328)	-	57451 (± 26427)		59922 (± 13291)	
K	581373 (± 251746)	-	440813 (± 208451)		502065 (± 109745)	
Ca	80530 (± 39497)	-	74257 (± 36174)		70454 (± 17619)	
S	30572 (± 15674)	-	29054 (± 13413)		27233 (± 6645)	
Mg	29178 (± 14640)	-	27828 (± 13089)		26122 (± 6856)	
Mn	1542 (± 696)	-	1271 (± 583)		1205 (± 292)	
Zn	376 (± 203)	-	360 (± 177)		309 (± 94)	
Cu	-	-	16.5 (± 6.2)		-	
Mo	-	-	9.74 (± 12.9)		-	
Ni	-	-	9.8 (± 7.46)		-	
B	165 (± 103)	-	207 (± 96)		175 (± 48)	

Linear combination fitting of Co K-edge XANES spectrum and Fe K-edge XANES spectrum of $Co_{2.25}Fe_{0.75}O_4$ treated hydroponic medium have been done in a range from -40 eV to 80 eV relative to the energy position of corresponding absorption edge. Ti K-edge XANES spectrum linear combination fitting to TiO_2 PVP treated hydroponic medium was also done in the range from -40eV to 80eV. Results of LCF are presented in the Table S5.5.

Table S5.5. Results of Linear combination fitting of Ce L3-edge XANES spectrum of $Ce_{0.75}Zr_{0.25}O_2$ treated soil sample and Zr K-edge XANES profile of $Ce_{0.75}Zr_{0.25}O_2$ grown lettuce tissue. The quality of the fit is shown in Figure 5.5.

Sample	Absorption Edge	Standards	Weight	Reduced chi-squared	R-factor
$Co_{2.25}Fe_{0.75}O_4$ **treated hydroponic medium**	Co K-edge	$CoCO_3$	0.140	0.0018295	0.0073131
		Co_3O_4	0.860		
	Fe K-edge	$Co_{2.25}Fe_{0.75}O_4$	0.445	0.0004226	0.0014848
		Fe_2O_3	0.555		
TiO_2 **PVP treated hydroponic medium**	Ti K-edge	TiO_2 PVP	0.962	0.0018378	0.0077598
		TiO_2 rutile	0.038		

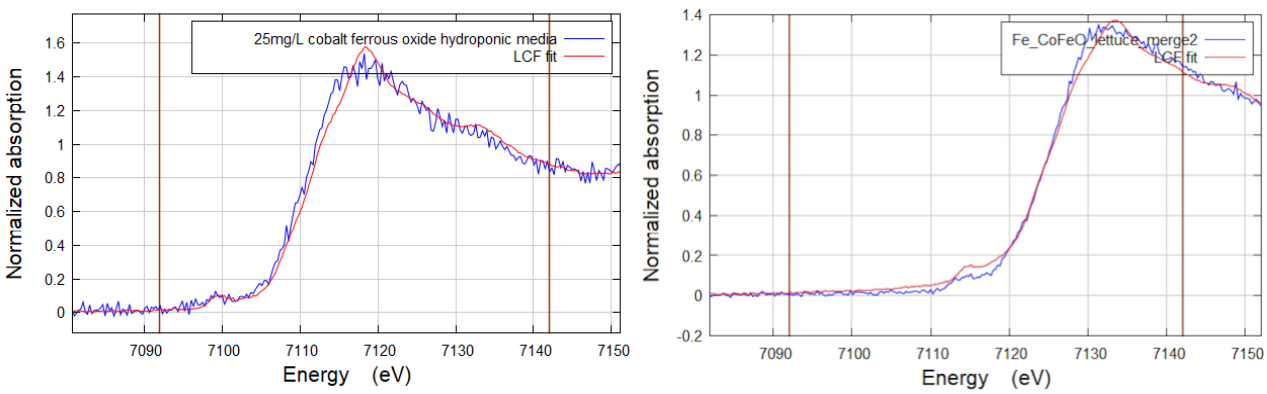


Figure S5.4. Linear combination fitting for Fe K-edge XANES spectrum of 25 mg L^{-1} $Co_{2.25}Fe_{0.75}O_4$ treated hydroponic media (left) and lettuce shoot tissue grown in the media (right). Media fit was performed using pristine $Co_{2.25}Fe_{0.75}O_4$, Fe_2O_3 and Fe_3O_4 reference standards.

Supplementary Information for: Chapter 6 – Nanomaterial interactions with nitrogen cycling soil microbial communities and ecotoxicological implications for *Eisenia fetida*

Jessica. J. Chadwick[1,2], Sami Ullah[1], Iseult Lynch[1], Cynthia Kallenbach[2]

[1] School of Geography, Earth and Environmental Sciences, University of Birmingham, B17, UK

[2] Department of Natural Resource Sciences, McGill University, Canada

Methods

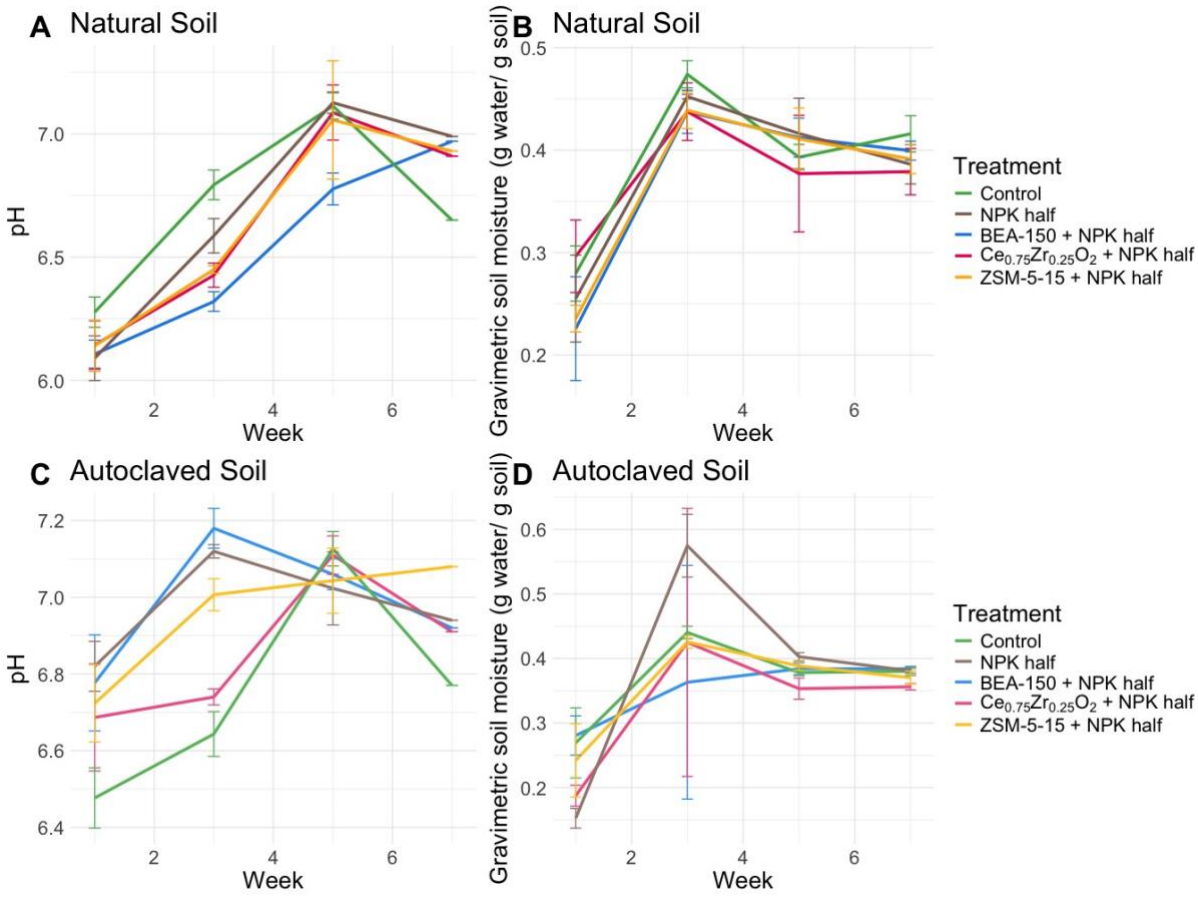


Figure S6.1. (A) Weekly changes in natural soil pH across the five different treatments. (B) Weekly changes in soil moisture for natural soil under different treatments. (C) and (D) are the same but for autoclaved soils.

Additional information for ICP-OES digestion of lettuce, soil and earthworm (*Eisenia fetida*) samples

Earthworm (*Eisenia fetida*) digestion analysed samples for Si and Al content, with standards for both made up in 2% HNO_3 and ranging from 0.05 to 10 ppm. Both lettuce and soil samples were analysed for Si, Al, Mn, Mg, K, P, Na, Ca, Cu, Zn, Fe and Ni, with lettuce samples also being analysed for Ce and Zr. All standards were made up in a single standard series ranging from 0.05 to 10ppm in a 2% HNO_3 background.

Table S6.1. Program details for Mars6 Microwave Digester heat-assisted digestion of dried lettuce, soil and earthworm (animal) tissue as based on the Mars 6 Microwave Acid Digestion Method Note Compendium. The digestion system utilised floor-mounted iWave temperature sensors to detect the solution temperature during digestion.

	Lettuce	Soil	*Eisenia fetida*
Sample mass (g)	0.5	0.5	0.5
Acid mix	10mL HNO_3	9mL HNO_3 and 3mL HF	10mL HNO_3
Temperature (˚C)	210	180	200
Ramp (mm:ss)	15:00	05:30	15:00
Hold (mm:ss)	15:00	09:30	15:00
Pressure (psi)	800	800	800
Power (W)	1000	1000	1000

Table S6.2. Extracellular enzyme assay experimental plate layout using MUB fluorescing substrate to control for background fluorescence of soil particles. This experimental layout was performed for NAG, LAP and TAP enzyme assays, with urease plates utilising the urease dependent conversion of urea to $NH_4^+$and being monitored using an absorbance assay for NH_4^+ detailed in 6.2.2ii.

Column #	**Contents**
1	buffer (control)
2	buffer + MUB (control)
3	buffer + substrate (control)
4	slurry + MUB (sample #1)
5	slurry + substrate (sample #1)
6	slurry + substrate (sample #1)
7	slurry + MUB (sample #2)
8	slurry + substrate (sample #2)
9	slurry + substrate (sample #2)
10	slurry + MUB (sample #3)
11	slurry + substrate (sample #3)
12	slurry + substrate (sample #3)

Results

Table S6.3. Statistical results of soil and leachate NO_3 and NH_4^+concentrations across time, amendment and soil type. Test results are relative to the control, autoclaved soil and week 1 results. Statistically significant results are indicated using '*'; p = 0.05 '*', p = 0.01 '**' and p = 0.001 '***'.

	Soil NO_3^-	Soil NH_4^+	Leachate NO_3^-	Leachate NH_4^+
	p-value	p-value	p-value	p-value
Intercept	< 0.001***	< 0.001***	< 0.001***	< 0.001***
Week 3	0.942	< 0.001***	< 0.001***	< 0.001***
Week 5	< 0.001***	< 0.001***	0.079	< 0.001***
Week 7	< 0.001***	< 0.001***	< 0.001***	< 0.001***
Natural soil	< 0.001***	< 0.001***	0.095	< 0.001***
BEA-150	0.058	< 0.001***	< 0.001***	< 0.001***
$Ce_{0.75}Zr_{0.25}O_2$	0.015*	< 0.001***	< 0.001***	0.184
NPK half	0.035*	< 0.001***	0.002**	0.010*
ZSM-5-15	0.018*	0.157	< 0.001***	< 0.001***
Week 3: Natural	0.7610	< 0.001***	0.022*	0.009
Week 5: Natural	< 0.001***	< 0.001***	0.067	< 0.001***
Week 7: Natural	< 0.001***	< 0.001***	0.998	< 0.001***
Week 3: BEA-150	0.673	< 0.001***	< 0.001***	< 0.001***
Week 5: BEA-150	< 0.001***	< 0.001***	< 0.001***	< 0.001***
Week 7: BEA-150	0.64	< 0.001***	< 0.001***	< 0.001***
Week 3: $Ce_{0.75}Zr_{0.25}O_2$	0.159	< 0.001***	< 0.001***	0.170
Week 5: $Ce_{0.75}Zr_{0.25}O_2$	< 0.001***	< 0.001***	< 0.001***	0.135
Week 7: $Ce_{0.75}Zr_{0.25}O_2$	0.022	< 0.001***	< 0.001***	0.124
Week 3: NPK half	0.089	< 0.001***	< 0.001***	0.009**
Week 5: NPK half	0.003**	< 0.001***	< 0.001***	0.009**
Week 7: NPK half	0.043*	< 0.001***	< 0.001***	0.008**
Week 3: ZSM-5-15	0.583	0.088	< 0.001***	0.046*
Week 5: ZSM-5-15	0.003**	0.010	< 0.001***	< 0.001***
Week 7: ZSM-5-15	0.020*	0.191	< 0.001***	< 0.001***
Natural: BEA-150	0.185	< 0.001***	0.013*	< 0.001***
Natural: $Ce_{0.75}Zr_{0.25}O_2$	0.043*	0.056	< 0.001***	0.004**
Natural: NPK half	0.051	0.029*	< 0.001***	< 0.001***
Natural: ZSM-5-15	0.037	< 0.001***	0.006**	< 0.001***
Week 3: BEA-150: Natural	0.976	< 0.001***	0.011*	0.182
Week 5: BEA-150: Natural	< 0.001***	< 0.001***	< 0.001***	< 0.001***
Week 7: BEA-150: Natural	0.112	< 0.001***	< 0.001***	< 0.001***
Week 3: $Ce_{0.75}Zr_{0.25}O_2$: Natural	0.200	0.150	0.003**	0.496
Week 5: $Ce_{0.75}Zr_{0.25}O_2$: Natural	< 0.001***	0.153	0.034*	< 0.001***
Week 7: $Ce_{0.75}Zr_{0.25}O_2$: Natural	0.051	0.088	< 0.001***	0.020*
Week 3: NPK half: Natural	0.058	0.015*	< 0.001***	< 0.001***
Week 5: NPK half: Natural	0.426	0.016*	0.368	< 0.001***
Week 7: NPK half: Natural	0.038*	0.023*	0.002**	< 0.001***
Week 3: ZSM-5-15: Natural	0.835	0.003**	0.014	0.004**
Week 5: ZSM-5-15: Natural	0.193	< 0.001***	< 0.001***	< 0.001***
Week 7: ZSM-5-15: Natural	0.025*	< 0.001***	< 0.001***	< 0.001***

Table S6.4. Concentration of $NH_4^+$and NO_3- ions in soil and leachate over the course of the lettuce growth period for the two soil conditions, natural and autoclaved, comparing between the five treatments. Data displayed are means and standard deviation. Missing data were below the limit of detection.

	Week	Control		$Ce_{0.75}Zr_{0.25}O_2$		NPK half		BEA-150		ZSM-5-15	
		Natural	Autoclaved	Natural	Autoclaved	Natural	Autoclaved	Natural	Autoclaved	Natural	Autoclaved
Soil											
NH_4^+ (mg kg^{-1} dry soil) (n=3)	1	1.77 (±0.21)	9.32 (±2.34)	3.50 (±0.82)	13.66 (±1.49)	9.94 (±3.53)	12.89 (±1.39)	4.37 (±0.93)	5.88 (±0.24)	2.41 (±0.93)	4.91 (±0.75)
	3	0.71 (±0.08)	2.60 (±0.12)	0.64 (±0.18)	3.17 (±0.05)	0.69 (±0.10)	3.16 (±0.53)	0.65 (±0.11)	2.55 (±0.63)	0.58 (±0.10)	1.73 (±1.51)
	5	0.60 (±0.04	1.38 (±0.47)	0.69 (±0.09)	2.10 (±0.08)	0.63 (±0.13)	2.02 (±0.78	0.66 (±0.08)	1.94 (±0.60)	0.49 (±0.15)	1.61 (±0.13)
	7	0.82 (±0.12)	0.93 (±0.07)	0.86 (±0.06)	1.23 (±0.30)	0.84 (±0.2)	1.16 (±0.37)	0.81 (±0.07)	0.90 (±0.18)	0.86 (±0.12)	1.04 (±0.47)
NO_3^- (mg kg^{-1} dry soil) (n=3)	1	6.58 (±2.30)	0.31 (±0.34)	9.39 (±0.87)	0.66 (±0.69)	8.91 (±0.44)	0.46 (±0.15)	8.75 (±0.31)	0.76 (±1.25)	9.16 (±0.31)	0.57 (±0.27)
	3	6.26 (±9.22)	-	16.0 (±4.23)	-	19.8 (±10.26)	-	10.5 (±4.25)	1.29 (±0.70)	11.31 (±0.70)	2.29 (±0.64)
	5	-	-	20.54 (±9.06)	-	9.47 (±7.48)	3.34 (±8.21)	21.91 (±8.83)	4.16 (±3.11)	8.80 (±6.78)	1.93 (±3.29)
	7	0.07 (±0.03)	-	0.23 (±0.04)	0.06 (±0.03)	0.17 (±0.03)	0.26 (±0.31)	0.12 (±0.02)	0.42 (±0.44)	0.10 (±0.02)	0.22 (±0.30)

	Week	Control		$Ce_{0.75}Zr_{0.25}O_2$		NPK half		BEA-150		ZSM-5-15	
		Natural	Autoclaved	Natural	Autoclaved	Natural	Autoclaved	Natural	Autoclaved	Natural	Autoclaved
Leachate											
NH_4^+ (mg kg^{-1} dry soil) (n=3)	1	0.24 (±0.02)	4.88 (±0.18)	0.35 (±0.19)	3.65 (±0.95)	1.39 (±0.95)	3.33 (±0.24)	0.95 (±0.39)	3.36 (±0.51)	0.68 (±0.26)	3.84 (±0.1)
	3	0.07 (±0.03)	6.54 (±1.46)	0.07 (±0.02)	6.08 (±2.15)	0.06 (±0.04)	8.80 (±1.76)	0.07 (±0.03)	6.21 (±2.55)	0.23 (±0.15)	9.44 (±2.73)
	5	0.04 (±0.01)	0.11 (±0.04)	0.03 (±0.01)	0.58 (±0.42)	0.04 (±0.01)	0.22 (±0.12)	0.02 (±0.02)	0.09 (±0.04)	0.04 (±0.01)	0.18 (±0.05)
	7	0.07 (±0.1)	0.36 (±0.41)	0.02 (±0.09)	0.14 (±0.07)	0.03 (±0.09)	0.14 (±0.07)	0.08 (±0.05)	0.11 (±0.1)	0.04 (±0.09)	0.03 (±0.1)
NO_3^- (mg kg^{-1} dry soil) (n=3)	1	4.76 (±2.06)	6.44 (±0.56)	-	8.85 (±2.07)	0.86 (±1.75)	9.73 (±2.37)	-	4.77 (±1.66)	0.05 (±0.08)	5.76 (±2.29)
	3	47.75 (±23.57)	22.31 (±8.57)	-	19.83 (±16.2)	-	29.03 (±13.45)	-	3.72 (±2.06)	-	3.46 (±4.73)
	5	2.32 (±2.11)	1.14 (±1.38)	54.53 (±12.89)	46.73 (±3.29)	36.75 (±21.86)	33.15 (±4.14)	59.58 (±5.28)	4.40 (±3.93)	41.54 (± 19.63)	2.71 (±2.76)
	7	0.34 (±0.23)	2.02 (±1.27)	1.21 (±0.72)	3.74 (±0.43)	1.03 (±0.4)	4.24 (±0.81)	1.21 (±0.18)	0.51 (±0.44)	1.38 (±0.77)	0.47 (±0.1)

Table S6.5. Statistical results of extracellular enzyme activity statistical testing relative to the control, autoclaved soil and week 1 results. Statistically significant results are indicated using '*'; p = 0.05 '*', p = 0.01 '**' and p = 0.001 '***'.

	LAP	TAP	NAG	Urease
	p-value	p-value	p-value	p-value
Intercept	< 0.001***	0.163	0.044*	0.827
Week 3	< 0.001***	0.915	0.009**	0.386
Week 5	0.062	0.872	0.016*	0.070
Week 7	0.831	0.370	0.032*	0.848
Natural soil	0.468	0.622	0.535	0.165
BEA-150	< 0.001***	0.617	0.931	0.720
$Ce_{0.75}Zr_{0.25}O_2$	0.949	0.954	0.690	0.223
NPK half	0.449	0.851	0.620	0.189
ZSM-5-15	0.259	0.001**	0.554	0.490
Week 3: Natural	< 0.001***	0.138	0.142	0.441
Week 5: Natural	0.055	0.16	0.505	< 0.001***
Week 7: Natural	0.013*	0.008**	0.911	0.913
Week 3: BEA-150	< 0.001***	0.161	0.122	0.074
Week 5: BEA-150	< 0.001***	0.069	0.984	< 0.001***
Week 7: BEA-150	< 0.001***	0.313	0.601	0.278
Week 3: $Ce_{0.75}Zr_{0.25}O_2$	0.464	0.760	0.144	0.166
Week 5: $Ce_{0.75}Zr_{0.25}O_2$	0.597	0.752	0.004**	0.054
Week 7: $Ce_{0.75}Zr_{0.25}O_2$	0.041*	0.567	< 0.001***	0.222
Week 3: NPK half	0.006**	0.718	0.017*	0.008**
Week 5: NPK half	0.081	0.871	< 0.001***	0.037*
Week 7: NPK half	0.909	0.734	< 0.001***	0.158
Week 3: ZSM-5-15	0.470	0.080	0.037*	0.325
Week 5: ZSM-5-15	0.676	0.067	< 0.001***	0.039*
Week 7: ZSM-5-15	0.688	0.047*	< 0.001***	0.850
Natural: BEA-150	0.537	0.851	0.950	0.166

	LAP	TAP	NAG	Urease
	p-value	p-value	p-value	p-value
Natural: $Ce_{0.75}Zr_{0.25}O_2$	0.117	0.903	0.705	0.497
Natural: NPK half	0.691	0.737	0.711	0.459
Natural: ZSM-5-15	0.027*	0.13	0.675	0.115
Week 3: BEA-150: Natural	0.001**	0.313	0.349	0.740
Week 5: BEA-150: Natural	0.183	0.593	0.508	< 0.001***
Week 7: BEA-150: Natural	0.214	0.190	0.524	0.683
Week 3: $Ce_{0.75}Zr_{0.25}O_2$: Natural	0.893	0.473	0.056	0.833
Week 5: $Ce_{0.75}Zr_{0.25}O_2$: Natural	0.670	0.801	< 0.001***	0.081
Week 7: $Ce_{0.75}Zr_{0.25}O_2$: Natural	0.007**	0.701	< 0.001***	0.590
Week 3: NPK half: Natural	0.011*	0.609	0.043*	0.351
Week 5: NPK half: Natural	0.653	0.778	< 0.001***	0.228
Week 7: NPK half: Natural	0.775	0.795	< 0.001***	0.740
Week 3: ZSM-5-15: Natural	0.164	0.323	0.037*	0.493
Week 5: ZSM-5-15: Natural	0.180	0.414	< 0.001***	0.078
Week 7: ZSM-5-15: Natural	0.092	0.172	< 0.001***	0.309

Table S6.6. Lettuce concentrations of nanomaterial constituent elements, macro- and micronutrients. Data presented are means and standard deviation. Values that were below the limit of detection are denoted with '-'.

Element	Compartment	Control		$Ce_{0.75}Zr_{0.25}O_2$		NPK half		BEA-150		ZSM-5-15	
		Natural	Autoclaved	Natural	Autoclaved	Natural	Autoclaved	Natural	Autoclaved	Natural	Autoclaved
Ce (mg kg^{-1})	Lettuce (n = 3)	0.00041 (± 0.00056)	0.00006 (± 0.00002)	0.00004 (± 0.00012)	0.00012 (± 0.00015)	0.00008 (± 0.00001)	0.00008 (± 0.00005)	0.00013 (± 0.00001)	0.00026 (± 0.00028)	-	0.00006 (± 0.0002)
Zr (mg kg^{-1})	Lettuce (n = 3)	0.00031 (± 0.00024)	0.00002 (± 0.00001)	0.00009 (± 0.00005)	-	0.00005 (± 0.00001)	0.00002 (± 0.00003)	0.00003 (± 0.00001)	0.00008 (± 0.00009)	0.0004 (± 0.00001)	0.00002 (± 0.00001)

Element	Compartment	Control		$Ce_{0.75}Zr_{0.25}O_2$		NPK half		BEA-150		ZSM-5-15	
		Natural	Autoclaved	Natural	Autoclaved	Natural	Autoclaved	Natural	Autoclaved	Natural	Autoclaved
Si (mg kg^{-1})	Lettuce (n = 3)	0.011 (± 0.0045)	0.012 (± 0.0005)	0.0075 (± 0.0023)	0.008 (± 0.0003)	0.0085 (± 0.0004)	0.01 (± 0.001)	0.0083 (± 0.0005)	0.01 (± 0.0021)	0.008 (± 0.0009)	0.008 (± 0.0009)
Al (mg kg^{-1})	Lettuce (n = 3)	0.27 (± 0.28)	0.0072 (± 0.0037)	0.0088 (± 0.0059)	0.0072 (± 0.0037)	0.0069 (± 0.0035)	0.0052 (± 0.0039)	0.0085 (± 0.004)	0.12 (± 0.19)	0.0058 (± 0.0021)	0.007 (± 0.0004)
Mn (mg kg^{-1})	Lettuce (n = 3)	0.0097 (± 0.006)	0.026 (± 0.0086)	0.0045 (± 0.001)	0.026 (± 0.0086)	0.0036 (± 0.0013)	0.03 (± 0.007)	0.005 (± 0.001)	0.051 (± 0.031)	0.0043 (± 0.0012)	0.005 (± 0.005)
Mg (mg kg^{-1})	Lettuce (n = 3)	1.09 (± 0.29)	0.52 (± 0.084)	0.92 (± 0.29)	0.91 (± 0.1)	0.65 (± 0.19)	0.7 (± 0.12)	0.92 (± 0.24)	0.86 (± 0.37)	0.88 (± 0.17)	0.036 (± 0.018)
Na (mg kg^{-1})	Lettuce (n = 3)	0.56 (± 0.04)	0.51 (± 0.20)	0.73 (± 0.40)	0.91 (± 0.09)	0.39 (± 0.088)	0.64 (± 0.25)	0.52 (± 0.19)	0.67 (± 0.28)	0.60 (± 0.25)	0.905 (± 0.384)
Fe (mg kg^{-1})	Lettuce (n = 3)	0.27 (± 0.27)	0.011 (± 0.0043)	0.016 (± 0.0047)	0.014 (± 0.002)	0.014 (± 0.005)	0.015 (± 0.006)	0.017 (± 0.005)	0.133 (± 0.208)	0.014 (± 0.003)	0.017 (± 0.014)
P (mg kg^{-1})	Lettuce (n = 3)	0.71 (± 0.09)	0.647 (± 0.260)	0.47 (± 0.11)	0.686 (± 0.360)	0.48 (± 0.09)	0.794 9± 0.129)	0.57 (± 0.35)	0.85 (± 0.18)	0.73 (± 0.36)	1.28 (± 0.83)
Ni (mg kg^{-1})	Lettuce (n = 3)	0.00026 (± 0.0003)	-	-	-	-	-	-	0.00005 (± 0.0003)	-	-
K (mg kg^{-1})	Lettuce (n = 3)	12.4 (± 0.68)	6.56 (± 1.01)	12.2 (± 4.12)	8.80 (± 1.93)	7.74 (± 2.79)	9.04 (± 1.19)	11.6 (± 4.39)	9.77 (± 0.70)	12.4 (± 4.34)	10.8 (± 1.80)
Zn (mg kg^{-1})	Lettuce (n = 3)	0.0071 (± 0.0037)	0.0039 (± 0.0004)	0.0032 (± 0.0002)	0.006 (± 0.002)	0.005 (± 0.001)	0.007 (± 0.002)	0.004 (± 0.001)	0.007 (± 0.002)	0.0043 (± 0.0011)	0.008 (± 0.004)
Ca (mg kg^{-1})	Lettuce (n = 3)	5.85 (± 1.18)	2.59 (± 0.60)	4.22 (± 0.79)	3.86 (± 0.35)	2.67 (± 1.1)	2.86 (± 0.56)	3.83 (± 1.26)	4.44 (± 3.04)	4.59 (± 1.19)	4.10 (± 2.25)
Cu (mg kg^{-1})	Lettuce (n = 3)	0.0031 (± 0.002)	0.0008 (± 0.0005)	0.0011 (± 0.0009)	0.0008 (± 0.0003)	0.00075 (± 0.00036)	0.0007 (± 0.0004)	0.00078 (± 0.00042)	0.001 (± 0.0009)	0.00065 (± 0.00035)	0.0007 (± 0.0005)

Supplementary Information for: Chapter 7 – Urea-Doped Amorphous Calcium Phosphate Application during Lettuce Growth Improves N-Use Efficiency Compared to Conventional Fertilisation

Jessica Chadwick[1,2], Peng Zhang[1], Iseult Lynch[1], Sami Ullah[1], Ryan Mushinski[2]

[1] School of Geography, Earth and Environmental Sciences, University of Birmingham, Edgbaston, Birmingham B15 2TT, UK

[2]School of Life Sciences, University of Warwick, Warwick, Coventry, CV4 7AL, UK

[*] Corresponding authors: Jessica J. Chadwick, jxc1326@student.bham.ac.uk; Ryan Mushinski, Ryan.Mushinski@warwick.ac.uk

Table S7.1. List of qPCR primers identified as functional genes for different steps of the Nitrogen (N) cycle.

Gene name	Forward primer	Reverse primer	Amplified	Source
Bacterial AmoA	GACTGGGAYTTCTGGMTKGAYTGGAA	TGYGACCACCAGTARAAWCCCCAG	+	Keeley *et al.*, 2020
Archaeal AmoA	GCMTTCAARTATCCRAGRCCRACRYTGCCW	TACMGATGGATGGCCGCNTGGWSMAAG	-	Keeley *et al.*, 2020
COMAMMOX AmoA	GGRACYTTYCAYATGCACACVGC	ACCACCAMGAVGTRTARACSGCAA	-	Keeley *et al.*, 2020
Periplasmic NxrB	GTGGAACAAYGTGGARACSAAGCC	SACRAASCGCCAYTCYTGGTC	+	Keeley *et al.*, 2020
Clade I NosZ	GAVGAYSTSACSCAYGGYTT	TGSADBGCVKRRCAGAA	-	Keeley *et al.*, 2020
Clade II NosZ	CGTTGCAYACNSARTTYGA	CKRTYCTTNGYNAKYTTRTT	-	Keeley *et al.*, 2020
Clade I NirS	GGNTAYGCNGTNCAYAT	CCNGTYTCYTTNACRTTNAC	-	Michotey *et al.*, 2000
Clade I NirK	TTYGTSTAYCACTGCGCVCC	GCYTCGATCAGRTTRTGGTT	+	Chen *et al.*, 2010
qNorB	GGNCAYCARGGNTAYGA	ACCCANAGRTGNACNACCCACCA	+	Braker and Tiedje, 2003
cNorB	GACAAGNNNTACTGGTGGT	TGNCCRTGNGCNGCNGT	-	Braker and Tiedje, 2003
Bacterial 16S rRNA	GTGCCAGCMGCCGCGGTAA	GGACTACHVGGGTWTCTAAT	+	Caporaso et al., 2012

Table S7.2. List of gBlock sequences for absolute quantification of N-cycling genes in soil microbes.

Gene	Primer sequences (F&R)	Primer sequence sites	Amplicon length	Source	Quantitative PCR thermal settings
Bacterial amoA (Betaproteobacteria)	F: GACTGGGAYTTCTGGMTKGAYTGGAA R: TGYGACCACCAGTARAAWCCCCAG	154-179 330-353	199	Keeley *et al.*, 2020	1) 3 minutes 98˚C 2) 40 cycles of: • 15s at 98˚C • 60s at 55˚C • 90s at 72°C 3) 72˚C for 10 minutes
Bacterial 16S rRNA	F: GTGCCAGCMGCCGCGGTAA R: GGACTACHVGGGTWTCTAAT	515F 806R	390	Caporaso et al., 2012	1) 94°C for 3 minutes 2) 40 cycles of: • 45s at 94°C f • 60s at 50°C • 90s at 72°C 3) 72˚C for 10 minutes
Periplasmic nxrB	F: GTGGAACAAYGTGGARACSAAGCC R: SACRAASCGCCAYTCYTGGTC	181-200 391-411	230	Keeley *et al.*, 2020	1) 3 minutes 98˚C 2) 40 cycles of: • 15s at 98˚C • 60s at 55˚C • 90s at 72°C 3) 72˚C for 10 minutes
nirK clade I	F: TTYGTSTAYCACTGCGCVCC R: GCYTCGATCAGRTTRTGGTT	502-521 1021-1040	538	Chen *et al.*, 2010	1) 3 minutes 98˚C 2) 40 cycles of: • 15s at 98˚C • 60s at 55˚C • 90s at 72°C 3) 72˚C for 10 minutes
qnorB	F: GGNCAYCARGGNTAYGA R: ACCCANAGRTGNACNACCCACCA	1204-1220 1444-1466	262	Braker and Tiedje, 2003	1) 15 minutes 95˚C 2) 40 cycles of: • 45s at 95˚C • 60s at 50˚C • 90s at 60˚C 3) 60s at 95˚C, 30s at 50˚C, 30s at 95˚C

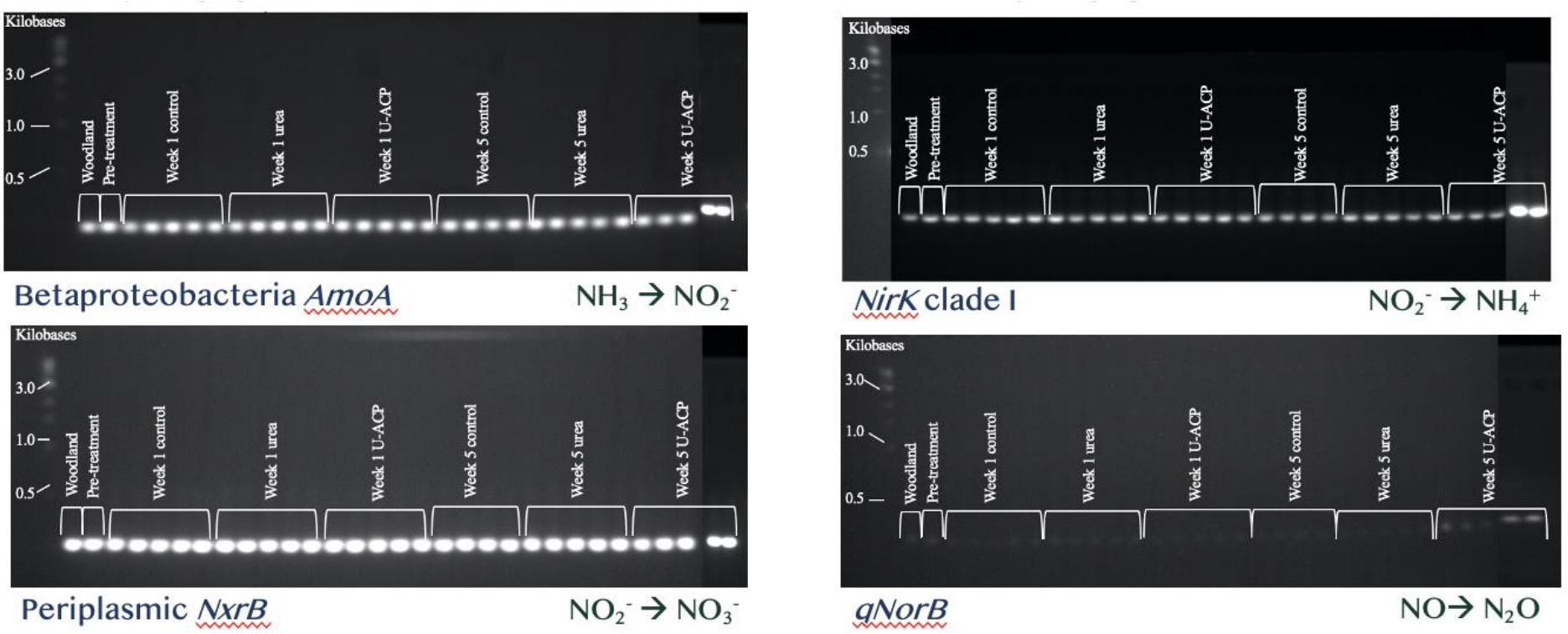


Figure S7.1. Labelled gel images of PCR products generated from (A) Betaproteobacteria AmoA gene primers; (B) periplasmic NxrB gene primers; (C) NirK clade I gene primers; and (D) qNorB gene primers, and four different soil DNA sources. Woodland soil DNA, pre-treatment experimental soil, treated experimental soil, and experimental soil after five weeks of the experiment were all used.

Hydroponics and Alternative Forms of Agriculture: Opportunities from Nanotechnology

This textbook chapter was published in “Nano-Enabled Sustainable and Precision Agriculture” by Academic Press (2023).

10

Hydroponics and alternative forms of agriculture: opportunities from nanotechnology

J.J. Chadwick[1], A. Witteveen[2], Peng Zhang[1,3] and Iseult Lynch[1]
[1]School of Geography, Earth and Environmental Sciences, University of Birmingham, Edgbaston, Birmingham, United Kingdom [2]Saturn Bioponics, Harborne, Birmingham, United Kingdom [3]Department of Environmental Science and Engineering, University of Science and Technology of China, Hefei, China

Learning objectives

Studying this chapter should provide the readers with sufficient knowledge to:

- understand how the rising food demand of the global population is driving diversification of crop growing alternatives such as vertical farming and technological innovation such as big data driven farm management;
- appreciate that modern agricultural techniques such as hydroponics differ significantly from soil-based agriculture, presenting new opportunities for nanotechnology to further enhance agricultural efficiency and reduce the associated pollution impacts;
- understand what is meant by precision agriculture and the ways that nanotechnology can aid and augment the insights gained from precision agriculture to optimize plant yields.

10.1 Introduction

Globally, soil quality is decreasing, putting additional pressure on our food system. As soil degradation continues and freshwater supplies become scarce, development of farming approaches that use both land and water more efficiently and productively to grow food is essential.[1] This need has created a niche for scientists and farmers to develop techniques to improve either land productivity or to use alternative agricultural techniques. 24% of UK farmers now employ some form of precision farming,[2] whereby a range of sensors, drones, or satellite imagery is used in order to generate data about the growing crop's specific needs and

Nano-enabled Sustainable and Precision Agriculture. DOI: https://doi.org/10.1016/B978-0-323-91233-4.00018-1
© 2023 Elsevier Inc. All rights reserved.

requirements in terms of water, fertilization, or other inputs. Employing nanotechnology with precision farming techniques is hoped to help further reduce the strain on resources, the range of ways nanotechnology can prove helpful in precision farming will be discussed further in this chapter.

As the human population has shifted from rural areas to cities, with urban populations making up 55% of the world's population of over 4 billion individuals, food sources are further away from centers of population density.[3] Additionally, with the globalization of the last century, food is transported to thousands of miles from where it was grown, with the UK food miles increasing on average 50% from 1978 (DEFRA, 2005). Local alternatives, such as urban agriculture and vertical farming, provide an opportunity to drastically reduce the air miles of our food, with city-based consumers having access to freshly grown crops far more easily. Using these alternatives to conventional farming is hoped to help meet the world's food demands, using less space and water, as well as requiring less transport.

Keyterm

Urban agriculture is the production and distribution of food grown in an urban area. It typically refers to plant crops but also extends to animal husbandry, beekeeping, and ornamental flower growing.

Precision agriculture lends itself to novel alternatives that could be further improved using nanotechnology. Food safety is also a core concern of the modern era. Vertical agriculture, or hydroponics, aims to provide dedicated infrastructure that is able to guarantee yields and provide ready-to-eat crops. As these crops are grown in densely populated areas, shelf life is extended, and the quality of the crops grown can be higher with far less travel time and less processing (and packaging) needed before transport. This also prevents more land from being required to produce the increasing quantities of food needed globally as the world's population grows. A secondary benefit is that areas that were previously used for agriculture can instead be used as biodiversity restoration areas and returned to their original habitats prior to their use for agriculture. Additionally, these rewilded former agricultural areas provide other ecosystem services which include provisions for humans, regulatory services, such as erosion control, improvements to air, soil and water quality, and natural hazard regulation, or cultural benefits, including recreation.[4] An estimated 5% of tropical deforestation is done for palm oil plantations, with deforestation for agriculture frequently generating newspaper headlines and international boycotts.[5,6] Limiting further destruction of wild spaces, such as the Amazon and Indonesian rainforests, is a global priority, as loss of these spaces has huge impacts on local indigenous communities, biodiversity, and climate change. By

presenting an alternative to soil-based agriculture, hydroponics, urban farming, and related approaches should eventually limit demand for new agricultural land and prevent further devastation of soil quality, potentially even allowing some current agricultural areas to become reforested, or rewilded.

Keyterm

Rewilding is the large-scale restoration of an area of land to its natural, uncultivated state. The area is then a natural ecosystem that is able to maintain itself without human input.

This chapter will compare several alternative forms of agriculture and interrogate the advantages and disadvantages of each, and the ways in which nanotechnology could aid or further improve them. Precision agriculture methods, and how nanotechnology can work concurrently with these, will also be discussed.

10.2 Hydroponics and alternative agricultural approaches

Protected cropping, or horticulture that takes place under controlled conditions, like that of a polytunnel, allows a myriad of benefits over conventional agriculture, enabling elevated levels of control of temperature, light quality and day length, and reducing the risk of pests. Hydroponics is an approach to growing crop plants that removes the need for soil and instead supplies plants with nutrient-rich aqueous solutions, typically via recirculation of the nutrient solution which can be tailored to the specific needs of the crops in question, and ideally adjusted in real time. Hydroponic structures use 60%–70% less water than regular conventional agriculture, and by utilizing vertical space can increase crop density three–fourfold per m^3 compared to traditional soil-based agriculture.

The recirculating aqueous solutions need to be enriched with all the nutrients that are essential for plant growth, including N, P, and K, but also with the micronutrients that are needed in far lower concentrations, such as manganese, zinc, and iron, among others. Hydroponics aims to solve many of the common issues seen in traditional agriculture. By using less land and water, it is a less resource-intensive form of farming than using a field. This means that the crops grown are able to always have the optimum conditions required, with the end goal of producing higher quality crops that are more nutritious and thus to make agriculture more productive. Some forms of protected cropping, such as vertical farms, allow total control over the growing environment which means that crops can be consistently produced across the year without the effect of

seasons, but with a large energy expenditure required to have the correct lighting and temperature. A comparison of soil-based and hydroponic farming techniques is shown in Table 10.1.

There are a wide range of different hydroponics techniques (Fig. 10.1) in which the crops are grown differently. The major distinctions are whether the nutrient solution culture is continuously recirculating or if the solution is run to waste. Recirculating hydroponic systems are more efficient for reducing nutrient waste but require regular nutrient and pH monitoring, ideally responsive to the plant's needs and adding different nutrients and pH correction in real time. Crops can also be grown in a solid substrate, for example, using rock wool slabs, a lightweight growing medium that is made of spun basaltic rock fibers which allow rock wool to maintain a moisture gradient and aeration that is effective for crop growth. Hydroponics is not the only alternative form of agriculture; aeroponics is a subset of hydroponics that instead of immersing plant roots in nutrient solutions suspends the plants in air and the roots are misted with the nutrient solution. There is also aquaponics, where hydroponics is integrated within an aquaculture system; here the nutrients are partially gained from cultivating fish and are then used to grow the crops, with water recirculated through the system. As opposed to traditional, soil-based farming, the range of crops that can be grown in hydroponic systems is limited currently. Predominantly leafy vegetables, such as lettuce or pak choi, are grown, but also other fruits, vegetables, and cereals can be grown, with the variety of crops possible expanding over time.

Table 10.1 Comparison of soil-based agriculture and hydroponics approaches.

	Soil-based agriculture	Hydroponics
NUE (nutrient use efficiency)	• Nutrients bind to soil particles • Nutrients subject to leaching or conversion into other compounds by soil microbes • Dependent on location, soil quality and nutritional content will alter regionally	• Closed system so can closely monitor nutrients left over at the end of the hydroponic stack • Lower nutrient levels needed so a reduction in nutrient losses to the environment (reduced agriculture-related pollution)
Scale	• Large-scale, commercial farms can cover many hectares	• Small scale, optimized for smaller scale growing in urban settings or warehouses • Hydroponic farms can cover many hectares
Resources used	• Soil has preexisting nutrients, with fertilizer added to provide consistent supply to crops • Pesticides and herbicides in common use	• Sealed growth room so reduced need for pesticides and no risk of competition from other plants • Nutrients must be entirely supplied by the hydroponic solution
Root secretions	• Root secretions released into soil, limiting their ability to travel • Root secretions important in root-microbe interactions, like with Rhizobia bacteria and mycorrhizal fungi	• Root secretions released into hydroponic solution and will travel through the rest of the hydroponic system—this can be positive or negative

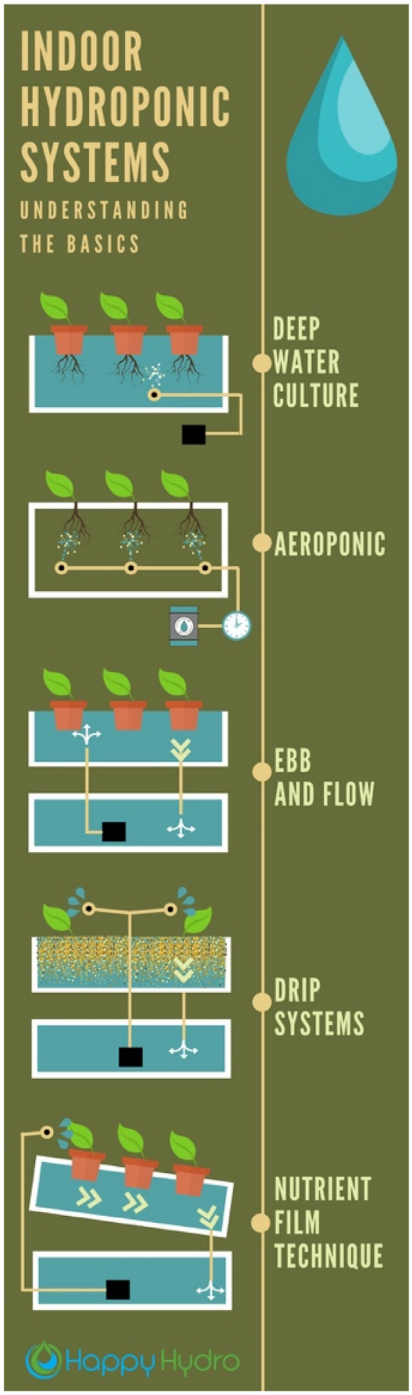


Figure 10.1 Outline of several different hydroponic systems. Deep water culture, ebb and flow, and nutrient film technique are all recirculating systems, while drop systems can be recirculating or not.[7] *Source: From McKeil, J.* Best Types of Hydroponics Systems and How They Work in 2019*, 2019. https://www.happyhydro.com/blogs/news/best-types-of-hydroponics-systems-and-how-they-work-in-2019 (accessed Mar 1, 2022).*

A perceived negative effect of growing crops using hydroponics is that the bacterial diversity of the nutrient medium is limited. Plants have coevolved with soil bacteria for many thousands of years, both aiding plant roots to gain nutrients and targeting plants as bacterial diseases. However, hydroponic solution has been shown to have similar levels of bacteria and fungi present as compared to compost[8,9] with similar levels of species diversity.[10] The bacterial concentration is particularly high around the roots due to root mucilage providing an optimal niche for microbes to thrive. Mycorrhizal fungi can be inoculated into hydroponic media, further reducing the need for high concentrations of nutrients, due to more efficient nutrient uptake. Combining fungal inoculation with more efficient sources of nutrients, such as nanofertilizers, could help to ensure that hydroponically grown crops can produce the required yields to be a competitive option for farmers.

The microbial activity seen in hydroponic systems is not always positive, however. Hydroponically grown plants are more prone to Pythium root rot than soil-grown crops are, due to the waterborne nature of the fungus which is easily transported via the recirculation of the medium. The zoospores are water mobile and so are able to spread effectively through the shared nutrient solution, infecting crop roots and causing the total root system to discolor through damage (see Fig. 10.2), potentially resulting in crop death. This has knock-on effects on the aerial component of the plants, stunting development and growth, and frequently causing wilting and yellow leaf discoloration, otherwise known as chlorosis. Good management practice can prevent Pythium spread, by the use of good sterilization techniques when using recirculating hydroponic systems and optimized environmental conditions, for example, the system must avoid very high or low temperatures and maintain dissolved oxygen in the nutrient solution.[11] Optimal environmental conditions need to be



Figure 10.2 Pythium root rot visible on the right, with a healthy rooted plant on the left.[12] Often there are no visible symptoms, with diseased plants having a reduced mass. *Source: From Mathias, M. Pythium in Hydroponics Can Be Tackled.* Fruit & Veg Tech. *2009, 9 (2), 4.*

maintained to prevent infection, such as avoiding waterlogging of the roots, having ambient growth temperatures, and avoiding overuse of nutrient additions. Similarly, poor management can lead to algal blooms in the nutrient medium which compete with the crop plants and can make them more susceptible to pathogen attacks.

Real-time sensing using nanosensors would allow closer monitoring of the nutrient solution content, something of particular importance in recirculating hydroponic systems. Real-time sensing has been demonstrated with silver nanoparticles, which could allow adaptation or the use of big data to analyze when or which plants should be removed to prevent outbreaks of disease in their earliest stages.[13] Fluorescent quantum dots have been used in conjunction with carbon nanoparticles to detect pathogenic bacteria in food, with higher concentrations of the pathogens resulting in linear increases in fluorescence.[14] If this technique were applied to hydroponics, it would be possible to detect relevant microbial pathogens by changing the aptamer (binding molecules made of peptides or oligonucleotides) and recording the fluorescence of the hydroponic medium or area around the crop roots.

If plants become infected, biofungicides are typically used, which could utilize nanotechnology rather than using traditional options. Chitosan can be added to hydroponic medium to aid the development of healthy microbial communities and has been used previously to prevent Pythium infections.[15,16] Chitosan is a natural derivative of the compound chitin, found in the exoskeleton of shellfish. Chitosan nanoparticles are popular, biodegradable polymers that have been shown to have antibacterial properties by disrupting bacterial cell membranes causing leakage of cell contents into the cytoplasm.[17] As such, the positive effect chitosan has on suppressing infections in hydroponics demonstrates a viable role for other nanomaterials in hydroponics.

Hydroponics is still a developing field, with relatively few commercial crops grown using this method. This is largely due to the cost of hydroponic facilities equipment, and the energy costs associated with running them, being unviable with the price that crops are sold competitively. Due to this, the majority of scientific research relating to hydroponics and nanomaterials is instead in the context of phytotoxicity and unraveling nanomaterials uptake by plants. This format of hydroponics differs from commercial hydroponics in that rather than utilizing stacks, such as those in Fig. 10.3, at the laboratory research scale hydroponic solutions are used in test tubes or petri dishes. A 2016 paper by Ref.[18] showed that hydroponically grown spinach had greater overall biomass, stem and root length, and greater concentrations of iron when treated with Fe_2O_3 (hematite) nanoparticles compared to untreated control plants. Similar results have been found using a range of metal and carbon-based nanofertilizers in common crop species including, tomato, cucumber, corn, wheat, and lettuce. Relating these findings to scalable commercial hydroponics is of interest



Figure 10.3 Vertical farm grown lettuces from the UK-based hydroponics company, Saturn Bioponics (Birmingham, United Kingdom). Hydroponics is a soilless farming technique that allows close control of the growing environment.

but this knowledge is presently lacking. More information on how best to apply nanomaterials in a hydroponic context is required, whether that is through the growth solution, as foliar sprays, or in sensing and controlled delivery of nutrients and pesticides. Understanding how hydroponically grown crops respond to nanomaterials is significant and has the potential to greatly aid the commercialization of hydroponics internationally. Additionally, looking at the impact on nutrient use efficiency and atmospheric losses by applying different nanomaterials in conjunction with hydroponics could be an area of interest for future research. An important question to explore is whether plant's responses are different when in hydroponics compared to soil systems, and this information will facilitate the design of nanomaterial systems optimized for hydroponics systems, via the application of safe and sustainable by design principles.[19]

10.3 Nanomaterials and precision agriculture

Precision agriculture is a form of sustainable intensification of farming that covers a wide range of modern technologies used to aid farmers' productivity and crop yields. The approaches range widely in terms of the methods applied, depending on the farm type, as precision farming is commonly used in both livestock and arable farming. Arable precision farming includes everything from altering the light quality used in vertical farming, to drone and satellite usage for crop analysis in the field to determine or control the timing of application of fertilizers or other interventions. A 2020 study of the UK farmers reflected that 60% of the UK cereal farmers used some form of precision farming to reduce their environmental impact (DEFRA, 2020), with 44% of all farmers using

precision farming stating that improving soil conditions was a reason for doing this, as seen in Fig. 10.4.

Precision farming has the capacity to improve farm management and offers clear advantages for indoor, greenhouse-based growing methods, such as vertical farming, providing a wider range of options for both farmers and consumers, reducing the pressures on land and water that exist from current agricultural methods. In the hydroponics context, accurate sensing of nutrient and trace element concentrations in the recirculating medium can allow adjustments in real time; while, as noted above, monitoring and early detection of fungal or bacterial spores can enable intervention through use of pesticides, isolation of the infected stack, replacement of medium or other automated or manual interventions. The bottom line is that access to real-time data allows farmers to make informed decisions at a much earlier point before crop damage becomes irreversible or extensive. Precision farming isn't perfect; however, with the use (interpretation) of complex data being a challenge and the need for expensive initial investments for sensing and monitoring devices by farmers being significant deterrents.

Many of the advantages of hydroponics arise from the accessibility of the nutrient medium to real-time analysis. However, in many cases separate sensors are needed for each element, and multianalyte detection of essential plant micronutrients such as Zn and Fe in the growth medium remains a challenge. A potential tool for the on-line monitoring of hydroponic solutions can be ion-selective electrodes (ISEs) that are also applied for the assessment of drinking water quality; however, these are not yet available for Fe, Cu, and Zn. Device

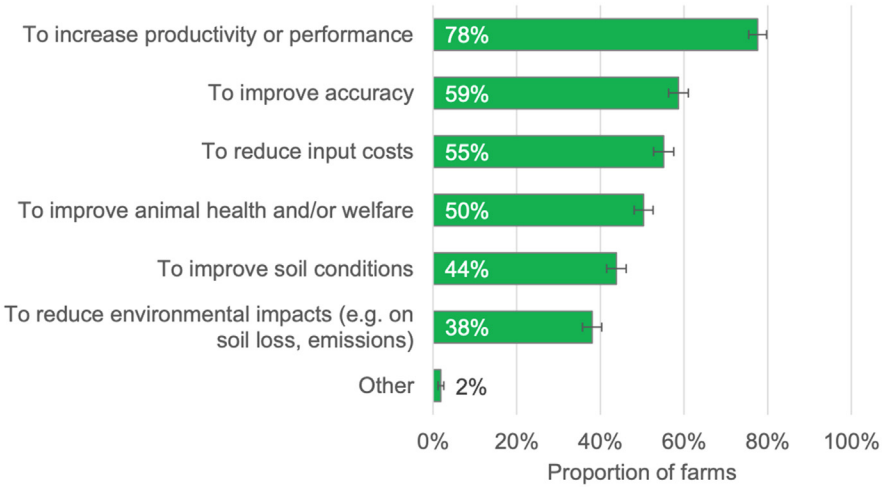


Figure 10.4 UK farmer's reasons for utilizing precision farming techniques. *Source: Image from Clark, C. Farm Practices Survey Autumn 2019—England; Farm Practices Survey; Department for Environment Food and Rural Affairs, 2020.*

optimization is needed to increase selectivity and sensitivity of combined ion-selective electrodes and to extend the useful life of the sensors by decreasing nonspecific binding/surface fouling. Nanotechnology offers enormous potential here, since much is known about how biomolecule interactions with nanoscale surfaces,[20] and indeed many nanomaterials are themselves antimicrobial and biocidal (e.g., silver, copper, and zinc-based nanomaterials, and chitosan as noted above) and thus reduce biofouling.

Using nanomaterials for nanosensors has huge potential to aid precision agriculture sensors networks. Using nitrate-sensitive nanosensors could help farmers' time the application of fertilization and irrigation more precisely, localizing nutrient input to specific areas. For example, the nanocomposite POT-MoS_2 (poly(3-octyl-thiophene and molybdenum disulfide)) when coated on a gold electrode was shown to be able to detect soil nitrate at all concentrations seen in agricultural fields. The use of the nanocomposite improves the sensitivity and selectivity of the sensor by utilizing its redox properties and hydrophobicity to allow anion exchange and prevent formation of a water layer around the electrode which can negatively affect sensitivity.[21] Alternatively, nanobiosensors (nanoscale sensors able to quantitatively detect a response by using a biologically derived component, e.g., enzyme, antibody, or peptide to then transduce the chemical signal into an electrochemical one for sensing) could be targeted to analyze changes in soil pH, pathogen and virus presence, and nutrient status.[22] These nanosensors could also be linked to nanoscale carriers of pesticides and fungicides in order to tailor the release of the chemicals in alignment with the real-time data coming from the sensors or be linked to irrigation systems for sustainable water management.[23]

The combination of nanomaterials in multielement sensors, with smart devices and interpretation algorithms based on artificial intelligence and machine learning logic to analyze data, will facilitate the transition to smart agricultural approaches to monitor the availability of nutrients/elements in the hydroponic solution and to modify its composition in real time. The productivity and quality of crops grown in hydroponic systems are highly dependent on the extent of nutrient acquisition from the growth medium, with bioavailability of nutrients affected by their forms (speciation) in the medium, and by interactions among nutrients (e.g., competition/antagonism). The selective removal of nutrients due to plant growth and evapotranspiration changes the concentration of nutrients in the hydroponic solution, which can adversely impact crop yield and quality, while accumulation of undesired counterions (i.e., Na^+, Cl^-) impact electrical conductivity of the solution itself thereby reducing sensing ability.

Zn is an important micronutrient in plants, and its deficiency leads to poor health, quality, and yield of crops. Portable sensors, based on graphene oxide and upconversion nanoparticles (in which the sequential absorption of two or more photons leads to the emission of light at shorter wavelength than the

excitation wavelength) have been developed for early detection of Zn deficiency in crops.[24] These sensors, which consist of hexagonal phase NaYF4:Er^{3+}, Yb^{3+} upconversion nanoparticles, functionalized with single-stranded DNA (UCNPs-ssDNA), can reliably detect mRNAs in RNA extracts from plants using a smartphone camera, and as such are a promising basis from which to build in-line sensors for hydroponics based on root secretions into the hydroponic medium.

All improvements in efficiency gained by using nanotechnology have the potential to save farmers money and improve the sustainability of the farming practice. With sensors focused on plant disease this aids also food safety for consumers and facilitates targeted treatment. Not only could the detection mechanisms used be nanomaterials based, but the resulting interventions and solutions, such as application of targeted and controlled-release pesticide delivery, could utilize nanotechnologies also. As mentioned in previous chapters, nanopesticides have huge potential to minimize careless pesticide use and prevent biodiversity losses and pollinator decline that result from misuse and overuse of pesticides. Additionally, nanofertilizers can also be used to aid in soil or water retention, providing a hands-off approach to soil irrigation. Normalized difference in vegetative index (NDVI) sensors are a commonly used measure for plant biomass based on the amount of red light absorbed and near infra-red light reflected. Nano-based light emitting diodes can be used in these sensors in order to determine the health of the crops and can be used as an indicator of nitrogen requirements of a crop at a given time.[25] An example of NDVI-produced images can be seen in Fig. 10.5.

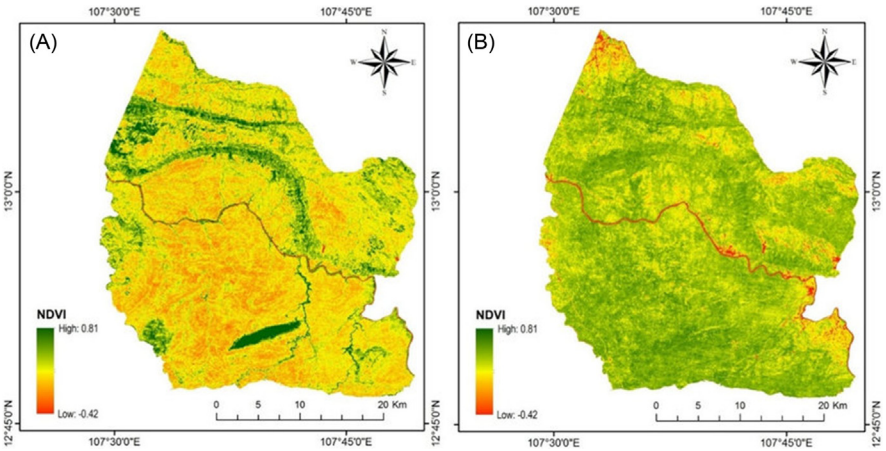


Figure 10.5 NDVI images in the dry (A) and rainy (B) season of a tropical broadleaf deciduous forest in Vietnam. High NDVI values indicate dense vegetation.[26] *NDVI*, Normalized difference in vegetative index. *Source: From Tran, A. T.; Nguyen, K. A.; Liou, Y. A.; Le, M. H.; Vu, V. T.; Nguyen, D. D. Classification and Observed Seasonal Phenology of Broadleaf Deciduous Forests in a Tropical Region by Using Multitemporal Sentinel-1A and Landsat 8 Data.* Forests *2021, 12 (2), 23.*

A roadmap for progress in the combination of nanotechnologies and artificial intelligence for precision agriculture was presented by Zhang et al.,[27] laying out the need for a systems approach, integration of datasets globally, and innovative modeling approaches to enable enhanced nanomaterials design for bespoke applications in agricultural sensing, pollution reduction, and precision application of fertilizers, pesticides, and other crop protection tools. Chapter 23 in this volume provides an overview of the current status of nanoinformatics approaches and their application for precision agriculture, including hydroponics systems.

10.4 Summary

Hydroponics is able to address many of the core concerns of conventional arable agriculture. Using less land and water are major global goals, highlighted in the sustainable development goals and regularly discussed at international conferences on climate change and global food and water security issues. Additionally, hydroponics can improve crop quality and safety, while bringing farming closer to where the majority of the population lives, that is, in urban areas, thus reducing unnecessary transport with its associated emissions.

Hydroponics is a new area in general, with precision farming overall worth $6 billion in 2020.[28] Precision farming is on an upward slope, with increases in its global value set to continue. These alternative agricultural methods have high take-up rates in the United Kingdom but there are concerns amongst farmers that they offer limited cost benefits or are not relevant to their farming (DEFRA, 2020).

Nanotechnology only began to be intensively researched in the early 2000s, making it a relatively young subject. As such, the overlap of the two areas has received limited research to date, and as such there are major knowledge gaps but early evidence suggesting major opportunities from the use of nanotechnologies and nanoscale materials to enhance hydroponic agriculture. Whether there are different concerns when using nanomaterials in hydroponics compared to in conventional soil-based agricultural systems is unknown, with positive results found when applying chitosan to suppress Pythium infections in hydroponic farms. Nanomaterials could have a wide range of roles in precision agriculture, forming nanobiosensors to detect moisture, pH, or nutrient status. The role of nanotechnology in precision agriculture is largely unexplored with further research required to realize some of the predicted applications.

References

1. Food and Agriculture Organization of the United Nations. *The State of the World's Land and Water Resources for Food and Agriculture*, 0 ed.; Routledge, **2021**. Available from: https://doi.org/10.4324/9780203142837.

2. Clark, C. Farm Practices Survey Autumn 2019—England*; Farm Practices Survey; Department for Environment Food and Rural Affairs*. Available from: https://assets.publishing.service.gov.uk/government/uploads/system/uploads/attachment_data/file/870305/fps-general-statsnotice-05mar20.pdf. **2020**.
3. United Nations. *World Population Prospects: The 2017 Revision, Key Findings and Advance Tables*; ESA/P/WP/248; Department of Economic and Social Affairs Population Division, **2017**.
4. Pereira, H. M.; Navarro, L. M., Eds. *Rewilding European Landscapes;* Springer International Publishing: Cham, **2015**. Available from: https://doi.org/10.1007/978-3-319-12039-3.
5. Cuypers, D.; Lust, A.; Geerken, T.; Gorissen, L.; Peters, G.; Karstensen, J.; Prieler, S.; Fisher, G.; Hizsnyik, E.; Van Velthuizen, H. European Commission; Directorate-General for the Environment; Vito; Centre for International Cooperation in Advanced Education and Research (Bonn), I. I. for A. S. A. (Laxenburg). *The Impact of EU Consumption on Deforestation: Comprehensive Analysis of the Impact of EU Consumption on Deforestation: Final Report*. Publications Office: Luxembourg, **2013a**.
6. Cuypers; et al. *The Impact of EU Consumption on Deforestation Com.Pdf*, **2013b**.
7. McKeil, J. *Best Types of Hydroponics Systems and How They Work in 2019*, **2019** https://www.happyhydro.com/blogs/news/best-types-of-hydroponics-systems-and-how-they-work-in-2019 (accessed Mar 1, 2022).
8. Berkelmann, B.; Wohanka, W.; Wolf, G. A. Characterisation of the Bacterial Flora in Circulating Nutrient Solutions of a Hydroponic System With Rockwool. *Acta Horticulturae; Int. Soc. Horticultural Sci. (ISHS)* **1994,** 372—381. Available from: https://doi.org/10.17660/ActaHortic.1994.361.37 Leuven, Belgium.
9. Waechter-Kristensen, B.; Caspersen, S.; Adalsteinsson, S.; Sundin, P.; Jensán, P. Organic Compounds and Micro-organisms in Closed, Hydroponic Culture: Occurrence and Effects on Plant Growth and Mineral Nutrition. *Acta Horticulturae; International Society for Horticultural Science (ISHS);* Leuven: Belgium, 1999, 197—204. *https://doi.org/10.17660/ActaHortic.1999.481.20*.
10. Chave, M.; Dabert, P.; Brun, R.; Godon, J.-J.; Poncet, C. Dynamics of Rhizoplane Bacterial Communities Subjected to Physicochemical Treatments in Hydroponic Crops. *Crop. Prot.* **2008,** *27* (3—5), 418—426. Available from: https://doi.org/10.1016/j.cropro.2007.07.010.
11. Raudales, R.; McGehee, C. Pythium Root Rot on Hydroponic Lettuce. *e-Gro Alert* **2016**. February.
12. Mathias, M. Pythium in Hydroponics Can Be Tackled. *Fruit & Veg Tech* **2009,** *9* (2), 4.
13. McFarland, A. D.; Van Duyne, R. P. Single Silver Nanoparticles as Real-Time Optical Sensors with Zeptomole Sensitivity. *Nano Lett* **2003,** *3* (8), 1057—1062. Available from: https://doi.org/10.1021/nl034372s.
14. Duan, N.; Wu, S.; Dai, S.; Miao, T.; Chen, J.; Wang, Z. Simultaneous Detection of Pathogenic Bacteria Using an Aptamer Based Biosensor and Dual Fluorescence Resonance Energy Transfer from Quantum Dots to Carbon Nanoparticles. *Microchim. Acta* **2015,** *182* (5—6), 917—923. Available from: https://doi.org/10.1007/s00604-014-1406-3.
15. Postma, J.; Stevens, L. H.; Wiegers, G. L.; Davelaar, E.; Nijhuis, E. H. Biological Control of *Pythium aphanidermatum* in Cucumber with a Combined Application of *Lysobacter enzymogenes* Strain 3.1T8 and Chitosan. *Biological Control* **2009,** *48* (3), 301—309. Available from: https://doi.org/10.1016/j.biocontrol.2008.11.006.
16. El Ghaouth, A.; Arul, J.; Grenier, J.; Benhamou, N.; Asselin, A.; Belanger, R. Effect of Chitosan on Cucumber Plants: Suppression of *Pythium aphanidermatum* and Induction of Defenses Reactions. *Cytol. Hystology* **1994**.
17. Qi, L.; Xu, Z.; Jiang, X.; Hu, C.; Zou, X. Preparation and Antibacterial Activity of Chitosan Nanoparticles. *Carbohydrate Research* **2004,** *339* (16), 2693—2700. Available from: https://doi.org/10.1016/j.carres.2004.09.007.
18. Jeyasubramanian, K.; Gopalakrishnan Thoppey, U. U.; Hikku, G. S.; Selvakumar, N.; Subramania, A.; Krishnamoorthy, K. Enhancement in Growth Rate and Productivity of

Spinach Grown in Hydroponics with Iron Oxide Nanoparticles. *RSC Adv* **2016,** *6* (19), 15451−15459. Available from: https://doi.org/10.1039/C5RA23425E.
19. Mech, A.; Gottardo, S.; Amenta, V.; Amodio, A.; Belz, S.; Bøwadt, S.; Drbohlavová, J.; Farcal, L.; Jantunen, P.; Małyska, A., et al. Safe- and Sustainable-by-Design: The Case of Smart Nanomaterials. A Perspective based on a European Workshop. *Regulatory Toxicology and Pharmacology* **2022,** *128*, 105093. Available from: https://www.sciencedirect.com/science/article/pii/S0273230021002348.
20. Wheeler, K. E.; Chetwynd, A. J.; Fahy, K. M.; Hong, B. S.; Tochihuitl, J. A.; Foster, L. A.; Lynch, I. Environmental Dimensions of the Protein Corona. *Nat Nanotechnol.* **2021,** *16* (6), 617−629. Available from: https://doi.org/10.1038/s41565-021-00924-1 Epub 2021 Jun 11. PMID: 34117462.
21. Ali, Md. A.; Wang, X.; Chen, Y.; Jiao, Y.; Mahal, N. K.; Moru, S.; Castellano, M. J.; Schnable, J. C.; Schnable, P. S.; Dong, L. Continuous Monitoring of Soil Nitrate Using a Miniature Sensor with Poly(3-Octyl-Thiophene) and Molybdenum Disulfide Nanocomposite. *ACS Appl. Mater. Interfaces* **2019,** *11* (32), 29195−29206. Available from: https://doi.org/10.1021/acsami.9b07120.
22. Sharma, A.; Rogers, K. R. Biosensors. *Meas. Sci. Technol* **1994**.
23. Fraceto, L. F.; Grillo, R.; de Medeiros, G. A.; Scognamiglio, V.; Rea, G.; Bartolucci, C. Nanotechnology in Agriculture: Which Innovation Potential Does It Have? *Front. Environ. Sci* **2016,** 4. Available from: https://doi.org/10.3389/fenvs.2016.00020.
24. Giust, D., et al. Graphene Oxide−Upconversion Nanoparticle Based Portable Sensors for Assessing Nutritional Deficiencies in Crops. *ACS Nano* **2018,** *12* (6), 6273−6279. Available from: https://doi.org/10.1021/acsnano.8b03261.(14).
25. Duhan, J. S.; Kumar, R.; Kumar, N.; Kaur, P.; Nehra, K.; Duhan, S. Nanotechnology: The New Perspective in Precision Agriculture. *Biotechnol. Rep.* **2017,** *15*, 11−23. Available from: https://doi.org/10.1016/j.btre.2017.03.002.
26. Tran, A. T.; Nguyen, K. A.; Liou, Y. A.; Le, M. H.; Vu, V. T.; Nguyen, D. D. Classification and Observed Seasonal Phenology of Broadleaf Deciduous Forests in a Tropical Region by Using Multitemporal Sentinel-1A and Landsat 8 Data. *Forests* **2021,** *12* (2), 235. Available from: https://doi.org/10.3390/f12020235.
27. Zhang, P.; Guo, Z.; Ullah, S., et al. Nanotechnology and Artificial Intelligence to Enable Sustainable and Precision Agriculture. *Nat. Plants* **2021,** *7*, 864−876. Available from: https://doi.org/10.1038/s41477-021-00946-6.
28. Global Industry Analysts, Inc. *Hydroponics - Global Market Trajectory & Analytics*, **2021**. https://www.researchandmarkets.com/reports/5028052/hydroponics-global-market-trajectory-and (accessed Mar 3, 2022).

Further reading

Sambo, P.; Nicoletto, C.; Giro, A.; Pii, Y.; Valentinuzzi, F.; Mimmo, T.; Lugli, P.; Orzes, G.; Mazzetto, F.; Astolfi, S., et al. Hydroponic Solutions for Soilless Production Systems: Issues and Opportunities in a Smart Agriculture Perspective. *Front. Plant Sci.* **2019,** *10*, 923. Available from: https://doi.org/10.3389/fpls.2019.00923.

Smith, A.; Watkiss, P.; Tweddle, G.; McKinnon, A.; Browne, M.; Hunt, A.; Trevelan, C.; Nash, C.; Cross, S. *The Validity of Food Miles as an Indicator of Sustainable Development; ED50254; Department for Environment Food and Rural Affairs*, **2005**; p. 117.